

# ALGEBRAS WITH MATCHINGS AND KNOT FLOER HOMOLOGY

PETER OZSVÁTH AND ZOLTÁN SZABÓ

ABSTRACT. Knot Floer homology is a knot invariant defined using holomorphic curves. In more recent work, taking cues from bordered Floer homology, the authors described another knot invariant, called “bordered knot Floer homology”, which has an explicit algebraic and combinatorial construction. In the present paper, we extend the holomorphic theory to bordered Heegaard diagrams for partial knot projections, and establish a pairing result for gluing such diagrams, in the spirit of the pairing theorem of bordered Floer homology. After making some model calculations, we obtain an identification of a variant of knot Floer homology with its algebraically defined relative. These results give a fast algorithm for computing knot Floer homology.

---

PSO was supported by NSF grant number DMS-1405114 and DMS-1708284.  
ZSz was supported by NSF grant numbers DMS-1606571 and DMS-1904628.

## 1. INTRODUCTION

The aim of the present paper is to identify the knot invariant from [22] with a certain specialization of the knot Floer homology from [19] and [24].

One version of knot Floer homology associates to a knot  $K$ , a bigraded module over  $\mathcal{R} = \mathbb{F}[U, V]/UV = 0$  (where  $\mathbb{F} = \mathbb{Z}/2\mathbb{Z}$  is the field with two elements), which we denote here by  $H_{\mathcal{R}}(K)$ . That module in turn is the homology of a chain complex, denoted here  $C_{\mathcal{R}}(\mathcal{H})$ , associated to a doubly-pointed genus  $g$  Heegaard diagram  $\mathcal{H}$ , whose differential counts pseudo-holomorphic disks  $u$  in  $\text{Sym}^g(\Sigma)$ , weighted with the monomial  $U^{n_w(u)}V^{n_z(u)}$ . Specializing further to  $V = 0$  (and then taking homology), we obtain the knot invariant denoted  $\text{HFK}^-(K)$  in [19]; and setting  $U = V = 0$ , we obtain the knot invariant  $\widehat{\text{HFK}}(K)$ . (Note that throughout the present paper, we are using knot Floer homology groups with coefficients mod 2, though we suppress this from the notation.) In [17], we described a Heegaard diagram associated to a knot projection, where the generators correspond to Kauffman states for the knot diagram; but the differentials still remained elusive counts of pseudo-holomorphic disks.

Taking algebraic clues from the bordered Floer homology of [10], in [21, 22], we defined chain complexes whose generators correspond to Kauffman states and whose differentials are determined by certain explicit algebraic constructions; we then verified that their homology groups are knot invariants. Specifically, the constructions from [22] give an oriented knot invariant  $\mathcal{G}(\vec{K})$ , that is a bigraded module over  $\mathcal{R}$ , whose  $V = 0$  specialization gives the knot invariant  $H^-(-\vec{K})$  from [21].

The aim of the present paper is to prove the following:

**Theorem 1.1.** *Bigraded knot Floer homology  $H_{\mathcal{R}}(K)$  (with coefficients mod 2) is identified with the bordered knot invariant  $\mathcal{G}(\vec{K})$  (again, with coefficients mod 2) from [22]; the bigraded knot Floer homology  $\text{HFK}^-(K)$  is identified with the bordered knot invariant  $H^-(\vec{K})$  from [21]; the bigraded knot Floer homology  $\widehat{\text{HFK}}(K)$  is identified with the  $U = V = 0$  specialization of  $\mathcal{G}(\vec{K})$ .*

(As the notation suggests, knot Floer homology is independent of the choice of orientation on  $K$ ; in view of the above theorem,  $\mathcal{G}(\vec{K})$  is independent of this choice, as well.)

The bordered knot invariants are defined in terms of a decorated knot projection. We start from the projection, cut it up into elementary pieces, associate bimodules to those pieces, and then define the invariant to be a (suitable) tensor product of the bimodules; compare [9, 8] for the three-dimensional analogue.

In its original formulation, knot Floer homology can be constructed using any Heegaard diagram representing a knot. We work here with the “standard Heegaard diagram” associated to a decorated knot projection, as used in [18]. After degenerating this Heegaard diagram, we obtain partial Heegaard diagrams, formalized in Section 2, which come in two kinds: the “lower diagrams” and the “upper diagrams”. Suitable counts of pseudo-holomorphic curves in upper diagrams leads to the definition of the “type  $D$  structure” associated to an upper diagram (Section 6), and counting pseudo-holomorphic curves in lower diagrams leads to the definition of the

“type  $A$  structure” associated to the lower diagram (Section 8). The underlying algebras for these modules are closely related to the ones defined in [21, 22]. Specifically, we will be working with curved modules over the algebra  $\mathcal{B}(2n, n)$  from [21] (which we abbreviate here by  $\mathcal{B}(n)$ ), with a curvature specified by a matching  $M$  (as described in Section 3), which in turn is very similar to working over the algebra  $\mathcal{A}(n, M)$  from [22].

A suitable tensor product of the type  $A$  and type  $D$  structures computes knot Floer homology, by an analogue of the pairing theorem from [10], proved in Section 9. The theory is generalized to bimodules in Section 10.

With the bordered theory in place, the verification of Theorem 1.1, which is completed in Section 15, rests on some model computations (see Section 13).

The pseudo-holomorphic curve counting here has a few complications beyond the material present in [10]. As in [7], we must account for “Reeb orbits” rather than merely Reeb chords. The present analysis is simpler, though, because our hypotheses on the partial diagrams exclude boundary degenerations on the “ $\alpha$ -side”. Rather, the boundary degenerations that occur here all happen on the “ $\beta$ -side”, and indeed they happen in a controlled manner that can be accounted for neatly in the algebra. With this understanding, the proof of the pairing theorem from [10] adapts readily.

Theorem 1.1 can be viewed as providing explicitly computable models for variants of knot Floer homology. Grid diagrams also give explicit combinatorial models for the necessary holomorphic curve counts; see [13, 14]. While the more algebraic bordered constructions studied here (and in [21, 22]) at present describe a specialized version of these invariants, their computations are much more efficient; see [23].

**1.1. Organization.** This paper is organized as follows. In Section 2, we formalize the partial Heegaard diagrams used in the bordered pseudo-holomorphic construction. Section 3 contains the algebraic background, with a formalization of the framework of curved algebras and the modules over them, which will be used throughout. Next we recall bordered algebras defined in [21], and show how they can be fit into the curved framework. The next few sections deal with upper diagrams, with the ultimate aim of defining their associated type  $D$  structures. In Section 4, we formalize the shadows of domains that connect upper Heegaard states, and use these to define a grading on the upper Heegaard states. In Section 5, we formulate the pseudo-holomorphic curves that represent these shadows, and lay out properties of their moduli spaces. In Section 6 we define the type  $D$  structure associated to an upper diagram, and verify that it satisfies the required structural identities, using the results from Section 5. In Section 7, we generalize the material from Section 5 to the curves relevant for the type  $A$  modules, which are defined in Section 8. In Section 9, we prove a pairing theorem for the modules associated to upper diagrams with lower diagrams, expressing knot Floer homology in terms of the modules associated to the two pieces. In Section 10, the material is adapted to the case of type  $DA$  bimodules associated to “middle diagrams”. A corresponding pairing theorem is established (Theorem 10.11). In fact, the above material is set up over a subalgebra of  $\mathcal{B}(n)$ , corresponding to restricting the idempotent ring. In Section 11, we extend the  $DA$  bimodules over all of  $\mathcal{B}(n)$ .

We would like to understand these bimodules for certain standard middle diagrams. For this description, we adapt the algebraically-defined bimodules from [22]; to the curved context. This adaptation is given in Section 12. Bimodules derived from these are identified with the bimodules associated to certain basic middle diagrams in Section 13. Combining these model computations with the pairing theorem for bimodules, we obtain an algebraic description of the type  $D$  modules associated to Heegaard diagrams for upper knot diagrams, in Section 14. This is readily adapted to a proof of Theorem 1.1 in Section 15.

**1.2. Acknowledgements.** The authors wish to express their gratitude to Robert Lipshitz and Dylan Thurston. Many of the ideas here were inspired by bordered Floer homology as described in [10]; and moreover the use of Reeb orbits also figured heavily in joint work with the first author which will appear soon [7].

We would also like to thank Andy Manion for sharing with us his work [11, 12]; and to thank Nate Dowlin, Ian Zemke, and Rumen Zarev for interesting conversations,

## 2. HEEGAARD DIAGRAMS

**2.1. Upper diagrams.** An *upper Heegaard diagram* is the following data:

- a surface  $\Sigma_0$  of genus  $g$  and  $2n$  boundary components, labelled  $Z_1, \dots, Z_{2n}$ ,
- a collection of disjoint, embedded arcs  $\{\alpha_i\}_{i=1}^{2n-1}$ , so that  $\alpha_i$  connects  $Z_i$  to  $Z_{i+1}$ ,
- a collection of disjoint embedded closed curves  $\{\alpha_i^c\}_{i=1}^g$  (which are also disjoint from  $\alpha_1, \dots, \alpha_{2n-1}$ ),
- another collection of embedded, mutually disjoint closed curves  $\{\beta_i\}_{i=1}^{g+n-1}$ .

We require this data to also satisfy the following properties:

- (UD-1) For each  $i \in \{1, \dots, 2n-1\}$ ,  $j \in \{1, \dots, g\}$ , and  $k \in \{1, \dots, g+n-1\}$ ,  $\alpha_i$  and  $\alpha_j^c$  curves are transverse to  $\beta_k$ .
- (UD-2) Both sets of  $\alpha$ - and the  $\beta$ -circles consist of homologically linearly independent curves (in  $H_1(\Sigma_0)$ ).
- (UD-3) The surface obtained by cutting  $\Sigma_0$  along  $\beta_1, \dots, \beta_{g+n-1}$ , which has  $n$  connected components, is required to contain exactly two boundary circles in each component.
- (UD-4) The subspace of  $H_1(\Sigma_0; \mathbb{Z})$  spanned by the curves  $\{\alpha_i^c\}_{i=1}^g$  meets transversely the space spanned by  $\{\beta_i\}_{i=1}^{g+n-1}$ .
- (UD-5) Letting  $\bar{\Sigma}$  denote the closed surface obtained by filling in  $\partial\Sigma_0$  with  $2n$  disks, the space  $H_1(\bar{\Sigma}; \mathbb{Z})$  is spanned by the images of the curves  $\{\alpha_i^c\}_{i=1}^g$  and  $\{\beta_i\}_{i=1}^{g+n-1}$ .

**Remark 2.1.** An upper diagram specifies a three-manifold  $Y$  whose boundary is a sphere, with an embedded collection of  $n$  arcs. Condition (UD-4) ensures that  $H_2(Y; \mathbb{Z}) = 0$ . (Compare [20, Proposition 2.15].) When  $g = 0$ , the three-manifold  $Y$  is a three-ball. Also, when  $g = 0$ , Condition (UD-5) is automatically satisfied.

Condition (UD-3) gives a matching  $M$  on  $\{1, \dots, 2n\}$  (a partition into two-element subsets), where  $\{i, j\} \in M$  if  $Z_i$  and  $Z_j$  can be connected by a path that does not cross any  $\beta_k$ .

We sometimes abbreviate the data

$$\mathcal{H}^\wedge = (\Sigma_0, Z_1, \dots, Z_{2n}, \{\alpha_1, \dots, \alpha_{2n-1}\}, \{\alpha_1^c, \dots, \alpha_g^c\}, \{\beta_1, \dots, \beta_{g+n-1}\}),$$

and let  $M(\mathcal{H}^\wedge)$  be the induced matching.

**Definition 2.2.** An upper Heegaard state is a subset  $\mathbf{x}$  of  $\Sigma_0$  consisting of  $g+n-1$  points in the intersection of the various  $\alpha$ - and  $\beta$ -curves, distributed so that each  $\beta$ -circle contains exactly one point in  $\mathbf{x}$ , each  $\alpha$ -circle contains exactly one point in  $\mathbf{x}$ , and no more than one point lies on any given  $\alpha$ -arc. Each Heegaard state  $\mathbf{x}$  determines a subset  $\alpha(\mathbf{x}) \subset \{1, \dots, 2n-1\}$  with cardinality  $n-1$  consisting of those  $i \in \{1, \dots, 2n-1\}$  with  $\mathbf{x} \cap \alpha_i \neq \emptyset$ .

**2.2. Lower diagrams.** A lower diagram  $\mathcal{H}^\vee$  is an upper diagram, equipped with an extra pair of basepoints  $w$  and  $z$  and one additional  $\beta$ -circle  $\beta_{g+n}$  so that exactly two of the  $n+1$  components in  $\Sigma_0 \setminus \beta$  contains one boundary component of  $\Sigma_0$  apiece, and these are marked by the basepoints  $w$  and  $z$  (and the remaining  $n-1$  components meet two boundary components of  $\Sigma_0$ ).

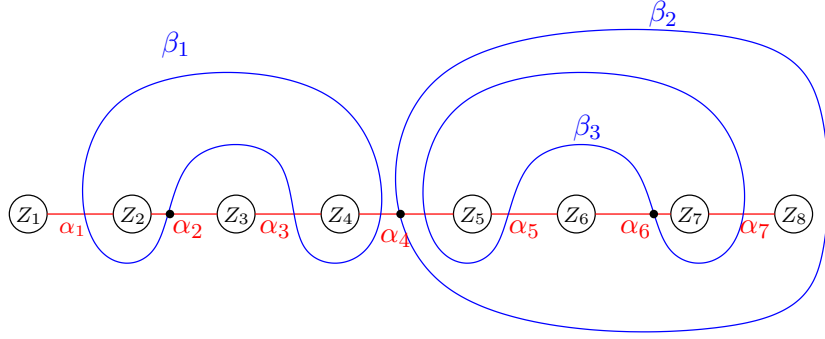


FIGURE 1. **An upper Heegaard diagram.** The black dots represent an upper Heegaard state  $\mathbf{x}$  with  $\alpha(\mathbf{x}) = \{2, 4, 6\}$

Note that a lower diagram also determines an equivalence relation  $M^\vee$  on the boundary circles  $Z_1, \dots, Z_{2n}$ , where  $\{i, j\} \in M^\vee$  if  $Z_i$  and  $Z_j$  can be connected by a path that does not cross any  $\beta_k$ .

A *lower Heegaard state*  $\mathbf{x}$  is a set of  $g + n$  points, where one lies on each  $\beta$ -circle, one lies on each  $\alpha$ -circle, and no more than one lies on each  $\alpha$ -arc. Each lower Heegaard state  $\mathbf{x}$  determines a subset  $\alpha(\mathbf{x})$  of  $\{1, \dots, 2n - 1\}$  with cardinality  $n$ , once again, consisting of those  $i = 1, \dots, 2n - 1$  with  $\mathbf{x} \cap \alpha_i \neq \emptyset$ .

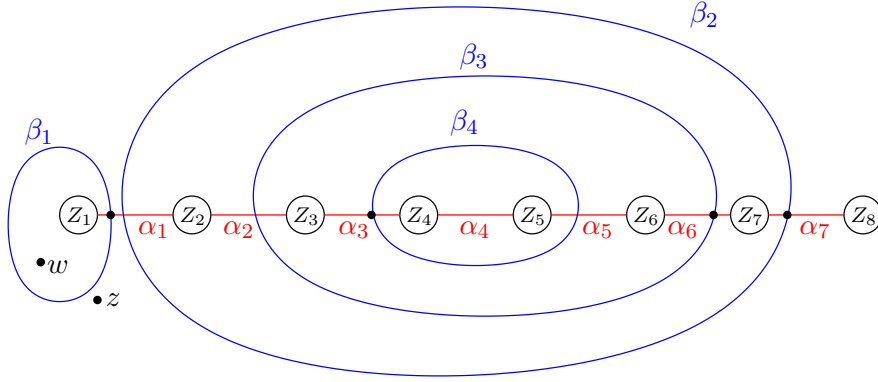


FIGURE 2. **A lower Heegaard diagram.** The basepoints  $w$  and  $z$  are marked; furthermore, a lower state  $\mathbf{x}$  with  $\alpha(\mathbf{x}) = \{1, 3, 6, 7\}$  is indicated by black dots.

### 2.3. Gluing upper and lower diagrams.

**Definition 2.3.** Let  $M_1$  and  $M_2$  be two matchings on  $\{1, \dots, 2n\}$ . We say that  $M_1$  and  $M_2$  are compatible if together they generate an equivalence relation with a single equivalence class.

It is convenient to phrase this geometrically in the following terms.

**Definition 2.4.** Let  $M$  be a matching on a finite set  $\{1, \dots, 2k\}$ . There is an associated one-manifold  $W(M)$ , whose boundary components correspond to the points

in  $\{1, \dots, 2k\}$ , and whose components correspond to  $\{i, j\} \in M$ ; that component connects the boundary component  $i$  to the boundary component  $j$ .

Suppose  $\{1, \dots, 2k\}$  is given with a matching  $M_1$  and another matching  $M_2$  on a subset  $S \subset \{1, \dots, 2k\}$ . Those two matchings together induce an equivalence relation  $M_3$  on  $\{1, \dots, 2k\} \setminus S$ . The associated spaces are related by

$$W(M_3) = W(M_2) \cup_S W(M_1).$$

In this language, the compatibility of  $M_1$  and  $M_2$  is equivalent to the condition that  $W(M_1) \cup_S W(M_2)$  has no closed components. See Figure 3.

**Definition 2.5.** Suppose that  $\mathcal{H}^\wedge$  and  $\mathcal{H}^\vee$  are upper and lower diagrams with the same number  $2n$  of boundary circles, and genera  $g_1$  and  $g_2$ . We say that  $\mathcal{H}^\wedge$  and  $\mathcal{H}^\vee$  are compatible if the corresponding matchings  $M(\mathcal{H}^\wedge)$  and  $M(\mathcal{H}^\vee)$  are compatible, in the sense of Definition 2.3

**Example 2.6.** The upper Heegaard diagram  $\mathcal{H}^\wedge$  from Figure 1 determines the matching on  $\{1, \dots, 8\}$ ,  $M^\wedge = \{\{1, 3\}, \{2, 4\}, \{5, 7\}, \{6, 8\}\}$ ; and the lower diagram  $\mathcal{H}^\vee$  from Figure 2 determines the matching  $M^\vee = \{\{2, 7\}, \{3, 6\}, \{4, 5\}\}$ . Together, they determine an equivalence relation with two equivalence classes,  $\{2, 4, 5, 7\}$  and  $\{1, 3, 6, 8\}$ ; thus,  $\mathcal{H}^\wedge$  and  $\mathcal{H}^\vee$  are not compatible, in the sense of Definition 2.5.

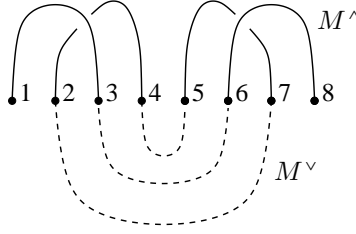


FIGURE 3. One-manifold associated to pairs of matchings.

**Proposition 2.7.** Suppose that  $\mathcal{H}^\wedge$  and  $\mathcal{H}^\vee$  are compatible upper and lower diagrams (with underlying surfaces  $\hat{\Sigma}_0$  and  $\check{\Sigma}_0$  respectively). Glue  $\hat{\Sigma}_0$  and  $\check{\Sigma}_0$  together along their boundaries to get a closed surface  $\Sigma$  of genus  $g = g_1 + g_2 + 2n - 1$ . Collect the  $\beta$ -circles for  $\mathcal{H}^\wedge$  and  $\mathcal{H}^\vee$  into a  $g$ -tuple, thought of now as circles in  $\Sigma$ ; and form a  $g$ -tuple of  $\alpha$ -circles consisting of the  $\alpha$ -circles in  $\mathcal{H}^\wedge$  and  $\mathcal{H}^\vee$  and further  $\alpha$ -circles formed by gluing  $\alpha$ -arcs in  $\mathcal{H}^\wedge$  to  $\alpha$ -arcs in  $\mathcal{H}^\vee$ . The result is a doubly-pointed Heegaard diagram.

**Proof.** It is straightforward to see that  $\Sigma$  has the stated genus, and that the  $\alpha$ -circles are homologically linearly independent. The compatibility condition guarantees that the complement of the  $\beta$ -circles is connected in  $\Sigma$ , and hence these circles are also linearly independent.  $\square$

We denote the doubly-pointed Heegaard diagram constructed in Proposition 2.7  $\mathcal{H}^\wedge \# \mathcal{H}^\vee$ .

**2.4. Examples.** The *standard upper diagram* is the diagram  $\mathcal{H}^\wedge(n)$  equipped with a planar surface,  $\alpha$ -arcs as in Figure 4 (with  $n = 4$ ),  $\beta$ -circles arranged as in the figure (after deleting  $\beta_4$ ), and no  $\alpha$ -circles. (That figure also contains two basepoints  $w$  and  $z$  which should be disregarded.) Note that the standard upper diagram has a single state  $\mathbf{x}$  with  $\alpha(\mathbf{x}) = \{2, \dots, 2n - 2\}$ .

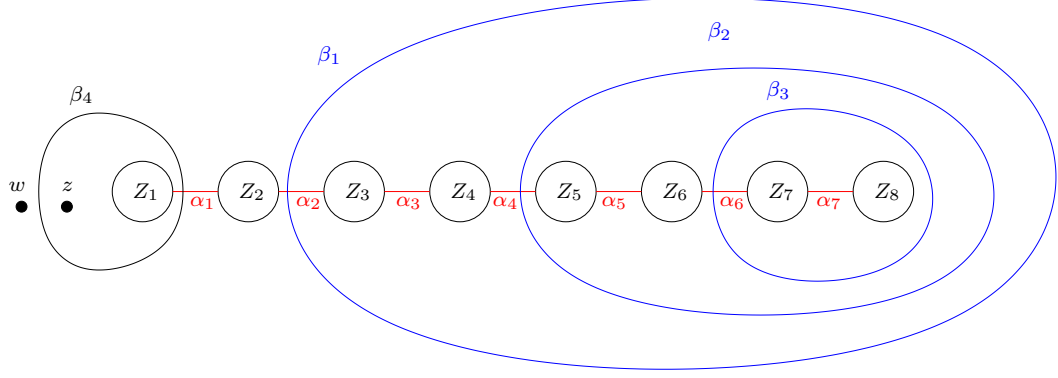


FIGURE 4. **Standard Heegaard diagrams**  $n = 4$ . This is the standard lower diagram; the standard upper diagram is obtained by removing the basepoints  $w$  and  $z$  and the circle  $\beta_4$ .

The *standard lower diagram* is obtained from the standard upper diagram by adding an extra  $\beta$ -circle around  $Z_1$ , and two adjacent basepoints  $w$  and  $z$  as shown in Figure 4.

Let  $\mathcal{H}^\wedge$  be any upper diagram drawn with Heegaard surface  $\Sigma_0$ , and fix an orientation preserving diffeomorphism  $\phi: \Sigma_0 \rightarrow \Sigma_0$ . There is a new upper Heegaard diagram

$$\phi(\mathcal{H}^\wedge) = (\Sigma_0, \alpha, \phi(\beta)) \cong (\Sigma_0, \phi^{-1}(\alpha), \beta).$$

We have illustrated this new upper diagram in the case where  $\phi$  is a half twist switching  $Z_2$  and  $Z_3$  in Figure 5.

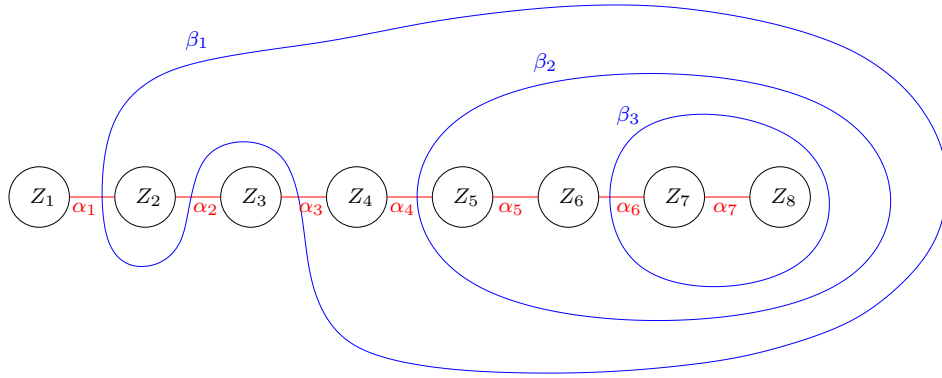


FIGURE 5. **Acting on the standard upper diagram by a half twist switching**  $Z_2$  and  $Z_3$ .



Let  $\mathcal{H}^\wedge$  be an upper diagram on a surface  $\Sigma_0$  of genus zero. Every mapping class of  $\mathbb{C}$  punctured at points  $\{p_1, \dots, p_{2n}\}$  can be represented by a diffeomorphism  $\phi_0$  of  $\Sigma_0$  to itself. Letting  $\phi_0$  act on  $\mathcal{H}^\wedge$ , we obtain an action of the mapping class group of  $\mathbb{C} \setminus \{p_1, \dots, p_{2n}\}$  (which in turn is identified with the quotient of the braid group on  $2n$  elements by the cyclic subgroup generated by a full twist; see [1]) on genus zero upper diagrams modulo isotopy. The braid group is generated by consecutive switches  $\sigma_i$ ; their corresponding mapping classes are represented by half twists: suppose that  $\gamma_i$  is a curve that encloses exactly two puncture points  $p_i$  and  $p_{i+1}$ , the half twist along  $\gamma_i$  is the mapping class  $\tau_{i,+}$  supported in the compact component of  $\mathbb{C} \setminus \gamma_i$  which switches  $p_i$  and  $p_{i+1}$ , and whose square is a Dehn twist along  $\gamma_i$ .

Gluing the standard upper diagram to  $\phi$  applied to the standard lower diagram induces a Heegaard diagram representing some knot in  $S^3$ , provided that the permutation  $\sigma$  induced by  $\phi$  has the property that the product of permutations

$$\sigma \cdot ((1, 2), (3, 4), \dots, (2n-1, 2n)) \cdot \sigma^{-1} \cdot ((1, 2), (3, 4), \dots, (2n-1, 2n))$$

has order  $n$ .

Consider a decorated knot projection, equipped with a height function, so that the marked edge contains the global minimum for the height function. Consider the associated Heegaard diagram (following [17]). Slicing the knot projection along a generic horizontal slice corresponds to decomposing the Heegaard diagram as the gluing of some upper and lower Heegaard diagrams; see Figure 6.

As usual, the Heegaard surface  $\Sigma$  is oriented as the boundary of the  $\alpha$ -handlebody.

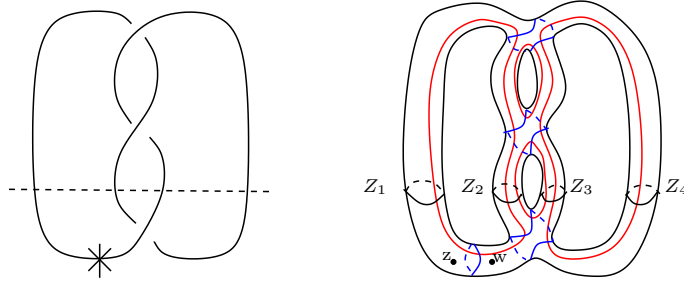


FIGURE 6. **Slicing the Heegaard diagram corresponding to a decorated knot projection.** Cutting the decorated projection on the left along the dotted line corresponds to slicing the Heegaard diagram along the right along the circles  $Z_1 \cup Z_2 \cup Z_3 \cup Z_4$ .

**2.5. Middle diagrams.** In this paper, we will define algebraic objects using holomorphic curve counts associated to upper and lower diagrams. Knot Floer homology then will be expressed as a pairing between the invariants of the upper and lower diagrams. To compute these individual objects, it will help to be able to decompose the knot diagram into further pieces, the *middle diagrams* we introduce presently.

**Definition 2.8.** A middle diagram is a Heegaard diagram obtained from an upper diagram with  $2m + 2n$  boundary components, by deleting the arc  $\alpha_{2m}$  which would

have connected  $Z_{2m}$  with  $Z_{2m+1}$ . Thus, the  $\alpha$ -arcs are labelled  $\alpha_i$  for

$$i \in \{1, \dots, 2m-1, 2m+1, \dots, 2m+2n-1\}.$$

Think of some boundary components of  $\Sigma_0$  as “incoming” boundary and other components as “outgoing” boundary. The incoming boundary components are labelled as  $\tilde{Z}_i = Z_i$  for  $i = 1, \dots, 2m$ ; and the outgoing boundary components  $\hat{Z}_i = Z_{2m+i}$  for  $i = 1, \dots, 2n$ ;  $\check{\alpha}_i = \alpha_i$  for  $i = 1, \dots, 2m-1$  and  $\hat{\alpha}_i = \alpha_{2m+i}$  for  $i = 1, \dots, 2n-1$ . The  $\beta$ -circles are labelled  $\{\beta_i\}_{i=1}^{g+m+n-1}$ . We abbreviate the resulting data

$$\mathcal{H}^{\parallel} = (\Sigma_0, (\tilde{Z}_1, \dots, \tilde{Z}_{2m}), (\hat{Z}_1, \dots, \hat{Z}_{2n}), \{\check{\alpha}_1, \dots, \check{\alpha}_{2m-1}\}, \{\hat{\alpha}_1, \dots, \hat{\alpha}_{2n-1}\}, \{\alpha_1^c, \dots, \alpha_g^c\}, \{\beta_1, \dots, \beta_{g+m+n-1}\}).$$

We will be primarily interested in five model middle diagrams: the *identity diagram*  $\mathcal{H}^{\natural} = \mathcal{H}^{\natural}(n)$  (Figure 7), the *middle diagram of a local maximum*  $\mathcal{H}_{c,n}^{\cap}$  (Figure 8), the *middle diagram of a local mimum*  $\mathcal{H}_{c,n}^{\cup}$  (Figure 9), the *middle diagram of a positive crossing*  $\mathcal{H}_{i,n}^+$ , and the *middle diagram of a negative crossing*  $\mathcal{H}_{i,n}^-$  (both in Figure 10).

We explain the interpretations of these Heegaard diagrams in terms of partial knot projection; though this connection will become important for us only much later (in Section 13). For  $\mathcal{H}_{c,n}^{\cap}$ , where  $2n$  denotes the number of input strands (so there are  $2n+2$  outputs), and  $c \in 1, \dots, 2n+1$  is chosen so that strands  $c$  and  $c+1$  come out of the local maximum. By contrast, for  $\mathcal{H}_{c,n}^{\cup}$ ,  $2n$  is the number of output strands and,  $c$  is choosen so that the output strands  $c$  and  $c+1$  connect to the local maximum. The diagrams for  $\mathcal{H}_{i,n}^+$  and  $\mathcal{H}_{i,n}^-$  both represent  $2n$  strands, so that the  $i$  and  $i+1^{st}$  ones cross. Orienting each strand upwards, the crossing is positive for  $\mathcal{H}^+$  and negative for  $\mathcal{H}^-$ . (In practice, the strands in a crossing region will not all be oriented pointing upward.)

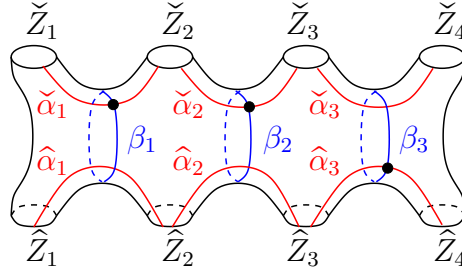


FIGURE 7. **Middle diagram of the identity  $\mathcal{H}^{\natural}(n)$ .** We have labelled a middle Heegaard state, with  $|\check{\alpha}(\mathbf{x})| = 2$ .

A *middle Heegaard state* is a set of  $g+m+n-1$  points of  $\Sigma_0$  in the locus where the various  $\alpha$ - and  $\beta$ -curves intersect, distributed so that one lies on each  $\beta$ -circle, one lies on each  $\alpha$ -circle, and no more than one lies on each  $\alpha$ -arc. For each middle Heegaard state, let  $\check{\alpha}(\mathbf{x}) \subset \{1, \dots, 2m-1\}$  consists of those  $i$  for which  $\mathbf{x} \cap \check{\alpha}_i \neq \emptyset$ ; and  $\hat{\alpha}(\mathbf{x}) \subset \{1, \dots, 2n-1\}$  consist of those  $j$  for which  $\mathbf{x} \cap \hat{\alpha}_j \neq \emptyset$ . Obviously,

$$(2.1) \quad |\check{\alpha}(\mathbf{x})| + |\hat{\alpha}(\mathbf{x})| = m+n-1.$$

We will be primarily interested in middle states with  $|\check{\alpha}(\mathbf{x})| = m$ .

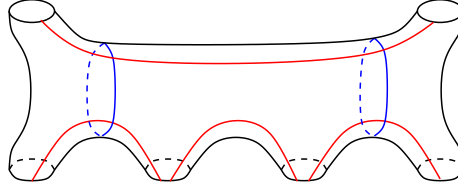


FIGURE 8. **Middle diagram of a local maximum**  $\mathcal{H}_{c,n}^\cap$ . We have drawn here the case when  $n = 1$  and  $c = 2$ .

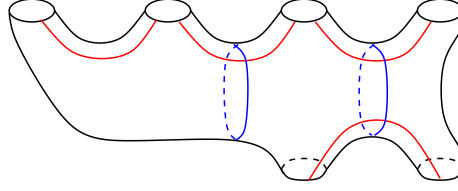


FIGURE 9. **Middle diagram of a local minimum**  $\mathcal{H}_{c,n}^\cup$ . We have drawn here the case where  $n = 2$  and  $c = 1$ .

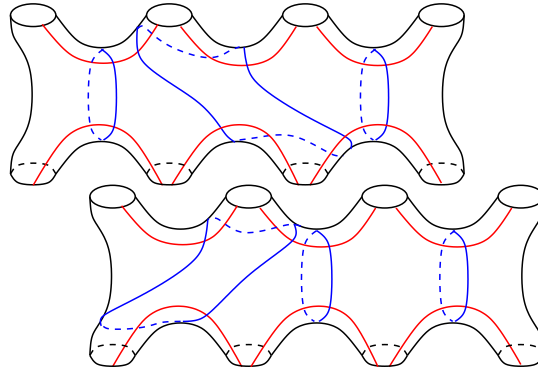


FIGURE 10. **Middle diagram of crossings**  $\mathcal{H}_{i,n}^+$  and  $\mathcal{H}_{i,n}^-$ .  $\mathcal{H}_{2,2}^-$  is above and  $\mathcal{H}_{1,2}^+$  is below.

An upper diagram can be thought of as a middle diagram with  $m = 0$ .

The  $\beta$ -circles induce an equivalence relation  $M^\parallel$  on the components of  $\partial\Sigma_0$ .

We should say a word about orientation conventions in pictures such as Figure 10. According to our conventions from [20], the Heegaard surface is oriented as the boundary of the  $\alpha$ -handlebody. Thus, the Heegaard diagram in picture in Figure 10 is oriented opposite to the orientation it inherits as the boundary of a neighborhood of the crossing apparent in the figure.

**2.6. Gluing middle diagrams to upper diagrams.** Let  $\mathcal{H}_1^\wedge$  be an upper diagram with  $2m$  outgoing boundary components, and  $\mathcal{H}^\parallel$  a middle diagram with  $2m$  incoming boundary components and  $2n$  outgoing ones. Combine the equivalence relation  $M(\mathcal{H}_1^\wedge)$  with the equivalence relation  $M(\mathcal{H}^\parallel)$  to obtain an equivalence

relation on all the boundary components of  $\mathcal{H}^\parallel$ . If every equivalence class contains an outgoing boundary component (of  $\mathcal{H}^\parallel$ ), then we say that  $\mathcal{H}_1^\wedge$  and  $\mathcal{H}^\parallel$  are *compatible*.

If  $\mathcal{H}_1^\wedge$  and  $\mathcal{H}^\parallel$  are compatible, we can glue the boundary of  $\mathcal{H}_1^\wedge$  to the incoming boundary of  $\mathcal{H}^\parallel$  to form a new upper diagram  $\mathcal{H}_2^\wedge = \mathcal{H}_1^\wedge \# \mathcal{H}^\parallel$ . Note that  $M(\mathcal{H}_2^\wedge)$  is the matching on  $\{1, \dots, 2n\}$ , thought of as labelling the outgoing boundary components of  $\mathcal{H}^\parallel$  induced by restricting  $M(\mathcal{H}_1^\wedge) \cup M(\mathcal{H}^\parallel)$  to the outgoing boundary of  $\mathcal{H}^\parallel$ . Each upper state on  $\mathcal{H}_2^\wedge$  can be restricted to give an upper state on  $\mathcal{H}_1^\wedge$  and a middle state in  $\mathcal{H}^\parallel$ . By Equation (2.1), for any middle state obtained in this manner,  $|\check{\alpha}(\mathbf{x})| = m$ .

We say that two upper diagrams  $\mathcal{H}_1^\wedge$  and  $\mathcal{H}_2^\wedge$  are *equivalent* if we can obtain  $\mathcal{H}_2^\wedge$  from  $\mathcal{H}_1^\wedge$  by isotopies, handle slides, and stabilizations/destabilizations. Handleslides here involve two  $\beta$  circles, two  $\alpha$  circles, or an  $\alpha$ -arc slid over an  $\alpha$ -circle.

Observe that if  $\mathcal{H}^\natural$  is the standard diagram for the identity with  $2n$  outgoing boundary components, then for  $\mathcal{H}_2^\wedge = \mathcal{H}_1^\wedge \# \mathcal{H}^\natural$ , we can slide each new outgoing  $\alpha$ -arc over its corresponding newly-formed  $\alpha$ -circle, and then destabilize that  $2n-1$  new  $\beta$ -circles with their newly-formed  $\alpha$ -circles, to get back the original Heegaard diagram  $\mathcal{H}_1^\wedge$ ; i.e.  $\mathcal{H}_1^\wedge$  and  $\mathcal{H}_2^\wedge$  are equivalent.

**2.7. The Heegaard diagram of a knot projection.** Fix the sphere with four boundary circles, and four  $\alpha$ -arcs connecting them in a circular configuration. Equip with a further  $\beta$ -circle. When the  $\beta$ -circle meets each of the four arcs exactly once, we can think of the configuration as specifying a crossing, where the type of the crossing depends on how the  $\beta$ -circle meets the  $\alpha$ -arcs. We denote the two diagrams  $H_+$  and  $H_-$ ; see Figure 11. (As in the case of  $\mathcal{H}^+$  and  $\mathcal{H}^-$ , the sign of the crossing using the usual conventions from knot theory agrees with the sign of  $H_\pm$  when both strands are oriented upwards.)

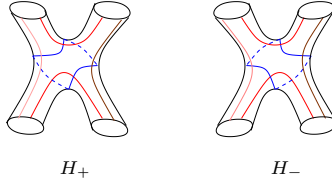


FIGURE 11. Crossing pieces.

We can glue  $H_+$  or  $H_-$  to two consecutive output circles  $Z_i$  and  $Z_{i+1}$  in an upper diagram  $\mathcal{H}_1^\wedge$  to get new upper diagrams  $\mathcal{H}_1^\wedge \cup_i H_+$  or  $\mathcal{H}_1^\wedge \cup_i H_-$ . These diagrams are easily seen to be equivalent to the diagram obtained by gluing  $\mathcal{H}_1^\wedge$  to the middle diagrams  $\mathcal{H}_{+,i}^\parallel$  and  $\mathcal{H}_{-,i}^\parallel$ .

We can relate this construction with the action of the mapping class group on the upper diagram discussed in Section 2.4.

Let  $\tau_{i,+}$  be the half twist whose square is a positive Dehn twist around a curve that encircles  $Z_i$  and  $Z_{i+1}$ . We have seen that  $\mathcal{H}^\wedge \cup_i H_+$  is equivalent to  $\mathcal{H}^\wedge \cup \mathcal{H}_{+,i}^\parallel$ . We claim these two diagrams are in turn equivalent to  $\tau_{i,+}(\mathcal{H}^\wedge)$ . This can be

seen by applying three handleslides to  $\mathcal{H}^\wedge \cup_i H_+$ , so that the newly-formed  $\alpha$ -circle and the  $\beta$ -circle supported in  $H_+$  meet in a single point. Destabilizing the resulting diagram, we obtain a new diagram which is diffeomorphic to  $\tau_{i,+}(\mathcal{H}^\wedge)$ ; see Figure 12. An analogous computation shows the equivalence between  $\mathcal{H}^\wedge \# \mathcal{H}_{i,n}^-$  and  $\tau_{i,-}(\mathcal{H}^\wedge)$ .

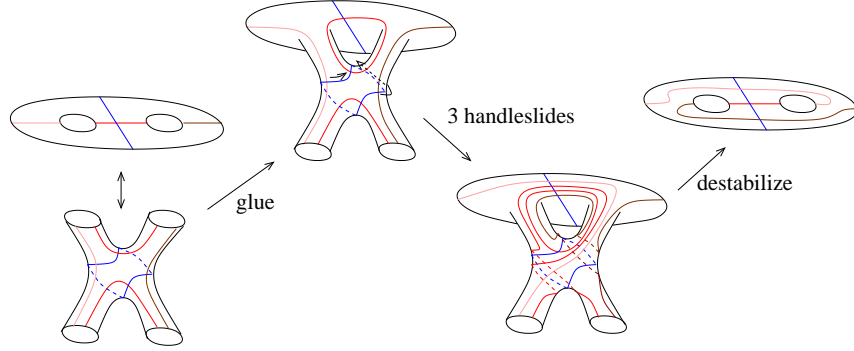


FIGURE 12. **Attaching  $H_+$  is equivalent to acting on a diagram by a half twist.** At the left, we have a portion of an upper diagram (with two consecutive boundary components separated by an arc; in general, they are separated by a collection of parallel arcs), which is glued to  $H_+$ . Performing three handleslides (the first two of which are indicated) and destabilizing is diffeomorphic to the original upper diagram and acting on its  $\alpha$ -curves by a half twist.

Suppose that  $K$  is a knot projection all of whose local maxima are global maxima, and whose local minima are global minima. The crossings correspond to the factorization of some mapping class  $\phi$  as a product of half twists. From the above discussion, it is clear that the Heegaard diagram of the knot projection is equivalent to the Heegaard diagram obtained by gluing the standard upper and lower diagrams  $\mathcal{H}^\wedge(n)$  and  $\mathcal{H}^\vee(n)$ , twisted by  $\phi$ ; i.e.  $\phi(\mathcal{H}^\wedge(n)) \# \mathcal{H}^\vee(n)$ .

### 3. ALGEBRA

We recall the algebraic preliminaries used in this paper, starting in Section 3.1 with an algebraic framework familiar from bordered Floer homology [10], applied to the case of algebras with curvature. In Subsection 3.2, we recall the bordered algebras from [21] and [22], and explain how to fit them into this framework.

**3.1. Algebraic framework.** For the purposes of the present paper, we find it convenient to work with smaller algebras than those from [22], but equipped with further algebraic structure, in the form of a *curvature* element. Such curved algebras have long played a role in Floer homology; see for example [4]. They have also played a role in categorified knot invariants; see for example [5]. Using curved algebras allows us to work with somewhat smaller algebras, and the curve counting involves fewer types of pseudo-holomorphic curves; see also [7].

The following is a straightforward adaptation of the algebraic material familiar in bordered Floer homology (see especially [10, Chapter 2] and [9, Chapter 2]) to the curved setting.

Fix a ground ring  $R$ . A *curved algebra* is a graded  $R$ -bimodule  $B$ , equipped with an associative multiplication

$$\mu_2: B \otimes_R B \rightarrow B$$

(with unit) and a preferred central element  $\mu_0 \in B$ . We denote the triple  $(B, \mu_0, \mu_2)$  by  $\mathcal{B}^\star$ .

A *curved module* over  $\mathcal{B}^\star$  is a right  $R$ -module  $M$ , equipped with right module maps  $m_1: M \rightarrow M$  and  $m_2: M \otimes_R B \rightarrow M$  satisfying the structure relations

$$(3.1) \quad m_1 \circ m_1 + m_2 \circ (\text{Id}_M \otimes \mu_0) = 0$$

$$(3.2) \quad m_1 \circ m_2 + m_2 \circ (m_1 \otimes \text{Id}_B) = 0$$

$$(3.3) \quad m_2 \circ (m_2 \otimes \text{Id}_B) = m_2 \circ (\text{Id}_M \otimes \mu_2)$$

This has a generalization to the  $\mathcal{A}_\infty$  context, as follows. A (curved)  $\mathcal{A}_\infty$  module  $M_{\mathcal{B}^\star}$  consists of a right  $R$ -module  $M$ , equipped with right  $R$ -module homomorphisms

$$m_i: M \otimes_R \overbrace{B \otimes_R \cdots \otimes_R B}^{i-1} \rightarrow B,$$

satisfying a sequence of  $\mathcal{A}_\infty$  relations, indexed by an integer  $k \geq 0$ , an element  $x \in M$ , and a (possibly empty) sequence  $b_1, \dots, b_k$  of algebra elements:

$$\begin{aligned} 0 = & \sum_{j=0}^k m_{k-j+1}(m_{j+1}(x, b_1, \dots, b_j), b_{j+1}, \dots, b_k) \\ & + \sum_{i=1}^{k-1} m_k(x, b_1, \dots, b_{i-1}, \mu_2(b_i, b_{i+1}), b_{i+2}, \dots, b_k) \\ & + \sum_{i=1}^{k+1} m_{k+2}(x, b_1, \dots, b_{i-1}, \mu_0, b_i, \dots, b_k). \end{aligned}$$

For example, when  $k = 0$ , the above relation gives Equation (3.1).

A (curved) type  $D$  structure is a left  $R$ -module  $X$  equipped with a left  $R$ -module homomorphism  $\delta^1: X \rightarrow B \otimes_R X$ , satisfying the structure relation

$$0 = \mu_0 \otimes \text{Id}_X + (\mu_2 \otimes \text{Id}_X) \circ (\text{Id}_B \otimes \delta^1) \circ \delta^1,$$

thought of as maps  $X \rightarrow B \otimes_R X$ . We will denote this data by  ${}^{\mathcal{B}^*}X$ . (This notion is equivalent to the notion of the *matrix factorizations* considered in [5].)

The definition of the tensor product  $M_{{}^{\mathcal{B}^*}} \boxtimes {}^{\mathcal{B}^*}X$  is the same as in the uncurved context. The verification that this is a chain complex is the same as in the uncurved case (see for example [10, Section 2.4]), except that the curved type  $D$  structure relations give rise to extra terms which are cancelled by the extra terms in the curved  $\mathcal{A}_\infty$  relation.

Bimodules also can be generalized to the curved case in a straightforward way. For example, let  $(B_1, \mu_0^{B_1})$  and  $(B_2, \mu_0^{B_2})$  be two curved algebras over ground rings  $R_1$  and  $R_2$  respectively. A curved type  $DA$  bimodule is a  $R_2$ - $R_1$ -bimodule  $X$ , equipped with operations

$$\delta_{\ell+1}^1: X \otimes_{R_1} \overbrace{B_1 \otimes_{R_1} \cdots \otimes_{R_1} B_1}^{\ell} \rightarrow B_2 \otimes_{R_2} X,$$

satisfying the structural relations for any  $x \in X$ ,

$$(3.4) \quad 0 = (\mu_2^{B_2} \otimes \text{Id}_X) \circ (\text{Id}_{B_2} \otimes \delta_1^1) \circ \delta_1^1(x) + \delta_2^1(x, \mu_0^{B_1}) + \mu_0^{B_2} \otimes x;$$

and, for each sequence  $b_1, \dots, b_k$  in  $B_1$  (with  $k \geq 1$ ),

$$(3.5) \quad \begin{aligned} 0 = & \sum_{j=0}^k \mu_2^{B_2} \circ (\text{Id} \otimes \delta_{k-j+1}^1) \circ (\delta_{j+1}^1(x, b_1, \dots, b_j), b_{j+1}, \dots, b_k) \\ & + \sum_{i=1}^{k-1} \delta_k^1(x, b_1, \dots, b_{i-1}, \mu_2^{B_1}(b_i, b_{i+1}), b_{i+2}, \dots, b_k) \\ & + \sum_{i=1}^{k+1} \delta_{k+2}^1(x, b_1, \dots, b_{i-1}, \mu_0^{B_1}, b_i, \dots, b_k). \end{aligned}$$

(Compare [9] in the uncurved case.) Note that the curvature on  $B_2$  appears in Equation (3.4), but not Equation (3.5).

**Example 3.1.** Fix curved algebras  $(B_1, \mu_0^{B_1})$  and  $(B_2, \mu_0^{B_2})$  over  $R$ , and suppose that  $\phi: B_1 \rightarrow B_2$  is an  $R$ -algebra homomorphism with the property that  $\phi(\mu_0^{B_1}) = \mu_0^{B_2}$ . Then  $\phi$  induces a type  $DA$  bimodule  ${}^{B_2}[\phi]_{B_1}$ , whose underlying  $R$ -bimodule is isomorphic to  ${}_R R_R$ , and whose operations are specified by  $\delta_2^1(x, b) = \phi(b) \otimes x$  (where  $x$  corresponds to  $\mathbf{1} \in {}_R R_R$ ) and  $\delta_k^1 \equiv 0$  for  $k \neq 2$ .

The above notions have obvious generalizations to the case where  $B$  is a differential graded algebra, i.e. it is equipped with a differential  $\mu_1$  (which satisfies a Leibniz rule) so that  $\mu_1(\mu_0) = 0$ .

In practice, we will often have another DGA  $\mathcal{A}''$  over  $R$ , and will consider various bimodules over  $\mathcal{B}^*$  and  $\mathcal{A}''$ . For example, thinking of  $\mathcal{A}'' \otimes \mathcal{B}^*$  as curved, with curvature  $\mathbf{1} \otimes \mu_0$ , we define a type  $DD$  bimodule  $X$  over  $\mathcal{A}''$  and  $\mathcal{B}^*$  to be a curved type  $D$  structure over  $\mathcal{A}'' \otimes \mathcal{B}^*$ .

**3.2. The bordered algebras.** In [21], to each pair of integers  $(m, k)$  with  $0 \leq k \leq m+1$ , we associated an algebra  $\mathcal{B}(m, k)$ . We recall the construction presently.

$\mathcal{B}(m, k)$  is constructed as the quotient of a larger algebra,  $\mathcal{B}_0(m, k)$ , associated to  $(m, k)$ . The base ring of  $\mathcal{B}_0(m, k)$  is the polynomial algebra  $\mathbb{F}[U_1, \dots, U_m]$ . Idempotents correspond to  $k$ -element subsets  $\mathbf{x}$  of  $\{0, \dots, m\}$  called *idempotent states*. We think of these as generators of a ring of idempotents  $I(m, k)$ .

Given idempotent states  $\mathbf{x}, \mathbf{y}$ , the  $\mathbb{F}[U_1, \dots, U_m]$ -module  $\mathbf{I}_{\mathbf{x}} \cdot \mathcal{B}_0(m, k) \cdot \mathbf{I}_{\mathbf{y}}$  is identified with  $\mathbb{F}[U_1, \dots, U_m]$ , given with a preferred generator  $\gamma_{\mathbf{x}, \mathbf{y}}$ . To specify the product, we proceed as follows. Each idempotent state  $\mathbf{x}$  has a *weight vector*  $v^{\mathbf{x}} \in \mathbb{Z}^m$ , with components  $i = 1, \dots, m$  given by  $v_i^{\mathbf{x}} = \#\{x \in \mathbf{x} \mid x \geq i\}$ . The multiplication is specified by

$$\gamma_{\mathbf{x}, \mathbf{y}} \cdot \gamma_{\mathbf{y}, \mathbf{z}} = U_1^{n_1} \cdots U_m^{n_m} \cdot \gamma_{\mathbf{x}, \mathbf{z}},$$

where

$$n_i = \frac{1}{2}(|v_i^{\mathbf{x}} - v_i^{\mathbf{y}}| + |v_i^{\mathbf{y}} - v_i^{\mathbf{z}}| - |v_i^{\mathbf{x}} - v_i^{\mathbf{z}}|).$$

For  $i = 1, \dots, m$ , let  $L_i$  be the sum of  $\gamma_{\mathbf{x}, \mathbf{y}}$ , taken over all pairs of idempotent states  $\mathbf{x}, \mathbf{y}$  so that there is some integer  $s$  with  $x_s = i$  and  $y_s = i-1$  and  $x_t = y_t$  for all  $t \neq s$ . Similarly, let  $R_i$  denote the sum of all the  $\gamma_{\mathbf{y}, \mathbf{x}}$  taken over the same pairs of idempotent states as above.

Under the identification  $\mathbf{I}_{\mathbf{x}} \cdot \mathcal{B}_0(m, k) \cdot \mathbf{I}_{\mathbf{y}} \cong \mathbb{F}[U_1, \dots, U_m]$ , the elements that correspond to monomials in the  $U_1, \dots, U_m$  are called *pure algebra elements in  $\mathcal{B}_0(m, k)$* . These elements are specified by their idempotents  $\mathbf{x}$  and  $\mathbf{y}$ , and their *relative weight vector*  $w(b) \in \mathbb{Q}^m$ , which in turn is uniquely characterized by

$$\omega_i(\gamma_{\mathbf{x}, \mathbf{y}}) = \frac{1}{2}|v_i^{\mathbf{x}} - v_i^{\mathbf{y}}| \quad \omega_i(U_j \cdot b) = \omega_i(b) + \begin{cases} 0 & \text{if } i \neq j \\ 1 & \text{if } i = j. \end{cases}$$

Let  $\mathcal{G} \subset \mathcal{B}_0(m, k)$  be the two-sided ideal generated by  $L_{i+1} \cdot L_i$ ,  $R_i \cdot R_{i+1}$  and, for all choices of  $\mathbf{x} = \{x_1, \dots, x_k\}$  with  $\mathbf{x} \cap \{j-1, j\} = \emptyset$ , the element  $\mathbf{I}_{\mathbf{x}} \cdot U_j$ . Then,

$$\mathcal{B}(m, k) = \mathcal{B}_0(m, k) / \mathcal{G}.$$

The pure algebra elements in  $\mathcal{B}(m, k)$  are those elements that are images of pure algebra elements in  $\mathcal{B}_0(m, k)$  under the above quotient map.

Idempotents  $\mathbf{x} = x_1 < \dots < x_k$  and  $\mathbf{y} = y_1 < \dots < y_k$  are said to be *too far* if for some  $t \in \{1, \dots, k\}$ ,  $|x_t - y_t| \geq 2$ . If  $\mathbf{x}$  and  $\mathbf{y}$  are too far, then  $\mathbf{I}_{\mathbf{x}} \cdot \mathcal{B}_0(m, k) \cdot \mathbf{I}_{\mathbf{y}} \in \mathcal{G}$ ; i.e.  $\mathbf{I}_{\mathbf{x}} \cdot \mathcal{B}(m, k) \cdot \mathbf{I}_{\mathbf{y}} = 0$ .

We restate here the concrete description of the ideal  $\mathcal{G}$  given in [21]:

**Proposition 3.2.** [21, Proposition 3.7] *Suppose that  $b = \mathbf{I}_{\mathbf{x}} \cdot b \cdot \mathbf{I}_{\mathbf{y}}$  is a pure algebra element in  $\mathcal{G}$ . Then, either  $\mathbf{x}$  and  $\mathbf{y}$  are too far, or there is a pair of integers  $i < j$  so that*

- $i, j \in \{0, \dots, m\} \setminus \mathbf{x} \cap \mathbf{y}$
- for all  $i < t < j$ ,  $t \in \mathbf{x} \cap \mathbf{y}$
- $\omega_t(b) \geq 1$  for all  $t = i+1, \dots, j$
- $\#\{x \in \mathbf{x} \mid x \leq i\} = \#\{y \in \mathbf{y} \mid y \leq i\}$ .



We specialize to the case of  $\mathcal{B}(n) = \mathcal{B}(2n, n)$ , which we think of as an algebra over the idempotent ring  $I(n) = I(2n, n)$ .

We will typically consider a subalgebra  $\mathcal{C}(n) \subset \mathcal{B}(2n, n)$  given by

$$\mathcal{C}(n) = \left( \sum_{\{\mathbf{x} | \mathbf{x} \cap \{0, 2n\} = \emptyset\}} \mathbf{I}_{\mathbf{x}} \right) \cdot \mathcal{B}(2n, n) \cdot \left( \sum_{\{\mathbf{x} | \mathbf{x} \cap \{0, 2n\} = \emptyset\}} \mathbf{I}_{\mathbf{x}} \right).$$

In particular, the elements  $L_1, R_1, L_{2n}, R_{2n}$  are not in this subalgebra; but  $U_1$  and  $U_{2n}$  are. Let  $I_0(n) \subset \mathcal{C}(n)$  denote the subring spanned by the idempotents  $\mathbf{I}_{\mathbf{x}}$  where  $\mathbf{x} \cap \{0, 2n\} = \emptyset$ . Thus,

$$\mathcal{C}(n) = I_0(n) \cdot \mathcal{B}(n) \cdot I_0(n).$$

Sometimes, we also consider

$$\mathcal{C}_0(n) = I_0(n) \cdot \mathcal{B}_0(n) \cdot I_0(n).$$

A *matching* is a partition of  $\{1, \dots, 2n\}$  into 2-element subsets. The matching  $M$  specifies a central algebra element in  $\mathcal{B}(n)$ ,

$$(3.6) \quad \mu_0^M = \sum_{\{i, j\} \in M} U_i U_j,$$

which we think of as specifying a curvature for  $\mathcal{B}^*(n) = (\mathcal{B}(n), \mu_0^M)$  or for

$$(3.7) \quad \mathcal{C}^*(n) = (\mathcal{C}(n), \mu_0^M).$$

We compare this with the algebraic set-up from [22]. In that paper, we defined an algebra  $\mathcal{A}(n, M)$  containing  $\mathcal{B}(n)$ , with new variables  $C_{i, j}$  for each  $\{i, j\} \in M$  satisfying  $dC_{i, j} = U_i U_j$  and  $C_{i, j}^2 = 0$ .

**Definition 3.3.** *The  $\mathcal{B}$ -to- $\mathcal{A}$  transformer is the type DA bimodule  ${}^{\mathcal{A}}T_{\mathcal{B}^*}$  which, as a bimodule over  $I(2n, n)$ , is identified with  $I(2n, n)$ , and with operations specified by*

$$\begin{aligned} \delta_1^1(\mathbf{1}) &= \sum_{(i, j) \in M} C_{i, j} \otimes \mathbf{1} \\ \delta_2^1(\mathbf{1}, b) &= b \otimes \mathbf{1} \\ \delta_\ell^1(\mathbf{1}, b_1, \dots, b_{\ell-1}) &= 0 \quad \text{for } \ell > 2. \end{aligned}$$

Thus, a curved type  $D$  structure over  $\mathcal{B}^*$  naturally gives rise to a type  $D$  structure over  $\mathcal{A}(n, M)$ ,  ${}^{\mathcal{B}^*}X \rightarrow {}^{\mathcal{A}}T_{\mathcal{B}^*} \boxtimes {}^{\mathcal{B}^*}X$ .

**3.3. Gradings.** Our algebras are equipped with two types of gradings: an Alexander grading, with values in some Abelian group, which is preserved by the algebra operations; and a homological grading, with values in  $\mathbb{Z}$ , so that  $\mu_i$  shifts by  $i - 2$  (and in particular, the element  $\mu_0$  has Alexander grading zero and homological grading  $-2$ ).

The weight function induces a grading on the algebra  $\mathcal{B}(n)$  with values in  $(\frac{1}{2}\mathbb{Z})^{2n} \subset \mathbb{Q}^{2n}$ . Choose for each  $\{i, j\} \in M$  a preferred ordering  $(i, j)$  of the integers  $i$  and  $j$ . There is an induced *Alexander vector*  $\mathbf{A}: M \rightarrow \mathbb{Q}$  defined by

$$(3.8) \quad \mathbf{A}_{\{i, j\}}(a) = \omega_i(a) - \omega_j(a),$$

where  $(i, j)$  is the ordering on  $\{i, j\}$ . Of course, this can be thought of as a grading with values in  $\mathbb{Q}^n$ . Since  $\mathbf{A}(\mu_0) = 0$ , the Alexander function induces a well-defined (Alexander-type)  $\mathbb{Q}^n$ -grading on the curved algebra  $\mathcal{B}^\star$ . Furthermore, there is an induced  $\mathbb{Q}$ -valued Alexander grading specified by the function on homogeneous algebra elements  $A = \sum_{\{i,j\} \in M} \mathbf{A}_{\{i,j\}}$ .

Sometimes, when we wish to distinguish this from Alexander gradings on modules, we write  $\mathbf{A}^M$ .

More abstractly, we can think of the matching as giving rise to a one-manifold  $W = W(M)$ , consisting of  $n$  arcs and boundary the points  $Y$  in  $\{1, \dots, 2n\}$  (i.e. each pair  $\{i, j\} \in M$  determines an arc connecting  $i$  and  $j$ ). The weight of a given algebra element gives an element of  $H^0(Y)$ ; and the Alexander grading can be thought of as an element of the cokernel  $H^0(W) \rightarrow H^0(Y)$ , which is identified with  $H^1(W, \partial W) \cong \mathbb{Q}^n$ . A choice of isomorphism above is equivalent to an orientation on  $W$ .

We have also a homological  $\Delta$ -grading, determined by

$$(3.9) \quad \Delta(a) = - \sum_i \omega_i(a)$$

if  $a \in \mathcal{B}$ . Note that  $\Delta(\mu_0) = -2$ , as required.

**3.4. Adapted bimodules.** We follow the algebraic set-up from [22, Section 2] with slight modifications.

We can think of  $\mathcal{B}(n)$  as an algebra associated to the zero-manifold  $Y_2$ , which consists of  $2n$  points. A matching on  $Y_2$ , which we think of as a one-manifold  $W_2$  with  $\partial W_2 = Y_2$ , specifies a curvature  $\mu_0 \in \mathcal{B}(Y_2)$ . There is an induced grading on  $\mathbf{A}_{W_2}$  on  $\mathcal{B}(Y_2)$  by  $H^1(W_2, Y_2)$ , for which  $\mathbf{A}_{W_2}(\mu_0) = 0$ . Thus, we think of  $\mathcal{B}^\star(Y_2, W_2)$  as graded by  $\mathbf{A}_{W_2}$ .

Fix cobordism  $W_1$  from  $Y_2$  to  $Y_1$ , and let  $W = W_1 \cup_{Y_2} W_2$ . If  $X$  is a  $H^1(W_1, \partial W_1)$ -graded vector space, then  $X \otimes \mathcal{B}^\star(Y_2, W_2)$  inherits a grading by  $H^1(W, \partial W)$ , using the natural map

$$(3.10) \quad H^1(W_1, \partial W_1) \oplus H^1(W_2, \partial W_2) \rightarrow H^1(W, \partial W).$$

**Definition 3.4.** Suppose that  $\mathcal{B}_2^\star$  is an algebra graded by  $H^1(W_2, Y_2)$ . Fix a cobordism  $W_1: Y_2 \rightarrow Y_1$ . A curved type DA bimodule  ${}^{\mathcal{B}_1^\star}X_{\mathcal{B}_2^\star}$  is called adapted to  $W_1$  if it is equipped with the following additional data:

- a grading of  $X$  by  $H^1(W_1, \partial W_1)$ , satisfying the following compatibility condition: if  $a_1, \dots, a_{\ell-1}$  are  $H^2(W_2, \partial W_2)$ -homogeneous elements, and  $\mathbf{x}$  is an  $H^1(W_1, \partial W_1)$ -homogeneous element, then  $\delta_\ell^1(\mathbf{x}, a_1, \dots, a_{\ell-1})$  is  $H^1(W, \partial W)$ -homogeneous, where  $W = W_1 \cup W_2$ , with grading given by

$$\mathbf{gr}(x) + \mathbf{A}(a_1) + \dots + \mathbf{A}(a_\ell),$$

viewed as an element of  $H^1(W, \partial W)$  using the Mayer-Vietoris maps from Equation (3.10).

- a grading of  $X$  by  $\mathbb{Q}$ , so that if  $\mathbf{x}, a_1, \dots, a_{\ell-1}$  are homogeneous, then  $\delta_\ell^1(\mathbf{x}, a_1, \dots, a_{\ell-1})$  is homogeneous of degree

$$\Delta_X(\mathbf{x}) + \Delta(a_1) + \dots + \Delta(a_{\ell-1}) - \ell + 2.$$

- $X$  is a finite-dimensional  $\mathbb{F}$ -vector space.

By contrast, recall that the adapted bimodules in the uncurved case ([22, Section 2]) were graded by  $H^1(W_1, \partial)$ , rather than  $H^1(W_1 \cup W_2, \partial)$ . This causes no additional difficulties. In particular, we have the following straightforward modification of [21, Proposition 3.19]:

**Proposition 3.5.** *Let  $W_3$  be an oriented one-manifold with  $Y_3 = \partial W_3$ . Fix also  $W_2: Y_3 \rightarrow Y_2$  and  $W_1: Y_2 \rightarrow Y_1$ . If  $\mathcal{B}_2^* Y_{\mathcal{B}_3^*}$  is adapted to  $W_2$  and  $\mathcal{B}_1^* X_{\mathcal{B}_2^*}$  is adapted to  $W_1$ , and  $W_1 \cup W_2$  has no closed components; then we can form their tensor product  $\mathcal{B}_1^* X_{\mathcal{B}_2^*} \boxtimes^{\mathcal{B}_2^*} Y_{\mathcal{B}_3^*}$  to get a curved DA bimodule  $\mathcal{B}_1^*(X \boxtimes Y)_{\mathcal{B}_3^*}$  adapted to  $W_1 \cup W_2$ .  $\square$*

## 4. GRADINGS ON UPPER HEEGAARD STATES

Throughout this section, we will fix an upper diagram  $\mathcal{H}^\wedge$  with  $2n$  boundary circles

$$\mathcal{H}^\wedge = (\Sigma_0, Z_1, \dots, Z_{2n}, \{\alpha_1, \dots, \alpha_{2n-1}\}, \{\alpha_1^c, \dots, \alpha_g^c\}, \{\beta_1, \dots, \beta_{g+n-1}\})$$

throughout. Let  $M$  be the matching on  $\{1, \dots, 2n\}$  induced by  $\mathcal{H}^\wedge$ .

In Section 6, we will explain how to associate a type  $D$  structure to  $\mathcal{H}^\wedge$ , over the curved algebra  $C^\star$  from Equation (3.7). This structure has a differential, which is defined by counting pseudo-holomorphic curves. Here, we explain the data needed to specify gradings on these structures.

**4.1. Preliminaries: filling in the Heegaard surface.** Before proceeding to the main material in this section, we introduce some notation which will be used throughout the paper.

Recall that the Heegaard surface  $\Sigma_0$  for  $\mathcal{H}^\wedge$  is an oriented, connected two-manifold of genus  $g$  with boundary  $\partial\Sigma_0 = Z = Z_1 \cup \dots \cup Z_{2n}$ . By attaching infinite cylinders  $Z \times [0, \infty)$  to  $\Sigma_0$ , we obtain an oriented two-manifold  $\Sigma$  with punctures  $p_1, \dots, p_{2n}$ . Filling in these punctures, we obtain a compact surface, denoted  $\overline{\Sigma}$ .

Extend  $\alpha$  in  $\Sigma$ , by attaching two rays in each cylinder  $Z_i \times [0, \infty)$  for  $i = 2, \dots, 2n-1$  and a single ray inside each of  $Z_1 \times [0, \infty)$  and  $Z_{2n} \times [0, \infty)$ . In the filled surface  $\overline{\Sigma}$  the union of  $\alpha$ -arcs completes to form a single closed interval. Let  $\overline{\alpha} \subset \overline{\Sigma}$  denote the subspace which is the union of the above defined interval and the union of curves  $\{\alpha_i^c\}_{i=1}^g$ .

**4.2. Gradings.** To each upper Heegaard state  $\mathbf{x}$  for  $\mathcal{H}^\wedge$ , there is an associated idempotent in  $I_0(n)$  (the ring generated by the idempotent states in  $\mathcal{C}(n) \subset \mathcal{B}(n)$ ), defined by the formula

$$\widehat{\mathbf{I}}(\mathbf{x}) = \mathbf{I}_{\{1, \dots, 2n-1\} \setminus \alpha(\mathbf{x})},$$

where  $\alpha(\mathbf{x})$  is defined as in Definition 2.2.

The complement of  $\overline{\alpha} \cup \beta$  inside  $\overline{\Sigma}$  can be written as a disjoint union of connected open sets called *elementary domains*.

**Definition 4.1.** *Given upper states  $\mathbf{x}$  and  $\mathbf{y}$ , a two-chain from  $\mathbf{x}$  to  $\mathbf{y}$  is a formal integral combination  $\phi$  of the elementary domains in  $\overline{\Sigma}$ , with the following property. If  $\partial_\alpha(\phi)$  resp.  $\partial_\beta(\phi)$  denotes the portion of the boundary of  $\phi$  contained in  $\alpha$  resp.  $\beta$ , we require that  $\partial(\partial_\alpha(\phi)) = \mathbf{y} - \mathbf{x}$  (and hence  $\partial(\partial_\beta(\phi)) = \mathbf{x} - \mathbf{y}$ ). Let  $\mathcal{D}(\mathbf{x}, \mathbf{y})$  denote the space of two-chains from  $\mathbf{x}$  to  $\mathbf{y}$ .*

Given  $\phi \in \mathcal{D}(\mathbf{x}, \mathbf{y})$  and  $\psi \in \mathcal{D}(\mathbf{y}, \mathbf{z})$ , their sum can be viewed as an element  $\phi * \psi \in \mathcal{D}(\mathbf{x}, \mathbf{z})$ .

**Definition 4.2.** *Let  $\phi \in \mathcal{D}(\mathbf{x}, \mathbf{y})$ . Define  $b_0(\phi)$  to be the element  $b \in \mathcal{B}_0(2n, n)$  characterized by the following two properties that*

- $\widehat{\mathbf{I}}(\mathbf{x}) \cdot b \cdot \widehat{\mathbf{I}}(\mathbf{y}) = b$ ; and
- for all  $i = 1, \dots, 2n$ ,  $\mathfrak{w}_i(b)$  is the average of the local multiplicities of  $\phi$  in the two elementary domains adjacent to  $Z_i$ .

We will also write  $\mathbf{w}(b) = \sum_{i=1}^{2n} \mathbf{w}_i(b)$ .

**Lemma 4.3.**  $b_0(\phi * \psi) = b_0(\phi) \cdot b_0(\psi)$ , where the right hand side is multiplication in  $\mathcal{B}_0(2n, n)$ .

**Proof.** This is clear from the additivity of the local multiplicities under juxtaposition.  $\square$

Each elementary domain  $\mathcal{D}_i$  in  $\overline{\Sigma}$  has an *Euler measure*, which is the integral of  $1/2\pi$  times the curvature of a metric for which the boundary consists of geodesics meeting at  $90^\circ$  angles along the corners.

For  $\phi \in \mathcal{D}(\mathbf{x}, \mathbf{y})$ , we define its *point measure*  $P(\phi)$  to be the sum  $n_{\mathbf{x}}(\phi) + n_{\mathbf{y}}(\phi)$ , so that each elementary domain  $\mathcal{D}$  contributes  $1/4$  times the number of components of  $\mathbf{x}$  and  $\mathbf{y}$  contained as corners of  $\mathcal{D}$ . The *Maslov grading* of  $\phi$  is defined by the formula:

$$(4.1) \quad \mathbf{m}(\phi) = e(\phi) + P(\phi).$$

**Lemma 4.4.** If  $\mathcal{D}(\mathbf{x}, \mathbf{y})$  is non-empty, then for any  $\phi \in \mathcal{D}(\mathbf{x}, \mathbf{y})$ , the integers  $\mathbf{m}(\phi) - \mathbf{w}(b_0(\phi))$  and  $\mathbf{w}_i(\phi) - \mathbf{w}_j(\phi)$  (with  $\{i, j\} \in M$ ) are independent of the choice of  $\phi$ .

**Proof.** Before verifying the independence of the choice of  $\phi$ , we start by verifying that  $\mathbf{m}(\phi)$ , which is evidently a rational number, is in fact an integer. This could be seen either by the interpretation of  $\mathbf{m}(\phi)$  as a Maslov index, but instead we recall here a more elementary argument. Since  $\mathbf{m}(\phi + \Sigma) = \mathbf{m}(\phi) + 2$ , it suffices to verify the integrality of  $\mathbf{m}(\phi)$  for positive  $\phi$ . If  $\phi$  is positive, it is elementary to construct a surface with corners  $F$  (cf. [20, Lemma 2.17]) at  $\mathbf{x}$  and  $\mathbf{y}$ ; this surface is equipped with a branched covering to  $\Sigma$  with branching at the intersection points of the  $\alpha$ - and the  $\beta$ -circles. Suppose for simplicity that each elementary domain is topologically a disk, so that the  $\alpha$  and  $\beta$ -arcs and circles give  $\Sigma$  the structure of a *CW* complex. The surface  $F$  has a *CW* complex structure, obtained by pulling back this *CW* complex structure. Consider the function  $f$  on subcomplexes of  $F$  that associates to each 2-cell 1, to each edge  $-1/2$ , and to each vertex  $1/4$ . Clearly,  $f(\mathcal{D}) = e(\mathcal{D})$  for each elementary domain. Moreover, since each interior edge is contained in two domains, and each interior vertex is contained in four elementary domains, it follows that

$$e(F) = \chi(F) + \frac{1}{2} \#(e \subset \partial F) + \sum_p \left( \frac{N_p}{4} - 1 \right) = \chi(F) + \sum_p \left( \frac{N_p - 2}{4} \right),$$

where  $N_p$  denotes the number of elementary domains that meet at a 0-cell in  $F$ . The integrality of  $\mathbf{m}(\phi)$  follows from the observation that at each corner point  $p$ ,  $\frac{N_p - 2}{4} + n_{p \cap \mathbf{x}}(\phi) + n_{p \cap \mathbf{y}}(\phi)$  is an integer. This argument can be easily adapted also to the case where the elementary domains are not disks.

If  $\phi, \phi' \in \mathcal{D}(\mathbf{x}, \mathbf{y})$  then  $\phi - \phi'$  can be written as a formal sum of components  $\mathcal{D}$  of  $\overline{\Sigma} \setminus \mathcal{B}$ . This is true since  $\alpha_1^c, \dots, \alpha_g^c$  are linearly independent in  $H_1(\overline{\Sigma})$  and the intersection of their span with the span of  $\beta_1, \dots, \beta_{g+n-1}$  is trivial (by Condition (UD-4)). Each of those latter components has  $e(\mathcal{D}) = 1$  and  $P(\mathcal{D}) = 1$ , contributing 2 to  $\mathbf{m}(\phi)$ ; similarly, the addition of  $\mathcal{D}$  contributes 2 to  $\mathbf{w}(b_0(\phi))$ .

To complete the lemma, note that if  $i$  and  $j$  are matched, then  $\mathbf{w}_i(\mathcal{D}) = \mathbf{w}_j(\mathcal{D})$  for any  $\mathcal{D}$  of  $\overline{\Sigma} \setminus \beta$ .  $\square$

Given  $\phi \in \mathcal{D}(\mathbf{x}, \mathbf{y})$ , let  $\hat{b}(\phi) \in \mathbf{I}_{\mathbf{x}} \cdot \mathcal{B} \cdot \mathbf{I}_{\mathbf{y}}$  denote the image of  $b_0(\phi)$  under the quotient map  $\mathcal{B}_0(n) \rightarrow \mathcal{B}(n)$ . Clearly,  $\hat{b}(\phi) \in \mathcal{C}(n) \subset \mathcal{B}(n)$ .

**Proposition 4.5.** *There is a function  $\mathbf{m}: \mathfrak{S}(\mathcal{H}^\wedge) \rightarrow \mathbb{Z}$  that is uniquely characterized up to an overall constant by the property that*

$$(4.2) \quad \mathbf{m}(\mathbf{x}) - \mathbf{m}(\mathbf{y}) = \mathbf{m}(\phi) - \mathbf{w}(b_0(\phi)),$$

for any  $\phi \in \mathcal{D}(\mathbf{x}, \mathbf{y})$ . Similarly, given an orientation for the one-manifold  $W$  specified by the matching  $M(\mathcal{H}^\wedge)$ , there is another function  $\mathbf{A}: \mathfrak{S}(\mathcal{H}^\wedge) \rightarrow \frac{1}{2}\mathbb{Z}^n$  with components  $\mathbf{A}_{\{i,j\}}$  corresponding to each  $\{i,j\} \in M$ , characterized by the following condition, uniquely up to overall translation by some vector in  $\frac{1}{2}\mathbb{Z}^n \subset \mathbb{Q}^n$ :

$$(4.3) \quad \mathbf{A}_{\{i,j\}}(\mathbf{x}) - \mathbf{A}_{\{i,j\}}(\mathbf{y}) = \mathbf{w}_i(b_0(\phi)) - \mathbf{w}_j(b_0(\phi)),$$

for any choice of  $\phi \in \mathcal{D}(\mathbf{x}, \mathbf{y})$ ; i.e.  $\mathbf{A}(\mathbf{x}) - \mathbf{A}(\mathbf{y}) = \mathbf{A}(b_0(\phi))$ , where the right-hand-side uses the  $\mathbb{Q}^n$ -valued Alexander vector grading on the algebra.

**Proof.** Fix  $\mathbf{x}$  and  $\mathbf{y}$ . Condition (UD-5) ensures that for any two upper states  $\mathbf{x}$  and  $\mathbf{y}$ , there is some  $\phi \in \mathcal{D}(\mathbf{x}, \mathbf{y})$ . Thus, according to Lemma 4.4, given  $\mathbf{x}$  and  $\mathbf{y}$ , the right-hand-side of Equation (4.2) is well-defined. To see that it can be written as  $\mathbf{m}(\mathbf{x}) - \mathbf{m}(\mathbf{y})$ , it suffices to observe that the right hand side of Equation (4.2) is additive under juxtaposition. This is mostly straightforward; see [25, Theorem 3.3] for an elementary proof of the additivity of  $\mathbf{m}$  under juxtapositions.

The corresponding statement for  $\mathbf{A}$  follows similarly.  $\square$

**Remark 4.6.** We could have chosen to work instead with elementary domains  $\mathcal{D}_i^0$ , which are the closures of the components of  $\Sigma_0 \setminus \alpha \cup \beta$ . Clearly each elementary domain  $\mathcal{D}_i$  in  $\overline{\Sigma}$  is obtained from some elementary domain  $\mathcal{D}_i^0$  in  $\Sigma_0$  by attaching half disks to each boundary component of  $\mathcal{D}_i$  obtained as  $Z_j \cap \mathcal{D}_i$  with  $j \neq 1$  or  $2n$ ; and attaching disks along the boundary components  $Z_1 \cap \mathcal{D}_i$  and  $Z_{2n} \cap \mathcal{D}_i$ . Thus, the Euler measure of each elementary domain in  $\overline{\Sigma}$  equals the Euler measure of the corresponding domain in  $\Sigma_0$  plus  $1/2$  for each boundary component induced by  $Z_j$  with  $j \neq 1$  or  $2n$  and  $1$  for the boundary components coming from  $Z_1$  or  $Z_{2n}$ . We could work with  $\mathcal{D}_0(\mathbf{x}, \mathbf{y})$ , which are domains in  $\Sigma_0$ . The Euler measure on elementary domains can be extended linearly to obtain an Euler measure of any  $\phi_0 \in \mathcal{D}_0(\mathbf{x}, \mathbf{y})$ . If  $\phi_0 \in \mathcal{D}_0(\mathbf{x}, \mathbf{y})$ , and  $\phi \in \mathcal{D}(\mathbf{x}, \mathbf{y})$  is the corresponding domain in  $\overline{\Sigma}$ , then

$$e(\phi) = e(\phi_0) + \mathbf{w}(b_0(\phi)).$$

With these conventions, then, Lemma 4.4 says that and

$$\mathbf{m}(\phi) - \mathbf{w}(b_0(\phi)) = e(\phi_0) + P(\phi_0)$$

is independent of the choice of  $\phi_0 \in \mathcal{D}_0(\mathbf{x}, \mathbf{y})$ .

5. HOLOMORPHIC CURVES USED FOR TYPE  $D$  STRUCTURES

We will describe now the holomorphic curves that go into the construction of the type  $D$  structure associated to an upper diagram, returning to the type  $A$  structure in Section 7. The curves counted in the present work are similar to the curves counted in [10]. Since our context here is slightly different, we recall material from [10], with an emphasis on the differences.

Fix some upper diagram

$$\mathcal{H}^\wedge = (\Sigma_0, Z_1, \dots, Z_{2n}, \{\alpha_1, \dots, \alpha_{2n-1}\}, \{\alpha_1^c, \dots, \alpha_g^c\}, \{\beta_1, \dots, \beta_{g+n-1}\}).$$

Filling in the boundary of  $\Sigma_0$  as explained in Section 4.1, we get  $\Sigma_0 \subset \Sigma \subset \overline{\Sigma}$ .

We will use Lipshitz's reformulation of Heegaard Floer homology [6], where the pseudo-holomorphic curve counting takes place in  $\Sigma \times [0, 1] \times \mathbb{R}$ . To this end, we will use the class of almost-complex structures appearing there (see also [10, Definition 5.1]), which we recall presently.

There are two projection maps

$$\pi_\Sigma: \Sigma \times [0, 1] \times \mathbb{R} \rightarrow \Sigma \quad \text{and} \quad \pi_{\mathbb{D}}: \Sigma \times [0, 1] \times \mathbb{R} \rightarrow [0, 1] \times \mathbb{R}.$$

The last projection map  $\pi_{\mathbb{D}}$  can be further decomposed into its components

$$s: \Sigma \times [0, 1] \times \mathbb{R} \rightarrow [0, 1] \quad \text{and} \quad t: \Sigma \times [0, 1] \times \mathbb{R} \rightarrow \mathbb{R}.$$

**Definition 5.1.** *An almost complex structure  $J$  on  $\overline{\Sigma} \times [0, 1] \times \mathbb{R}$  is called admissible if*

- *The projection  $\pi_{\mathbb{D}}$  is  $J$ -holomorphic.*
- *$J$  preserves the subspace  $\ker(d_p \pi_\Sigma) \subset T_p(\Sigma \times [0, 1] \times \mathbb{R})$ .*
- *The  $\mathbb{R}$ -action is  $J$ -holomorphic.*
- *The complex structure is split in some  $\mathbb{R}$ -invariant neighborhood of*

$$\{p_1, \dots, p_{2n}\} \times [0, 1] \times \mathbb{R},$$

*where the  $p_i$  are the punctures.*

We will consider  $J$ -holomorphic curves

$$u: (S, \partial S) \rightarrow (\Sigma \times [0, 1] \times \mathbb{R}, (\alpha \times \{1\} \times \mathbb{R}) \cup (\beta \cup \{0\} \times \mathbb{R})),$$

with certain asymptotic conditions. To state those, we view  $\Sigma \times [0, 1] \times \mathbb{R}$  as having three kinds of infinities,  $\Sigma \times [0, 1] \times \{+\infty\}$ ,  $\Sigma \times [0, 1] \times \{-\infty\}$ , and  $\{p_i\} \times [0, 1] \times \mathbb{R}$ ; the first two of these are referred to as  $+\infty$  and  $-\infty$  respectively. Let

$$(5.1) \quad d = g + n - 1.$$

The asymptotics of the holomorphic curves we consider are as follows:

- At  $\pm\infty$ ,  $u$  is asymptotic to a  $d$ -tuple of chords of the form  $x_i \times [0, 1] \times \{\pm\infty\}$ , where  $\mathbf{x} = \{x_i\}_{i=1}^d$  is an upper Heegaard state.
- For boundary punctures  $p_i$ , at  $\{p_i\} \times [0, 1] \times \mathbb{R}$ , the curve  $u$  is asymptotic to a collection of Reeb chords  $\rho_i \times 1 \times t_i$ ; where  $\rho_i$  is a Reeb chord in  $\partial\Sigma_0 = Z_1 \cup \dots \cup Z_{2n}$  with endpoints on  $\mathbf{a} = \alpha \cap Z$ . These ends are called *east infinity* boundaries of  $u$ , and  $t_i$  is called its *height*.

- For interior punctures  $p_i$ , at  $\{p_i\} \times [0, 1] \times \mathbb{R}$ , the curve  $u$  is asymptotic to a collection of Reeb orbits  $\{o_i\} \times s_i \times t_i$  for  $0 < s_i < 1$ , where  $o_i$  is the simple Reeb orbit corresponding to the puncture  $p_i$ . These ends are called *middle infinity*, and the values  $t_i$  are also called their *height*.

We give the details in this section.

**5.1. Naming Reeb chords.** A Reeb chord is an arc  $\rho$  in some boundary component  $Z_i$ , with endpoints on the intersection points between  $Z_i$  and  $\alpha_{i-1} \cup \alpha_i$ . As such, it has an initial point  $\rho^-$  and a terminal point  $\rho^+$ .

When describing Reeb chords, we will use the following notation. Each circle boundary component  $Z_i$  with  $i = 2, \dots, 2n-1$  meets two  $\alpha$ -curves  $\alpha_{i-1}$  and  $\alpha_i$ , and so the boundary circle is divided into two Reeb chords. Label  $L_i$  the chord that goes from  $\alpha_{i-1}$  to  $\alpha_i$  with respect to the boundary orientation of the circle, and  $R_i$  the one which goes from  $\alpha_i$  to  $\alpha_{i-1}$ ; see Figure 13. All Reeb chords on  $Z_i$  can thus be represented as words in the  $L_i$  and  $R_i$  that alternate between the two letters. In particular, the two Reeb chords that cover the circle once can be written as  $L_i R_i$  and  $R_i L_i$ ; moreover,  $L_i R_i$  starts and ends at  $\alpha_{i-1}$  and  $R_i L_i$  starts and ends at  $\alpha_i$ .

The boundary component  $Z_1$  meets only one  $\alpha$ -arc,  $\alpha_1$ ; and hence all Reeb chords are multiples of the same Reeb chord from  $\alpha_1$  to itself. For consistency with the above, we label this basic Reeb chord, that covers  $Z_1$  once,  $R_1 L_1$  (although independently,  $R_1$  and  $L_1$  do not make sense); similarly, we label the Reeb chord that covers  $Z_{2n}$  once  $L_{2n} R_{2n}$ .

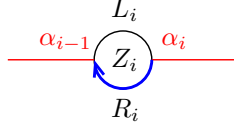


FIGURE 13. **Names of Reeb chords.** The Reeb chord  $R_i$  is indicated by the oriented half circle.

**5.2. Pre-flowlines.** We start with a more precise formulation of the asymptotic conditions for our holomorphic curves.

**Definition 5.2.** A decorated source  $\mathcal{S}$  is the following collection of data:

- (1) a smooth oriented surface  $S$  with boundary and punctures (some of which can be on the boundary)
- (2) a labeling of each boundary puncture of  $S$  by one of  $+$ ,  $-$ , or  $\mathbf{e}$
- (3) a labeling of each  $\mathbf{e}$  puncture on  $S$  by a Reeb chord
- (4) a labeling of each interior puncture by a Reeb orbit.

Let  $\mathbf{E}(\mathcal{S}) \subset S$  denote the set of punctures marked  $\mathbf{e}$ ;  $\Omega(\mathcal{S}) \subset S$  denote the set of interior punctures, and  $\mathbf{P}(\mathcal{S}) = \mathbf{E}(\mathcal{S}) \cup \Omega(\mathcal{S})$ .

**Remark 5.3.** In Section 7.6, our decorated sources will also include boundary punctures marked by  $w$ . Unlike the  $\mathbf{e}$  punctures, such punctures are not labelled by Reeb chords.



We recall what it means for a map to be asymptotic to a given Reeb chord  $\rho$  at  $q$ . Suppose that  $S$  is a decorated source with a puncture  $q$  on its boundary, thought of as a point in  $\overline{S}$ .  $f: S \rightarrow \Sigma$  is a smooth map with a continuous extension  $\overline{f}: \overline{S} \rightarrow \overline{\Sigma}$ , so that  $f(q) = z_i$ . Let

$$\mathbb{D}^+ = \{z = x + iy \in \mathbb{C} \mid |z| \leq 1, y \geq 0\}$$

and let  $\phi: \mathbb{D}^+ \rightarrow \overline{\mathcal{S}}$  be a holomorphic parameterization around the puncture  $q$ , i.e. so that  $\phi(0) = q$ . If the chord  $\rho$  is supported in  $Z_i$ , consider the identification of the corresponding puncture in  $\Sigma$ ,

$$\psi: S^1 \times [0, \infty) \rightarrow \Sigma,$$

with image  $Z_i \times [0, \infty) \subset \Sigma$ . We say that  $u$  is asymptotic to  $\rho$  at the puncture  $q$  if the family of function  $[0, 1] \rightarrow S^1$  indexed by  $r \in (0, 1]$  specified by

$$\theta \mapsto \pi_{S^1} \circ \psi^{-1} \circ \pi_{\Sigma} \circ u \circ \phi(re^{i\theta})$$

converges to  $\rho$  as  $C^\infty$  functions from  $[0, 1]$  to  $S^1$ , as  $r \mapsto 0$ .

This definition has a straightforward adaptation to interior punctures  $q$  in  $\Sigma$ , where  $o$  is some Reeb orbit. In that case, we choose a parameterization around  $q$  by the punctured disk  $\{z \in \mathbb{C} \setminus \{0\} \mid |z| \leq 1\}$  about  $q$ , and we require that the  $C^\infty$  functions from  $S^1 \rightarrow S^1$  indexed by  $r \in (0, 1]$  defined by

$$\theta \mapsto \pi_{S^1} \circ \psi^{-1} \circ \pi_{\Sigma} \circ u \circ \phi(re^{2\pi i\theta})$$

converge to the given Reeb orbit as  $r \mapsto 0$ .

A *generalized upper Heegaard state* is a  $d$ -element subset of points  $\mathbf{x} = \{x_i\}_{i=1}^d$  in  $\Sigma_0$ , each of which is contained in the intersection of the various  $\alpha$ - and  $\beta$ -curves, distributed so that each  $\beta$ -circle contains exactly one point in  $\mathbf{x}$ , each  $\alpha$ -circle contains exactly one some point in  $\mathbf{x}$ , and no more than one point lies on any given  $\alpha$ -circle. Note that a generalized upper Heegaard state can have more than one element on the same  $\alpha$ -arc.

Analogous to [10, Section 5.2], given a decorated source  $\mathcal{S}$ , we consider maps as follows:

**Definition 5.4.** A pre-flowline is a map

$$u: (\mathcal{S}, \partial\mathcal{S}) \rightarrow (\Sigma \times [0, 1] \times \mathbb{R}, (\alpha \times \{1\} \times \mathbb{R}) \cup (\beta \times \{0\} \times \mathbb{R}))$$

subject to the constraints:

- (M-1)  $u: \mathcal{S} \rightarrow \Sigma \times [0, 1] \times \mathbb{R}$  is proper.
- (M-2)  $u$  extends to a proper map  $\overline{u}: S'_b \rightarrow \overline{\Sigma} \times [0, 1] \times \mathbb{R}$ , where  $S'_b$  is obtained from  $\mathcal{S}$  by filling in the interior and the  $\mathbf{e}$  punctures (so  $S_b \subset S'_b \subset \overline{S}$ )
- (M-3)  $\pi_{\mathbb{D}} \circ u$  is a  $d$ -fold branched cover (with  $d$  as in Equation (5.1)).
- (M-4) At each  $-$ -puncture  $q$  of  $\mathcal{S}$ ,  $\lim_{z \rightarrow q} (t \circ u)(z) = -\infty$ .
- (M-5) At each  $+$ -puncture  $q$  of  $\mathcal{S}$ ,  $\lim_{z \rightarrow q} (t \circ u)(z) = +\infty$ .
- (M-6) At each  $\mathbf{e}$ -puncture  $q$  of  $\mathcal{S}$ ,  $\lim_{z \rightarrow q} (\pi_{\Sigma} \circ u)(z)$  is the Reeb chord  $\rho$  labeling  $q$ . The same holds for middle infinity punctures  $q$ , with limits to the corresponding Reeb orbit.
- (M-7) There are a generalized upper Heegaard states  $\mathbf{x}$  and  $\mathbf{y}$  with the property that as  $t \mapsto -\infty$ ,  $\pi_{\Sigma} \circ u$  is asymptotic to  $\mathbf{x}$  and as  $t \mapsto +\infty$ ,  $\pi_{\Sigma} \circ u$  is asymptotic to  $\mathbf{y}$ .

(M-8) For each  $t \in \mathbb{R}$  and  $i = 1, \dots, d$ ,  $u^{-1}(\beta_i \times \{0\} \times \{t\})$  consists of exactly one point. Similarly, for each  $t \in \mathbb{R}$  and each  $i = 1, \dots, g$ ,  $u^{-1}(\alpha_i^c \times \{1\} \times \{t\})$  consists of exactly one point.

By the definition of branched covers of manifolds with boundary, Condition (M-3) ensures that  $\pi_{\mathbb{D}} \circ u$  (and indeed  $t \circ u$ ) has no critical points over  $\partial[0, 1] \times \mathbb{R}$ .

**Definition 5.5.** Let  $\mathbf{x}$  and  $\mathbf{y}$  be generalized upper Heegaard states, and  $u$  a pre-flowline that connects them. The Reeb asymptotics of  $u$  is the ordered partition of Reeb chords  $\vec{P} = (P_1, \dots, P_\ell)$  appearing in the asymptotics of  $u$ , ordered by the value of  $t \circ u$ .

Property (M-8) is called *weak boundary monotonicity*. We will often consider curves satisfying the following additional condition, called *strong boundary monotonicity*:

(M-8s) For each  $t \in \mathbb{R}$  and  $i = 1, \dots, 2n-1$ ,  $u^{-1}(\alpha_i \times \{1\} \times \{t\})$  consists of at most one point.

If  $u$  satisfies this stronger condition, then  $u$  is asymptotic to upper Heegaard states  $\mathbf{x}$  and  $\mathbf{y}$  over  $-\infty$  and  $+\infty$  respectively.

**Remark 5.6.** Pre-flows can be thought of as Whitney disks in  $\text{Sym}^{g+n-1}(\bar{\Sigma})$ , mapping one of the boundary arcs into the smooth torus  $\beta_1 \times \dots \times \beta_{g+n-1}$ , and the other boundary arc  $a$  into the singular space  $\alpha_1^c \times \dots \times \alpha_g^c \times \text{Sym}^{n-1}(I)$ , where  $I = \bar{\alpha}_1 \cup \dots \cup \bar{\alpha}_{2n-1}$ . The strong monotonicity condition guarantees that the arc  $a$  in fact maps into a smooth part of  $\alpha_1^c \times \dots \times \alpha_g^c \times \text{Sym}^{n-1}(I)$ .

**5.3. On boundary monotonicity.** If  $\boldsymbol{\rho} = \{\rho_1, \dots, \rho_m, o_1, \dots, o_k\}$  is a set of Reeb chords and orbits, let  $\boldsymbol{\rho}^- = \{\rho_1^-, \dots, \rho_m^-\}$  be the multi-set (i.e. set with repeated entries) of initial points of the Reeb chords, and  $\boldsymbol{\rho}^+ = \{\rho_1^+, \dots, \rho_m^+\}$  be the multi-set of terminal points.

Strong boundary monotonicity can be formulated in terms of the initial generalized Heegaard state  $\mathbf{x}$  and the Reeb asymptotics.

**Definition 5.7.** Let  $\mathbf{x}$  be a generalized upper Heegaard state and  $(\boldsymbol{\rho}_1, \dots, \boldsymbol{\rho}_\ell)$ , a sequence of sets of Reeb chords and orbits. We formulate strong boundary monotonicity of  $(\mathbf{x}, \boldsymbol{\rho}_1, \dots, \boldsymbol{\rho}_\ell)$  inductively in  $\ell$ ; at the same time, we also define the terminal  $\alpha$ -set of a strongly boundary monotone sequence  $\alpha(\mathbf{x}, \boldsymbol{\rho}_1, \dots, \boldsymbol{\rho}_\ell) \subset \{1, \dots, 2n-1\}$ , as follows. When  $\ell = 0$ ,  $(\mathbf{x})$  is called strongly boundary monotone if  $\mathbf{x}$  is an upper Heegaard state; and its terminal  $\alpha$ -set is defined to be the set of  $i = 1, \dots, 2n-1$  so that  $\mathbf{x} \cap \alpha_i \neq \emptyset$ . (Note that this definition of  $\alpha(\mathbf{x})$  coincides with the earlier definition given in Definition 2.2.) For  $\ell \geq 1$ , we say that  $(\mathbf{x}, \boldsymbol{\rho}_1, \dots, \boldsymbol{\rho}_\ell)$  is strongly boundary monotone if all of the following conditions hold:

- The sequence  $(\mathbf{x}, \boldsymbol{\rho}_1, \dots, \boldsymbol{\rho}_{\ell-1})$  is strongly boundary monotone.
- No two points in  $\boldsymbol{\rho}_\ell^-$  lies on the same  $\alpha$ -arc, and no two points in  $\boldsymbol{\rho}_\ell^+$  lies on the same  $\alpha$ -arc.
- Letting  $A_-$  resp.  $A_+ \subset \{1, \dots, 2n-1\}$  consist of all  $i$  so that  $\boldsymbol{\rho}_\ell^- \cap \alpha_i \neq \emptyset$  resp.  $\boldsymbol{\rho}_\ell^+ \cap \alpha_i \neq \emptyset$ , we require that

$$A_- \subset \alpha(\mathbf{x}, \boldsymbol{\rho}_1, \dots, \boldsymbol{\rho}_{\ell-1}).$$

- The set

$$\alpha(\mathbf{x}, \boldsymbol{\rho}_1, \dots, \boldsymbol{\rho}_\ell) = A_+ \cup \left( \alpha(\mathbf{x}, \boldsymbol{\rho}_1, \dots, \boldsymbol{\rho}_{\ell-1}) \setminus A_- \right)$$

consists of  $n - 1$  elements.

Note that Condition (M-3) for a pseudo-holomorphic flowline follows from the other conditions, as follows. It is clear that  $\pi_{\mathbb{D}} \circ u$  is a pseudo-holomorphic map from  $\mathcal{S}$  to  $[0, 1] \times \mathbb{R}$ . Since  $\mathcal{S}$  has positive and negative punctures,  $t \circ u$  is not constant, so  $\pi_{\mathbb{D}} \circ u$  is a branched cover. The degree of the branching is determined by Property (M-7).

The following is a variant of [10, Lemma 5.53]:

**Lemma 5.8.** *Suppose that  $u$  is a weakly boundary monotone flowline from  $\mathbf{x}$  to  $\mathbf{y}$  with asymptotics specified by  $\vec{\rho}$ . Then,  $(\mathbf{x}, \vec{\rho})$  is strongly boundary monotone if and only if  $u$  is strongly boundary monotone.*

**Proof.** Fix  $\tau \in \mathbb{R}$ , so  $(t \circ u)^{-1}(\tau)$  contains none of the punctures of  $\mathcal{S}$ , and let

$$\alpha(u, \tau) = \{i \in \{1, \dots, 2n - 1\} \mid u^{-1}(\alpha_i \times \{1\} \times \{\tau\}) \neq \emptyset\}.$$

Let  $q$  be some puncture on  $\mathcal{S}$  labelled by  $\rho$ , a Reeb chord with  $\rho^-$  on  $\alpha_i$  and  $\rho^+$  on  $\alpha_j$ . Since  $t \circ u$  is strictly monotone on the arc through  $q$  (in view of Property (M-3)), it follows that for all sufficiently small  $\epsilon > 0$ ,  $i \in \alpha(u, t(q) - \epsilon)$  and  $j \in \alpha(u, t(q) + \epsilon)$ . In fact, by continuity (and induction on  $\ell$ ), we see that  $\alpha(\mathbf{x}, \boldsymbol{\rho}_1, \dots, \boldsymbol{\rho}_{\ell-1}) = \alpha(u, \tau)$  for all  $\tau$  with  $t_{\ell-1} < \tau < t_\ell$ , where  $t_i$  denotes the  $t$ -value of the punctures labelled by  $\boldsymbol{\rho}_i$ , and  $t_0 = -\infty$ . It follows easily that the two formulations of boundary monotonicity coincide: strong boundary monotonicity on  $u$  is a condition on  $\alpha(u, \tau)$  and strong boundary monotonicity of  $(\mathbf{x}, \vec{\rho})$  is the corresponding condition on the  $\alpha(\mathbf{x}, \boldsymbol{\rho}_1, \dots, \boldsymbol{\rho}_\ell)$ .  $\square$

The following result will allow us to restrict attention to moduli spaces containing only strongly boundary monotone sequences:

**Proposition 5.9.** *Suppose that  $\mathbf{x}$  and  $\mathbf{y}$  are upper Heegaard states. If  $u$  is a weakly, but not strongly boundary monotone pre-flowline representing  $\phi \in \mathcal{D}(\mathbf{x}, \mathbf{y})$ , then  $b_0(\phi)$  is in the ideal  $\mathcal{I} \subset \mathcal{B}_0$ ; i.e. its image in  $\mathcal{B}$  vanishes.*

**Proof.** Let  $X \subset \mathbb{R}$  denote the set of points  $\tau \in \mathbb{R}$  for which  $u^{-1}(\alpha_i \times \{1\} \times \{\tau\})$  consists of more than one point for some  $i$ . The set  $X$  is bounded below since  $u$  is asymptotic to an upper Heegaard state  $\mathbf{x}$  as  $t \mapsto -\infty$ . Thus, it has an infimum  $\tau_0$ . There must be some puncture  $p \in \partial \overline{\mathcal{S}}$  asymptotic to a Reeb chord  $\rho$  that ends on  $\alpha_i$ , with  $t(u(p)) = \tau_0$ , and another point  $q \in \partial \overline{\mathcal{S}}$  with  $\pi_\Sigma(u(q)) \in \overline{\alpha}_i$  and  $t(u(q)) = \tau_0$ . The initial point of  $\rho$  cannot be on  $\alpha_i$ , for that would violate boundary monotonicity for the portion of the curve in values  $< \tau_0$ .

Given a pre-flowline  $u$  and generic  $\tau < \tau_0$ , we construct certain pure algebra elements  $b_\tau, c_\tau \in \mathcal{B}_0$  with  $\hat{\mathbf{I}}(\mathbf{x}) \cdot b_\tau = b_\tau$ , and  $b_0(\phi) = b_\tau \cdot c_\tau$ .

The algebra element  $b_\tau$  for any  $\tau < \tau_0$  is specified by its initial idempotent  $\hat{\mathbf{I}}(\mathbf{x})$ , and its weight, which is given by the sum of the weights of all the Reeb chords and orbits in  $(t \circ u)^{-1}((-\infty, \tau))$ . Note that  $b_\tau = \hat{\mathbf{I}}(\mathbf{x}) \cdot b_\tau \cdot \mathbf{I}_{\mathbf{x}_\tau}$ , where

$$\mathbf{x}_\tau = \{1, \dots, 2n - 1\} \setminus \{i \mid \pi_\Sigma(u(1, \tau)) \cap \alpha_i \neq \emptyset\},$$

and  $\mathbf{I}_{\mathbf{x}_\tau}$  denotes its corresponding idempotent.

Assume that the initial point of  $\rho$  is on  $\alpha_{i-1}$ , so that  $\rho$  is of the form  $L_i(R_i L_i)^k$ . (The case where the initial point of  $\rho$  is on  $\alpha_{i+1}$  will follow similarly.) We could write  $b_0(\phi) = b_{\tau_0-\epsilon} \cdot c_{\tau_0-\epsilon}$ , where  $\hat{\mathbf{I}}(\mathbf{x}) \cdot b_{\tau_0-\epsilon} \cdot \mathbf{I}_{\mathbf{x}_{\tau_0-\epsilon}} = b_{\tau_0-\epsilon}$  and  $i-1, i \notin \mathbf{I}_{\mathbf{x}_\tau}$ .

There are two cases. Either  $\mathbf{w}_i(c_{\tau_0-\epsilon}) \geq 1$ , in which case  $c_{\tau_0-\epsilon} = U_i \cdot c'$  for some algebra element  $c'$ ; so  $c_{\tau_0-\epsilon} \in \mathcal{G}$ . If  $\mathbf{w}_i(c_{\tau_0-\epsilon}) = 1/2$ , then  $c_{\tau_0-\epsilon}$  moves one of its coordinates from  $\geq i+1$  to  $\leq i-1$ , so once again  $c_{\tau_0-\epsilon} \in \mathcal{G}$ .  $\square$

#### 5.4. Pseudo-holomorphic flows.

**Definition 5.10.** *A pseudo-holomorphic flowline is a pre-flow satisfying the following further hypothesis:*

(M-9h) *The map  $u$  is  $(j, J)$ -holomorphic with respect to some fixed admissible almost-complex structure  $J$  (Definition 5.1) and complex structure  $j$  on  $\mathcal{S}$ .*

Recall that  $\bar{\Sigma}$  is equipped with  $2n$  points  $z_1, \dots, z_{2n}$ . If  $u$  is a pseudo-holomorphic flow, then  $f = \pi_\Sigma \circ u$  is a local branched cover over  $z_i$ , with branching specified by the Reeb chords.

Generalized pseudo-holomorphic flowlines can be collected into homology classes. Specifically, if  $u$  is a pre-flowline from  $\mathbf{x}$  to  $\mathbf{y}$ , then the projection to  $\Sigma$  induces a two-chain from  $\mathbf{x}$  to  $\mathbf{y}$ , in the sense of Definition 4.1, obtained from assembling the local multiplicities of  $\pi_\Sigma \circ u$ . We call the two-chain so obtained  $\mathbf{S}(u)$ , the *shadow* of  $u$ .

Fix an admissible almost-complex structure  $J$ . We will consider moduli spaces  $\mathcal{M}^B(\mathbf{x}, \mathbf{y}; \mathcal{S}; \vec{P})$  of curves from a decorated source asymptotic to  $\mathbf{x}$  and  $\mathbf{y}$  at  $-\infty$  and  $+\infty$  respectively, with given shadow  $B \in \mathcal{D}(\mathbf{x}, \mathbf{y})$ , and respecting the partition  $\vec{P}$ . We will typically take the quotient of these moduli spaces by the natural  $\mathbb{R}$  action, to get moduli spaces

$$\widehat{\mathcal{M}}^B(\mathbf{x}, \mathbf{y}; \mathcal{S}; \vec{P}) = \mathcal{M}^B(\mathbf{x}, \mathbf{y}; \mathcal{S}; \vec{P}) / \mathbb{R}.$$

**Example 5.11.** *Consider the top picture in Figure 14, showing a shaded domain  $B$  connecting upper states  $\mathbf{x}$  and  $\mathbf{y}$ . (We have illustrated only two components of each Heegaard state; assume for all  $i > 2$ ,  $x_i = y_i$ .) The two holomorphic disks crossing  $L_i$  and  $L_{i+1}$  can be translated relative to one other to obtain a one-parameter family of holomorphic curves in  $\mathcal{M}^B(\mathbf{x}, \mathbf{y}, (\{L_i\}, \{L_{i+1}\}))$  (which are not boundary monotone) and  $\mathcal{M}^B(\mathbf{x}, \mathbf{y}, (\{L_{i+1}\}, \{L_i\}))$  (which are boundary monotone), and a single curve in  $\mathcal{M}^B(\mathbf{x}, \mathbf{y}, (\{L_i, L_{i+1}\}))$ . Note that  $b_0(B) = \hat{\mathbf{I}}(\mathbf{x}) \cdot L_{i+1} L_i \in \mathcal{G}$ .*

**Example 5.12.** *Consider the second line in Figure 14. Here, the shaded domain supports holomorphic curves in six different moduli spaces,  $\mathcal{M}^B(\mathbf{x}, \mathbf{y}, \vec{p})$ , with partitions  $\vec{p} = (\{L_i\}, \{R_i\})$ ,  $(\{R_i\}, \{L_i\})$ ,  $(\{L_i \cdot R_i\})$ ,  $(\{R_i \cdot L_i\})$ ,  $(o_i)$ , and  $(\{R_i, L_i\})$ . The first two are not boundary monotone, and the four are. (The first five are two-dimensional moduli spaces and the last one is one-dimensional.) Now,  $b_0(B) = \hat{\mathbf{I}}(\mathbf{x}) \cdot U_i \cdot \hat{\mathbf{I}}(\mathbf{y})$  (noting that  $\hat{\mathbf{I}}(\mathbf{x}) = \hat{\mathbf{I}}(\mathbf{y})$ , and  $i-1, i \notin \{1, \dots, 2n-1\} \setminus \alpha(\mathbf{x})$ ).*

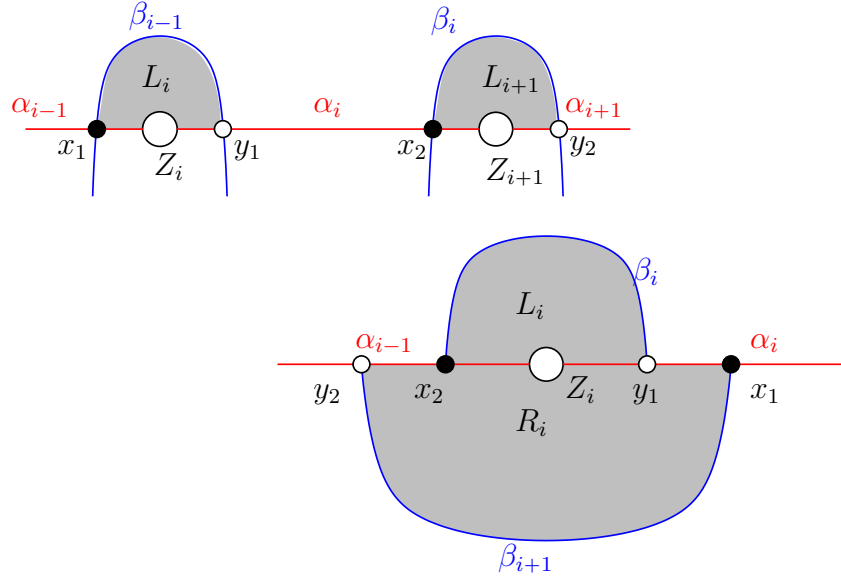


FIGURE 14. Some moduli spaces.

### 5.5. The expected dimension of the moduli spaces.

**Definition 5.13.** A Reeb sequence  $\vec{\rho} = (\rho_1, \dots, \rho_\ell)$  is an ordered sequence of Reeb orbits and chords.

A Reeb sequence  $\vec{\rho} = (\rho_1, \dots, \rho_\ell)$  gives rise to a partition of Reeb chords, where each term consists of one element sets,  $\vec{\rho} = (\{\rho_1\}, \dots, \{\rho_\ell\})$ . We call such a partition *simple*. We will use interchangeably a Reeb sequence with its associated simple partition; e.g. we say that  $(\mathbf{x}, \vec{\rho})$  is boundary monotone if  $\mathbf{x}$ , together with the simple partition associated to  $\vec{\rho}$  is. Similarly, given a Reeb sequence  $\vec{\rho}$ , when we write  $m^B(\mathbf{x}, \mathbf{y}, \mathcal{S}, \vec{\rho})$ , we mean the moduli space with associated simple partition.

Fix  $(B, \vec{\rho})$  with  $B \in \mathcal{D}(\mathbf{x}, \mathbf{y})$ , and  $\vec{\rho}$  is a sequence of Reeb chords and orbits. We say that  $(B, \vec{\rho})$  is *compatible* if the sum of the weights of  $\vec{\rho}$  agree with the local multiplicities of  $B$  around the boundary, and  $(B, \vec{\rho})$  is strongly boundary monotone.

**Definition 5.14.** Let  $|o(\vec{\rho})|$  be the number of Reeb orbits appearing in  $\vec{\rho}$ , and  $|\text{cho}(\vec{\rho})|$  be the number of chords. If  $(B, \vec{\rho})$  is compatible, we can define the embedded Euler characteristic, the embedded index, and the embedded moduli space:

$$(5.2) \quad \chi_{\text{emb}}(B) = d + e(B) - n_{\mathbf{x}}(B) - n_{\mathbf{y}}(B)$$

$$(5.3) \quad \text{ind}(B, \mathbf{x}, \mathbf{y}; \vec{\rho}) = e(B) + n_{\mathbf{x}}(B) + n_{\mathbf{y}}(B) + 2|o(\vec{\rho})| + |\text{cho}(\vec{\rho})| - 2\omega_{\partial}(B)$$

$$(5.4) \quad m^B(\mathbf{x}, \mathbf{y}, \vec{\rho}) = \bigcup_{\chi(\mathcal{S}) = \chi_{\text{emb}}(B)} m^B(\mathbf{x}, \mathbf{y}, \mathcal{S}; \vec{\rho}),$$

where  $\omega_{\partial}(B)$  is the total weight of  $B$  at the boundary; i.e.

$$\omega_{\partial}(B) = \sum_{\rho_i} \omega(\rho_i).$$

Note also that  $\text{ind}(B, \mathbf{x}, \mathbf{y}; \vec{\rho}) = \mathbf{m}(B)$ , in cases where each Reeb chord in  $\vec{\rho}$  has length  $1/2$  and each orbit has length  $1$ .

**Remark 5.15.** *When comparing the above formulas with, for example, [10, Section 5.7.1], bear in mind that there, the Euler measure of  $B$  is defined in terms of the Heegaard surface with boundary  $(\Sigma_0)$ ; whereas here we think of it as the Euler measure in  $\overline{\Sigma}$  instead.*

The following is a straightforward adaptation of [10, Proposition 5.29]:

**Proposition 5.16.** *If  $M^B(\mathbf{x}, \mathbf{y}, \mathcal{S}; \vec{\rho})$  is represented by some pseudo-holomorphic  $u$ , then  $\chi(\mathcal{S}) = \chi_{\text{emb}}(B)$  if and only if  $u$  is embedded. In this case, the expected dimension of the moduli space is computed by  $\text{ind}(B, \mathbf{x}, \mathbf{y}; \vec{\rho})$ . Moreover, if a strongly monotone moduli space  $M^B(\mathbf{x}, \mathbf{y}, \mathcal{S}; \vec{\rho})$  has a non-embedded holomorphic representative, then its expected dimension is  $\leq \text{ind}(B, \mathbf{x}, \mathbf{y}; \vec{\rho}) - 2$ .*

**Proof.** The proof is as in [10, Proposition 5.29], which in turn follows [6].

Suppose that  $u$  is a weakly boundary monotone pre-flow. Let  $b_\Sigma$  be the ramification number of  $\pi_\Sigma \circ u$ , defined so that each interior branch point contributes  $1$ ; each boundary branched points contribute  $1/2$ . We think of  $\overline{S}$  as a manifold with corners, one for each  $\pm\infty$  puncture (but the Reeb orbit punctures fill in to give ordinary boundary). Let  $e(\overline{S})$  denote the corresponding Euler measure.

By the Riemann-Hurwitz formula,

$$(5.5) \quad \chi(\overline{S}) = e(\overline{S}) + \frac{d}{2} = e(B) + \frac{d}{2} - b_\Sigma.$$

Let  $\tau_R(u)$  denote a copy of  $u$  translated by  $R$  units in the  $\mathbb{R}$ -direction. Since  $u$  is embedded, for small  $\epsilon$ ,  $u$  and  $\tau_\epsilon(u)$  intersect only near branch points of  $f = \pi_\Sigma \circ u$ ; and since both are pseudo-holomorphic, their algebraic intersection number is precisely  $b_\Sigma$ . When  $R$  is large,

$$u \cdot \tau_R(u) = n_{\mathbf{x}}(B) + n_{\mathbf{y}}(B) - \frac{d}{2}.$$

As in [6], the intersection number  $u \cap \tau_t(u)$  is independent of  $t$ , so in particular

$$(5.6) \quad u \cdot \tau_R(u) = u \cdot \tau_\epsilon(u).$$

(In [10], the intersection number is not independent of  $t$ ; rather, there are possible correction terms when Reeb chords are slid past one another. This contribution takes the form of a linking number near the boundary which, in the present context vanishes.) Thus, Equation (5.6) shows that

$$b_\Sigma = n_{\mathbf{x}}(B) + n_{\mathbf{y}}(B) - \frac{d}{2}.$$

Substituting this back into Equation (5.5) shows that

$$\chi(\overline{S}) = d + e(B) - n_{\mathbf{x}}(B) - n_{\mathbf{y}}(B) = \chi_{\text{emb}}(B),$$

in the case where  $u$  is embedded.

When  $u$  is pseudo-holomorphic, but not embedded, it has  $s > 0$  (positive) double points (and no negative double-points). By boundary monotonicity, do not occur

on the boundary. In this case  $u \cdot \tau_\epsilon(u) = b_\Sigma + 2s$ , Equation (5.6) shows that  $b_\Sigma + 2s = n_{\mathbf{x}}(B) + n_{\mathbf{y}}(B) - \frac{d}{2}$ , and so

$$\chi(\overline{S}) = \chi_{\text{emb}}(B) + 2s > \chi_{\text{emb}}(\overline{S}).$$

Suppose once again that  $u$  is embedded. Thinking of  $\overline{S}$  as a branched cover of the disk with branching  $b_{\mathbb{D}}$ , we have that

$$b_{\mathbb{D}} = d - \chi(\overline{S}) = n_{\mathbf{x}}(u) + n_{\mathbf{y}}(u) - e(B).$$

From the point of view of the symmetric product, since  $u$  is embedded,  $b_{\mathbb{D}}$  is the intersection number of the disk corresponding to  $u$  with the diagonal locus in the symmetric product. In the case where the sequence  $\vec{\rho}$  is empty,  $\text{ind}(u)$  is computed by a Maslov index, which, according a result of Rasmussen [24], equals  $2e(\mathbf{S}(u)) + b_{\mathbb{D}}$ . Thus, in this case where  $\ell = 0$ ,

$$\text{ind}(u) = e(B) + n_{\mathbf{x}}(B) + n_{\mathbf{y}}(B).$$

In general, each Reeb chord and orbit gives a correction to the above formula for the index. If a Reeb chord has weight  $w$ , its correction is  $1 - 2w$ . This can be seen by looking, for example, at a model computation as shown on the right in Figure 15. In this example, we have arranged for the source to be a  $\mathcal{S}$  is a disk with a single Reeb chord with weight  $w$ ;  $B$  has  $e(B) = 2w$ ; and the moduli space of pseudo-holomorphic representatives (modulo  $\mathbb{R}$ ) is rigid, and hence has index 1. For the Reeb orbit with weight  $w$ , a similar rigid solution can be found with  $e = \frac{w+1}{2}$ ,  $n_{\mathbf{x}}(B) + n_{\mathbf{y}}(B) = \frac{w-1}{2}$ .

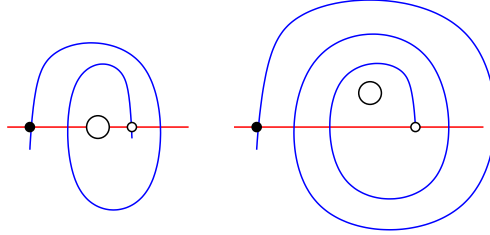


FIGURE 15. Model computations for the index.

Finally, when  $u$  is not embedded, and has  $s$  double points, the intersection number with the diagonal corresponds to  $b_{\mathbb{D}} + 2s$ , so  $\text{ind}(u) = \text{ind}(B, \mathbf{x}, \mathbf{y}; \boldsymbol{\rho}) - 2s$ .  $\square$

**5.6. Boundary degenerations.** We formalize the notion of  $\beta$ -boundary degenerations.

**Definition 5.17.** Let  $\mathbb{H} \subset \mathbb{C}$  (the “lower half plane”) consist of  $\{x + iy \mid x, y \in \mathbb{R}, y \leq 0\}$ , so  $\partial\mathbb{H} = \mathbb{R}$ . A boundary degeneration consists of the following data.

- a smooth, oriented surface  $R_b$  with boundary and punctures, exactly  $d$  of which are on the boundary.
- a labelling of the interior punctures of  $R_b$  by Reeb orbits
- a complex structure  $j_b$  on  $R_b$ .
- a smooth map  $w: (R_b, \partial R_b) \rightarrow (\Sigma \times \mathbb{H}, \beta \times \mathbb{R} \times \{0\})$ .

- a constant  $\tau \in \mathbb{R}$ .

These data are required to satisfy the following conditions:

- (1) The map  $w: R_b \rightarrow \Sigma \times \mathbb{H}$  is proper, and it extends to a proper map  $\bar{w}: R'_b \rightarrow \bar{\Sigma} \times \mathbb{H}$ , where  $R'_b$  is obtained from  $R_b$  by filling in the  $\mathbf{e}$  punctures (so  $R_b \subset R'_b \subset \bar{R}_b$ ).
- (2) The map  $\pi_{\mathbb{H}} \circ w$  is a  $d$ -fold branched cover.
- (3) At each interior puncture of  $R_b$ ,  $\pi_{\Sigma} \circ w$  is asymptotic to the Reeb orbits which labels the puncture.
- (4) For each  $t \in \mathbb{R} = \partial\mathbb{H}$  and  $i = 1, \dots, d$ ,  $w^{-1}(\beta_i \times \{t\})$  consists of exactly one point.
- (5) The map  $w$  is holomorphic, with respect to  $j_b$  on the domain and the split complex structure  $j \times j_{\mathbb{H}}$  on the range.

The map  $w: R_b \rightarrow \Sigma \times \mathbb{H}$  extends to a map

$$\bar{w}: \bar{R}_b \rightarrow \bar{\Sigma} \times \bar{\mathbb{H}}.$$

**Definition 5.18.** Think of the boundary punctures in  $R_b$  as a  $d$ -tuple of points in  $\bar{R}_b$ . The images of these points under  $\bar{\pi}_{\mathbb{H}} \circ \bar{w}$  gives a point, denoted  $\text{ev}^{\beta}(w)$ , in  $\beta_1 \times \dots \times \beta_d = \mathbb{T}_{\beta}$ .

The boundary degeneration induces a map  $u: (R_b, \partial R_b) \rightarrow (\Sigma \times [0, 1] \times \mathbb{R}, \beta \times \mathbb{R})$ , so that  $\pi_{\Sigma} \circ u = \pi_{\Sigma} \circ w$ ,  $s \circ u = 0$ , and  $t \circ u \equiv \tau$ .

Such a boundary degeneration  $w$  has a shadow which is a two-chain  $B$  which is a formal linear combination of the components of  $\Sigma \setminus \beta$ .

For  $\{r, s\} \in M$ , there is a two-chain  $\mathcal{B}_{\{r, s\}}$  corresponding to the component of  $\Sigma \setminus \beta$  containing  $z_r$  and  $z_s$ . Let  $\hat{\mathcal{N}}_j^{\mathcal{B}_{\{r, s\}}}$  denote the moduli space of boundary degenerations with shadow  $\mathcal{B}_{\{r, s\}}$  as above modulo the (real two-dimensional) group of automorphisms of  $\mathbb{H}$ .

**Proposition 5.19.** For a generic complex structure  $j$  on  $\Sigma$ , the moduli space  $\mathcal{N}_j^{\mathcal{B}_{\{r, s\}}}$  of boundary degeneration is a smooth manifold of dimension  $d = g + n - 1$ .

**Proof.** This follows from the fact that the corresponding moduli space is somewhere injective near the boundary; see [6, Proposition 3.9 and Lemma 3.10]; see also [20, Proposition 3.14] and [16].  $\square$

There is an evaluation map  $\text{ev}^{\beta}: \mathcal{N}_j^{\mathcal{B}_{\{r, s\}}} \rightarrow \mathbb{T}_{\beta}$ . Given  $\mathbf{x} \in \mathbb{T}_{\beta}$ , let

$$\mathcal{N}_j^{\mathcal{B}_{\{r, s\}}}(\mathbf{x}) = (\text{ev}^{\beta})^{-1}(\mathbf{x}).$$

The following result will be important:

**Lemma 5.20.** The evaluation map  $\text{ev}^{\beta}: \mathcal{N}_j^{\mathcal{B}_{\{r, s\}}} \rightarrow \mathbb{T}_{\beta}$  has odd degree.

**Proof.** Consider first the case where  $g = 0$ . In this case,  $\text{ev}^{\beta}$  is clearly a homeomorphism: the boundary degeneration consist of  $d - 1$  constant disks, and one disk that maps to  $\mathcal{B}_{\{r, s\}}$  with degree one. We can move the constants around on



at  $d - 1$  dimensional portion of  $\mathbb{T}_\beta$  and reparameterize the remaining component to obtain the claimed homeomorphism. In cases where  $g > 0$ , gluing spheres gives the desired degree statement [6, Section 12]; see also [20, Section 10].  $\square$

### 5.7. Regular moduli spaces of embedded curves.

**Definition 5.21.** A Reeb sequence  $(\rho_1, \dots, \rho_\ell)$  is called *typical* if each chord  $\rho_i$  appearing in the sequence covers half of some boundary circle (i.e. it is one of  $L_i$  or  $R_i$ ), and each Reeb orbit covers some boundary circle exactly once.

**Theorem 5.22.** Choose a generic  $J$ . Let  $B$  be a shadow with  $\mathbf{m}(B) \leq 2$  and  $\vec{\rho}$  is a typical Reeb sequence. Then, the moduli spaces  $M^B(\mathbf{x}, \mathbf{y}, \mathcal{S}; \vec{\rho})$  is a smooth manifold of dimension given by  $\mathbf{m}(B)$ . Moreover, if  $\mathbf{m}(B) \leq 1$  and  $\vec{\rho}$  is not typical, then  $M^B(\mathbf{x}, \mathbf{y}, \mathcal{S}; \vec{\rho})$  is empty.

**Proof.** Consider first the moduli space  $M^B(\mathbf{x}, \mathbf{y}, \mathcal{S})$ , where the order of the punctures is left unspecified. Standard arguments show that, for generic  $J$ , the corresponding moduli space is a manifold transversely cut out by the  $\bar{\partial}$  operator; see [10, Proposition 5.6]. Moreover, the evaluation map at the punctures gives a map from the moduli space to  $\mathbb{R}^E$ , where here  $E = E(\mathcal{S})$  denotes the number of east punctures of  $\mathcal{S}$ . There is a dense set of  $J$  for which the evaluation map is transverse to the various diagonals in  $\mathbb{R}^E$ , so that their preimages give submanifolds of  $M^B(\mathbf{x}, \mathbf{y}, \mathcal{S})$ ; the moduli spaces  $M^B(\mathbf{x}, \mathbf{y}, \mathcal{S}; \vec{\rho})$  are the complement of these submanifolds.

This transversality argument shows that  $M^B(\mathbf{x}, \mathbf{y}, \mathcal{S}; \vec{\rho})$  is a smooth manifold with dimension (as computed in Proposition 5.16) given by

$$\begin{aligned} \text{ind}(B, \mathbf{x}, \mathbf{y}; \vec{\rho}) &= e(B) + n_{\mathbf{x}}(B) + n_{\mathbf{y}}(B) + 2|o(\vec{\rho})| + |\text{cho}(\vec{\rho})| - 2 \sum_{\rho_i} \omega(\rho_i) \\ &= \mathbf{m}(B) - \sum_{o \in o(\vec{\rho})} (2\omega(o) - 2) - \sum_{\rho \in \text{cho}(\vec{\rho})} (2\omega(\rho) - 1) \\ &\leq \mathbf{m}(B), \end{aligned}$$

with equality exactly when each orbit has length one and each chord has length  $1/2$ .  $\square$

**Remark 5.23.** The above general position can be seen from the point of view of the symmetric product as follows. As in Remark 5.6, we think of our pseudo-holomorphic curves as giving pseudo-holomorphic disks in  $\text{Sym}^d(\bar{\Sigma})$ . The subspace  $\alpha_1^c \times \dots \times \alpha_g^c \times \text{Sym}^{n-1}(I)$  is equipped with codimension one walls of the form  $\{p_i\} \times \text{Sym}^{n-2}(I)$ , with  $p_i \in \bar{\Sigma}$ . Typical sequences arise for holomorphic disks that are transverse to these walls; chords or orbits with larger weight occur when the curves have higher order contact with the submanifolds.

**5.8. Ends of one-dimensional moduli spaces.** We will consider ends of one-dimensional moduli spaces  $\widehat{M}^B(\mathbf{x}, \mathbf{y}, \mathcal{S}; \vec{P})$ . These will include ends that consist of two-story buildings. Another kind of end consists of the formation of an “orbit curve” at east infinity. This occurs when some Reeb orbit constraint  $o_i$  in  $\vec{P}$  slides off to  $s = 1$ . (See Figure 16.) Other ends occur when two consecutive parts in  $\vec{P}$  collide. We call these *collision ends*.

In formulating these ends, we use the following terminology from [10]:

**Definition 5.24.** An ordered pair of Reeb chords  $\rho$  and  $\sigma$  are called *weakly composable* if  $\rho^+$  and  $\sigma^-$  are contained on the same  $\alpha$ -arc. Moreover, if  $\rho$  and  $\sigma$  are weakly composable, they are further called *strongly composable* if  $\rho^+ = \sigma^-$ . If  $\rho$  and  $\sigma$  are strongly composable we can join them to get a new Reeb chord  $\rho \uplus \sigma$ .

Thus,  $L_i$  and  $L_{i+1}$  are weakly but not strongly composable, while  $L_i$  and  $R_i$  are strongly composable.

**Definition 5.25.** A collision end is called *invisible* if  $\rho_i$  and  $\rho_{i+1}$  are the same Reeb orbit. Otherwise, it is called *visible*.

**Theorem 5.26.** Let  $\mathcal{H}^\wedge$  be an upper diagram and  $M$  its associated matching. Fix upper Heegaard states  $\mathbf{x}$  and  $\mathbf{y}$  and a typical Reeb sequence  $\vec{\rho}$ . Suppose moreover that  $(\mathbf{x}, \vec{\rho})$  is strongly boundary monotone, and  $B \in \mathcal{D}(\mathbf{x}, \mathbf{y})$  has vanishing local multiplicity somewhere. Fix  $\mathcal{S}$  and  $\vec{\rho}$  so that  $\text{ind}(B, \mathbf{x}, \mathbf{y}; \mathcal{S}, \vec{\rho}) = 2$ . Let  $\widehat{M} = \widehat{M}^B(\mathbf{x}, \mathbf{y}; \mathcal{S}; \vec{\rho})$ . The total number of ends of  $\widehat{M}$  of the following types are even in number:

(DE-1) Two-story ends, which are of the form

$$\widehat{M}^{B_1}(\mathbf{x}, \mathbf{w}; \mathcal{S}_1; \rho_1, \dots, \rho_i) \times \widehat{M}^{B_2}(\mathbf{w}, \mathbf{y}; \mathcal{S}_2; \rho_{i+1}, \dots, \rho_\ell),$$

taken over all upper Heegaard states  $\mathbf{w}$  and choices of  $\mathcal{S}_1$  and  $\mathcal{S}_2$  so that  $\mathcal{S}_1 \natural \mathcal{S}_2 = \mathcal{S}$ , and  $B_1 \natural B_2 = B$ .

(DE-2) Orbit curve ends, of the form  $\widehat{M}^B(\mathbf{x}, \mathbf{y}; \mathcal{S}; \rho_1, \dots, \rho_{i-1}, v_j, \rho_{i+1}, \dots, \rho_\ell)$ , where some Reeb orbit component  $\rho_i = o_j$  slides off to  $s = 1$  and is replaced by a Reeb chord  $v_j$  that covers  $Z_j$  with multiplicity 1. (When  $j \neq 1$  or  $2n$ , there are two possible choices:  $v_j = R_j L_j$  or  $L_j R_j$ .)

(DE-3) Visible collision ends where at least one of  $\rho_i$  or  $\rho_{i+1}$  is a Reeb orbit.

(DE-4) Collision ends where  $\rho_i$  and  $\rho_{i+1}$  are Reeb chords, where one of the two conditions are satisfied:  $\rho_i$  and  $\rho_{i+1}$  are not weakly composable, or they are strongly composable.

(DE-5) An end consisting of a boundary degeneration that meets a constant flow-line. In this special case,  $\vec{\rho}$  consists of exactly two constraints, which are matched Reeb orbits, and  $\mathbf{x} = \mathbf{y}$ . Moreover, if  $\{r, s\} \in M$ , then the number of boundary degeneration ends of the union

$$M(\mathbf{x}, \mathbf{x}, \{e_r\}, \{e_s\}) \cup M(\mathbf{x}, \mathbf{x}, \{e_s\}, \{e_r\})$$

is odd.

The above result is proved in Section 7.

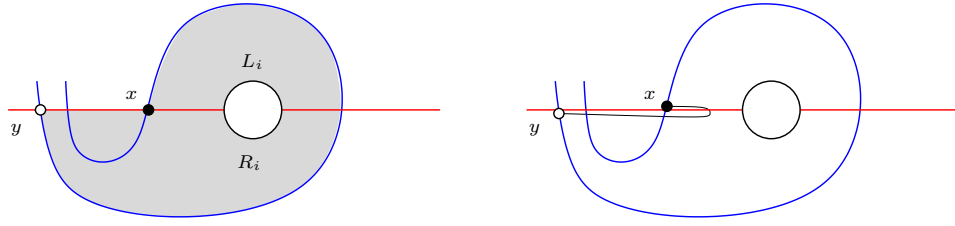


FIGURE 16. **Orbit curve end.** Consider the moduli space  $\widehat{m}^B(x, y, \{o_i\})$ , where  $B$  is shaded on the left. This one-dimensional moduli space has an end which is a two-story building, and another which is an orbit curve end with  $v_i = L_i R_i$ .

6. TYPE  $D$  MODULES

Let  $\mathcal{H}^\wedge$  be an upper diagram, and let  $M$  be its corresponding matching. Let  $W$  be the one-manifold associated to  $M$  (as in Definition 2.4), and fix an orientation on  $W$ ; i.e. a choice of preferred  $i$  for each  $\{i, j\} \in M$ . (This latter data is needed to define the  $\mathbb{Q}^n$ -valued Alexander grading.)

Choose an admissible almost-complex structure  $J$  over  $\mathcal{H}^\wedge$  (as in Definition 5.1). Let  $R(\mathcal{H}^\wedge)$  be the vector space generated over  $\mathbb{F}$  by the upper states. For  $\alpha(\mathbf{x})$  as in Definition 2.2, let

$$(6.1) \quad \hat{\mathbf{I}}(\mathbf{x}) = \mathbf{I}_{\{1, \dots, 2n-1\} \setminus \alpha(\mathbf{x})}$$

thought of as an idempotent in the algebra  $\mathcal{C}(n)$ . The left action of the idempotent subalgebra of  $\mathcal{C}(n)$  is specified by the condition that  $\hat{\mathbf{I}}(\mathbf{x}) \cdot \mathbf{x} = \mathbf{x}$ .

Consider the functions  $\mathbf{m}: \mathfrak{S}(\mathcal{H}^\wedge) \rightarrow \mathbb{Z}$  and  $\mathbf{A}: \mathfrak{S}(\mathcal{H}^\wedge) \rightarrow \frac{1}{2}\mathbb{Z}^n$  defined in Equations (4.2) and 4.3 above. These endow  $R(\mathcal{H}^\wedge)$  with a  $\mathbb{Z}$ -valued  $\Delta$ -grading and a  $\frac{1}{2}\mathbb{Z}^n$ -valued Alexander grading, denoted  $\mathbf{A}$ .

Let  $\mathbf{x}, \mathbf{y}$  be upper Heegaard states, and  $B \in \mathcal{D}(\mathbf{x}, \mathbf{y})$ . Let  $m^B(\mathbf{x}, \mathbf{y})$  be the union of  $m^B(\mathbf{x}, \mathbf{y}; \vec{\rho})$  (as in Equation (5.4)), taken over all typical sequences  $\vec{\rho}$  of Reeb chords and orbits that are compatible with  $B$ . Recall that by Theorem 5.22,  $m^B(\mathbf{x}, \mathbf{y})$  has expected dimension  $\mathbf{m}(B)$  (independent of the typical sequence  $\vec{\rho}$ ).

Define the operation

$$\delta^1: R(\mathcal{H}^\wedge) \rightarrow \mathcal{C}(n) \otimes R(\mathcal{H}^\wedge)$$

by

$$(6.2) \quad \delta^1(\mathbf{x}) = \sum_{\{\mathbf{y} \in \mathfrak{S}, B \in \mathcal{D}(\mathbf{x}, \mathbf{y}) \mid \mathbf{m}(B)=1\}} \# \widehat{m}^B(\mathbf{x}, \mathbf{y}) \cdot \hat{b}(B) \otimes \mathbf{y},$$

where  $\hat{b}(B) \in \mathcal{C}(n) \subset \mathcal{B}(2n, n)$  is as in Section 4.

**Proposition 6.1.** *The sum appearing on the right of Equation (6.2) is finite.*

**Proof.** The non-zero terms arise from  $B \in \mathcal{D}(\mathbf{x}, \mathbf{y})$  with  $\mathbf{m}(B) = 1$ , which have pseudo-holomorphic representatives. We must show that there are only finitely many such  $B$ . To this end, fix some  $B_0 \in \mathcal{D}(\mathbf{x}, \mathbf{y})$ . Our hypothesis on upper diagrams (Property (UD-4)) ensures that for any other  $B \in \mathcal{D}(\mathbf{x}, \mathbf{y})$ , we can find integers  $n_{\{r,s\}}$  so that

$$B = B_0 + \sum_{\{r,s\} \in M} n_{\{r,s\}} \cdot \mathcal{B}_{\{r,s\}}.$$

If  $B$  has a holomorphic representative, then all of its local multiplicities must be non-negative, giving a lower bound on each  $n_{\{r,s\}}$ . Since

$$\mathbf{m}(B) = \mathbf{m}(B_0) + 2 \sum_{\{r,s\} \in M} n_{\{r,s\}},$$

condition that  $\mathbf{m}(B) = 1$  also places an upper bound on all the  $n_{\{r,s\}}$ , proving the desired finiteness statement.  $\square$

**Proposition 6.2.** *The map  $\delta^1$  respects (relative) gradings in the following sense: if  $b \otimes \mathbf{y}$  appears with non-zero multiplicity in  $\delta^1(\mathbf{x})$ , then*

$$\begin{aligned}\mathbf{m}(\mathbf{x}) - 1 &= \Delta(b) + \mathbf{m}(\mathbf{y}) \\ \mathbf{A}(\mathbf{x}) &= \mathbf{A}(b) + \mathbf{A}(\mathbf{y}).\end{aligned}$$

**Proof.** The above equations follow at once from Equations (4.2), (4.3), and the definitions of the gradings on the algebra, Equations (3.9) and (3.8).  $\square$

**Proposition 6.3.** *The map  $\delta^1$  defined above satisfies a curved type  $D$  structure relation, with curvature  $\mu_0 = \sum_{\{r,s\} \in M} U_r \cdot U_s$ .*

**Proof.** Choose  $\mathbf{x}$  and  $\mathbf{z}$  so that there is some  $B \in \mathcal{D}(\mathbf{x}, \mathbf{y})$  with  $\mathbf{m}(B) = 2$ . Consider the ends of the moduli spaces  $\widehat{M}^B(\mathbf{x}, \mathbf{z}, \mathcal{S}; \vec{P})$ , where we take the union over all choices of typical Reeb sequences  $[\vec{P}] = (\rho_1, \dots, \rho_\ell)$  and all choices of source  $\mathcal{S}$ . We can assume without loss of generality that the homology class  $B$  of the curve does not cover all of  $\Sigma$ ; for otherwise, the corresponding term in  $(\mu_2 \otimes \text{Id}_{R(\mathcal{H}^\wedge)}) \circ (\text{Id}_C \otimes \delta^1) \circ \delta^1$  vanishes; there are no non-zero algebra elements with positive weight everywhere.

These moduli spaces are one-dimensional according to Theorem 5.22. Next we appeal to Theorem 5.26, observing cancellations of the counts of various ends cancel. The various collision ends where at least one of  $\rho_i$  or  $\rho_{i+1}$  is a Reeb orbit cancel with one another. Specifically, consider a typical Reeb sequence  $(\rho_1, \dots, \rho_i, \rho_{i+1}, \dots, \rho_\ell)$  with a visible collision end for  $\rho_i$  and  $\rho_{i+1}$ , where at least one of the two is a Reeb orbit (i.e. in the terminology of Theorem 5.26, this is an end of type (DE-3)). These ends correspond to the corresponding collision end of the moduli space where the order of  $\rho_i$  and  $\rho_{i+1}$  are permuted. (This is a different moduli space, since the collision is visible.) Similarly, if  $\rho_i$  and  $\rho_{i+1}$  are two Reeb chords that are not weakly composable (a subcase of (DE-4)), we can permute them to get another moduli space with a corresponding end. When  $\rho_i$  and  $\rho_{i+1}$  are strongly composable chords, the corresponding ends cancel against orbit ends (Type (DE-2)).

The two types of ends left unaccounted for are the two-story ends (Type (DE-1)) and the boundary degeneration ends (Type (DE-5)). The fact there is an even number of remaining ends gives the type  $D$  structure relation.  $\square$

The above three propositions can be summarized as follows: the vector space  $R(\mathcal{H}^\wedge)$ , with differential as in Equation (6.2) is a curved type  $D$  structure, with a homological grading induced by  $\mathbf{m}$  and Alexander gradings  $\mathbf{A}$ .

The following invariance property of this curved type  $D$  structure will be important for us:

**Proposition 6.4.** *If  $J_0$  and  $J_1$  are any two generic almost-complex structures, there is a type  $D$  structure quasi-isomorphism of graded type  $D$  structures*

$$R(\mathcal{H}^\wedge, J_0) \simeq R(\mathcal{H}^\wedge, J_1).$$

**Proof.** As usual, one must show that a path  $\{J_t\}_{t \in [0,1]}$  induces a type  $D$  morphism. This is done via the straightforward modification of Theorem 5.26 to varying

$\{J_t\}$ , and considering moduli spaces between generators  $\mathbf{x}$  and  $\mathbf{y}$  where the with index 1. Specifically, fix a generic one-parameter family  $\{J_t\}_{t \in [0,1]}$  of almost-complex structures, and consider the moduli space  $\mathcal{M}^B(\mathbf{x}, \mathbf{y}; \{J_t\})$  of  $J_t$ -holomorphic curves, where  $t$  is the second parameter in the projection to  $[0, 1] \times \mathbb{R}$  (parameterized by pairs  $(s, t)$ ). For such moduli spaces, the ends of Type (DE-5) do not exist (such moduli spaces connect a generator to itself; and indeed they count curves with index 2). With this remark in place, the above proof of Proposition 6.3 shows that there is an even number of two-story ends. This immediately shows that the map

$$h^1(\mathbf{x}) = \sum_{\mathbf{y} \in \mathfrak{S}, B \in \mathcal{D}(\mathbf{x}, \mathbf{y})} \hat{b}(B) \otimes \# \mathcal{M}^B(\mathbf{x}, \mathbf{y}; \{J_t\}) \cdot \mathbf{y}.$$

gives a type  $D$  morphism

$$h^1: R(\mathcal{H}^\wedge, J_0) \rightarrow \mathcal{C}(n) \otimes R(\mathcal{H}^\wedge, J_1).$$

Homotopies of paths of complex structures induce homotopies of type  $D$  morphisms and the identity path induces the identity map as usual; so it follows that  $h^1$  is a type  $D$  quasi-isomorphism.

Verifying that the maps are graded is straightforward.  $\square$

**Remark 6.5.** *The above proposition shows that the quasi-isomorphism type of the type  $D$  structure of an upper Heegaard diagram is independent of the analytical choices (of almost-complex structures) made. One could aim for more invariance. One could think of an upper Heegaard diagram as in fact representing an upper knot diagram, and then try to prove dependence of the type  $D$  structure only on the upper knot diagram; and indeed one could try to show that it is an invariant of the tangle represented by the diagram. We do not pursue this route, in the interest of minimizing the road to Theorem 1.1.*

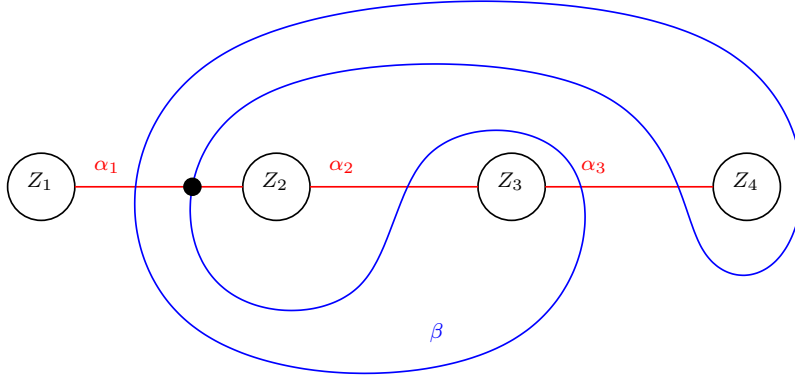


FIGURE 17. **Upper Heegaard diagram.** This diagram has five Heegaard states, corresponding to the five intersection points of  $\beta$  with  $\alpha_1 \cup \alpha_2 \cup \alpha_3$ . One of these ( $x_2$  in the text) is indicated in black.

**6.1. Examples.** We start with a simple example. Consider the upper Heegaard diagram from Figure 17. This has five Heegaard states, which we label from left to

right,  $x_1, x_2, t, y_1, y_2$ . Since we have  $d = 1$ , the curve counting is straightforward, and we find that the type  $D$  structure is as indicated in the following diagram:

$$(6.3) \quad \begin{array}{ccccccc} & & & L_2 L_3 & & & \\ & & & \curvearrowright & & & \\ x_1 & \xrightarrow{U_4} & x_2 & \xrightarrow{L_2 U_1} & t & \xrightarrow{L_3} & y_1 & \xrightarrow{U_2} & y_2 \\ & \xleftarrow{U_3} & & \xleftarrow{R_2} & & \xleftarrow{R_3 U_4} & & \xleftarrow{U_1} & \\ & & & \curvearrowleft & & & & & \\ & & & R_3 R_2 & & & & & \end{array}$$

We give a (very simple) family of examples which will play a fundamental role in our future computations.

For  $n > 1$ , consider the matching  $M = \{\{1, 2\}, \{3, 4\}, \dots, \{2i-1, 2i\}, \dots, \{2n-1, 2n\}\}$  on  $\{1, \dots, 2n\}$  where  $2i-1$  is matched with  $2i$  for  $i = 1, \dots, n$ . Let  $\mathbf{s} = \{2i-1\}_{i=1}^n$ , and  $\mu_0 = \sum_{i=1}^n U_{2i-1} U_{2i}$ . The type  $d$  structure with a single generator  $\mathbf{x}$  satisfying  $\mathbf{I}_{\mathbf{s}} \cdot \mathbf{x} = \mathbf{x}$  and  $\delta^1(\mathbf{x}) = 0$  can be viewed as a curved module over  $\mathcal{C}(n)$  since  $\mathbf{I}_{\mathbf{s}} \cdot \mu_0 = 0$ . We write this type  $D$  structure  ${}^{\mathcal{C}^*}k$ ,

**Lemma 6.6.** *For any  $n > 1$ , let  $\mathcal{H}^\wedge$  denote the standard upper diagram with  $2n$  local maxima (pictured in Figure 4; after deleting  $\beta_4$  and the basepoints  $w$  and  $z$ ). There is an identification of type  $D$  structures*

$$R(\mathcal{H}^\wedge) \cong {}^{\mathcal{C}^*}k.$$

**Proof.** The diagram has exactly one Heegaard state  $\mathbf{x}$ ; it has  $\mathbf{I}_{\mathbf{s}} \cdot \mathbf{x} = \mathbf{x}$ ; and there are no holomorphic curves that can induce  $\delta^1$ -actions.  $\square$

## 7. MORE HOLOMORPHIC CURVES

We describe here the pseudo-holomorphic curves used in the constructions of the type  $A$  modules for a given lower diagram  $\mathcal{H}^\vee$ . The moduli spaces we consider here are similar to the ones considered in Section 5, except that now the limiting values as  $t \mapsto \pm\infty$  are lower (rather than upper) Heegaard states; moreover, the partitions we consider here  $P = (\rho_1, \dots, \rho_\ell)$  of the east and interior punctures need not be simple (c.f. Definition 5.2): each term in the partition  $\rho_i$  is some (non-empty) subset of chords and orbits. More formally:

**Definition 7.1.** *a constraint packet  $\rho$  is a pair consisting of a set of Reeb orbits, denoted  $\text{orb}(\rho)$ ; and a set of Reeb chords, denoted  $\text{cho}(\rho)$ .*

Thus, in our curve counting, for the partition  $(\rho_1, \dots, \rho_\ell)$ , each term  $\rho_i$  is a constraint packet. Sometimes, we find it convenient to generalize this slightly: a *generalized constraint packet*, consisting of *multi-sets* of Reeb orbits and chords (i.e. the same chord or orbit can occur with positive multiplicity).

The differential and, indeed, all the module actions (of sequences of algebra elements on the module) will count pseudo-holomorphic curves with constraint packets specified by algebra elements; and these constraint packets will have a rather special form (cf. Definition 8.6). In particular, each constraint packet in the algebra action definition will contain at most one Reeb orbit.

We will prove an  $\mathcal{A}_\infty$  relation for modules, which will involve analyzing ends of one-dimensional moduli spaces. Two story building degenerations correspond to terms in the  $\mathcal{A}_\infty$  relation involving two applications of the module actions. In [10], these moduli spaces have another kind of end, called *join curve ends*, which correspond to the differential in the bordered algebra. By contrast, in the present case, join curve ends of the various moduli spaces which we consider cancel in pairs. (One could construct a larger algebra than the one considered here, equipped with a differential, so that the join curve ends of moduli spaces correspond to terms in the differential of the algebra. The present algebra can be thought of as the homology of this larger algebra.) See Figure 20 for an illustration. As [10], there are also *collision ends*, which correspond to multiplication in the algebra. There is another new kind of end, corresponding to the formation of  $\beta$ -boundary degenerations. Some of these cancel against orbit curve ends; the remaining orbit ends are accounted for by the curvature of our algebra.

Our goal here is to formulate the moduli spaces we consider precisely, and to describe the ends of one-dimensional moduli spaces. The algebraic interpretations of the counts of these ends described above will be given in detail in Section 8.

**7.1. Pseudo-holomorphic flows in lower diagrams.** We will need to name Reeb chords for lower diagrams as shown in Figure 18; i.e. switched from the conventions from the type  $D$  side; c.f. Figure 13). This will be useful for the gluing of diagrams. As a point of comparison: the chord labelled  $L_i$  on the  $D$  side has initial point on  $\alpha_{i-1}$  and terminal point on  $\alpha_i$ ; while the chord labelled  $L_i$  on the  $A$  side has initial point on  $\alpha_i$  and terminal point on  $\alpha_{i-1}$ .

Strong boundary monotonicity is a closed condition, in the following sense:



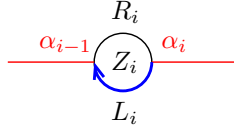


FIGURE 18. **Names of Reeb chords for lower diagrams.** The Reeb chord  $L_i$  is indicated by the oriented half circle.

**Lemma 7.2.** *Suppose that  $u$  is a pseudo-holomorphic flowline which appears in the Gromov limit of a sequence of strongly boundary monotone curves. Then  $u$ , is strongly boundary monotone, as well.*

**Proof.** This follows exactly as in [10, Lemma 5.55]: strong boundary monotonicity can be phrased in terms of the monotonicity of the function  $t \circ u$  restricted to each boundary component. Monotone functions can limit to constant functions, but in that case, there is an  $\alpha$ -boundary degeneration component, which in turn is ruled out by Condition (AM-9).  $\square$

Given a lower diagram  $(\Sigma, \alpha, \beta, w, z)$ , the operations on the type  $A$  module are defined by counting  $J$ -holomorphic curves

$$u: (S, \partial S) \rightarrow (\Sigma \times [0, 1] \times \mathbb{R}, (\alpha \times \{1\} \times \mathbb{R}) \cup (\beta \cup \{0\} \times \mathbb{R})),$$

subject to the constraints (M-1)-(M-7) and (M-8), with the understanding that presently, we set

$$(7.1) \quad d = g + n.$$

We will make the following further hypothesis:

(AM-9) At least one of  $n_w(u)$  or  $n_z(u)$  vanishes.

The strong boundary monotonicity condition on such a map  $u$  looks exactly as it did earlier (c.f. Condition (M-8s)). As in Section 5, this condition can be formulated in terms of combinatorial data. Specifically, given a lower generator  $\mathbf{x}$  and a sequence of sets of Reeb chords and orbits  $(\rho_1, \dots, \rho_\ell)$ , define the terminal  $\alpha$ -set and strong boundary monotonicity of  $(\mathbf{x}, \rho_1, \dots, \rho_\ell)$  as in Definition 5.7, with the understanding that now  $\mathbf{x}$  is a lower, rather than upper, Heegaard state.

Given lower Heegaard states  $\mathbf{x}, \mathbf{y}$ , a marked source  $\mathcal{S}$  a strongly boundary monotone sequence  $\rho_1, \dots, \rho_\ell = \vec{\rho}$ , we can form moduli spaces of such pseudo-holomorphic flows, denoted  $\widehat{M}(\mathbf{x}, \mathbf{y}, \mathcal{S}, \rho_1, \dots, \rho_\ell)$  or simply  $\widehat{M}(\mathbf{x}, \mathbf{y}, \mathcal{S}; \vec{\rho})$ .

Lemma 5.8 has the following straightforward adaptation:

**Lemma 7.3.** *If  $(\mathbf{x}, \vec{\rho})$  is strongly boundary monotone and  $u \in M^B(\mathbf{x}, \mathbf{y}, \mathcal{S}, \vec{\rho})$ , then  $u$  is strongly boundary monotone. Conversely, if  $u \in M^B(\mathbf{x}, \mathbf{y}, \mathcal{S}, \vec{\rho})$  is strongly boundary monotone, then  $(\mathbf{x}, \vec{\rho})$  is strongly boundary monotone.*  $\square$

Let  $\rho$  be a constraint packet consisting entirely of chords (i.e. it contains no orbits). Think of each  $\rho \in \rho$  as a path in  $[0, 1] \times Z$ . Let  $\text{inv}(\rho)$  denote the minimal number of crossings between the various chords. Given any point  $p \in Z$ , let  $m([\rho], p)$  denote the multiplicity with which the Reeb chords in  $\rho$  cover  $p$ , with the convention that

if  $p = \alpha_i \cap Z_i$  or  $\alpha_{i-1} \cap Z_i$ , then  $m([\rho], p)$  is the average of  $m([\rho], p')$  over the two nearby choices  $p' \in Z$  on both sides of  $p$ . For example, if  $p = \alpha_i \cap Z_i$  or  $\alpha_{i-1} \cap Z_i$ , then  $m(L_i, p) = 1/2$ .

Let

$$(7.2) \quad \iota(\rho) = \text{inv}(\rho) - m([\rho], \rho^-).$$

(Note that  $m([\rho], \rho^-) = m([\rho], \rho^+)$ .)

**Example 7.4.** If  $\rho$  is a single Reeb chord, then  $\iota(\{\rho\}) = -\omega(\rho)$ .

**Example 7.5.** Fix integers  $a, b \geq 0$ ,  $i \in \{2, \dots, 2n-1\}$ , and let  $\rho_1 = (L_i R_i)^\alpha L_i$ ,  $\rho_2 = (R_i L_i)^\beta R_i$ , and  $\rho = \{\{\rho_1\}, \{\rho_2\}\}$ . Then,

$$\begin{aligned} \text{inv}(\rho_1, \rho_2) &= |\alpha - \beta| \\ m([\{\rho_1, \rho_2\}], \{\rho_1, \rho_2\}^-) &= 2(\alpha + \beta + 1). \end{aligned}$$

Note that  $\iota(\{(L_i R_i)^{\alpha+\beta+1}\}) = -\alpha - \beta - 1$ , so

$$\iota(\rho) - \iota(\{(L_i R_i)^{\alpha+\beta+1}\}) = |\alpha - \beta| - \alpha - \beta - 1 \leq -1,$$

with equality iff  $a = 0$  or  $b = 0$ .

**Example 7.6.** Fix integers  $a, b \geq 1$ ,  $i \in \{2, \dots, 2n-1\}$ ; let  $\rho_1 = (L_i R_i)^a$ ,  $\rho_2 = (R_i L_i)^b$ , and  $\rho = \{\rho_1, \rho_2\}$ . Then

$$\begin{aligned} \text{inv}(\{\rho_1\}, \{\rho_2\}) &= |a - b| \\ m([\{\rho_1, \rho_2\}], \{\rho_1, \rho_2\}^-) &= 2a + 2b. \end{aligned}$$

Note that  $\iota(\rho_1) = -a$ ,  $\iota(\rho_2) = -b$ ; so

$$\iota(\{\rho_1, \rho_2\}) = |a - b| - 2a - 2b < -a - b = \iota(\{\rho_1\}) + \iota(\{\rho_2\}).$$

**7.2. The chamber structure on  $\mathbb{T}_\beta$ .** We will be interested in some further structure on  $\mathbb{T}_\beta$  induced by the boundary degenerations, as defined in Definition 5.17 (using  $d$  now as in Equation (7.1)).

For each  $\{j, k\} \in M^\vee$ , there is a corresponding component of  $\mathcal{B}_{\{j, k\}}$  of  $\Sigma_0 \setminus \mathcal{B}$ , which contains the two boundary components  $Z_j$  and  $Z_k$ ; or equivalently, component  $\mathcal{B}_{\{j, k\}} \subset \Sigma \setminus \mathcal{B}$  which contains the two punctures corresponding to  $Z_j$  and  $Z_k$ .

Let  $t: \mathbb{H} \cong [0, \infty) \times \mathbb{R} \rightarrow \mathbb{R}$  denote the projection to the second factor. Given  $w \in \mathcal{N}_J^{\mathcal{B}_{\{j, k\}}}$ , we have two punctures  $q_1$  and  $q_2$ , labelled by orbits  $j$  and  $k$  respectively. Let  $\delta(w) = t \circ w(q_1) - t \circ w(q_2)$ . Note that  $\delta(w)$  is not invariant under conformal automorphisms of  $\mathbb{H}$ ; but the sign of  $\delta(w)$  is.

**Lemma 7.7.** For generic  $J$ , the subspace of  $d$ -dimensional torus  $\mathbb{T}_\beta$

$$\mathcal{W}^{o_j=o_k} = \{\mathbf{x} \in \mathbb{T}_\beta \mid \exists v \in \hat{\mathcal{N}}^{\mathcal{B}_{\{j, k\}}}(\mathbf{x}) \text{ so that } \delta(v) = 0\}$$

is the image under a smooth map of a smooth manifold of dimension  $d-1$ .

**Proof.** The map  $\delta: \mathcal{N}^{\mathcal{B}_{\{j, k\}}}(\mathbf{x}) \rightarrow \mathbb{R}$  is a smooth map. By transversality arguments, for generic  $J$ , 0 is a regular value, so  $\delta^{-1}(0)$  is a submanifold. Similarly, if we take the quotient by the automorphism of group of  $\mathbb{H}$ , the quotient of  $\delta^{-1}(0)$  is a codimension one submanifold of  $\hat{\mathcal{N}}^{\mathcal{B}_{\{j, k\}}}(\mathbf{x})$ . Now,  $\mathcal{W}^{o_j=o_k}$  is the image of this submanifold under the evaluation map  $\text{ev}^\beta$  from Definition 5.18.  $\square$

We have the following analogue of Lemma 5.20 for lower diagrams:

**Lemma 7.8.** *The evaluation map  $\text{ev}^\beta: \mathcal{N}_J^{\mathcal{B}_{\{r,s\}}} \rightarrow \mathbb{T}_\beta$  has odd degree.*

It follows that the complement of  $\mathcal{W}^{o_j=o_k}$  in  $\mathbb{T}_\beta$  consists of two (disjoint) chambers:

$$\begin{aligned} \mathcal{C}^{o_j > o_k} &= \{\mathbf{x} \in \mathbb{T}_\beta \mid \#(w \in \mathcal{N}_{\{j,k\}}^{\mathcal{B}}(\mathbf{x}) \text{ so that } \delta(w) > 0) \equiv 1 \pmod{2}\} \\ \mathcal{C}^{o_j < o_k} &= \{\mathbf{x} \in \mathbb{T}_\beta \mid \#(w \in \mathcal{N}_{\{j,k\}}^{\mathcal{B}}(\mathbf{x}) \text{ so that } \delta(w) < 0) \equiv 1 \pmod{2}\} \end{aligned}$$

### 7.3. Smooth moduli spaces.

**Definition 7.9.** *Let  $\mathbf{x}$  and  $\mathbf{y}$  be lower states, suppose that  $(B, \rho_1, \dots, \rho_\ell) = (B, \vec{\rho})$  is strongly boundary monotone. Define*

$$(7.3) \quad \chi_{\text{emb}}(B, \vec{\rho}) = d + e(B) - n_{\mathbf{x}}(B) - n_{\mathbf{y}}(B) - \sum_{i=1}^{\ell} \left( \iota(\text{cho}(\rho_i)) + \mathfrak{w}(\text{cho}(\rho_i)) \right)$$

$$(7.4) \quad \begin{aligned} \text{ind}(B, \mathbf{x}, \mathbf{y}; \vec{\rho}) &= e(B) + n_{\mathbf{x}}(B) + n_{\mathbf{y}}(B) + \ell \\ &\quad - \mathfrak{w}(\vec{\rho}) + \iota(\text{cho}(\vec{\rho})) + \sum_{o \in o(\vec{\rho})} (1 - \mathfrak{w}(o)), \end{aligned}$$

where

$$\iota(\vec{\rho}) = \sum_{i=1}^{\ell} \iota(\text{cho}(\rho_i)) \quad \text{and} \quad \mathfrak{w}(\rho) = \sum_{i=1}^{\ell} \mathfrak{w}(\rho_i),$$

**Remark 7.10.** *Note that in the special case where each packet in  $\vec{\rho}$  contains a single chord (so we write  $\vec{\rho} = \vec{\rho}$ ), Example 7.4 shows that  $\iota(\vec{\rho}) = -\mathfrak{w}(\vec{\rho})$ ; so the above definition of the embedded index is consistent with Equation (5.2).*

We have the following analogue of Proposition 5.16

**Proposition 7.11.** *Suppose that  $(\mathbf{x}, \vec{\rho})$  is strongly boundary monotone. If  $\mathcal{M}^B(\mathbf{x}, \mathbf{y}, \mathcal{S}; \vec{\rho})$  is represented by some pseudo-holomorphic  $u$ , then  $\chi(\mathcal{S}) = \chi_{\text{emb}}(B)$  if and only if  $u$  is embedded. In this case, the expected dimension of the moduli space is computed by  $\text{ind}(B, \mathbf{x}, \mathbf{y}; \vec{\rho})$ . Moreover, if a strongly monotone moduli space  $\mathcal{M}^B(\mathbf{x}, \mathbf{y}, \mathcal{S}; \vec{\rho})$  has a non-embedded holomorphic representative, then its expected dimension  $\leq \text{ind}(B, \mathbf{x}, \mathbf{y}; \vec{\rho}) - 2$ .*

**Proof.** To deduce Equation (7.3), we apply the proof of Proposition 5.16. As in that proof, we compare the intersection number  $u \cap \tau_R(u) = n_{\mathbf{x}}(B) + n_{\mathbf{y}} - \frac{d}{2}$  with  $u \cap \tau_\epsilon(u)$ . In that argument, we used the fact that  $\tau_\epsilon(u) = b_\Sigma$ . In the present case, however, there are additional intersection points from  $u \cap \tau_\epsilon(u)$  that come from the double points at the boundary (arising from the constraint packets). Thus,

$$u \cap \tau_\epsilon(u) = b_\Sigma + \sum_{i=1}^{\ell} N(\text{cho}(\rho_i)),$$

where  $N(\rho_i)$  is the number of intersection points of  $u \cap \tau_\epsilon(u)$  that come from the constraint packet  $\rho_i$ . We will show that

$$(7.5) \quad N(\text{cho}(\rho)) = -\iota(\text{cho}(\rho)) - \mathfrak{w}(\text{cho}(\rho)).$$

To see this, note that contributions arise only for pairs of chords in the packet that are contained in some fixed boundary component  $\widehat{Z}_j$ . Suppose then that there are exactly two chords  $\rho_1$  and  $\rho_2$  in  $\boldsymbol{\rho}$  that are contained in  $\widehat{Z}_j$ . Suppose that the length of  $\rho_1$  is  $a$  and the length of  $\rho_2$  is  $b$ . (Here, we normalize so that the whole boundary has length 1; so in particular  $L_i$  has length  $\frac{1}{2}$ .) By boundary monotonicity,  $a + b$  is an integer. In our local model, the surface has a component where  $f$  is modelled on  $\tau \mapsto \tau^{2a}$  and another modeled on  $\tau \mapsto c \cdot \tau^{2b}$ , for  $\tau \in \mathbb{C}$  with  $\operatorname{Re}(\tau) \geq 0$ , and some  $c \in \mathbb{R}^{<0}$ . To count double points, we can halve the number of double points on the maps  $\tau \mapsto \tau^{2a}$  and  $\tau \mapsto c \cdot \tau^{2b}$  for  $\tau \in \mathbb{C}$ . Counting double points there is equivalent to counting the intersection number of the quadratic function  $(z - \tau^{2a})(z - c\tau^{2b})$  with the discriminant locus, which in turn is equivalent to the order of vanishing of the function

$$(\tau^{2a} + c\tau^{2b})^2 - 4c\tau^{2(a+b)} = (\tau^{2a} - c\tau^{2b})^2 = \min(4a, 4b),$$

which, by Examples 7.5 and 7.6, verifies Equation (7.5). (Note that the when  $a$  has fractional length, we are using Example 7.5 with  $a = \alpha + \frac{1}{2}$ ,  $b = \beta + \frac{1}{2}$ .)

Having verified Equation (7.5), Equation (7.3) follows at once.

Deducing the index from the Euler characteristic as in proof of Proposition 5.16, noting that

$$\operatorname{ind} = 2e + b_{\mathbb{D}} - \sum_{i=1}^{\ell} (|\boldsymbol{\rho}_i| - 1) + \sum_{\rho \in \operatorname{cho}(\boldsymbol{\rho}_i)} (1 - 2\omega(\rho)) + \sum_{o \in \operatorname{orb}(\boldsymbol{\rho}_i)} (2 - 2\omega(o)).$$

□

**Example 7.12.** Consider the shadow in Figure 19. This shadow occurs for four different boundary monotone moduli spaces:  $\widehat{\mathcal{M}}^B(\mathbf{x}, \mathbf{y}, (\{o_i\}; \mathcal{S}_1))$ , where  $\mathcal{S}_1$  is a disk with four boundary punctures, and a single orbit puncture;  $\widehat{\mathcal{M}}^B(\mathbf{x}, \mathbf{y}, (\{L_i R_i\}; \mathcal{S}_2))$ , where  $\mathcal{S}_2$  is a disk with five boundary punctures (one of which is an East infinity boundary puncture, labelled by  $L_i R_i$ );  $\widehat{\mathcal{M}}^B(\mathbf{x}, \mathbf{y}, (\{R_i L_i\}; \mathcal{S}_3))$ , similar to the above moduli space, and finally,  $\widehat{\mathcal{M}}^B(\mathbf{x}, \mathbf{y}, (\{L_i, R_i\}; \mathcal{S}_4))$ , where  $\mathcal{S}_4$  is a disjoint union of two three-punctured disks (one of which has an East infinity puncture labelled by  $L_i$  and the other of which has a puncture labelled by  $R_i$ ). The dimensions of these moduli spaces are 2, 1, 1, and 0 respectively.

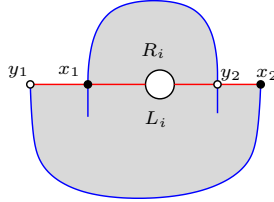


FIGURE 19. Moduli spaces with given shadow.

There are evaluation maps  $\operatorname{ev}_i^{\beta}: \mathcal{M}(\mathbf{x}, \mathbf{y}, \boldsymbol{\rho}_1, \dots, \boldsymbol{\rho}_{\ell}) \rightarrow \mathbb{T}_{\beta}$ , obtained as follows. Suppose that the punctures at level  $\boldsymbol{\rho}_i$  are mapped via  $t$  to  $\tau \in \mathbb{R}$ ; then

$$\operatorname{ev}_i^{\beta}(v) = \pi_{\Sigma}^{-1}(\{(0, \tau)\}).$$

These maps descend to give maps

$$(7.6) \quad \text{ev}_i^\beta: \widehat{\mathcal{M}}(\mathbf{x}, \mathbf{y}, \boldsymbol{\rho}_1, \dots, \boldsymbol{\rho}_\ell) \rightarrow \mathbb{T}_\beta.$$

The following is a mild elaboration on Theorem 5.22 (see [10, Proposition 5.6]):

**Theorem 7.13.** *Choose a generic  $\{J_t\}$ . Suppose that  $(\mathbf{x}, \vec{\rho})$  is boundary monotone. If  $\text{ind}(B, \mathbf{x}, \mathbf{y}; \vec{\rho}) \leq 2$ , then the moduli space  $\mathcal{M}^B(\mathbf{x}, \mathbf{y}, \mathcal{S}; \vec{\rho})$  is a smooth manifold of dimension given by  $\text{ind}(B, \mathbf{x}, \mathbf{y}; \vec{\rho})$ . Moreover,  $\text{ev}_i^\beta$  are transverse to all of the walls  $\mathcal{W}^{o_j=o_k}$  for all  $\{r, s\} \in M^\vee$ ; in particular, all the disks  $v$  appearing in the zero-dimensional moduli spaces  $\widehat{\mathcal{M}}^B(\mathbf{x}, \mathbf{y}, \mathcal{S}, \vec{\rho})$  with  $\text{ind}(B, \mathbf{x}, \mathbf{y}; \vec{\rho}) = 1$  have  $\text{ev}_i^\beta \in \mathcal{C}^{o_j > o_k}$  or  $\mathcal{C}^{o_j < o_k}$ .*

**Proof.** For generic  $\{J_t\}$ , the moduli spaces  $\mathcal{M}^B(\mathbf{x}, \mathbf{y}; \mathcal{S})$  are transversely cut out by the  $\bar{\partial}$  operator. The  $t$  evaluations of the various punctures give a map from this moduli space to  $\mathbb{R}^P$ , where the set  $P$  corresponds with the interior and  $\mathbf{e}$ -punctures of  $\mathcal{S}$ . This map  $\text{ev}_P: \mathcal{M}^B(\mathbf{x}, \mathbf{y}; \mathcal{S}) \rightarrow \mathbb{R}^P$  is a submersion. The moduli space  $\mathcal{M}^B(\mathbf{x}, \mathbf{y}; \mathcal{S}; \vec{\rho})$  can be thought of as the preimage under this evaluation map of a suitable diagonal  $\Delta_P$  in  $\mathbb{R}^P$ . (For example, if some subset  $\{p_1, \dots, p_k\}$  of punctures are assigned to the same constraint packet, then the corresponding diagonal in  $\mathbb{R}^P$  consists of those  $P$ -tuples whose components at  $p_1, \dots, p_k$  coincide.) It follows readily that  $\mathcal{M}^B(\mathbf{x}, \mathbf{y}, \mathcal{S}; \vec{\rho})$  is a smooth manifold of dimension given by  $\text{ind}(B, \mathbf{x}, \mathbf{y}; \vec{\rho})$ .

At each puncture  $p$ , we also have a corresponding evaluation map  $\text{ev}_p^\beta: \mathcal{M}^B(\mathbf{x}, \mathbf{y}; \mathcal{S})$  defined by  $\text{ev}_p^\beta(v) = \pi_\Sigma^{-1}(\{(0, t(v(p)))\})$ ; taking the product over each puncture gives a submersion

$$\text{ev}_P^\beta: \mathcal{M}^B(\mathbf{x}, \mathbf{y}; \mathcal{S}) \rightarrow (\mathbb{T}_\beta)^P.$$

It follows that for generic  $\{J_t\}$ , the evaluations are transverse to the diagonals in  $\mathbb{R}^P$  and the walls  $\mathcal{W}^{o_j=o_k}$  from Lemma 7.7; in particular, for generic  $\{J_t\}$ ,  $\text{ev}_i^\beta$  on  $\widehat{\mathcal{M}}(\mathbf{x}, \mathbf{y}, \boldsymbol{\rho}_1, \dots, \boldsymbol{\rho}_\ell)$  (which is obtained by evaluating  $\text{ev}_p^\beta$  at any puncture  $p$  belonging to the  $i^{\text{th}}$  packet) is transverse to the codimension one walls  $\mathcal{W}^{o_j=o_k}$ . (Compare [10, Proposition 5.6]; see also [15, Section 3.4].)  $\square$

If a holomorphic curve  $v$  represents a point in  $\widehat{\mathcal{M}}^B(\mathbf{x}, \mathbf{y}; \mathcal{S}; \vec{\rho})$  with  $\text{ev}_i^\beta \in \mathcal{C}^{o_j > o_k}$  or  $\mathcal{C}^{o_j < o_k}$ , we write  $v \in \mathcal{C}_i^{o_j > o_k}$  or  $\mathcal{C}_i^{o_j < o_k}$ .

**7.4. Ends of one-dimensional moduli spaces.** We set up some preliminaries used in the description of the ends of one-dimensional moduli spaces.

**Definition 7.14.** *Observe that there are two special Reeb orbits which are not matched with any other Reeb orbit. If  $o_j$  is one of these orbits, recall that the corresponding component of  $\Sigma \setminus \beta$ , which we denote  $\mathcal{B}_{\{j\}}$ , contains one of the two basepoints  $w$  or  $z$ . We call the other orbits non-special. An orbit marking is a partition of the orbits into two types, the even ones and the odd ones, so that the following conditions hold:*

- each even one is matched with an odd one in  $M^\vee$ .
- there is exactly one even special orbit and one odd one.

**Definition 7.15.** Fix an orbit marking. A constraint packet is called *allowed* by the orbit marking, or simply *allowed*, if it satisfies the following properties:

- ( $\rho$ -1) Each of the chords appearing in  $\rho$  are disjoint from one another.
- ( $\rho$ -2) It contains at most one orbit, and that orbit is simple. If it contains no orbits, it is called *orbitless*.
- ( $\rho$ -3) If  $\rho$  contains an even type orbit, then it contains exactly one Reeb chord, as well; and the chord is disjoint from the orbit.
- ( $\rho$ -4) If  $\rho$  contains an odd type orbit, then it contains no Reeb chords.

Given two constraint packets  $\rho_1$  and  $\rho_2$ , a *contained collision* is a new (possibly generalized) constraint packet  $\sigma$ , where  $\text{orb}(\sigma) = \text{orb}(\rho_1) \cup \text{orb}(\rho_2)$  as multi-sets (i.e. it might consist of the same orbit with multiplicity 2), and  $\text{cho}(\sigma)$  is the union of the following three sets:

- those Reeb chords in  $\rho_1$  that cannot be prepended onto any Reeb chord in  $\rho_2$
- those Reeb chords in  $\rho_2$  that cannot be appended to any Reeb chord in  $\rho_1$
- the joins  $\rho_1 \uplus \rho_2$  of all possible pairs of joinable (i.e. “strongly composable”) Reeb chords  $\rho_1 \in \text{cho}(\rho_1)$  and  $\rho_2 \in \text{cho}(\rho_2)$ .

The contained collision is called *visible* if no orbit in  $\text{orb}(\sigma)$  is contained in both  $\text{orb}(\rho_1)$  and  $\text{orb}(\rho_2)$ . The collision is called *strongly composable* if whenever the chords  $\rho_1 \in \text{cho}(\rho_1)$  and  $\rho_2 \in \text{cho}(\rho_2)$  are weakly composable (as in Definition 5.24), they are in fact strongly composable.

**Remark 7.16.** A collision between two constraint packets  $\rho_1$  and  $\rho_2$  might be merely a generalized constraint packet. For example, both  $\rho_1$  and  $\rho_2$  may contain the same orbit, and their collision can contain the same orbit with multiplicity two. When the collision is contained and visible this does not occur: the multi-set of orbits in the collision is in fact a set. (Indeed, if the collision occurs in a boundary monotone sequence, it is also easy to see that the multi-set of chords is also a set.)

**Definition 7.17.** Suppose that  $\rho_1$  and  $\rho_2$  are allowed constraint packets (in the sense of Definition 7.15), which also have the property that there are  $\{j, k\} \in M^\vee$  so that  $o_j \in \text{orb}(\rho_1)$  and  $o_k \in \text{orb}(\rho_2)$ . In this case,  $\text{cho}(\rho_1) \cup \text{cho}(\rho_2)$  consists of a single chord, which we denote  $\sigma$ . We say that the constraint packet is  $\{\sigma\}$  (i.e. with the two orbits removed) is the boundary degeneration collision of  $\rho_1$  and  $\rho_2$ .

With these remarks in place, we state the following analogue of [10, Theorem 5.61], which will be used in Section 8 in the verification of the  $\mathcal{A}_\infty$  relation:

**Theorem 7.18.** Let  $\mathcal{H}^\vee$  be a lower diagram and  $M^\vee$  the induced relation among  $\{1, \dots, 2n\}$ . Choose also an orbit marking as in Definition 7.14. Fix a lower Heegaard state  $\mathbf{x}$  and a sequence of constraint packets  $\vec{\rho}$  with the following properties:

- $(\mathbf{x}, \vec{\rho})$  is strongly boundary monotone.
- Each constraint packet  $\rho_i$  is allowed, in the sense of Definition 7.15

Let  $\mathbf{y}$  be a lower Heegaard state, and  $B \in \pi_2(\mathbf{x}, \mathbf{y})$ , whose local multiplicity vanishes either at  $w$  or  $z$  (or both). Choose  $\mathcal{S}$  and  $\vec{P}$  so that  $[\vec{P}] = (\rho_1, \dots, \rho_\ell)$  and so that  $\chi(\mathcal{S}) = \chi_{\text{emb}}(B)$ ; and suppose that  $\text{ind}(B, \mathbf{x}, \mathbf{y}; \vec{\rho}) = 2$ , and abbreviate

$\widehat{m} = \widehat{m}^B(\mathbf{x}, \mathbf{y}; \mathcal{S}; \vec{\rho})$ . The total number of ends of  $\widehat{m}$  of the following types are even in number:

(AE-1) Two-story ends, which are of the form

$$\widehat{m}(\mathbf{x}, \mathbf{w}; \mathcal{S}_1; \rho_1, \dots, \rho_i) \times \widehat{m}(\mathbf{w}, \mathbf{y}; \mathcal{S}_2; \rho_{i+1}, \dots, \rho_\ell),$$

taken over all lower Heegaard states  $\mathbf{w}$  and choices of  $\mathcal{S}_1$  and  $\mathcal{S}_2$  so that  $\mathcal{S}_1 \natural \mathcal{S}_2 = \mathcal{S}$ , and  $B_1 \natural B_2 = B$ .

(AE-2) Orbit curve ends, of the form  $\widehat{m}^B(\mathbf{x}, \mathbf{y}, \mathcal{S}'; \rho_1, \dots, \rho_{i-1}, \sigma, \rho_{i+1}, \dots, \rho_\ell)$ , where  $\text{orb}(\sigma) = \text{orb}(\rho_i) \setminus \{o_r\}$ ,  $\text{cho}(\sigma) = \text{cho}(\rho_i) \cup \{v_r\}$  where  $v_r$  is a Reeb chord that covers the boundary component  $Z_r$  with multiplicity 1.

(AE-3) Contained collision ends for two consecutive packets  $\rho_i$  and  $\rho_{i+1}$ , which correspond to points in  $\widehat{m}^{B'}(\mathbf{x}, \mathbf{y}, \mathcal{S}; \rho_1, \dots, \rho_{i-1}, \sigma, \rho_{i+2}, \dots, \rho_\ell)$  with the following properties:

(C-1) The collision is visible.

(C-2) The packets  $\rho_i$  and  $\rho_{i+1}$  are strongly composable.

(C-3) The packet  $\sigma$  is a contained collision of  $\rho_i$  and  $\rho_{i+1}$

(C-4) The chords in  $\sigma$  are disjoint from one another.

(AE-4) Join ends, of the form  $\widehat{m}^B(\mathbf{x}, \mathbf{y}, \mathcal{S}'; \rho_1, \dots, \rho_{i-1}, \sigma, \rho_{i+1}, \dots, \rho_\ell)$ ,  $\text{orb}(\sigma) = \text{orb}(\rho_i)$ , and the following conditions hold:

(J-1)  $(\mathbf{x}, \rho_1, \dots, \rho_{i-1}, \sigma, \rho_{i+1}, \dots, \rho_\ell)$  is strongly boundary monotone.

(J-2) There is some  $\rho \in \text{cho}(\rho_i)$  with the property that  $\rho = \rho_1 \uplus \rho_2$ , and  $\text{cho}(\sigma) = (\text{cho}(\rho_i) \setminus \{\rho\}) \cup \{\rho_1, \rho_2\}$ .

(J-3) In the above decomposition, at least one of  $\rho_1$  and  $\rho_2$  covers only half of a boundary component.

(AE-5) Boundary degeneration collisions  $\sigma$  between two consecutive packets  $\rho_i$  and  $\rho_{i+1}$ ; when  $o_j \in \text{orb}(\rho_i)$ ,  $o_k \in \text{orb}(\rho_{i+1})$  and  $\{j, k\} \in M^\vee$ ; these correspond to points in  $\widehat{m}^{B'}(\mathbf{x}, \mathbf{y}, \mathcal{S}'; \rho_1, \dots, \rho_{i-1}, \sigma, \rho_{i+1}, \dots, \rho_\ell)$  in the chamber  $C^{o_j < o_k}$ . The homology class  $B'$  is obtained from  $B$  by removing a copy of  $\mathcal{B}_{\{r, s\}}$ .

(AE-6) Special boundary degeneration ends, when  $\rho_i$  contains a special Reeb orbit  $o_k$ . When  $\sigma = \rho_i \setminus \{o_k\}$  is non-empty, these are identified with

$$\widehat{m}^{B'}(\mathbf{x}, \mathbf{y}, \mathcal{S}'; \rho_1, \dots, \rho_{i-1}, \sigma, \rho_{i+2}, \dots, \rho_\ell)$$

for  $B = B' + \mathcal{B}_{\{k\}}$ ; when  $\rho_i = \{o_k\}$ , then  $\ell = 1$ ,  $\mathbf{x} = \mathbf{y}$ ,  $B = \mathcal{B}_{\{k\}}$ , and the end is unique.

**Remark 7.19.** In the above statement, some of the sources  $\mathcal{S}'$  are different from the original source  $\mathcal{S}$ . We have not spelled out the precise relationship between  $\mathcal{S}'$  and  $\mathcal{S}$ ; it is clear from the context.

**Remark 7.20.** The packets  $\sigma$  that appear in the join curve ends are not allowed in the sense of Definition 7.15; moreover, packets appearing in contained collision ends need not be allowed.

Let

$$\widehat{m}^B(\mathbf{x}, \mathbf{y}, \vec{P}) = \bigcup_{\mathcal{S}} \widehat{m}^B(\mathbf{x}, \mathbf{y}, \mathcal{S}; \vec{P}).$$

See Figure 20 for a picture of a join curve end.

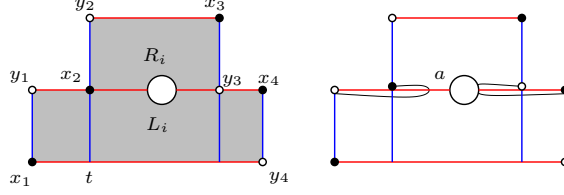


FIGURE 20. **Join curve end.** The moduli space corresponding to the shaded homotopy class, from  $\mathbf{x} = \{x_1, x_2, x_3, x_4\}$  to  $\mathbf{y} = \{y_1, y_2, y_3, y_4\}$  with the Reeb chord  $L_i R_i$  has a join curve end as the cut parameter  $a \mapsto 0$ . (There is another end which is a two-story building, corresponding to a flow from  $\{x_1, x_2, x_3, x_4\}$  to  $\{y_1, t, x_3, x_4\}$ , followed by the flow from  $\{y_1, t, x_3, x_4\}$  to  $\{y_1, y_2, y_3, y_4\}$  that crosses  $L_i R_i$ .)

**Example 7.21.** Suppose that  $\mathbf{x}$  and  $\mathbf{y}$  are generators. Let  $c$  denote the number of points in  $\widehat{\mathcal{M}}^B(\mathbf{x}, \mathbf{y}, (\{L_i, R_i\}))$ . Let  $a$  be the number of two-story ends of  $\widehat{\mathcal{M}}^B(\mathbf{x}, \mathbf{y}, (\{L_i R_i\}))$ ; and  $b$  be the number of two-story ends of  $\widehat{\mathcal{M}}^B(\mathbf{x}, \mathbf{y}, (\{R_i L_i\}))$ . The above theorem applied to  $\widehat{\mathcal{M}}^B(\mathbf{x}, \mathbf{y}, (\{L_i R_i\}))$  implies that  $a + c \equiv 0 \pmod{2}$ ; and applied to  $\widehat{\mathcal{M}}^B(\mathbf{x}, \mathbf{y}, (\{R_i L_i\}))$  gives  $b + c \equiv 0 \pmod{2}$ .

**Example 7.22.** Suppose that  $\mathbf{x}$  and  $\mathbf{y}$  are generators. The above theorem implies that the number of two-story ends of  $\widehat{\mathcal{M}}^B(\mathbf{x}, \mathbf{y}, \{L_i R_i L_i\})$  is even; in particular, there are no join curve ends because the constraint packet  $\{L_i, R_i L_i\}$  is not part of a boundary monotone sequence.

**Example 7.23.** Suppose that  $\mathbf{x}$  and  $\mathbf{y}$  are generators. Let  $c_1$  denote the number of points in  $\widehat{\mathcal{M}}(\mathbf{x}, \mathbf{y}, \{L_i, R_i L_i R_i\})$ ,  $c_2$  denote the number of points in  $\widehat{\mathcal{M}}(\mathbf{x}, \mathbf{y}, \{R_i, L_i R_i L_i\})$ ,  $a$  denote the number of two-story ends of  $\widehat{\mathcal{M}}(\mathbf{x}, \mathbf{y}, \{L_i R_i L_i R_i\})$  and  $b$  the number of two-story ends of  $\widehat{\mathcal{M}}(\mathbf{x}, \mathbf{y}, \{R_i L_i R_i L_i\})$ . The above theorem implies that

$$a + c_1 + c_2 \equiv 0 \pmod{2}$$

$$b + c_1 + c_2 \equiv 0 \pmod{2}.$$

**Example 7.24.** The above theorem shows that there is an even number of two-story ends of  $\widehat{\mathcal{M}}(\mathbf{x}, \mathbf{y}, (\{L_{i+1}\}, \{L_i\}))$ , since the collision between  $L_{i+1}$  and  $L_i$  is weakly, but not strongly, composable. (Note that there are three types of such two-story ends.)

**Example 7.25.** Consider the moduli space  $\widehat{\mathcal{M}}(\mathbf{x}, \mathbf{y}, \{L_i R_i\}, \{L_i R_i\})$ . Let  $a$  denote the number of two-story ends (again, of three possible types);  $b$  denote the number of join curve ends (of two types, corresponding to the sequence  $(\{L_i, R_i\}, \{L_i R_i\})$  or the sequence  $(\{L_i R_i\}, \{L_i, R_i\})$ ; and  $c$  be the number of points in  $\widehat{\mathcal{M}}(\mathbf{x}, \mathbf{y}, \{L_i R_i L_i R_i\})$ . Then,  $a + b + c \equiv 0 \pmod{2}$ .

**Example 7.26.** Let  $a$  be the number of two-story ends of the moduli space  $\widehat{\mathcal{M}}^B(\mathbf{x}, \mathbf{y}, \{o_i, R_{i+1}\})$ , and  $b_1$  denote the number of points in  $\widehat{\mathcal{M}}^B(\mathbf{x}, \mathbf{y}, \{L_i R_i, R_{i+1}\})$ , and  $b_2$  denote the number of points in  $\widehat{\mathcal{M}}^B(\mathbf{x}, \mathbf{y}, \{R_i L_i, R_{i+1}\})$ . Then,  $a + b_1 + b_2 \equiv 0 \pmod{2}$ .



**7.5. Curves at East infinity.** We recall (with very minor adaptation) the material from [10, Section 5.3]. Let  $Z = \bigcup_{i=1}^{2n} Z_i$  be the boundary of  $\Sigma_0$ . Let  $\mathbf{a} = Z \cap \bigcup_{i=1}^{2n-1} \alpha_i$ . We consider moduli spaces of holomorphic curves in  $\mathbb{R} \times Z \times [0, 1] \times \mathbb{R}$ . The ends of the first  $\mathbb{R}$  factor are called east and west infinity; the ends of the second  $\mathbb{R}$  factor are called  $\pm\infty$ . There is an  $\mathbb{R} \times \mathbb{R}$ -action on  $\mathbb{R} \times Z \times [0, 1] \times \mathbb{R}$ , projection maps  $\pi_{\mathbb{R} \times Z}$  (onto the first two factors),  $s$  (to  $[0, 1]$ ) and  $t$  (to the last  $\mathbb{R}$  factor). Fix a split complex structure  $J$  on  $\mathbb{R} \times Z \times [0, 1] \times \mathbb{R}$ .

**Definition 7.27.** An east source  $\mathcal{T}$  is:

- a smooth two-manifold  $T$  with boundary and punctures
- a labeling of each puncture of  $T$  by  $\mathbf{e}$  or  $\mathbf{w}$
- a labeling of each  $\mathbf{w}$  or  $\mathbf{e}$  puncture  $q$  by a Reeb orbit, if the  $q$  is in the interior of  $T$ , and a labeling of  $q$  by a chord in  $(Z, \mathbf{a})$  if the puncture is on the boundary of  $T$ .

Given a east source  $\mathcal{T}$ , we consider maps:

$$v: (T, \partial T) \rightarrow (\mathbb{R} \times Z \times [0, 1] \times \mathbb{R}, \mathbb{R} \times \mathbf{a} \times \{1\} \times \mathbb{R})$$

satisfying:

- (E-1)  $v$  is  $(j, J)$ -holomorphic with respect to some almost-complex structure  $j$  on  $T$ .
- (E-2)  $v$  is proper.
- (E-3)  $(s, t): v \rightarrow [0, 1] \times \mathbb{R}$  is constant.
- (E-4) At each  $\mathbf{w}$  puncture  $q$  of  $T$  labeled by  $\rho$  (a chord or orbit),  $\lim_{z \rightarrow q} \pi_{\Sigma} \circ v(z)$  is  $\rho \subset \{-\infty\} \times Z$ .
- (E-5) At each  $\mathbf{e}$  puncture  $q$  of  $T$  labeled by  $\rho$  (a chord or orbit),  $\lim_{z \rightarrow q} \pi_{\Sigma} \circ v(z)$  is  $\rho \subset \{+\infty\} \times Z$ .

Note that if  $T$  has non-empty boundary, then  $s \circ v = 1$ .

**Definition 7.28.** Let  $\mathcal{E}(\mathcal{T})$  denote the moduli space of holomorphic maps from  $T$  satisfying Properties (E-1)-(E-5) above.

For each puncture  $q$  in  $\mathcal{T}$ , there is a corresponding evaluation  $\text{ev}_q: \mathcal{E}(\mathcal{T}) \rightarrow \mathbb{R}$  which computes the  $t \circ v$  on the component of  $T$  containing  $q$ . There are evaluation maps

$$\begin{aligned} \text{ev}_{\mathbf{w}} &= \prod_{q \in \mathbf{W}(\mathcal{T})} \text{ev}_q: \mathcal{E}(\mathcal{T}) \rightarrow ([0, 1] \times \mathbb{R})^{|\mathbf{W}(\mathcal{T})|} \\ \text{ev}_{\mathbf{e}} &= \prod_{q \in \mathbf{E}(\mathcal{T})} \text{ev}_q: \mathcal{E}(\mathcal{T}) \rightarrow ([0, 1] \times \mathbb{R})^{|\mathbf{E}(\mathcal{T})|}. \end{aligned}$$

Consider the  $t$ -projection of the evaluation map; e.g.  $t \circ \text{ev}_{\mathbf{w}} \rightarrow \mathbb{R}^{|\mathbf{W}(\mathcal{T})|}$ . Given an east source  $\mathcal{T}$ , and ordered partitions  $P_{\mathbf{w}}$  and  $P_{\mathbf{e}}$ , we let  $\mathcal{E}(\mathcal{T}; P_{\mathbf{w}}, P_{\mathbf{e}}) \subset \mathcal{E}(\mathcal{T})$  be the subspaces obtained by cutting down by the partial diagonals associated to  $t \circ \text{ev}_{\mathbf{w}}$  and  $t \circ \text{ev}_{\mathbf{e}}$ .

The following is [10, Proposition 5.14]; compare [15, Section 3.3]:

**Proposition 7.29.** *If  $\mathcal{T}$  has the property that all of the components of  $T$  are topological disks, then  $\mathcal{E}(\mathcal{T})$  is transversely cut out by the  $\bar{\partial}$  equation for any split complex structure on  $\mathbb{R} \times Z \times [0, 1] \times \mathbb{R}$ .*

Let  $\hat{\mathcal{E}}(\mathcal{T}) = \mathcal{E}(\mathcal{T})/\mathbb{R} \times \mathbb{R}$ .

The following particular components are illustrated in Figure 21.

A *trivial component* is a component of  $\mathcal{T}$  with exactly two punctures, one  $\mathbf{e}$  and one  $\mathbf{w}$ , both labelled by the same Reeb chord. The holomorphic map to  $\mathbb{R} \times Z$  is invariant under translation by  $\mathbb{R}$ .

A *join component* is a component of  $\mathcal{T}$  which is a topological disk with two west boundary punctures and one east boundary puncture. Labeling, in counterclockwise order  $(e, \rho_e)$ ,  $(w, \rho_1)$ , and  $(w, \rho_2)$ . There is a holomorphic map from such a component if and only if  $\rho_e = \rho_2 \uplus \rho_1$ ; if it exists, it is unique up to translation. The puncture  $(w, \rho_1)$  is called the *top puncture* and  $(w, \rho_2)$  is called the *bottom puncture*. A *join curve* is a curve that consists of one join component and a collection of trivial components.

An *split component* is defined similarly, only now there the punctures in counterclockwise order, are  $(w, \rho_w)$ ,  $(e, \rho_1)$  and  $(e, \rho_2)$ . Again, there is a holomorphic map if and only if  $\rho_w = \rho_1 \uplus \rho_2$ . The puncture  $(e, \rho_2)$  is called the *top puncture* and  $(e, \rho_1)$  is called the *bottom puncture*.

**Remark 7.30.** *Note that there are join and split curves that cover the cylinder with arbitrarily large multiplicity; on the left of Figure 21, we have illustrated a split curve that covers the cylinder with multiplicity one, and these are the split curves that will occur in our considerations for type D structures. When considering type A modules, though, we will be forced to consider join and split curve ends that cover the boundary cylinder with higher multiplicity.*

An *orbit component* is a disk with a single boundary puncture, labelled  $(w, \rho)$ , and a single orbit puncture  $(e, o)$  in its interior, so that  $o$  is a simple orbit. There is a holomorphic map from such a component if and only if  $\rho$  is one of the two chords that covers the boundary component containing  $o$  with multiplicity one.

**Remark 7.31.** *There are other components with disk sources one might consider. For example, the “shuffle curves” from [10, Section 5.3] have a natural analogue, which one might call “orbit-shuffle curves”. These have a west puncture that is an orbit, another west puncture labelled by a chord  $\rho$  on the same boundary component as  $o$ , and a single east puncture labelled by  $\rho \uplus u$ , where  $u$  is one of the two curves that covers the boundary once. The map to  $\mathbb{R} \times Z$  has a single branch point in the interior. These curves, however, will not enter our considerations. This is because in an allowed constraint packet (in the sense of Definition 7.15), the orbits are disjoint from the chords. These other curves would enter if we were to try to define the theory over  $\mathcal{A}$  from [22], which we can avoid by some algebraic considerations; see Section 15.*

**7.6. Curves at West infinity.** Unlike in [10], generalized flowlines can degenerate also at west infinity. In formulating this degeneration, we need to generalize slightly the notion of a decorated source and pre-flowline, as follows:

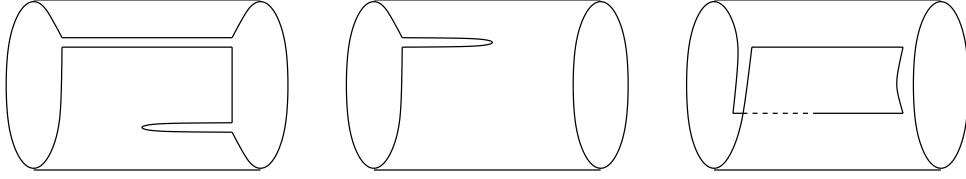


FIGURE 21. **Curves at East infinity.** The boundary on the left is glued to the source, and the boundary to the right is the “east infinity” portion. We have illustrated from left to right: a split curve, an orbit curve, and an orbit shuffle curve. The join curve is obtained by reflecting the leftmost picture through a vertical axis.

**Definition 7.32.** A decorated source with West punctures is a decorated source as in Definition 5.2 equipped with a further set of boundary punctures that are labelled  $\mathbf{w}$ . A pre-flowline with west punctures is a map

$$u: (\mathcal{S}, \partial\mathcal{S}) \rightarrow (\Sigma \times [0, 1] \times \mathbb{R}, (\boldsymbol{\alpha} \times \{1\} \times \mathbb{R}) \cup (\boldsymbol{\beta} \times \{0\} \times \mathbb{R}))$$

where  $\mathcal{S}$  is equipped with boundary punctures  $\mathbf{W}(\mathcal{S})$  with the following properties:

- for each west puncture  $q$ ,  $\lim_{z \rightarrow q} u(z)$  converges to a point in  $\Sigma \times 0 \times \mathbb{R}$ ; i.e. if we fill in the west punctures to form a source curve  $\mathcal{S}'$  (without West punctures),  $u$  extends uniquely to a  $u': \mathcal{S}' \rightarrow \Sigma \times [0, 1] \times \mathbb{R}$
- The extension  $u'$  obtained as above is a pre-flowline in the sense of Definition 5.4.
- The set of west punctures in  $\mathcal{S}$  comes with an ordered partition into  $d$ -tuples  $q_1, \dots, q_d$ , so that

$$\pi_{\mathbb{D}} \circ u(q_1) = \dots = \pi_{\mathbb{D}} \circ u(q_d).$$

We call this the disk partition of the punctures at West infinity.

A pseudo-holomorphic flowline with West punctures is a pre-flowline with West punctures which, when filled in, give a pseudo-holomorphic flowline in the sense of Definition 5.10.

Obviously, when  $\mathbf{W}(\mathcal{S}) = \emptyset$ , the above definition agrees with the usual definition of a source curve and pre-flowline (Definitions 5.2 and 5.4 respectively).

For a pre-flowline  $u$ , let  $[\mathbf{W}(\mathcal{S})]$  denote the set of  $d$ -tuples in the disk partition; equivalently, it is the set of equivalence classes of West punctures on  $\mathcal{S}$ , modulo the equivalence relation  $q \sim q'$  if  $t \circ u(q) = t \circ u(q')$ . In particular,

$$|[\mathbf{W}(\mathcal{S})]| = |\mathbf{W}(\mathcal{S})|/d.$$

Fix a pre-flowline  $u$  with west punctures, and  $\mathbf{q} = \{q_1, \dots, q_d\} \in [\mathbf{W}(\mathcal{S})]$ . There is a corresponding evaluation

$$\text{ev}_{\mathbf{q}}^{\beta}(u) = \pi_{\Sigma}(u(q_1)) \times \dots \times \pi_{\Sigma}(u(q_d)).$$

By boundary monotonicity,  $\text{ev}_{\mathbf{q}}^{\beta}(u) \in \beta_1 \times \dots \times \beta_g$

Taking the product over  $[\mathbf{W}(\mathcal{S})]$ , we obtain a map

$$\text{ev}_{\mathbf{e}}^{\beta} \in (\mathbb{T}_{\beta})^{[\mathbf{W}(\mathcal{S})]}$$

We consider moduli spaces of holomorphic curves in  $\Sigma \times \mathbb{H}$ , generalizing the boundary degenerations of Definition 5.17.

**Definition 7.33.** A boundary degeneration with West punctures is a map

$$w: (R_b, \partial R_b) \rightarrow (\Sigma \times \mathbb{H}, \beta \times \mathbb{R})$$

whose  $d$  punctures over the point at infinity in  $\mathbb{H}$  are called east punctures; and equipped with additional punctures in  $\partial R_b$ , called west punctures with the following properties:

- for each west puncture  $q$ ,  $\lim_{z \rightarrow q} u(z)$  converges to a point in  $\Sigma \times \mathbb{R} \subset \Sigma \times \mathbb{H}$ ; i.e. if we fill in the west punctures to form a source curve  $R'_b$ , then  $w$  extends uniquely to a continuous map

$$w': (R'_b, \partial R'_b) \rightarrow (\Sigma \times \mathbb{H}, \Sigma \times \mathbb{R}).$$

- The extension  $w'$  obtained as above is a boundary degeneration as in Definition 5.17.
- The set of west punctures in  $R_b$  comes with a partition into  $d$ -tuples  $q_1, \dots, q_d$  so that

$$\pi_{\mathbb{H}} \circ u(q_1) = \dots = \pi_{\mathbb{H}} \circ u(q_d).$$

**Definition 7.34.** A boundary degeneration level is a finite union of boundary degenerations with West punctures. We can think of its source curve  $\mathcal{R}$  (which has possibly many components) as marked with a set of East punctures  $\mathbf{E}(\mathcal{R})$  and west punctures  $\mathbf{W}(\mathcal{R})$ ; punctures of each type come in  $d$ -tuples (again, referred to as the disk partition).

For a boundary degeneration level, let  $[\mathbf{E}(\mathcal{R})]$  resp.  $[\mathbf{W}(\mathcal{R})]$  and denote the set of  $d$ -tuples in the disk partition of  $\mathbf{E}(\mathcal{R})$  resp.  $\mathbf{W}(\mathcal{R})$ .

For a boundary degeneration level, we have, as before, evaluations

$$\text{ev}_{\mathbf{e}}^{\beta}(w) \in (\mathbb{T}_{\beta})^{[\mathbf{E}(\mathcal{R})]} \quad \text{and} \quad \text{ev}_{\mathbf{w}}^{\beta}(w) \in (\mathbb{T}_{\beta})^{[\mathbf{W}(\mathcal{R})]}.$$

**7.7. Compactness.** As in [10, Section 5.4], we use the Eliashberg-Givental-Hofer compactness [3].

**Definition 7.35.** A holomorphic story is the following data:

- a sequence  $(w_{\ell}, \dots, w_1, u, v_1, \dots, v_k)$  for some  $\ell \geq 0$ ,  $k \geq 0$  where  $u$  is a pseudo-holomorphic flowline with West punctures, with source  $\mathcal{S}$ ;  $\{w_i\}_{i=1}^{\ell}$  is a sequence of boundary degeneration levels, where  $w_i$  has source  $\mathcal{R}_i$ ;  $\{v_i\}_{i=1}^k$  is a sequence of curves at East infinity.
- One-to-one correspondences between the following objects:  $\mathbf{W}(\mathcal{S})$  and  $\mathbf{E}(\mathcal{R}_1)$ ;  $\mathbf{W}(\mathcal{R}_i)$  and  $\mathbf{E}(\mathcal{R}_{i+1})$  for  $i = 1, \dots, \ell - 1$  (which respect the disk partition);  $\mathbf{E}(\mathcal{S})$  and  $\mathbf{W}(\mathcal{T}_1)$ ;  $\mathbf{E}(\mathcal{T}_i)$  and  $\mathbf{W}(\mathcal{T}_{i+1})$  (for  $i = 1, \dots, k - 1$ ),

so that the following conditions hold:

- $u \in \mathcal{M}^B(\mathbf{x}, \mathbf{y}; \mathcal{S})$
- $v_i \in \mathcal{E}(\mathcal{T}_i)$
- $w_i \in \mathcal{N}(\mathcal{R}_i)$

- $\text{ev}_{\mathbf{e}}(u) = \text{ev}_{\mathbf{w}}(v_1)$  in  $\mathbb{R}^{\mathbf{E}(\mathcal{S})}/\mathbb{R} \cong \mathbb{R}^{\mathbf{W}(\mathcal{I}_1)}/\mathbb{R}$  (here, and in the next few conditions, we use the isomorphism of product spaces induced by the one-to-one correspondence between punctures).
- $\text{ev}_{\mathbf{e}}(v_i) = \text{ev}_{\mathbf{w}}(v_{i+1})$  in  $\mathbb{R}^{\mathbf{E}(\mathcal{I}_i)}/\mathbb{R} \cong \mathbb{R}^{\mathbf{W}(\mathcal{I}_{i+1})}/\mathbb{R}$  for  $i = 1, \dots, k-1$ .
- $\text{ev}_{\mathbf{w}}^{\beta}(u) = \text{ev}_{\mathbf{e}}^{\beta}(w_1)$  in  $(\mathbb{T}_{\beta})^{[\mathbf{W}(\mathcal{S})]} \cong (\mathbb{T}_{\beta})^{[\mathbf{E}(w_1)]}$
- $\text{ev}_{\mathbf{w}}^{\beta}(v_w) = \text{ev}_{\mathbf{e}}^{\beta}(w_{i+1})$  in  $(\mathbb{T}_{\beta})^{[\mathbf{W}(\mathcal{R}_i)]} \cong (\mathbb{T}_{\beta})^{[\mathbf{E}(\mathcal{R}_{i+1})]}$  for  $i = 1, \dots, \ell-1$ .

A holomorphic story with  $\{k, \ell\} = \{0, 1\}$  is called a simple holomorphic comb. A holomorphic comb of height  $N$  is a sequence  $(w_{j,\ell_j}, \dots, w_{j,1}, u_j, v_{j,1}, \dots, v_{j,k_j})$  for  $j = 1, \dots, N$  of holomorphic stories with  $u_j$  a stable curve in  $\mathcal{M}^{B_j}(\mathbf{x}_j, \mathbf{x}_{j+1}; \mathcal{S}_j)$  for some sequence of generalized generators  $\mathbf{x}_1, \dots, \mathbf{x}_{N+1}$ .

**Remark 7.36.** In the above statement, we require the curves  $u_j$  to be stable. This excludes where all the components of the source  $\mathcal{S}_j$  are disks with exactly two punctures: one at  $+\infty$ , another at  $-\infty$ , and  $\pi_{\Sigma} \circ u_j$  is a constant map (to  $\mathbf{x}_j = \mathbf{x}_{j+1}$ ).

As in [10, Section 5.4] (following [3]), the space of holomorphic combs can be used to construct a compactification of  $\widehat{\mathcal{M}}(\mathbf{x}, \mathbf{y}; \mathcal{S})$ , denoted  $\overline{\mathcal{M}}(\mathbf{x}, \mathbf{y}; \mathcal{S})$ ; and similarly a compactification  $\overline{\mathcal{M}}(\mathbf{x}, \mathbf{y}; \mathcal{S}; \vec{\rho})$  of  $\widehat{\mathcal{M}}(\mathbf{x}, \mathbf{y}; \vec{\rho})$ . This is a compactification in the following sense:

**Proposition 7.37.** If  $\{U_n\}$  is a sequence of holomorphic combs in a fixed homology class, then  $\{U_n\}$  has a subsequence which converges to a (possibly) nodal holomorphic curve in the same homology class.

**Proof.** See [10, Proposition 5.24] for the compactness result at east infinity. The west infinity curves are extracted by a more standard Gromov compactification, rescaling from the  $\mathbb{D}$  factor to  $\mathbb{H}$ , as in the proof of [6, Lemma 3.82].  $\square$

Let  $([0, 1] \times \mathbb{R})^{\vec{\rho}}$  denote the space of functions from all of the punctures on the source to  $[0, 1] \times \mathbb{R}$ . Note that if two punctures  $p$  and  $q$  correspond to the same level  $\rho_i$ , then their  $t$  values coincide. The evaluation maps

$$\text{ev}: \widehat{\mathcal{M}}^B(\mathbf{x}, \mathbf{y}, \vec{\rho}) \rightarrow ([0, 1] \times \mathbb{R})^{\vec{\rho}}/\mathbb{R}$$

extend continuously to the space of holomorphic stories, where now we evaluate on all east-most punctures.

Each curve at west infinity  $w$  has a shadow  $B$ , which determines the total multiplicity of the Reeb orbits. When the shadow is  $\mathcal{B}_{\{j,k\}}$ , there are exactly two Reeb orbits,  $o_j$  and  $o_k$ ; in this case, we call the curve at west infinity a *simple boundary degeneration component*. There are also two special orbits that are not matched, with corresponding shadows  $\mathcal{B}_{\{j\}}$  containing no other orbit. We also call the corresponding boundary degeneration components simple. A *simple boundary degeneration* is a curve all of whose components are either trivial or simple west components.

When  $w$  is a simple boundary degeneration, and  $\text{ev}(w) \in C^{o_k > o_j}$ , we call  $o_k$  the *top orbit* and  $o_j$  the *bottom orbit*; see Figure 22.

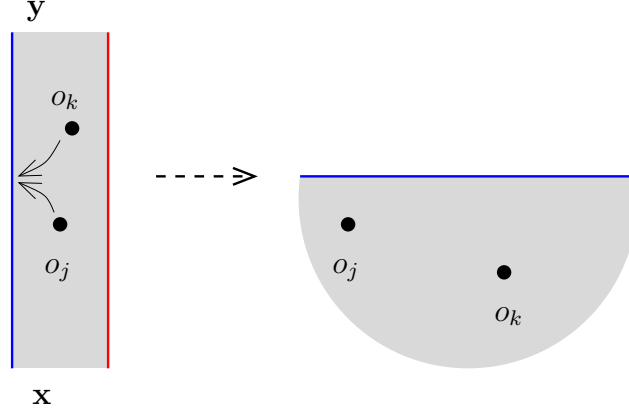


FIGURE 22. **Extracting a boundary degeneration.** As the two orbits on the left come together, we can rescale (and rotate) to construct a boundary degeneration as pictured on the right.

**7.8. Gluing.** The ends of two-dimensional moduli spaces stated in Theorem 7.18 are modeled by certain gluing results, which we collect here; compare [10, Section 5.5].

The following is [10, Proposition 5.39]. To state it, use the following terminology from there. If  $(u, v)$  is a simple holomorphic comb, with  $v \in \mathcal{E}(\mathcal{T})$ , a *smeared neighborhood* of  $(u, v)$  in  $\overline{\mathcal{M}}^B(\mathbf{x}, \mathbf{y}, \mathcal{S}, P)$  is an open neighborhood of

$$\{(u, v') | v' \in \mathcal{E}(\mathcal{T}), (u, v') \in \overline{\mathcal{M}}^B(\mathbf{x}, \mathbf{y}; \mathcal{S}; P)\}.$$

Also, given  $p, q \in \mathcal{T}$ , let  $\overline{\text{ev}}_{p,q}: \overline{\mathcal{M}}(\mathbf{x}, \mathbf{y}; \mathcal{S}) \rightarrow [-\infty, \infty]$  be the continuous extension of  $\text{ev}_{p,q}$ .

**Proposition 7.38.** *Suppose that  $(u, v)$  is a simple holomorphic comb in  $\overline{\mathcal{M}}^B(\mathbf{x}, \mathbf{y}; \mathcal{S}, P)$ . Assume that  $v$  is a split curve and there are two parts  $P_1$  and  $P_2$  such that for each split component of  $\mathcal{T}$ , its bottom puncture belongs to  $P_1$  and its top puncture belongs to  $P_2$ . Assume that  $\text{ind}(B, \mathbf{x}, \mathbf{y}; \mathcal{S}, P) = 2$ . Let  $q_1 \in P_2$  and  $q_2 \in P_1$  be the top and bottom punctures, respectively, on one of the split components of  $\mathcal{T}$ . Then for generic  $J$ , there is a smeared neighborhood  $U$  of  $(u, v)$  in  $\overline{\mathcal{M}}^B(\mathbf{x}, \mathbf{y}; \mathcal{S}, P)$  so that  $\overline{\text{ev}}_{q_1, q_2}: U \rightarrow \mathbb{R}_+$  is proper near 0 and of odd degree near  $(u, v)$ .*

The above is proved in [10, Proposition 5.39].

The following result is also used in [10] (see especially the proof of [10, Theorem 5.61]):

**Proposition 7.39.** *Let  $\mathcal{S}$  be a source curve equipped with some ordered partition  $P$ , and  $P'$  be the ordered partition where consecutive packets  $P_j$  and  $P_{j+1}$  in  $P$  collide. Suppose that  $\text{ind}(B, \mathbf{x}, \mathbf{y}; \mathcal{S}', P') = 2$ . Suppose that  $(u, v)$  is a simple holomorphic comb in  $\overline{\mathcal{M}}^B(\mathbf{x}, \mathbf{y}; \mathcal{S}', P')$ , so that  $u \in \mathcal{M}^B(\mathbf{x}, \mathbf{y}; \mathcal{S}, P)$  is a smooth point and  $v$  is a join curve. Let  $\Delta_P \subset \mathbb{R}^P$  denote the diagonal that specifies the collision of levels  $j$  and  $j+1$ , and suppose that  $u$  is a smooth, isolated point*

in  $\mathcal{M}(\mathbf{x}, \mathbf{y}; \mathcal{S}, P) \times_{\text{ev}_P} \Delta_P$ . Then, there is a smeared neighborhood  $U$  of  $(u, v) \in \overline{\mathcal{M}}^B(\mathbf{x}, \mathbf{y}, \mathcal{S}'; P')$  with the property that  $U \times_{\text{ev}_{P'}} \Delta_{P'}$  is homeomorphic to  $[0, 1]$ .

**Proof.** Note first that since the domain of  $v$  is a planar surface,  $v$  represents a smooth point in its moduli space  $\mathcal{E}$ . (See [10, Proposition 5.16].) The hypothesis that  $u$  is a smooth point includes the statement that the evaluation map is transverse to the diagonal where the two chords to be joined are mapped to the same  $t$ -position. Thus,  $u$  and  $v$  have neighborhoods  $U_u$  and  $U_v$ , so that  $(u, v)$  is a transverse intersection point of  $\text{ev}: U_u \rightarrow \mathbb{R}^{\mathbf{E}(\mathcal{S})}$  and  $\text{ev}: U_v \rightarrow \mathbb{R}^{\mathbf{W}(\mathcal{S})}$ . Thus, gluing gives an identification of a neighborhood of  $(u, v)$  that is identified with  $U_u \times_{\text{ev}} U_v \times [0, 1]$ . In fact, the image of  $\text{ev}(U_v)$  is the diagonal  $\Delta_P$  (that determines the portion of  $\mathcal{M}^B(\mathbf{x}, \mathbf{y}, \mathcal{S}; P')$  where the two consecutive packets  $P_j$  and  $P_{j+1}$  collide). Thus, gluing identifies a neighborhood of  $(u, v)$  with  $(U_u \times_{\text{ev}_P} \Delta_P) \times [0, 1]$ . By assumption,  $U_u \times_{\text{ev}_P} \Delta_P$  consists of the point  $u$ .  $\square$

In a similar vein, we have the following analogue for orbit curves. To state it, fix some  $q_0 \in \mathcal{S}$ , and let  $p \in \mathcal{S}$  be a puncture marked by an orbit. The map

$$(7.7) \quad s \circ \text{ev}_{\{p\}}: \mathcal{M}(\mathbf{x}, \mathbf{y}; \mathcal{S}) \rightarrow (0, 1)$$

specified by  $s \circ \text{ev}_p(u) = s \circ u(q)$ , extends continuously to a map

$$\overline{s \circ \text{ev}_{\{p\}}}: \overline{\mathcal{M}}(\mathbf{x}, \mathbf{y}; \mathcal{S}) \rightarrow [0, 1].$$

**Proposition 7.40.** *Suppose that  $(u_0, v)$  is a simple holomorphic comb in  $\overline{\mathcal{M}}^B(\mathbf{x}, \mathbf{y}; \mathcal{S})$ , and assume that  $v$  is an orbit curve with orbit  $o_j$ . Let  $\mathcal{S}_0$  denote the source for  $u_0$ ; it has a distinguished boundary puncture  $p_0$  labelled by some length one chord  $v_j$ ; and  $\mathcal{S}$  is obtained by replacing this boundary puncture with an interior puncture  $p$  labelled by  $o_j$ . Choose also the following data:*

- a set of punctures  $P$  on  $\mathcal{S}$ ; and let  $P_0$  be the corresponding collection of punctures on  $\mathcal{S}_0$  (i.e. with  $p$  replaced by  $p_0$ )
- a smooth manifold  $M$
- a smooth map  $\phi: M \rightarrow \mathbb{R}^P \cong \mathbb{R}^{P_0}$
- a point  $u_0 \times m_0 \in \mathcal{M}(\mathbf{x}, \mathbf{y}; \mathcal{S}_0) \times_{\text{ev}_{P_0}} M$ .

Suppose that:

- $\phi$  is transverse to  $\text{ev}_P: \mathcal{M}^B(\mathbf{x}, \mathbf{y}; \mathcal{S}_0) \rightarrow \mathbb{R}^{P_0} = \mathbb{R}^P$
- $\phi$  is transverse to  $\text{ev}_P: \mathcal{M}^B(\mathbf{x}, \mathbf{y}; \mathcal{S}) \rightarrow \mathbb{R}^P$
- the fibered product  $\mathcal{M}^B(\mathbf{x}, \mathbf{y}; \mathcal{S}_0) \times_{\text{ev}_{P_0}} M$  is two-dimensional.
- $u_0 \times m_0$  is an (isolated) point in  $\mathcal{M}^B(\mathbf{x}, \mathbf{u}; \mathcal{S}_0) \times_{\text{ev}_{P_0}} M$ .

Then, there is a smeared neighborhood  $U$  of  $(u_0, v)$  in  $\overline{\mathcal{M}}^B(\mathbf{x}, \mathbf{y}; \mathcal{S})$  so that  $U \times_{\overline{\text{ev}_{P_0}}} M$  is homeomorphic to  $u_0 \times m_0 \times (0, 1] = (0, 1]$ . Moreover,

$$u_0 \times m_0 \times (0, 1] \subset \overline{\mathcal{M}}^B(\mathbf{x}, \mathbf{y}; \mathcal{S}) \times_{\overline{\text{ev}_{P_0}}} M \xrightarrow{\overline{s \circ \text{ev}_{\{p\}}}} [0, 1]$$

is proper and of odd degree near 1.

**Proof.** This proof is similar to the proof of Proposition 7.39. Again, the moduli space  $\mathcal{E}$  for an orbit curve is smooth. In this case, the evaluation map

$$\text{ev}: \mathcal{E}(\mathcal{T}, P) \rightarrow \mathbb{R}^P$$

is a diffeomorphism near  $v$ , so gluing gives a smeared neighborhood of  $(u_0, v)$  in  $\overline{\mathcal{M}}(\mathbf{x}, \mathbf{y}; \mathcal{S})$  which is homeomorphic to  $U_0 \times (0, 1]$ , where  $U_0$  is a neighborhood of  $u_0$  in  $\mathcal{M}(\mathbf{x}, \mathbf{y}; \mathcal{S}_0)$ . Similarly,  $(U_0 \times (0, 1]) \times_{\text{ev}_{P_0}} M$  is identified with  $(U_0 \times_{\text{ev}_{P_0}} M) \times (0, 1]$ . Since  $p$  is an interior puncture, it follows that  $s \circ \text{ev}_p(u \times m \times t) < 0$  for  $t < 1$ ; it is straightforward also to see that  $s \circ \overline{\text{ev}}_p(u \times m \times 1) = 1$ . The degree statement follows.  $\square$

The following is similar to Proposition 7.40. To state it, we generalize the notion of smeared neighborhood in the following straightforward manner to simple combs  $(w, u)$  where  $w$  is a curve at West infinity.

Let  $(w, u)$  be a simple holomorphic curve with  $w \in \mathcal{N}(\mathcal{R})$ , and  $u$  a pseudo-holomorphic flowline with west punctures. A *smeared neighborhood* of  $(w, u)$  in is an open neighborhood in  $\overline{\mathcal{M}}^B(\mathbf{x}, \mathbf{y}, \mathcal{S})$  of the set

$$\{(w, u') \in \mathcal{N}(\mathcal{R}), (w, u) \in \overline{\mathcal{M}}(\mathbf{x}, \mathbf{y}, \mathcal{S})\}$$

In this neighborhood,  $u$  is to be thought of as a curve with West punctures (over the  $t$ -value where it meets  $w$ ).

**Proposition 7.41.** *Suppose that  $(w, u_0)$  is a simple holomorphic comb in  $\overline{\mathcal{M}}^B(\mathbf{x}, \mathbf{y}; \mathcal{S})$ , and assume that  $w$  is a simple boundary degeneration with some puncture  $p$  labelled by an orbit  $o_j$ . Let  $\mathbf{q}$  denote the  $d$ -tuple of west punctures in  $u_0$ . Fix also the following data:*

- a smooth manifold  $M$
- a smooth map  $\phi: M \rightarrow \mathbb{R}^{P_0}$ , where  $P_0$  denotes the set of punctures which do not appear in the boundary degeneration component
- an auxiliary puncture  $q_0 \in P_0$  with  $t \circ u_0(q_0) = t \circ u_0(q)$  for all  $q \in \mathbf{q}$ .

Assume that:

(W-1)  $\phi$  is transverse to

$$\text{ev}_{P_0}: \mathcal{M}^{B_0}(\mathbf{x}, \mathbf{y}; \mathcal{S}_0) \rightarrow \mathbb{R}^{P_0},$$

where  $\mathcal{B}_{\{r, s\}} + B_0 = B$  and  $\mathcal{B}_{\{r, s\}}$  is the shadow of  $w$ .

(W-2)  $\phi \times 0: M \rightarrow \mathbb{R}^{P_0} \times \mathbb{R}$  is transverse to

$$\text{ev}_{P_0} \times (\text{ev}_{p_1} - \text{ev}_{q_0}): \mathcal{M}^B(\mathbf{x}, \mathbf{y}; \mathcal{S}) \rightarrow \mathbb{R}^{P_0} \times \mathbb{R}$$

(W-3) the fibered product  $\mathcal{M}^B(\mathbf{x}, \mathbf{y}; \mathcal{S}) \times_{\text{ev}_{P_0} \times \text{ev}_{p_1} - \text{ev}_{q_0}} (M \times 0)$  is two-dimensional,

(W-4)  $(w \times u_0) \times m_0$  is a point in  $\overline{\mathcal{M}}(\mathbf{x}, \mathbf{y}; \mathcal{S}) \times_{\text{ev}_{P_0}} M$ .

Then there is a smeared neighborhood  $U$  of  $(w, u_0)$  in  $\overline{\mathcal{M}}^B(\mathbf{x}, \mathbf{y}; \mathcal{S})$  with the following properties:

- The map  $\overline{s \circ \text{ev}}_p: U \times_{\text{ev}_{P_0}} M \rightarrow [0, 1]$  is proper near 0.
- The above map has odd degree near  $(w, u_0)$ .



**Proof.** Each simple boundary degeneration  $w$  is transversely cut out in the moduli space  $\widehat{\mathcal{N}}^{\mathcal{B}_{\{j,k\}}}(\mathbf{x}; \mathcal{R})$ . We are assuming that  $u$  is also transversely cut out in  $\widehat{\mathcal{M}}^{B_0}(\mathbf{x}, \mathbf{y}; \mathcal{S}; P_2)$ . It follows from standard gluing results (see [10, Proposition 5.31]; see also [2, Section 5.3]) that for sufficiently small open neighborhoods  $U_w$  and  $U_{u_0}$  of  $w$  and  $u_0$ , there is an open neighborhood in  $\overline{\mathcal{M}}^B(\mathbf{x}, \mathbf{y}; \mathcal{R}; \mathcal{S}_0; P)$  which is homeomorphic to  $(U_w \times_{\text{ev}^\beta} U_{u_0}) \times [0, 1) \times (-1, 1)$ . Here, the interval  $[0, 1)$  parameterizes the gluing parameter, and the interval  $(-1, 1)$  parameterizes the  $t$  value of the  $d$ -tuple of west punctures over  $u_0$ . Since  $\text{ev}^\beta: U_w \rightarrow \mathbb{T}_\beta$  has odd degree (Lemma 5.20), this neighborhood is identified with an odd number of copies of  $U_{u_0} \times [0, 1) \times (-1, 1)$ . Choosing  $U_{u_0}$  sufficiently small that  $U_{u_0} \times_{\text{ev}_{P_0}} M$  consists of the single point  $(u_0, m_0)$ , we have that the smeared neighborhood  $U$  of  $(w, u_0)$  has the property that  $U \times_{\text{ev}_{P_0}} M$  is identified with an odd number of copies of  $[0, 1) \times (-1, 1)$ .

Pick one such component  $\overline{\mathcal{M}}$ , and let  $\mathcal{M}$  denote its interior. Consider the maps

$$F_1 = s \circ \text{ev}_p: \mathcal{M} \rightarrow (0, 1) \quad \text{and} \quad F_2 = \text{ev}_p - \text{ev}_{q_0}: \mathcal{M} \rightarrow \mathbb{R}.$$

The maps  $F_1$  and  $F_2$  extend continuously to give maps  $\overline{F}_i: \overline{\mathcal{M}} \rightarrow \mathbb{R}$  for  $i = 1, 2$ ; and in fact  $\overline{F}_1: \overline{\mathcal{M}} \rightarrow [0, 1)$  is proper near 0.

Clearly, the restriction of  $\overline{F}_2$  to  $0 \times (-1, 1)$  has odd degree near 0. Moreover, since  $p$  is an interior puncture,  $F_1(s, t) > 0$  for all  $s > 0$  and  $t \in (-1, 1)$ . Also,  $\overline{F}_1(0, t) = 0$ . It follows that  $F: [0, 1) \times (-1, 1) \rightarrow \mathbb{R} \times \mathbb{R}$  has odd degree. Clearly, the neighborhood of

$$\mathcal{M} \times_{\text{ev}_{P_0} \times (\text{ev}_p - \text{ev}_{q_0})} (M \times 0)$$

is given as  $F_2^{-1}(0)$ , and the restriction of  $s \circ \text{ev}_p$  to this set is  $F_1$ . It follows that the degree of  $s \circ \text{ev}_p$  to  $U \times_{\text{ev}_{P_0}} M$  agrees with an odd multiple of the degree of  $F_1|_{F_2^{-1}(0)}$ , which agrees with the degree of  $F$ , which we have shown to be odd.  $\square$

In the above proposition, we measured the distance of the boundary degeneration by measuring  $s \circ u(p)$ , where  $p$  is the puncture which goes into the boundary degeneration. In the next very similar proposition, we measure the distance to the boundary by  $t \circ u(p_1) - t \circ u(p_2)$ , where now  $\{p_1, p_2\}$  are the two punctures which go into the boundary degeneration.

**Proposition 7.42.** *Suppose that  $(w, u_0)$  is a simple holomorphic comb in  $\overline{\mathcal{M}}^B(\mathbf{x}, \mathbf{y}; \mathcal{S})$ , and assume that  $w$  is a simple boundary degeneration with exactly two punctures  $p_1$  and  $p_2$ , labelled by orbits  $o_j$  and  $o_k$  respectively. Fix also the following data:*

- a smooth manifold  $M$
- a smooth map  $\phi: M \rightarrow \mathbb{R}^{P_0}$ , where  $P_0$  denotes the set of punctures which do not appear in the boundary degeneration component
- an auxiliary puncture  $q_0 \in P_0$  with  $t \circ u(q_0) = t \circ u_0(q)$  for all  $q \in \mathbf{q}$ .

Assume that:

- $\phi$  is transverse to

$$\text{ev}_{P_0}: \mathcal{M}^{B_0}(\mathbf{x}, \mathbf{y}; \mathcal{S}_0) \rightarrow \mathbb{R}^{P_0},$$

where  $\mathcal{B}_{\{r,s\}} + B_0 = B$  and  $\mathcal{B}_{\{r,s\}}$  is the shadow of  $w$ .

- $\phi$  is transverse to

$$\text{ev}_{P_0} \times (\text{ev}_{p_1} - \text{ev}_{q_0}): \mathcal{M}^B(\mathbf{x}, \mathbf{y}; \mathcal{S}) \rightarrow \mathbb{R}^{P_0} \times \mathbb{R},$$

where  $\mathcal{B}_{\{r,s\}} + B_0 = B$  and  $\mathcal{B}_{\{r,s\}}$  is the shadow of  $w$ .

- the fibered product  $\mathcal{M}^B(\mathbf{x}, \mathbf{y}; \mathcal{S}) \times_{\text{ev}_{P_0} \times \text{ev}_{p_1} - \text{ev}_{q_0}} (M \times 0)$  is two-dimensional,
- $(w \times u_0) \times m_0$  is a point in  $\overline{\mathcal{M}}(\mathbf{x}, \mathbf{y}; \mathcal{S}) \times_{\text{ev}_{P_0}} M$ .
- The map  $\text{ev}_{\mathbf{q}}^\beta: \mathcal{M}(\mathbf{x}, \mathbf{y}; \mathcal{S}) \rightarrow \mathbb{T}_\beta$  is transverse to the wall  $\mathcal{W}^{o_j=o_k}$ .

Then there is a smeared neighborhood  $U$  of  $(w, u_0)$  in  $\overline{\mathcal{M}}^B(\mathbf{x}, \mathbf{y}; \mathcal{S})$  with the following properties:

- Let  $f: U \times_{\text{ev}_{P_0} \times (\text{ev}_{p_1} - \text{ev}_{q_0})} (M \times 0) \rightarrow \mathbb{R}$  be defined by  $u \mapsto t \circ u(p_1) - t \circ u(p_2)$  is proper, sending the portion of  $U$  in the interior  $\mathcal{M}^B(\mathbf{x}, \mathbf{y}; \mathcal{S})$  to  $\mathbb{R} \setminus 0$ , and mapping ideal combs to 0.
- if  $\text{ev}_{\mathbf{q}}^\beta(u_0)$  is in the  $\mathcal{C}^{o_j > o_k}$ , then  $f$  has odd degree near  $(w, u_0)$  for  $\epsilon > 0$  and even degree for  $\epsilon < 0$ ; if  $\text{ev}_{\mathbf{q}}^\beta(u_0)$  is in  $\mathcal{C}^{o_j < o_k}$   $f$  has even degree for  $\epsilon > 0$  and odd degree for  $\epsilon < 0$ .

**Proof.** As in the proof of Proposition 7.41, we can choose a smeared neighborhood  $U$  so that  $U \times_{\text{ev}_{P_0}} M$  is identified with an odd number of copies of  $[0, 1) \times (-1, 1)$ , indexed by simple boundary degenerations  $\{w_i\}$ . Since  $\text{ev}_{\mathbf{q}}^\beta$  is not on a wall, it follows that for each such boundary degeneration,  $t \circ w_i(p_1) - t \circ w_i(p_2)$  is non-zero. Thus, we can give each component of  $U \times_{\text{ev}_{P_0}} M$  an *associated sign*, which is positive or negative, according to the sign of the difference  $t \circ w_i(p_1) - t \circ w_i(p_2)$ .

Choosing  $U$  sufficiently small, we can ensure that  $t \circ u(p_1) - t \circ u(p_2)$  is non-zero; and in fact, on each component  $\mathcal{M}$ , the sign of  $t \circ u(p_1) - t \circ u(p_2)$  is determined by the associated sign of the component.

Pick any component  $\overline{\mathcal{M}}$  with positive sign, and let  $\mathcal{M}$  denote its interior.

Consider the maps

$$F_1 = t \circ \text{ev}_{p_1} - t \circ \text{ev}_{p_2}: \mathcal{M} \rightarrow \mathbb{R}^{>0} \quad \text{and} \quad F_2 = \text{ev}_{p_1} - \text{ev}_{q_0}: \mathcal{M} \rightarrow \mathbb{R}.$$

The maps  $F_1$  and  $F_2$  extend continuously to  $\overline{\mathcal{M}}$  to give maps  $\overline{F}_1: \overline{\mathcal{M}} \rightarrow \mathbb{R}^{\geq 0}$  and  $\overline{F}_2: \overline{\mathcal{M}} \rightarrow \mathbb{R}$ .

Clearly, the restriction of  $\overline{F}_2$  to

$$0 \times (-1, 1) = \partial \overline{\mathcal{M}}$$

has odd degree near 0. Moreover,  $F_1(s, t) > 0$  for all  $s > 0$  and  $t \in (-1, 1)$ , with  $\overline{F}(0, t) = 0$ . It follows that  $\overline{F}: \overline{\mathcal{M}} \rightarrow [0, 1) \times (-1, 1)$  has odd degree; and this is the same as the degree of the restriction  $F_1|_{F_2^{-1}(0)}$ .

If the component  $\overline{\mathcal{M}}$  has negative associated sign, the map  $F_1 = t \circ \text{ev}_{p_1} - t \circ \text{ev}_{p_2}$  maps to  $\mathbb{R}^{<0}$ , and indeed the above argument shows that

$$\overline{F}: \overline{\mathcal{M}} \rightarrow \mathbb{R}^{\leq 0} \times \mathbb{R}$$

has odd degree over the origin.

Now, if  $\text{ev}_{\mathbf{q}}^\beta(u_0) \in \mathcal{C}^{o_j > o_k}$ , there is an odd number of positive associated components and an even number of negative associated ones; whereas if  $\text{ev}_{\mathbf{q}}^\beta(u_0) \in \mathcal{C}^{o_j < o_k}$ , there

is an odd number of negative associated components and an even number of positive ones. The degree statement now follows.  $\square$

### 7.9. Ends of one-dimensional moduli spaces.

**Proof of Theorem 7.18.** Consider the limiting comb in the end of the one-dimensional moduli space  $\widehat{\mathcal{M}}$ , whose existence is guaranteed by Gromov compactness (cf. Proposition 7.37). This limit contains no  $\alpha$ -boundary degenerations, because such a degeneration covers both basepoints  $w$  and  $z$ .

Suppose next that a  $\beta$ -boundary degeneration occurs in the limit. By the dimension formula, the boundary degeneration must be simple (otherwise, the remaining curve has codimension greater than one). There are two cases, according to whether or not the boundary degeneration is special.

Suppose first that boundary degeneration is not special. Then there are two different orbits  $o_j$  and  $o_k$  on the boundary degeneration, and, by the hypotheses on allowed constraint packets, it follows that the boundary degeneration occurs as two packets collide. Moreover, since  $o_j$  and  $o_k$  are matched in  $M^\vee$ , and our packets are allowed, one of the two orbits is even, and so it is constrained to lie at the same level as a chord. Thus, the collision is a “boundary degeneration collision” in the sense of Definition 7.17. Moreover, the hypotheses of Proposition 7.41 are satisfied, using for  $M$  the diagonal which specifies the chord packets. That proposition now ensures that there is an odd number of such ends, and they are all in the chamber as specified in (AE-5).

Suppose that the boundary degeneration is special. There are two subcases, in the notation of (AE-6), according to whether or not  $\sigma = \rho_i \setminus \{o_k\}$  is empty. If  $\sigma$  is non-empty, we can apply Proposition 7.42, to find an odd number of ends. If  $\sigma$  is empty, the dimension formula ensures that the limiting curve lies in a moduli space with expected dimension zero. This moduli space is empty, unless it corresponds to the constant flowline. That is the case where  $\ell = 1$ ,  $\mathbf{x} = \mathbf{y}$ , and  $B = \mathcal{B}_{\{k\}}$ . These ends occur with an odd multiplicity, where we glue the constant flowline at  $\mathbf{x} = \mathbf{y}$  to the odd number of simple boundary degenerations  $w$  with  $\text{ev}^\beta(w) = \mathbf{x}$ , according to Lemma 5.20. This completes the cases where  $\beta$ -boundary degenerations occur.

The classification of the remaining ends follows very similarly to the proof of [10, Theorem 5.61]. In the present case, we have the possibility of orbit curves forming. Each such end appears with odd multiplicity by Proposition 7.40.

The fact that the chords in the collision are disjoint from one another (Condition (C-4)) follows from the dimension formula: combining the index formula the computation from Example 7.6, it follows that boundary-monotone collisions between non-disjoint constraint packets occur in codimension greater than one.

As in [10], boundary monotonicity and the non-existence of  $\alpha$ -boundary degenerations implies that in every collision, the joined chords are strongly composable.

We argue that collisions that are not visible occur with even multiplicity. To see this, observe that if the limiting curve has two punctures  $q_1$  and  $q_2$ , both of which are marked by the same orbit  $o_i$ , and  $t(u(q_1)) = t(u(q_2))$ , then that curve can be obtained as a limit of curves in  $\mathcal{M}(\mathbf{x}, \mathbf{y}, \mathcal{S}, \rho_1, \dots, \rho_\ell)$ , so that  $q_1$  belongs to the

packet  $\rho_i$  (and  $q_2$  to  $\rho_{i+1}$ ); or it can be obtained as a limit of curves in the same moduli space but where  $q_2$  belongs to  $\rho_{i+1}$ . Thus, these two ends cancel.

For the join curve ends as in Case (AE-4), the decomposition must satisfy Property (J-3); for other decompositions occur in larger codimension than one. (See the computation from Example 7.5.)  $\square$

**Proof of Theorem 5.26.** This follows as in the proof of Theorem 7.18. The key difference is that in the present case, orbits are never constrained to lie in the same level as other Reeb chords; and indeed if  $j$  and  $k$  are matched in  $M^\wedge$ , i.e. both appear in a boundary degeneration, only one of  $o_j$  or  $o_k$  is allowed to appear in a constraint packet. It follows that the only boundary degenerations that can appear are special ones. The dimension formula once again ensures that the remaining curve, in this case, is a constant.  $\square$

## 8. TYPE A MODULES

Let  $\mathcal{H}^\vee$  be a lower diagram, and  $M$  a matching on  $\{1, \dots, 2n\}$ . Let  $M^\vee$  be the equivalence relation on  $\{1, \dots, 2n\}$  induced by  $\mathcal{H}^\vee$ . Together,  $M$  and  $M^\vee$  generate an equivalence relation on  $\{1, \dots, 2n\}$ . The matching  $M$  is called *compatible* with  $\mathcal{H}^\vee$  if the equivalence relation has one equivalence class in it.

Our aim here is to prove the following:

**Theorem 8.1.** *Fix a lower diagram  $\mathcal{H}^\vee$  and a matching  $M$  on  $\{1, \dots, 2n\}$  compatible with  $M^\vee$ . Fix also a generic almost-complex structure for  $\mathcal{H}^\vee$ . Let  $Q(\mathcal{H}^\vee, M)$  be the free  $\mathbb{F}[U, V]/UV$ -module generated by lower states. This can be endowed with the following further structures:*

- A rational-valued Alexander grading  $\mathbf{A}$  (Equation (4.3) below)
- An integer-valued relative grading  $\mathbf{m}$  (Equation (8.3))
- A collection of maps

$$m_{1+\ell}: Q \otimes \overbrace{\mathcal{B} \otimes \cdots \otimes \mathcal{B}}^\ell \rightarrow Q$$

for  $\ell \in \mathbb{Z}^{\geq 0}$ , defined by counting pseudo-holomorphic flows (Equation (8.5)).

The result is a curved  $\mathcal{A}_\infty$  module over  $\mathcal{B}$ , with curvature  $\sum_{\{i,j\} \in M} U_i U_j$ , which has the following grading properties:

- $U$  drops  $\mathbf{A}$  by 1;  $V$  raises  $\mathbf{A}$  by 1; and the operations  $m_{1+\ell}$  preserve  $\mathbf{A}$
- $U$  drops  $\mathbf{m}$  by 1;  $V$  drops  $\mathbf{m}$  by 1, and the operations  $m_{1+\ell}$  respect  $\mathbf{m}$ , in the sense that if  $\mathbf{x} \in Q$  is a homogeneous module element, and  $a_1, \dots, a_\ell$  is a sequence of homogeneous algebra elements, then  $m_{1+\ell}(\mathbf{x}, a_1, \dots, a_\ell)$  is also homogeneous, with grading given by

$$(8.1) \quad \mathbf{gr}(m_{1+\ell}(\mathbf{x}, a_1, \dots, a_\ell)) = \mathbf{gr}(\mathbf{x}) + \ell - 1 + \sum_{i=1}^{\ell} \mathbf{m}(a_i).$$

Constraint packets are related to algebra elements in  $\mathcal{C}$  in Section 8.1. Once that is complete, the proof will be given in the end of Section 8.2. Invariance properties will be dealt with in Subsection 8.3, and examples will be given in Subsection 8.4

**8.1. Algebra elements and constraints.** An ingredient to constructing type A modules to lower diagrams is the relationship between constraint packets (c.f. Definition 7.1) and the algebra  $\mathcal{C}$ , which we formulate presently.

If  $\rho$  is a Reeb chord for a lower diagram, then it has a corresponding algebra element  $\tilde{b}(\rho)$  obtained by multiplying together the letters that represent the chord, as in Figure 18. For example, the chord  $\rho$  that covers  $Z_i$  with multiplicity one and which starts and ends at  $\alpha_i$  has

$$a(\rho) = L_i \cdot R_i = \left( \sum_{\{\mathbf{s} \mid i \in \mathbf{s}, i-1 \notin \mathbf{s}\}} \mathbf{I}_{\mathbf{s}} \right) \cdot U_i$$

We generalize this construction to certain kinds of chord packets, as follows.

If  $\rho$  is a Reeb chord, let  $\rho^-$  denote its initial  $\alpha$ -arc, and  $\rho^+$  denote its terminal  $\alpha$ -arc.

**Definition 8.2.** *A set of Reeb chords  $\{\rho_1, \dots, \rho_j\}$  is called algebraic if for any pair of distinct chords  $\rho_a$  and  $\rho_b$ ,*

- *the chords  $\rho_a$  and  $\rho_b$  are on different boundary components  $Z_i$  and  $Z_j$ ,*
- *the initial points  $\rho_a^-$  and  $\rho_b^-$  are on different  $\alpha$ -curves; and*
- *the terminal points  $\rho_a^+$  and  $\rho_b^+$  are on different  $\alpha$ -curves.*

Let  $\rho$  be a set of Reeb chords that is algebraic, in the above sense, we can associate an algebra element to  $\rho$ , defined as follows. Let  $\alpha(\rho^+)$  be the curve  $\alpha_i$  with  $\rho^+ \in \alpha_i$ ; define  $\alpha(\rho^-)$  similarly. Let

$$I^-(\rho) = \sum_{\{\mathbf{s} \mid \{\alpha(\rho_1^-), \dots, \alpha(\rho_j^-)\} \subset \{\alpha_i\}_{i \in \mathbf{s}}\}} I_{\mathbf{s}} \quad \text{and} \quad I^+(\rho) = \sum_{\{\mathbf{s} \mid \{\alpha(\rho_1^+), \dots, \alpha(\rho_j^+)\} \subset \{\alpha_i\}_{i \in \mathbf{s}}\}} I_{\mathbf{s}}$$

Then,  $\check{b}_0(\rho)$  be the algebra element  $a_0 \in \mathcal{B}_0(2n, n)$  with

$$a = I^- \cdot a \cdot I^+$$

and whose weight  $w_i(a)$  is the average local multiplicity at  $Z_i$ . Let  $\check{b}(\rho)$  be the image of  $\check{b}_0(\rho)$  in  $\mathcal{C}(n)$ .

**8.2. Constructing the  $\mathcal{A}_\infty$  module.** We will fix throughout a lower diagram  $\mathcal{H}^\vee$  and a compatible  $M$  on  $\{1, \dots, 2n\}$ .

Sometimes it is useful to enlarge the equivalence relation to include the points  $w$  and  $z$ , as follows. We extend  $M^\vee$  to a matching  $M_*^\vee$  on the set  $\{w, z, 1, \dots, 2n\}$ , so that  $i$  is matched with  $w$  resp.  $z$  if  $\check{Z}_i$  can be connected to  $w$  resp.  $z$  without crossing any  $\alpha$ -circles. Then,  $M$  and  $M_*^\vee$  extended in this manner define an equivalence relation on  $\{w, z, 1, \dots, 2n\}$ . If  $M$  and  $M^\vee$  are compatible, the associated one-manifold  $W(M) \cup W(M_*^\vee)$  is homeomorphic to an interval from  $w$  and  $z$ .

Traversing the arc  $W(M) \cup W(M_*^\vee)$  (starting at  $w$  and ending at  $z$ ), we encounter placemarkers for the orbits  $\{1, \dots, 2n\}$  in some order. Let  $f_0: \{1, \dots, 2n\}$  denote the order in which the placemarkers are encountered along this arc. We will define a function

$$f: \{1, \dots, 2n\} \rightarrow \{1, \dots, 2n\},$$

obtained by post-composing  $f_0$  with the involution on  $\{1, \dots, 2n\}$  that switches  $2i-1$  and  $2i$  for  $i = 1, \dots, n$ . Thus, the resulting function has  $f(i) = 1$  if the orbit  $o_i$  is the second orbit we encounter on the arc;  $f(i) = 2$  if  $o_i$  is the first;  $f(i) = 3$  if  $o_i$  is the fourth, and  $f(i) = 4$  if  $o_i$  is the third, etc. See Figure 23.

**Definition 8.3.** *The function  $f: \{1, \dots, 2n\}$  is called the induced ordering on the boundary components, induced by  $M^\vee$  and  $M$ .*

Observe that if  $i$  is chosen so that  $Z_i$  and  $w$  are contained in the same component of  $\Sigma \setminus \beta$ , then  $f(i) = 2n-1$ . We call the Reeb orbit  $o_i$  *even* resp. *odd* if  $f(i)$  is even resp. odd; i.e.  $f$  induces an orbit marking, in the sense of Definition 7.14.

**Remark 8.4.** *The function  $f$  can be thought of as a relabeling of the Reeb orbits, which might seem somewhat artificial at the moment. It is, however, a reordering which very convenient for the purpose of the pairing theorem; cf. Section 9.*

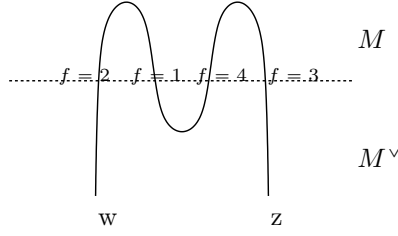


FIGURE 23. **Labeling the orbits.** The matchings  $M^\vee$ ,  $M$ , and the basepoint  $z$  order the Reeb orbits as indicated.

We will give  $Q(\mathcal{H}^\vee, M)$  the structure of a bimodule, which is a right module over the idempotent ring  $I_0(n) \subset \mathcal{C}(n)$  and a left module over  $\mathcal{R} = \mathbb{F}[U, V]/UV = 0$ . As a left  $\mathcal{R}$ -module it is freely generated by all lower states. The idempotent in  $\mathcal{C}(n)$  associated to a lower state is defined be

$$\check{\mathbf{I}}(\mathbf{x}) = \mathbf{I}_{\alpha(\mathbf{x})},$$

where  $\alpha(\mathbf{x})$  is as in Definition 2.2. (Note that this is different from the idempotent for upper states, as in Equation (6.1).) The right action of the idempotent subalgebra of  $\mathcal{C}(n)$  is specified by the condition that  $\mathbf{x} \cdot \check{\mathbf{I}}(\mathbf{x}) = \mathbf{x}$ .

**Lemma 8.5.** *Given  $\mathbf{x}, \mathbf{y} \in \mathfrak{S}$ , the quantity*

$$\mathbf{A}(B) = n_z(B) - n_w(B) + \sum_{i=1}^{2n} (-1)^{f(i)} \omega_i(B)$$

*is independent of the choice of  $B \in \mathcal{D}(\mathbf{x}, \mathbf{y})$ .*

**Proof.** This follows from the fact that  $\mathbf{A}(B)$  vanishes on each component  $B$  of  $\Sigma \setminus \beta$ . (Compare the proof of Lemma 4.4.)  $\square$

Since  $\mathbf{A}(B_1 * B_2) = \mathbf{A}(B_1) + \mathbf{A}(B_2)$ , there is a function  $\mathbf{A}: \mathfrak{S} \rightarrow \mathbb{Q}$ , uniquely characterized up to an overall additive indeterminacy, so that

$$(8.2) \quad \mathbf{A}(\mathbf{x}) - \mathbf{A}(\mathbf{y}) = \mathbf{A}(B)$$

for  $B \in \mathcal{D}(\mathbf{x}, \mathbf{y})$ . This induces a  $\mathbb{Q}$ -valued grading on  $Q(\mathcal{H}^\vee, M) = \bigoplus_{s \in \mathbb{Q}} Q(\mathcal{H}^\vee, M, s)$ , with the convention that

$$\begin{aligned} U: Q(\mathcal{H}^\vee, M, s) &\rightarrow Q(\mathcal{H}^\vee, M, s-1) \\ V: Q(\mathcal{H}^\vee, M, s) &\rightarrow Q(\mathcal{H}^\vee, M, s+1). \end{aligned}$$

Chose a generic admissible almost-complex structure for  $\mathcal{H}^\vee$ . We use this to endow  $Q(\mathcal{H}^\vee, M)$  with the structure of a right  $\mathcal{A}_\infty$  module over  $\mathcal{C}(n)$ , as follows.

**Definition 8.6.** *Fix a Heegaard state  $\mathbf{x}$  and a sequence  $\vec{a} = (a_1, \dots, a_\ell)$  of pure algebra elements in  $\mathcal{B}_0(2n, n)$ . A sequence of constraint packets  $\boldsymbol{\rho}_1, \dots, \boldsymbol{\rho}_k$  is called  $(\mathbf{x}, \vec{a})$ -compatible if there is a sequence  $1 \leq k_1 < \dots < k_\ell \leq k$  so that the following conditions hold:*

- the constraint packets  $\boldsymbol{\rho}_{k_i}$  are algebraic, in the sense of Definition 8.2

- $\check{\mathbf{I}}(\mathbf{x}) \cdot \check{b}_0(\boldsymbol{\rho}_{k_1}) \otimes \cdots \otimes \check{b}_0(\boldsymbol{\rho}_{k_\ell}) = \check{\mathbf{I}}(\mathbf{x}) \cdot a_1 \otimes \cdots \otimes a_\ell$ , as elements of  $Q(\mathcal{H}^\vee, M) \otimes \mathcal{C}_0(n)^{\otimes \ell}$
- for each  $t \notin \{k_1, \dots, k_\ell\}$ , the constraint packet  $\boldsymbol{\rho}_t$  is either of the form  $\{o_i\}$  where  $f(i)$  is odd; or it is of the form  $\{o_i, v_j\}$ , where
  - $f(i)$  is even
  - $\{i, j\} \in M$
  - $v_j$  is one of the two Reeb chords that covers  $Z_j$  with multiplicity one.

Constraint packets  $\boldsymbol{\rho}_j$  with  $j \in \{k_1, \dots, k_\ell\}$  are called *orbitless*. Let  $[\mathbf{x}, a_1, \dots, a_\ell]$  be the set of all sequences of constraint packets  $\boldsymbol{\rho}_1, \dots, \boldsymbol{\rho}_h$  that are  $(\mathbf{x}, \vec{a})$ -compatible.

When considering boundary-monotone sequences, we can use  $\mathcal{C}(n)$  instead of  $\mathcal{C}_0(n)$ , according to the following:

**Lemma 8.7.** *If  $(\mathbf{x}, \boldsymbol{\rho}_1, \dots, \boldsymbol{\rho}_k)$  is a strongly boundary monotone sequence which is  $\vec{a} = (a_1, \dots, a_\ell)$ -compatible for some sequence of algebra elements in  $\mathcal{B}_0$ ; then the projection of  $\mathbf{x} \otimes a_1 \otimes \cdots \otimes a_\ell$  in  $Q \otimes \mathcal{C}(n)^{\otimes \ell}$  is non-zero.*

**Proof.** We use Proposition 3.2. Consider the packet at time  $t$ ,  $\boldsymbol{\rho}_t$ , and let  $\mathbf{I}_{\mathbf{x}_-}$  and  $\mathbf{I}_{\mathbf{x}_+}$  be the idempotents immediately before and after.

We claim that  $\mathbf{x}_-$  and  $\mathbf{x}_+$  cannot be too far. This follows from the fact that  $\boldsymbol{\rho}$  contains two chords  $\rho_1$  and  $\rho_2$  so that the terminal point of  $\rho_1$  is the initial point of  $\rho_2$ , then the initial point of  $\rho_2$  also appears in  $\mathbf{I}_{\mathbf{x}_-}$ . This is immediate.

It remains to exclude the other possibility from Proposition 3.2. That can be excluded by the following reasoning. Suppose that  $\boldsymbol{\rho}$  contains a sequence of chords  $\rho_i, \dots, \rho_j$  with the following properties:

- $\rho_t$  is supported on  $\check{Z}_t$  for  $t = i, \dots, j$
- either  $\mathbf{I}_{\mathbf{x}_-}$  or  $\mathbf{I}_{\mathbf{x}_+}$  does not contain  $\alpha_i$ .
- $\mathbf{w}(\rho_t) \geq 1$  for  $t = i + 1, \dots, j - 1$

A straightforward proof by induction, using boundary monotonicity, shows that endpoints of  $\rho_j$  are on  $\alpha_j$ .

From Proposition 3.2, it follows that the pure algebra element  $\mathbf{I}_{\mathbf{x}_-} \cdot b_0(\boldsymbol{\rho}) \mathbf{I}_{\mathbf{x}_+}$  is not in  $\mathcal{J}$ ; i.e. its projection to  $\mathcal{B}$  is non-zero.  $\square$

**Definition 8.8.** *Given  $(B, \boldsymbol{\rho}_1, \dots, \boldsymbol{\rho}_h)$ , the  $U$ -weight is the quantity  $\gamma$  which is be the multiplicity of  $B$  at  $\mathbf{w}$  plus the number of constraint packets among the  $\boldsymbol{\rho}_1, \dots, \boldsymbol{\rho}_h$  consisting of a single Reeb orbit (or, equivalently, the total count of odd Reeb orbits appearing in the  $\boldsymbol{\rho}_1, \dots, \boldsymbol{\rho}_h$ ); and the  $V$ -weight  $\delta = \delta(B, \boldsymbol{\rho}_1, \dots, \boldsymbol{\rho}_h)$  is the local multiplicity of the domain  $B$  at the basepoint  $\mathbf{z}$ .*

**Lemma 8.9.** *If  $\mathcal{D}(\mathbf{x}, \mathbf{y})$  is non-empty, then for  $B \in \mathcal{D}(\mathbf{x}, \mathbf{y})$ , the integer*

$$(8.3) \quad \mathbf{m}(B) = e(B) + P(B) - \mathbf{w}_\partial(B) - n_{\mathbf{w}}(B) - n_{\mathbf{z}}(B)$$

*is independent of  $B$ .*

**Proof.** This follows as in Lemma 4.4, with the observation that now  $e(\mathcal{D}) + P(\mathcal{D}) - \mathbf{w}_\partial(\mathcal{D}) - n_{\mathbf{w}}(\mathcal{D}) - n_{\mathbf{z}}(\mathcal{D})$  vanishes components  $\mathcal{D}$  of  $\Sigma \setminus \mathcal{B}$ .  $\square$



Correspondingly, we have a function  $\mathbf{m}: \mathfrak{S} \rightarrow \mathbb{Z}$  uniquely characterized up to an overall additive constant by the property that

$$(8.4) \quad \mathbf{gr}(\mathbf{x}) - \mathbf{gr}(\mathbf{y}) = \mathbf{m}(B)$$

for any  $B \in \mathcal{D}(\mathbf{x}, \mathbf{y})$ .

**Lemma 8.10.** *Fix  $\mathbf{x}, \mathbf{y} \in \mathfrak{S}$ , a sequence of pure algebra elements  $\vec{a} = (a_1, \dots, a_\ell)$ , an  $(\mathbf{x}, \vec{a})$ -compatible sequence of constraint packets  $\rho_1, \dots, \rho_h$ , and  $B \in \mathcal{D}(\mathbf{x}, \mathbf{y})$ . If there is a pre-flowline  $u$  whose shadow is  $B$  and whose packet sequence is  $(\rho_1, \dots, \rho_\ell)$ , then*

$$\mathbf{gr}(\mathbf{x}) + \ell - \sum_i \mathbf{w}_{i=1}^\ell(a_i) = \mathbf{gr}(\mathbf{y}) - \gamma(B) - \delta(B) + \text{ind}(B, \mathbf{x}, \mathbf{y}, \rho_1, \dots, \rho_h).$$

**Proof.** By the definition of  $\mathbf{gr}$  and  $\mathbf{m}$ ,

$$\mathbf{gr}(\mathbf{x}) - \mathbf{gr}(\mathbf{y}) = e(B) + n_{\mathbf{x}}(B) + n_{\mathbf{y}}(B) - \mathbf{w}_{\partial}(B) - n_{\mathbf{w}}(B) - n_{\mathbf{z}}(B).$$

Since all the orbits in appearing in  $\rho_i$  have weight 1, the index formula gives

$$\text{ind}(B, \vec{\rho}_i) = e(B) + n_{\mathbf{x}}(B) + n_{\mathbf{y}}(B) + h - \mathbf{w}_{\partial}(B) + \sum \iota(\text{cho}(\rho_i)).$$

Indeed,  $\iota(\text{cho}(\rho_i)) = -\mathbf{w}(\text{cho}(\rho_i))$ , so taking the difference of these two equations, we find that

$$\begin{aligned} \mathbf{gr}(\mathbf{x}) - \mathbf{gr}(\mathbf{y}) - \text{ind}(B, \vec{\rho}) &= -h - n_{\mathbf{w}}(B) - n_{\mathbf{z}}(B) + \sum_{i=1}^h \mathbf{w}(\text{cho}(\rho_i)) \\ &= -\ell - n_{\mathbf{w}}(B) - n_{\mathbf{z}}(B) - \#(\text{odd orbits}) + \sum_{i=1}^{\ell} \mathbf{w}(a_i) \\ &= -\ell - \gamma(B) - \delta(B) + \sum_{i=1}^{\ell} \mathbf{w}(a_i). \end{aligned}$$

Going from the second to the third line uses the fact that the packets containing an even orbit also contain a weight one chord.  $\square$

Fix a lower Heegaard state  $\mathbf{x}$  and a sequence of pure algebra elements  $a_1, \dots, a_\ell$  so that  $\check{\mathbf{I}}(\mathbf{x}) \cdot a_1 \otimes \dots \otimes a_\ell \neq 0$ . Define

$$(8.5) \quad m_{1+\ell}(\mathbf{x}, a_1, \dots, a_\ell) = \sum_{\{\mathbf{y} \in \mathfrak{S}, (\rho_1, \dots, \rho_h) \in \llbracket \mathbf{x}, a_1, \dots, a_\ell \rrbracket\}} U^\gamma V^\delta \# \mathcal{M}(\mathbf{x}, \mathbf{y}, \rho_1, \dots, \rho_h) \cdot \mathbf{y},$$

where  $\gamma = \gamma(\rho_1, \dots, \rho_h)$  is the multiplicity at  $\mathbf{w}$  of the domain  $B$  determined by the sequence  $\mathbf{x}, \mathbf{y}, \rho_1, \dots, \rho_h$  plus the number of constraint packets among the  $(\rho_1, \dots, \rho_h)$  consisting of a single Reeb orbit. When  $\check{\mathbf{I}}(\mathbf{x}) \otimes a_1 \otimes \dots \otimes a_\ell = 0$ , we define the action  $m_{1+\ell}(\mathbf{x}, a_1, \dots, a_\ell) = 0$ .

For example, the  $\mathbf{y}$  coefficient of  $m_1(\mathbf{x})$  is computed by counting points in

$$\mathcal{M}(\mathbf{x}, \mathbf{y}, \rho_1, \dots, \rho_h),$$

where each  $\rho_t$  is either an odd Reeb orbit, or it is the constraint packet consisting of some even Reeb orbit covering some boundary component once together with a Reeb chord that covers its matching (using  $M$ ) boundary component exactly once.

As another example, the  $\mathbf{y}$  coefficient of  $m_2(\mathbf{x}, U_2)$  is computed by counting points in  $\mathcal{M}(\mathbf{x}, \mathbf{y}; \boldsymbol{\rho}_1, \dots, \boldsymbol{\rho}_h)$ , where exactly one of  $\boldsymbol{\rho}_t$  is Reeb chord  $R_2 L_2$  or the Reeb chord  $L_2 R_2$ , and all other constraints packets have an orbit or an orbit and a chord as above.

We claim that the sum appearing in Equation (8.5) is finite, according to the following:

**Lemma 8.11.** *Given  $(\mathbf{x}, a_1, \dots, a_\ell)$  and  $\mathbf{y}$ , there are only finitely many homology classes  $B$  of holomorphic disks that can represent  $\mathcal{M}(\mathbf{x}, \mathbf{y}, \boldsymbol{\rho}_1, \dots, \boldsymbol{\rho}_h)$ , where  $\boldsymbol{\rho}_1, \dots, \boldsymbol{\rho}_h$  is  $(\mathbf{x}, \vec{a})$ -compatible, and for which one of  $\gamma = 0$  or  $\delta = 0$ .*

**Proof.** Fix  $\mathbf{x}, \mathbf{y}$ , and let  $B \in \mathcal{D}(\mathbf{x}, \mathbf{y})$  representing some  $(\mathbf{x}, \vec{a})$  compatible sequence  $(\boldsymbol{\rho}_1, \dots, \boldsymbol{\rho}_h)$ . The following bounds are immediate:

- (b-1) For  $\{i, j\} \in M^\vee$ , the quantity  $\omega_i(B) - \omega_j(B)$  is independent of the choice of  $B$  (depending only on  $\mathbf{x}$  and  $\mathbf{y}$ ).
- (b-2)  $\omega_{f^{-1}(2)}(B) - n_w(B)$  is independent of  $B$ .
- (b-3)  $\omega_{f^{-1}(2n-1)}(B) - n_z(B)$  is independent of  $B$ .
- (b-4) while for  $\{i, j\} \in M$  with  $f(i)$  odd,

$$\omega_i(B) - \omega_j(B) - \#(o_i \in \boldsymbol{\rho}_1, \dots, \boldsymbol{\rho}_h)$$

depends only on  $\mathbf{x}, \mathbf{y}$ , and  $\vec{a}$ .

Thus, for fixed  $(\mathbf{x}, \vec{a})$  and  $\mathbf{y}$ , there are constants  $c_i$  so that

$$(8.6) \quad c_i = \omega_{f^{-1}(2i-1)}(B) - n_w(B) - \#(o_k \in \boldsymbol{\rho}_1, \dots, \boldsymbol{\rho}_h \text{ with } f(k) \text{ odd and } f(k) \leq 2i-1).$$

The case  $i = n$ , together with the fact that  $\omega_{f^{-1}(2n-1)}(B) - n_z(B)$ , is independent of  $B$  shows that

$$n_z(B) - n_w(B) - \#(o_k \in \boldsymbol{\rho}_1, \dots, \boldsymbol{\rho}_h \text{ with } f(k) \text{ odd}) = \delta - \gamma$$

is independent of the choice of  $B$ . Since  $UV = 0$ , we obtain an upper bound on the  $U$ -power  $\gamma$  appearing on any term in  $m_{1+\ell}(\mathbf{x}, a_1, \dots, a_\ell)$ .

Equation (8.6) implies that for any odd  $i$ ,  $\omega_{f^{-1}(i)}(B) \leq c_i + \gamma$ . By (b-2) and (b-1), we can conclude a similar bound for even  $i$ , as well. Since  $\gamma$  is bounded above as above, we obtain a universal bound on  $\omega_i(B)$  for any  $B$  that contributes to  $m_\ell(\mathbf{x}, a_1, \dots, a_\ell)$ . It is elementary to see that there are only finitely many non-negative homology classes of  $B \in \mathcal{D}(\mathbf{x}, \mathbf{y})$  with a universal bound on  $\omega_i(B)$  bounded for all  $i$ .  $\square$

**Proposition 8.12.** *The operations defined above endow  $Q(\mathcal{H}^\vee, M)$  with the structure of right  $\mathcal{A}_\infty$  module over  $\mathcal{C}(n)$  (which is also a free left module over  $\mathcal{R}$ ).*

**Proof.** Let  $\mathbf{x}$  be an lower Heegaard state, and  $a_1, \dots, a_\ell$  be a sequence of algebra elements so that  $\mathbf{x} \otimes a_1 \otimes \dots \otimes a_\ell \neq 0$ . As usual, the  $\mathcal{A}_\infty$  relations are proved by looking at ends of one-dimensional moduli spaces. Specifically, we consider  $\widehat{\mathcal{M}}(\mathbf{x}, \mathbf{z}, \boldsymbol{\rho}_1, \dots, \boldsymbol{\rho}_h)$ , where we take the union over all sequences of algebraic constraint packets  $(\boldsymbol{\rho}_1, \dots, \boldsymbol{\rho}_h) \in \llbracket \mathbf{x}, a_1, \dots, a_\ell \rrbracket$ .

The condition that  $\check{\mathbf{I}}(\mathbf{x}) \cdot a_1 \otimes \dots \otimes a_\ell \neq 0$  ensures that the corresponding compatible constraint packets  $(\mathbf{x}, \boldsymbol{\rho}_1, \dots, \boldsymbol{\rho}_h)$  are strongly boundary monotone. (See

Lemma 7.3.) The homology classes that have non-zero contribution cannot have positive multiplicity at both  $w$  and  $z$ , since we have the relation in our algebra that  $UV = 0$ . It is easy to see that each constraint packet is allowed, in the sense of Definition 7.15.

Contributions of the two-story ends (Type (AE-1)) correspond to the terms

$$m_{\ell-i+1}(m_{i+1}(\mathbf{x}, a_1, \dots, a_i), a_{i+1}, \dots, a_\ell)$$

appearing in the  $\mathcal{A}_\infty$  relation.

Orbit curve ends (Type (AE-2)) occur in two types. When the constraint packet is of the form  $\{o_j, v_k\}$  (so that  $f(j)$  is even), its corresponding orbit curve ends corresponds to a term in

$$(8.7) \quad m_{\ell+2}(\mathbf{x}, a_1, \dots, a_i, \mu_0, a_{i+1}, \dots, a_\ell).$$

If the constraint packet is of the form  $\{o_j\}$  (so that  $f(j)$  is odd), we call the corresponding orbit curve end an *odd orbit curve end*. In the course of this proof, we will find other ends that cancel these odd orbit curve ends.

We turn now to visible collision ends (Type (AE-3)), first considering visible collision ends where the two constraint packets  $\rho_i$  and  $\rho_{i+1}$  are orbitless. These contribution correspond to the terms in the  $\mathcal{A}_\infty$  relation of the form

$$m_\ell(\mathbf{x}, a_1, \dots, a_{i-1}, a_i \cdot a_{i+1}, a_{i+2}, \dots, a_\ell).$$

Consider next collision ends where exactly one of  $\rho_i$  or  $\rho_{i+1}$  is orbitless. In this case, we can find an alternative choice of  $i^{th}$  and  $(i+1)^{st}$  constraint packet  $\rho'_i$  and  $\rho'_{i+1}$ , so that the corresponding ends of  $\mathcal{M}(\mathbf{x}, \mathbf{y}, \rho_1, \dots, \rho_{i-1}, \rho_i, \rho_{i+1}, \rho_{i+2}, \dots, \rho_\ell)$  and  $\mathcal{M}(\mathbf{x}, \mathbf{y}, \rho_1, \dots, \rho_{i-1}, \rho'_i, \rho'_{i+1}, \rho_{i+2}, \dots, \rho_\ell)$  cancel. We choose  $\rho'_i = \rho_{i+1}$  and  $\rho'_{i+1} = \rho_i$  except in the special case where one of  $\rho_i$  or  $\rho_{i+1}$  (which we can assume without loss of generality is  $\rho_i$ ) consists of an even orbit  $o_j$  and matching chord  $v$  that covers  $Z_k$  with multiplicity 1, and  $\rho_{i+1}$  also contains some chord  $\rho$  supported in  $Z_k$ . In that case, there is a unique, possibly different long chord  $v'$  covering  $Z_k$  with multiplicity one, so that  $v \uplus \rho = \rho \uplus v'$ . Then,  $\rho'_{i+1} = \{o_j, v'\}$ , and  $\rho'_i = \rho_{i+1}$ ; see Figure 24. (We are cancelling here contributions corresponding to ends of different moduli spaces; but the domains  $B$  each pair of moduli spaces is the same, as are the total number of odd orbits in the corresponding Reeb sequences; so the  $U$  and  $V$  exponents for the contributions are the same, and the cancellation occurs.)

Similar cancellations occur when both  $\rho_i$  and  $\rho_{i+1}$  contain orbits, but the orbit in  $\rho_i$  is not matched (via  $M^\vee$ ) with the one in  $\rho_{i+1}$ .

When the orbit in  $\rho_i$  is matched with the orbit in  $\rho_{i+1}$  there are two kinds of collision ends: those that are contained (Type (AE-3)), and those that are not (Type (AE-5)); see Figure 26. Ends where the collision is contained once again cancel corresponding ends of moduli spaces where the order of the two packets is permuted.

The total number of remaining (i.e. uncontained) collision ends of this moduli space and the one obtained by permuting  $\rho_i$  and  $\rho_{i+1}$  counts points in

$$\mathcal{M}(\mathbf{x}, \mathbf{z}, \rho_1, \dots, \rho_{i-1}, \sigma, \rho_{i+2}, \dots, \rho_\ell),$$

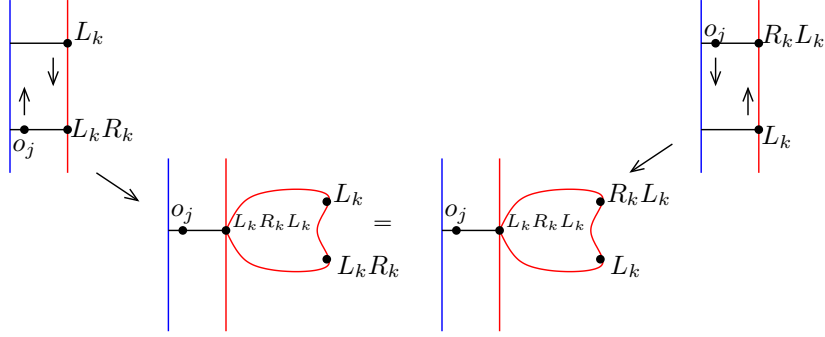


FIGURE 24. **Cancellations of collision ends.** For this collision cancellation, we use the two decompositions of  $L_k R_k L_k$  as  $L_k \uplus R_k L_k = L_k R_k \uplus L_k$ . (In the picture, we assume that  $f(k)$  and  $f(j)$  are consecutive integers, and  $f(k)$  is odd.)

where  $\sigma = \{v_k\}$  is one of the two Reeb chords that covers the component  $Z_k$  with  $f(k)$  odd. These cancel against the odd orbit curve ends described above. See Figure 26. Note that in this case, the homology classes  $B$  and  $B'$  of the curves representing the two cancelling ends do not coincide: an uncontained collision end removes a boundary degeneration. Nonetheless, the boundary degenerations considered here have  $n_w(v) = n_z(v) = 0$ ; and the total number of odd orbits remains unchanged, so the  $U$  and  $V$  exponents of the two ends coincide.

The same cancellation occurs for ends of Type (AE-6) (the “special boundary degenerations”), where the even unmatched Reeb orbit (i.e.  $o_j$  with  $f(j) = 2$ ) is removed: it cancels with a corresponding odd orbit end. (See Figure 25.) Cancellation occurs because the moduli space with the boundary degeneration end contributes the same  $U$  and  $V$  powers as the moduli space with the odd orbit end. To see this, let  $B$  denotes the homology class with the special boundary degeneration; let  $(\rho_1, \dots, \rho_\ell)$  denote the Reeb sequence for the moduli space containing the special boundary degeneration end; let  $(\rho_1, \dots, \rho_{i-1}, \sigma, \rho_{i+1}, \dots, \rho_\ell)$  be the sequence associated with the boundary degeneration end; and let  $B'$  be the homology class where the boundary degeneration is removed (and the one where the corresponding odd orbit end occurs). Clearly,  $n_w(B') = n_w(B) - 1$ , while the odd orbit end is associated with the sequence  $(\rho_1, \dots, \rho_{i-1}, \{o_j\}, \rho_{i+1}, \dots, \rho_\ell)$ , which has one odd orbit more than the original sequence moduli space that has one additional odd orbit in its interior than  $\rho_1, \dots, \rho_\ell$ . Thus, the  $U$  exponents of both moduli spaces coincide. Moreover, since  $n_z(B) = n_z(B')$ , the  $V$  exponents coincide, as well.

By contrast, ends of Type (AE-6), involving the other unmatched Reeb orbit  $o_j$  (with  $f(j) = 1$ ) do not contribute. This is true because  $\mathcal{B}_{\{j\}}$  also crosses the  $z$  basepoint, so the homology class contributes a multiple of  $V$ . By Equation (8.5), moduli spaces containing this orbit are counted with a multiple of  $U$ . Since we have specialized to  $UV = 0$ , this end does not contribute.

Consider next the join ends (Type (AE-4)). We argue ultimately that these all count with even multiplicity, as follows.

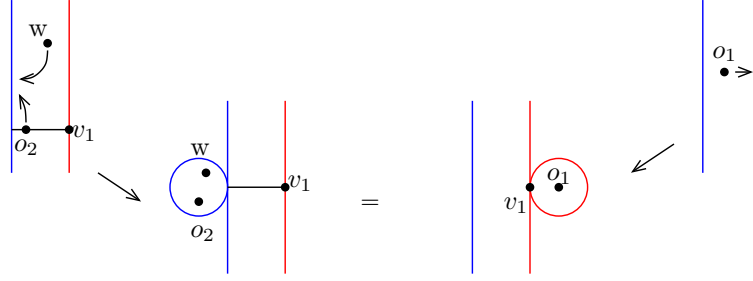


FIGURE 25. **Special boundary degeneration cancelling an odd orbit end.** Orbits here are labelled by their  $f$ -values.

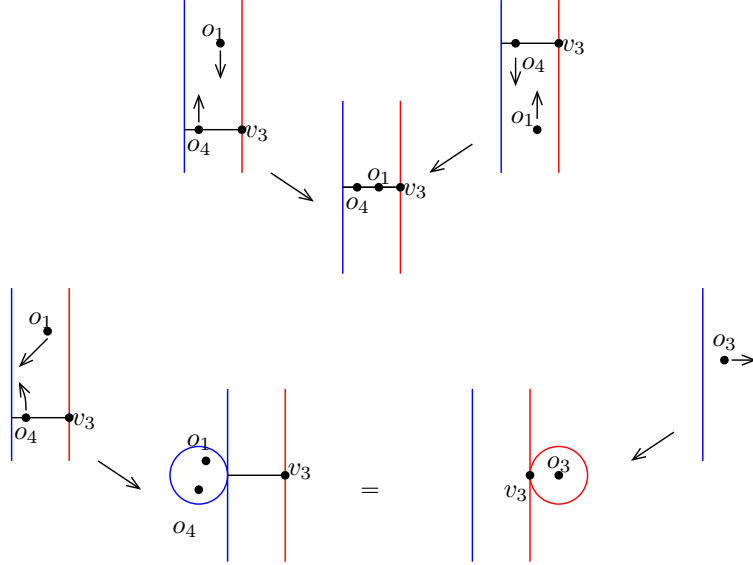


FIGURE 26. **Cancellations when two packets contain orbits.** The top row indicates cancellations of two contained collision ends. The bottom row indicates the cancelation of an uncontained collision end with an odd orbit end. In this picture, we subscript each orbit by its  $f$ -value.

Suppose that  $\rho_i$  contains some chord  $\rho$  supported in  $Z_i$ , which we can split as  $\rho = \rho_1 \uplus \rho_2$ . We investigate the corresponding join ends  $\rho_1, \dots, \rho_{i-1}, \sigma, \rho_{i+1}, \dots, \rho_\ell$ , where

$$\text{cho}(\sigma) = (\text{cho}(\rho_i) \setminus \{\rho\}) \cup \{\rho_1, \rho_2\}.$$

If the two endpoints of  $\rho$  are distinct, then this corresponding join curve end cannot appear in a moduli space of boundary monotone curves. That is, suppose that  $\rho$  has two distinct endpoints and it has a decomposition as  $\rho = \rho_1 \uplus \rho_2$ . Then it is elementary to see that either  $\rho_1^+ = \rho_2^+$  or  $\rho_1^- = \rho_2^-$ ; i.e. the chords  $\rho_1$  and  $\rho_2$  cannot appear in the same constraint packet, for a boundary monotone sequence.

Consider next the case where the two endpoints of  $\rho$  are the same, and consider there is a join curve end corresponding to a splitting  $\rho = \rho_1 \uplus \rho_2$ . Such ends appear boundary monotone moduli spaces only when the two endpoints of  $\rho_1$  (and hence also of  $\rho_2$ ) are distinct. For example, we know  $\rho_1^- = \rho_2^+$ , so if  $\rho_1^- = \rho_1^+$ , then  $\rho_2^+ = \rho_1^+$ , so  $\rho_1$  and  $\rho_2$  cannot appear in the same constraint packet.

We are left with the case where  $\rho = \rho_1 \uplus \rho_2$ , and the two endpoints of  $\rho_1$  are distinct, as are the two endpoints of  $\rho_2$ . We can then form  $\rho' = \rho_2 \uplus \rho_1$ . When  $\rho_1$  or  $\rho_2$  covers only half of the corresponding boundary component  $Z_i$ , this splitting of  $\rho'$  gives rise to a join curve end in moduli space

$$\widehat{m}(\rho_1, \dots, \rho_{i-1}, \rho'_i, \rho_{i+1}, \dots, \rho_h),$$

where  $\text{orb}(\rho'_i) = \text{orb}(\rho_i)$  and

$$\text{cho}(\rho'_i) = (\text{cho}(\rho_i) \setminus \{\rho_1 \uplus \rho_2\}) \cup \{\rho_2 \uplus \rho_1\}.$$

Clearly, both  $(\rho_1, \dots, \rho_{i-1}, \rho'_i, \rho_{i+1}, \dots, \rho_h)$  is also consistent with  $(\mathbf{x}, a_1, \dots, a_h)$ . Moreover, this join curve end occurs with the same multiplicity as the corresponding join curve of

$$\widehat{m}(\rho_1, \dots, \rho_{i-1}, \rho_i, \rho_{i+1}, \dots, \rho_h),$$

corresponding to the splitting  $\rho = \rho_1 \uplus \rho_2$ .

We have thus set up a one-to-one correspondence between pairs of join curve ends of different moduli spaces that are consistent with the same algebra actions, so the join curve ends of the moduli spaces counted in the  $\mathcal{A}_\infty$  relations cancel in pairs. See Figure 27 for some examples. (Observe that join curve ends can appear for splittings of the chord  $(L_k R_k)^m$  or  $(L_k R_k)^m$  for arbitrarily large  $m$ . In this case, the join curve at East infinity covers the cylinder with multiplicity  $m$ . Moreover, according to Theorem 7.18 there are only two codimension one join ends corresponding to splittings of  $(L_k R_k)^m$ ; and they are  $\{L_k, (R_k L_k)^{m-1} R_k\}$  and  $\{R_k, (L_k R_k)^{m-1} L_k\}$ . The same two ends appear when the chord is replaced by  $(R_k L_k)^m$ . Figure 27 illustrates  $m = 1$  and  $2$ .)

This cancellation completes the verification of the  $\mathcal{A}_\infty$  relation.  $\square$

We can synthesize these parts to give the following:

**Proof of Theorem 8.1.** The Alexander grading was defined in Equations (8.2) (which is valid thanks to Lemma 8.5. Actions were defined in Equation (8.5), which was shown to be a valid definition in Lemma 8.11. The grading  $\mathbf{m}$  was defined in Equation (8.4) (which is valid thanks to Lemma 8.9). The  $\mathcal{A}_\infty$  relations were verified in Proposition 8.12. The fact that the operations preserve  $\mathbf{A}$  is obvious from Lemma 8.5. The fact that they respect  $\mathbf{m}$  (Equation (8.1)) follows readily from Lemma 8.10.  $\square$

**8.3. Invariance properties.** The following is an adaptation of [10, Proposition 7.19]:

**Proposition 8.13.** *If  $J_0$  and  $J_1$  are any two generic paths of almost-complex structures, there is an  $\mathcal{A}_\infty$  homotopy equivalence*

$$Q(\mathcal{H}^\vee, M, J_0) \simeq Q(\mathcal{H}^\vee, M, J_1).$$

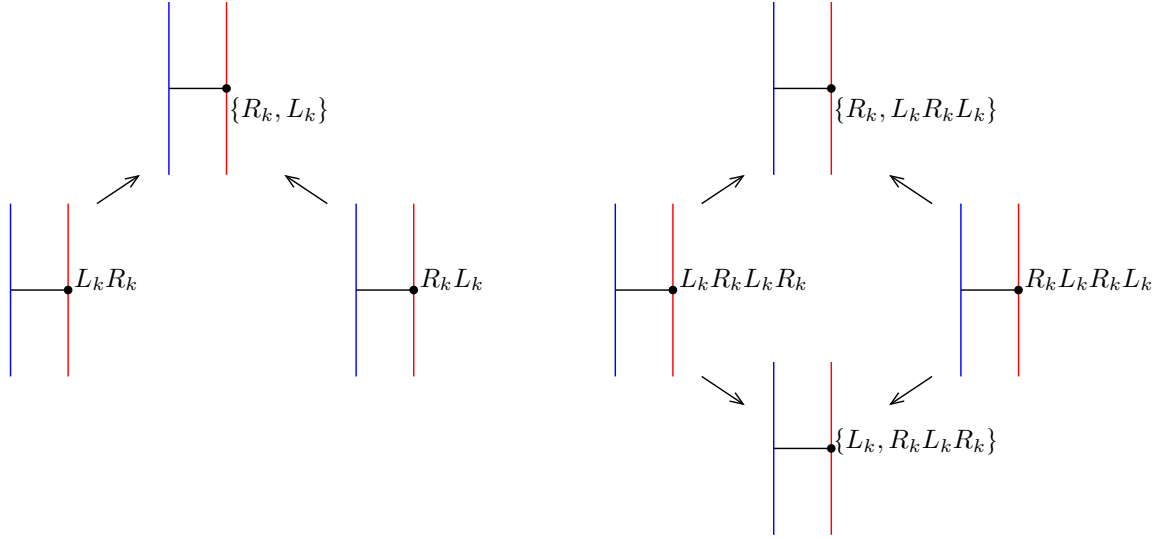


FIGURE 27. **Cancellations of join ends.** The two one-dimensional moduli spaces shown at the left (containing Reeb chords  $L_k R_k$  and  $R_k L_k$ ) have the same ends. The two one-dimensional moduli spaces on the right (containing length two Reeb chords  $L_k R_k L_k R_k$  and  $R_k L_k R_k L_k$  and) each now have two different kinds of join curve ends; but again these two ends of the two moduli spaces are in one-to-one correspondence with each other.

**Proof.** This is mostly standard; so we sketch the proof. A morphism

$$f: Q(\mathcal{H}^\vee, M, J_0) \rightarrow Q(\mathcal{H}^\vee, M, J_1)$$

is constructed by counting points in moduli spaces  $\mathcal{M}^B(\mathbf{x}, \mathbf{y}; \rho_1, \dots, \rho_h)$ , where now the moduli spaces are taken with respect to a path of paths of almost-complex structures that interpolate from  $J_0$  to  $J_1$ . The proof that this morphism satisfies the structure equation of an  $\mathcal{A}_\infty$  homomorphism is similar to the proof of Proposition 8.12. An analogue of Theorem 7.18 identifies ends of these moduli spaces, and cancellations are analogous to the ones in Proposition 8.12: two-story ends correspond to terms of the form

$$\sum_{i=1}^{1+\ell} f_{\ell-i+1}(m_i(\mathbf{x}, a_1, \dots, a_{i-1}), a_i, \dots, a_\ell) + m_{\ell-i+1}(f_i(\mathbf{x}, a_1, \dots, a_{i-1}), a_i, \dots, a_\ell);$$

even orbit ends contribute terms of the form

$$\sum_{i=1}^{\ell} f_{\ell+2}(\mathbf{x}, a_1, \dots, a_{i-1}, \mu_0, a_i, \dots, a_\ell);$$

while odd orbit ends cancel with boundary degeneration collisions. Join curve ends cancel in pairs, and contained collisions correspond to terms of the form

$$\sum_{i=1}^{\ell} f_{\ell}(\mathbf{x}, \dots, a_{i-1}, \mu_2(a_i, a_{i+1}), a_{i+2}, \dots, a_\ell).$$

Adding up these contributions give the  $\mathcal{A}_\infty$  homomorphism relation.

The homotopy inverse  $g$  is constructed by turning the one-parameter family of paths around, and the homotopy relation

$$f \circ g \simeq \text{Id}$$

is verified by considering a variation of one-parameter families.  $\square$

More topological invariance properties of this module can be established by adapting methods from [10, Section 7.3]; the above result is the only one necessary for the purposes of this paper.

**8.4. Examples.** Consider the algebra  $C^\star(1)$ , using the only matching on the single pair of strands. There is an isomorphism

$$(8.8) \quad \Psi: C^\star(1) \rightarrow \mathcal{R} = \mathbb{F}[U, V]/UV,$$

with  $\Psi(U_1) = U$  and  $\Psi(U_2) = V$ . Let  ${}^{\mathcal{R}}[\Psi]_{C(1)}$  be the associated bimodule. Note that  ${}^{\mathcal{R}}[\Psi]_{C(1)} = {}^{\mathcal{R}}[\Psi]_{C^\star(1)}$ , as the curvature in  $C^\star(1)$  vanishes.

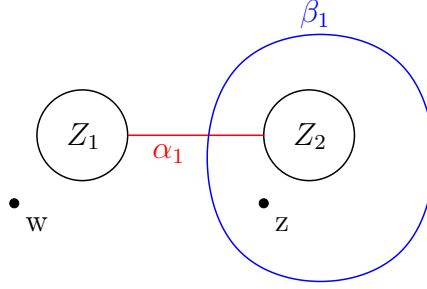


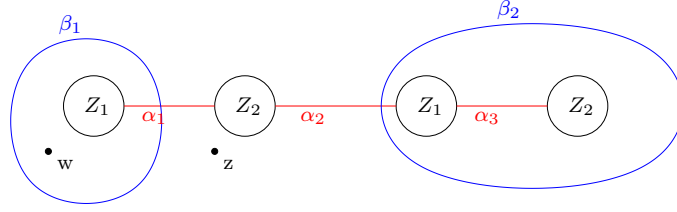
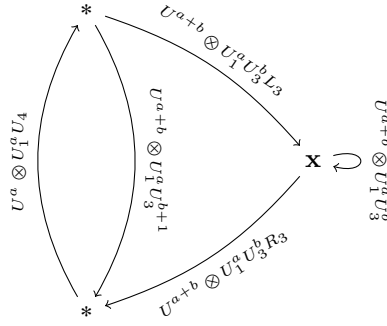
FIGURE 28. Standard lower diagram with  $n = 1$ .

**Lemma 8.14.** *For the standard lower diagram  $\mathcal{H}^\vee$  with two strands, there is an identification  $Q(\mathcal{H}^\vee) = {}^{\mathcal{R}}[\Psi]_{C^\star(1)}$ .*

**Proof.** Consider the diagram pictured in Figure 28. It has a unique generator  $x$ . Homology classes of disks are multiples of the two components  $\mathcal{D}_1$  and  $\mathcal{D}_2$  of  $\Sigma \setminus \beta_1$ , labelled so that  $\mathcal{D}_i$  contains the boundary component  $Z_i$ . A curve representing the homology class  $k \cdot \mathcal{D}_1$  has index one if and only if contains a single Reeb chord on its boundary with length  $k$  (and no internal punctures). In that case, there is a unique holomorphic representative, giving rise to the action  $m_2(x, U_1^k) = U^k \otimes x$ . Arguing similarly on the other side, we find that  $m_2(x, U_2^k) = V^k \otimes x$ . This completes the verification.  $\square$

We consider a less trivial example; the standard lower diagram with  $n = 2$ , and (compatible) matching  $M = \{\{1, 4\}, \{2, 3\}\}$ . (See Figure 29.) For simplicity, we consider the  $V = 0$  specialization. In this case, the module has a simple description, described by the following graph:



FIGURE 29. **Standard lower diagram with  $n = 2$ .**

(8.9)

Each path from  $x$  to itself (and choices of  $a$  and  $b$  for each edge) gives an  $\mathcal{A}_\infty$  action. The inputs are obtained by concatenating the second tensor factor on each edge, and the output is obtained by multiplying together the first tensor factor in each edge. So, for example, we have actions

$$\begin{aligned} m_2(x, U_1) &= U \otimes x \\ m_4(x, R_3, U_4, L_3) &= 1 \otimes x. \end{aligned}$$

The above two actions can be seen by looking at embedded disks in the Heegaard diagram. Indeed, all of the other above actions are determined by the existence of the above two actions, and the (curved)  $\mathcal{A}_\infty$  structure relations. For example, applying the above two actions, and the  $\mathcal{A}_\infty$  relation with inputs  $R_3, U_4, L_3, U_1$ , we can conclude that

$$m_4(x, R_3, U_4, L_3 U_1) = U \otimes x.$$

Applying the  $\mathcal{A}_\infty$  relations with input sequence  $R_3, U_4, U_1, L_3$  gives

$$m_4(x, R_3, U_1 U_4, L_3) = U \otimes x.$$

Finally, applying the input sequence  $R_3, L_3$ , we can conclude that

$$m_2(x, U_3) = U \otimes x.$$

It is straightforward, if a little cumbersome, to generalize to the  $V$ -unspecialized case; compare [22, Section 7].

## 9. THE PAIRING THEOREM

Start with a doubly-pointed Heegaard diagram  $\mathcal{H}$  for an oriented knot  $\vec{K}$  in  $S^3$ , together with a decomposition along a union  $Z$  of  $2n$  circles along which  $\mathcal{H}$  decomposes as a union of a lower and an upper diagram,  $\mathcal{H} = \mathcal{H}^\vee \cup_Z \mathcal{H}^\wedge$ . For example, we could consider the doubly-pointed Heegaard diagram for a knot projection as in [17], sliced in two along  $2n$  circles corresponding to a horizontal cut of the diagram, arranged so that the distinguished edge is in the bottom; see for example Figure 6. Letting  $M^\wedge$  and  $M^\vee$  be the matchings induced by  $\mathcal{H}^\wedge$  and  $\mathcal{H}^\vee$  respectively, the hypothesis ensures that  $M^\wedge$  is compatible with  $M^\vee$ , in the sense of Definition 2.3.

Let  $C_{\mathcal{R}}(\mathcal{H})$  denote the Heegaard-Floer complex of the doubly-pointed diagram  $\mathcal{H}$ : i.e. if  $C$  is the free  $\mathcal{R}$ -module generated by Heegaard states of  $\mathcal{H}$ , equipped with the differential specified by

$$(9.1) \quad \partial \mathbf{x} = \sum_{\mathbf{y} \in \mathfrak{S}(\mathcal{H})} \sum_{B \in \mathcal{D}(\mathbf{x}, \mathbf{y})} \# \widehat{m}^B(\mathbf{x}, \mathbf{y}) \cdot U^{n_w(B)} V^{n_z(B)} \cdot \mathbf{y}.$$

The homology of this complex  $C_{\mathcal{R}}(\mathcal{H}) = (C, \partial)$ , thought of as a bigraded  $\mathcal{R}$ -module, is the knot invariant  $H_{\mathcal{R}}(K)$  discussed in the introduction.

Our aim here is to prove the following pairing theorem, describing knot Floer homology in terms of type  $D$  and type  $A$  structures.

**Theorem 9.1.** *For  $\mathcal{H} = \mathcal{H}^\vee \cup_Z \mathcal{H}^\wedge$  as above there is a quasi-isomorphism of bigraded chain complexes over  $\mathcal{R}$*

$$C_{\mathcal{R}}(\mathcal{H}) \simeq Q(\mathcal{H}^\vee) \boxtimes R(\mathcal{H}^\wedge).$$

The proof will occupy the rest of this section. Like the of the pairing theorem from [10, Chapter 9], we “deformation the diagonal”. The key novelty here is to deform our orbits as well as chords, as in [7]. However, the boundary degenerations present in the current set-up cause this step to be more intricate.

As usual, the proof begins by inserting a sufficiently long neck, to identify the Floer complex  $C_{\mathcal{R}}(\mathcal{H})$  with another complex which is isomorphic to  $C$  as a  $\mathcal{R}$ -module, and whose differential  $\partial^{(0)}$  counts points in a fibered product of moduli spaces coming from the two sides. In our case, the fibered product is a fibered product over  $[0, 1] \times \mathbb{R}$  (thought of as having coordinates  $(s, t)$ ) of moduli spaces of pseudo-holomorphic curves in  $\mathcal{H}^\vee$  and  $\mathcal{H}^\wedge$ . This identification is spelled out in Subsection 9.1. Note that this identification works slightly differently when  $n = 1$ . In this outline we will assume  $n > 1$ ; the case where  $n = 1$  is handled in Subsection 9.8.

In Section 9.2, we give an independent proof that  $\partial^{(0)}$  is indeed a differential. Although this is not logically necessary (it follows from the identification with the Heegaard Floer differential), elements of the proof will be used throughout.

We will compare the fibered product complex with another chain complex, described in Subsection 9.3, that corresponds to deforming the  $s$ -coordinate matchings to the boundary. Again, the underlying  $\mathcal{R}$ -module is  $C$ , but the differential  $\partial^\sharp$  now, instead of counting points in the fibered product, counts curves where orbits for the

curves in  $\mathcal{H}^\wedge$  match with long chords on the  $\mathcal{H}^\vee$ -side. These moduli spaces allow for some additional orbits on the type  $\mathcal{H}^\vee$  side; details are given in Subsection 9.3.

Interpolating between these two extremes is a sequence of complexes (Subsection 9.4),  $\{(C, \partial^{(k)})\}_{k=0}^{2n}$ , where  $\partial^{(2n)} = \partial^\sharp$ .

Isomorphisms  $\Phi_k: (C, \partial^{(k)}) \rightarrow (C, \partial^{(k+1)})$  are constructed in Section 9.5, using moduli spaces in which the  $s$ -matching on Reeb orbits are deformed by a parameter  $r \in (0, 1)$ . Looking at ends of these moduli spaces give the desired relation

$$\partial^{(k+1)} \circ \Phi_k + \Phi_k \circ \partial^{(k)} = 0.$$

By an energy argument, these maps are isomorphisms.

Having fully deformed the  $s$ -parameter in the matching to obtain  $(C, \partial^\sharp)$ , we can now deform the  $t$ -parameter in the matching as in [10, Chapter 9] (“time dilation”); see Section 9.6. We now proceed to establish these steps.

**9.1. The Heegaard Floer differential and matched curves.** The discussion here is closely modelled on [10, Section 9.1].

Let  $\Sigma_1$  denote the Heegaard surface for  $\mathcal{H}^\vee$  and  $\Sigma_2$  denote the surface for  $\mathcal{H}^\wedge$ .

**Definition 9.2.** Let  $\mathcal{H} = \mathcal{H}^\vee \# \mathcal{H}^\wedge$ . States  $\mathbf{x}_1 \in \mathfrak{S}(\mathcal{H}^\vee)$ ,  $\mathbf{x}_2 \in \mathfrak{S}(\mathcal{H}^\wedge)$  are called matching states if  $\alpha(\mathbf{x}_1)$  is the complement of  $\alpha(\mathbf{x}_2)$  (i.e.  $\check{\mathbf{I}}(\mathbf{x}_1) = \hat{\mathbf{I}}(\mathbf{x}_2)$ )

There is a one-to-one correspondence between pairs of matching states  $\mathbf{x}_1$  and  $\mathbf{x}_2$  and Heegaard states for  $\mathcal{H}^\vee \# \mathcal{H}^\wedge$ . Thus, the generators of  $C_{\mathcal{R}}(\mathcal{H})$  correspond to the generators of  $Q(\mathcal{H}^\vee) \otimes R(\mathcal{H}^\wedge)$ , where the latter tensor product is over the idempotent subalgebra  $I_0(n) \subset C(n)$ .

In the Heegaard Floer differential for  $C_{\mathcal{R}}(\mathcal{H})$ , the holomorphic disk counting for the homology class  $B$  is weighted by  $U^{n_w(B)} V^{n_z(B)}$ . Since in  $\mathcal{R}$  we impose the relation  $UV = 0$ , it follows that the homology classes with non-zero contribution have vanishing local multiplicity at  $w$  or  $z$ .

For  $x \in \alpha_i$ , we write  $\alpha(x) = i$ . This definition will be used both for  $x \in \Sigma_1$  and  $\Sigma_2$ .

**Definition 9.3.** Let  $\rho_1$  be a Reeb chord in  $\mathcal{H}^\wedge$  and  $\rho_2$  be a Reeb chord in  $\mathcal{H}^\vee$ . We say that  $\rho_1$  and  $\rho_2$  are matching chords if the following two conditions hold:

- $\mathbf{w}(\rho_1) = \mathbf{w}(\rho_2)$
- $\alpha(\rho_1^-) \neq \alpha(\rho_2^-)$ .

The first condition implies that if  $\rho_1$  is a chord on  $\check{Z}_i$ , then  $\rho_2$  is a chord in  $\hat{Z}_i$ . The second condition means that the initial point of a chord is on  $\alpha_{i-1}$  if and only if the initial point of its matching chord is on  $\alpha_i$ . It is equivalent to replace the second condition by the condition  $\alpha(\rho_1^+) \neq \alpha(\rho_2^+)$ . Note that chords in  $\check{Z}_1$  or  $\check{Z}_{2n}$  do not match with any chords in  $\hat{Z}_1$  or  $\hat{Z}_{2n}$ .

A more succinct description of the matching condition can be given following our labeling conventions from Figure 13 (for the upper diagram) and 18 (for the lower diagram): with these conventions,  $\rho_1$  and  $\rho_2$  are matching precisely if their labels are the same.

**Definition 9.4.** Suppose  $n > 1$ . Fix two pairs  $(\mathbf{x}_1, \mathbf{x}_2)$  and  $(\mathbf{y}_1, \mathbf{y}_2)$  of matching states, i.e. where  $\mathbf{x}_1, \mathbf{y}_1 \in \mathfrak{S}(\mathcal{H}^\vee)$ ,  $\mathbf{x}_2, \mathbf{y}_2 \in \mathfrak{S}(\mathcal{H}^\wedge)$ , so that  $\mathbf{x} = \mathbf{x}_1 \# \mathbf{x}_2$  and  $\mathbf{y} = \mathbf{y}_1 \# \mathbf{y}_2$  are Heegaard states for  $\mathcal{H}$ . A matched pair consists of the following data

- a holomorphic curve  $u_1$  in  $\mathcal{H}^\vee$  with source  $\mathcal{S}_1$  representing homology class  $B_1 \in \mathcal{D}(\mathbf{x}_1, \mathbf{y}_1)$ .
- a holomorphic curve  $u_2$  in  $\mathcal{H}^\wedge$  with source  $\mathcal{S}_2$  representing homology class  $B_2 \in \mathcal{D}(\mathbf{x}_2, \mathbf{y}_2)$
- a bijection  $\psi: \mathbf{P}(\mathcal{S}_2) \rightarrow \mathbf{P}(\mathcal{S}_1)$

with the following properties:

- For each  $q \in \mathbf{P}(\mathcal{S}_2)$  marked with a Reeb orbit or chord, the corresponding puncture  $\psi(q) \in \mathbf{P}(\mathcal{S}_1)$  is marked with the matching Reeb orbit or chord.
- For each  $q \in \mathbf{P}(\mathcal{S}_2)$ ,

$$(s \circ u_1(\psi(q)), t \circ u_1(\psi(q))) = (s \circ u_2(q), t \circ u_2(q)).$$

If  $B_1$  and  $B_2$  induce  $B \in \mathcal{D}(\mathbf{x}, \mathbf{y})$ , let  $MM_{\mathfrak{h}}^B(\mathbf{x}_1, \mathbf{y}_1; \mathbf{x}_2, \mathbf{y}_2; \mathcal{S}_1, \mathcal{S}_2; \psi)$  denote the moduli space of matched pairs.

**Lemma 9.5.** Assume that  $\rho_1, \sigma_1$  are Reeb chords on two different boundary components in  $\Sigma_1$  and  $\rho_2, \sigma_2$  are the matching Reeb chords in  $\Sigma_2$ . The four numbers  $\{\alpha(\rho_1^+), \alpha(\sigma_1^+), \alpha(\rho_2^+), \alpha(\sigma_2^+)\}$  are distinct if and only if the four numbers  $\{\alpha(\rho_1^-), \alpha(\sigma_1^-), \alpha(\rho_2^-), \alpha(\sigma_2^-)\}$  are.

**Proof.** Let  $\xi_1$  and  $\xi_2$  be matching chords, then clearly

$$\{\alpha(\xi_1^-), \alpha(\xi_2^-)\} = \{\alpha(\xi_1^+), \alpha(\xi_2^+)\}.$$

The lemma follows readily.  $\square$

**Lemma 9.6.** Let  $(\mathbf{x}_1, \mathbf{x}_2)$  and  $(\mathbf{y}_1, \mathbf{y}_2)$  be two pairs of matching states, and fix a matched pair  $(u_1, u_2)$  connecting  $\mathbf{x}_1 \# \mathbf{x}_2$  to  $\mathbf{y}_1 \# \mathbf{y}_2$ , with  $u_1 \in \mathcal{M}(\mathbf{x}_1, \mathbf{y}_1, \boldsymbol{\rho}_1, \dots, \boldsymbol{\rho}_m)$  and  $u_2 \in \mathcal{M}(\mathbf{x}_2, \mathbf{y}_2, \boldsymbol{\rho}'_1, \dots, \boldsymbol{\rho}'_m)$  (where the chords in  $\boldsymbol{\rho}_i$  all match, in the sense of Definition 9.3 with chords in  $\boldsymbol{\rho}'_i$ ). Then, both  $u_1$  and  $u_2$  are strongly boundary monotone; moreover,  $\alpha(\mathbf{x}_1, \boldsymbol{\rho}_1, \dots, \boldsymbol{\rho}_\ell)$  is complementary to  $\alpha(\mathbf{x}_2, \boldsymbol{\rho}'_1, \dots, \boldsymbol{\rho}'_\ell)$  for all  $\ell = 0, \dots, m$ .

**Proof.** We prove the following by induction on  $\ell$ :

- (1)  $(\mathbf{x}_1, \boldsymbol{\rho}_1, \dots, \boldsymbol{\rho}_\ell)$  and  $(\mathbf{x}_2, \boldsymbol{\rho}'_1, \dots, \boldsymbol{\rho}'_\ell)$  are strongly boundary monotone
- (2)  $\alpha(\mathbf{x}_1, \boldsymbol{\rho}_1, \dots, \boldsymbol{\rho}_\ell)$  and  $\alpha(\mathbf{x}_2, \boldsymbol{\rho}'_1, \dots, \boldsymbol{\rho}'_\ell)$  are disjoint.

The case where  $\ell = 0$  is simply the hypothesis that  $\mathbf{x}_1$  and  $\mathbf{x}_2$  are matching states. Given a subset  $\mathfrak{s}$ , let

$$\alpha(\mathfrak{s}) = \{k \in 1, \dots, 2n-1 \mid \alpha_k \cap \mathfrak{s} \neq \emptyset\}.$$

Recall that  $\boldsymbol{\rho}_i^-$  denotes the set of initial points of all the chords in  $\boldsymbol{\rho}_i$ . Let  $A_- = \alpha(\boldsymbol{\rho}_i^-)$  and  $A_+ = \alpha(\boldsymbol{\rho}_i^+)$ . Continuity ensures that  $A_- \subset \alpha(\mathbf{x}_1, \boldsymbol{\rho}_1, \dots, \boldsymbol{\rho}_{\ell-1})$  and  $B_- \subset \alpha(\mathbf{x}_2, \boldsymbol{\rho}'_1, \dots, \boldsymbol{\rho}'_{\ell-1})$ . Weak boundary monotonicity implies that  $|A_-| = |\boldsymbol{\rho}_i^-|$

and  $|B_-| = |\rho_i'^-|$ . By the induction hypothesis,  $A_-$  and  $B_-$  are disjoint. From Lemma 9.5, it follows that

$$|A_-| = |\rho_i^-|, |B_-| = |\rho_i'^-|, |A_- \cap B_-| = \emptyset \Rightarrow |A_+| = |\rho_i^+|, |B_+| = |\rho_i'^+|, |A_+ \cap B_+| = \emptyset.$$

In particular, we have verified that  $A_+$  and  $B_+$  are disjoint. It follows at once that

$$\alpha(\mathbf{x}_1, \rho_1, \dots, \rho_i) = (\alpha(\mathbf{x}, \rho_1, \dots, \rho_{\ell-1}) \setminus A_-) \cup A_+$$

is disjoint from

$$\alpha(\mathbf{x}_2, \rho_1', \dots, \rho_i') = (\alpha(\mathbf{x}_2, \rho_1', \dots, \rho_{\ell-1}') \setminus B_-) \cup B_+,$$

verifying Property (2) for the inductive step.

Since  $|A_+| = |A_-|$ , it follows that

$$|\alpha(\mathbf{x}_1, \rho_1, \dots, \rho_i)| = |\alpha(\mathbf{x}_1, \rho_1, \dots, \rho_{i-1})| - |A_+ \cap (\alpha(\mathbf{x}_1, \rho_1, \dots, \rho_{i-1}) \setminus A_-)|.$$

We show that  $A_+ \cap (\alpha(\mathbf{x}_1, \rho_1, \dots, \rho_{i-1}) \setminus A_-)$  is empty; for if it were non-empty, there would be some chord  $\rho_1 \in \rho_i$  with  $\rho_1^+ \neq \rho_1^-$ , and  $\alpha(\rho_1^+) \in \alpha(\mathbf{x}_1, \rho_1, \dots, \rho_{i-1})$ . But for any chord with  $\rho_1^+ \neq \rho_1^-$ , the matching chord  $\rho_2$  satisfies  $\alpha(\rho_1^+) = \alpha(\rho_2^-)$ ; so  $\alpha(\rho_2^-) \in \alpha(\mathbf{x}_2, \rho_1', \dots, \rho_{i-1}')$ . But  $\alpha(\rho_2^-)$  is contained in both  $\alpha(\mathbf{x}_1, \rho_1, \dots, \rho_{i-1})$  and  $\alpha(\mathbf{x}_2, \rho_1', \dots, \rho_{i-1}')$ , violating an inductive hypothesis. We conclude that  $|A_+ \cap (\alpha(\mathbf{x}_1, \rho_1, \dots, \rho_{i-1}) \setminus A_-)| = 0$ , so

$$|\alpha(\mathbf{x}_1, \rho_1, \dots, \rho_i)| = |\alpha(\mathbf{x}_1, \rho_1, \dots, \rho_{i-1})|.$$

A symmetric argument shows that

$$|\alpha(\mathbf{x}_2, \rho_1', \dots, \rho_i')| = |\alpha(\mathbf{x}_2, \rho_1', \dots, \rho_{i-1}')|,$$

verifying Property (1) for the inductive step.  $\square$

Recall that the expected dimensions of the moduli spaces  $\mathcal{M}^{B_i}(\mathbf{x}_i, \mathbf{y}_i; \mathcal{S}_i)$  for  $i = 1, 2$  are given by the indices

$$\begin{aligned} \text{ind}(B_1, \mathcal{S}_1) &= g_1 + n + 2e(B_1) - \chi(\mathcal{S}_1) + 2o_1 + c_1 - 2\omega_1 \\ \text{ind}(B_2, \mathcal{S}_2) &= g_2 + n - 1 + 2e(B_2) - \chi(\mathcal{S}_2) + 2o_2 + c_2 - 2\omega_2, \end{aligned}$$

where  $o_i$  denotes the number of interior punctures of  $\mathcal{S}_i$ ,  $c_i$  denotes the number of boundary punctures of  $\mathcal{S}_i$ , and  $\omega_i$  denotes the total weight of  $B_i$  at the boundary. (In comparing this formula with, for example, [10, Equation 9.8], note that the convention on the Euler measures here are different from the ones used in [10]; c.f. Remark 5.15.)

**Definition 9.7.** *The index of a matched pair is defined by the formula*

$$\begin{aligned} (9.2) \quad \text{ind}(B_1, \mathcal{S}_1; B_2, \mathcal{S}_2) &= \text{ind}(B_1, \mathcal{S}_1) + \text{ind}(B_2, \mathcal{S}_2) - c - 2o \\ &= g + 2e(B_1) + 2e(B_2) - \chi(\mathcal{S}_1) - \chi(\mathcal{S}_2) + 2o + c - 4\omega, \end{aligned}$$

where  $g = g_1 + g_2 + 2n - 1$  is the genus of  $\mathcal{H} \wedge \# \mathcal{H}^\vee$ ,  $c = c_1 = c_2$ ,  $o = o_1 = o_2$ , and  $\omega = \omega_1 = \omega_2$ .

We can think of the moduli space  $mm_{\mathfrak{h}}^B(\mathbf{x}_1, \mathbf{y}_1; \mathbf{x}_2, \mathbf{y}_2; \mathcal{S}_1, \mathcal{S}_2; \psi)$  as a fibered product

$$mm_{\mathfrak{h}}^B(\mathbf{x}_1, \mathbf{y}_1; \mathbf{x}_2, \mathbf{y}_2; \mathcal{S}_1, \mathcal{S}_2; \psi) = m^{B_1}(\mathbf{x}_1, \mathbf{y}_1, \mathcal{S}_1) \times_{\text{ev}} m^{B_2}(\mathbf{x}_2, \mathbf{y}_2, \mathcal{S}_2)$$

where  $\times_{\text{ev}}$  denotes the fibered product over the evaluation maps at the punctures

$$\text{ev}_1: M^{B_1}(\mathbf{x}_1, \mathbf{y}_1, \mathcal{S}_1) \rightarrow ([0, 1] \times \mathbb{R})^k \quad \text{ev}_2: M^{B_2}(\mathbf{x}_2, \mathbf{y}_2, \mathcal{S}_2) \rightarrow ([0, 1] \times \mathbb{R})^k,$$

where  $k = |\mathbf{P}(\mathcal{S}_1)| = |\mathbf{P}(\mathcal{S}_2)| = c + o$ . Then, the index of the moduli space is the expected dimension of the moduli space of matched pairs inherited from its description as a fibered product over  $([0, 1] \times \mathbb{R})^k$ .

The moduli space  $mm_{\natural}(\mathbf{x}_1, \mathbf{y}_1; \mathbf{x}_2, \mathbf{y}_2; \mathcal{S}_1, \mathcal{S}_2; \psi)$  comes with an  $\mathbb{R}$  action which is free except in the special case where both sides consist of trivial strips. The quotient is denoted by

$$\widehat{mm}(\mathbf{x}_1, \mathbf{y}_1; \mathbf{x}_2, \mathbf{y}_2; \mathcal{S}_1, \mathcal{S}_2; \psi) = mm_{\natural}(\mathbf{x}_1, \mathbf{y}_1; \mathbf{x}_2, \mathbf{y}_2; \mathcal{S}_1, \mathcal{S}_2; \psi)/\mathbb{R}.$$

**Lemma 9.8.** *Fix  $B_1 \in \mathcal{D}(\mathbf{x}_1, \mathbf{y}_1)$  and  $B_2 \in \mathcal{D}(\mathbf{x}_2, \mathbf{y}_2)$  so that  $\omega_i(B_1) = \omega_i(B_2)$  for  $i = 1, \dots, 2n$ , and at least one of  $n_w(B_1)$  or  $n_z(B_1)$  vanishes. For generic admissible almost complex structures on  $\Sigma_i \times [0, 1] \times \mathbb{R}$ , and  $\text{ind}(B_1, \mathcal{S}_1; B_2, \mathcal{S}_2) \leq 2$ , the moduli space of matched pairs*

$$mm_{\natural}^B(\mathbf{x}_1, \mathbf{y}_1; \mathbf{x}_2, \mathbf{y}_2; \mathcal{S}_1, \mathcal{S}_2; \psi)$$

*is transversely cut out by the  $\bar{\partial}$ -equation and the evaluation map; in particular, this moduli space is a manifold whose dimension is given by Equation (9.2).*

**Proof.** This is essentially [10, Lemma 9.4].  $\square$

The data  $(\mathcal{S}_1, \mathcal{S}_2, \psi: \mathbf{P}(\mathcal{S}_2) \rightarrow \mathbf{P}(\mathcal{S}_1))$  of a matched pair can be used to form a new source curve  $\mathcal{S}_1 \natural_{\psi} \mathcal{S}_2$ , obtained by gluing punctures to punctures (i.e. connected sum for orbits and boundary connected sum for boundary punctures). If  $B_1 \in \mathcal{D}(\mathbf{x}_1, \mathbf{y}_1)$ ,  $B_2 \in \mathcal{D}(\mathbf{x}_2, \mathbf{y}_2)$  are represented by a matched pair, we can construct  $B = B_1 \natural B_2 \in \mathcal{D}(\mathbf{x}, \mathbf{y})$ , where  $\mathbf{x} = \mathbf{x}_1 \# \mathbf{x}_2$  and  $\mathbf{y} = \mathbf{y}_1 \# \mathbf{y}_2$ , represented by a (not necessarily holomorphic) curve with source  $\mathcal{S} = \mathcal{S}_1 \natural_{\psi} \mathcal{S}_2$ .

It is elementary to see that

$$(9.3) \quad e(B_1 \natural B_2) = e(B_1) + e(B_2) - 2\omega$$

$$(9.4) \quad \chi(\mathcal{S}_1 \natural_{\psi} \mathcal{S}_2) = \chi(\mathcal{S}_1) + \chi(\mathcal{S}_2) - 2o - c.$$

It is an easy consequence that

$$\text{ind}(B_1 \natural B_2, \mathcal{S}_1 \natural_{\psi} \mathcal{S}_2) = \text{ind}(B_1, \mathcal{S}_1; B_2, \mathcal{S}_2),$$

identifying expected dimension of the moduli space of curves in  $\mathcal{S}_1 \natural_{\psi} \mathcal{S}_2$  with expected dimension of the moduli spaces of matched pairs. Our goal is to refine this to an identification of moduli spaces.

As in Definition 5.4, let

$$\chi_{\text{emb}}(B) = g + e(B) - n_{\mathbf{x}}(B) - n_{\mathbf{y}}(B)$$

$$\text{ind}(B) = e(B) + n_{\mathbf{x}}(B) + n_{\mathbf{y}}(B).$$

**Proposition 9.9.** *Fix  $\mathbf{x} = \mathbf{x}_1 \# \mathbf{x}_2$  and  $\mathbf{y} = \mathbf{y}_1 \# \mathbf{y}_2$ , and decompose  $B \in \mathcal{D}(\mathbf{x}, \mathbf{y})$  as  $B = B_1 \natural B_2$ , with  $B_i \in \mathcal{D}(\mathbf{x}_i, \mathbf{y}_i)$ . Fix source curves  $\mathcal{S}_1$  and  $\mathcal{S}_2$  together with a one-to-one correspondence  $\psi: \mathbf{P}(\mathcal{S}_2) \rightarrow \mathbf{P}(\mathcal{S}_1)$  which is consistent with the chord and orbit labels, so we can form  $\mathcal{S} = \mathcal{S}_1 \natural_{\psi} \mathcal{S}_2$ . Suppose that  $M^B(\mathbf{x}, \mathbf{y}; \mathcal{S})$  (i.e. the moduli space for curves in  $\mathcal{H}$ ) and  $M^{B_i}(\mathbf{x}_i, \mathbf{y}_i; \mathcal{S}_i)$  (which are moduli spaces for curves in  $\mathcal{H}_i$ ) are non-empty for  $i = 1, 2$ . Then,  $\chi(\mathcal{S}) = \chi_{\text{emb}}(B)$  if and only*

if  $\chi(\mathcal{S}_i) = \chi_{\text{emb}}(B_i)$  for  $i = 1, 2$ ; and all the chords in  $\mathbf{P}(\mathcal{S}_1)$  have weight  $1/2$  and all the orbits have length 1.

**Proof.** Let  $\mathbf{w}$  denote the total weight of  $B_1$  at the boundary,  $o$  denote the number of orbits in  $\mathcal{S}_1$ , and  $c$  the number of chords. Since  $g = g_1 + g_2 + 2n - 1$ , it follows immediately from Equation (9.3) that

$$\chi_{\text{emb}}(B_1 \sharp B_2) = \chi_{\text{emb}}(B_1) + \chi_{\text{emb}}(B_2) - 2\mathbf{w};$$

so using Equation (9.4), it follows that

$$\chi(\mathcal{S}) - \chi_{\text{emb}}(B) = (\chi(\mathcal{S}_1) - \chi_{\text{emb}}(B_1)) + (\chi(\mathcal{S}_2) - \chi_{\text{emb}}(B_2)) + 2\mathbf{w} - c - 2o.$$

Clearly,  $2\mathbf{w} - c - 2o \geq 0$ , with equality iff each orbit has weight 1 and each chord has weight  $1/2$ . Also, the hypotheses that  $m^B(\mathcal{S}) \neq \emptyset$  and  $m^{B_i}(\mathcal{S}_i) \neq \emptyset$  for  $i = 1, 2$  ensure that

$$\chi(\mathcal{S}) \geq \chi_{\text{emb}}(B), \quad \chi(\mathcal{S}_i) \geq \chi_{\text{emb}}(B_i)$$

with equality iff the curves are embedded.  $\square$

The Gromov compactification of the space of matched curves is provided by a space of matched combs, which we define presently.

Let  $(w_{\ell_1}, \dots, w_1, u, v_1, \dots, v_k)$  be a story with total source  $\overline{\mathcal{S}}$ . Let  $\mathbf{E}(\overline{\mathcal{S}})$  be the eastmost punctures in  $\overline{\mathcal{S}}$  (i.e. these are the East punctures on curves that are not matched with west punctures on other curves at East infinity),  $\Omega(\overline{\mathcal{S}})$  be all the orbit-marked punctures in all the components of  $\overline{\mathcal{S}}$ , and

$$\mathbf{P}(\overline{\mathcal{S}}) = \mathbf{E}(\overline{\mathcal{S}}) \cup \Omega(\overline{\mathcal{S}}).$$

**Definition 9.10.** Given  $\mathbf{x}_1, \mathbf{y}_1 \in \mathfrak{S}(\mathcal{H}^\vee)$  and  $\mathbf{x}_2, \mathbf{y}_2 \in \mathfrak{S}(\mathcal{H}^\wedge)$ , a matched story from  $\mathbf{x} = \mathbf{x}_1 \# \mathbf{x}_2$  to  $\mathbf{y} = \mathbf{y}_1 \# \mathbf{y}_2$  consists of the following data:

- a pair of holomorphic stories

$$\overline{u}_1 = (w_{\ell_1}^1, \dots, w_1^1, u^1, v_1^1, \dots, v_{k_1}^1) \quad \text{and} \quad \overline{u}_2 = (w_{\ell_2}^2, \dots, w_1^2, u^2, v_1^2, \dots, v_{k_2}^2),$$

- a one-to-one correspondence

$$\psi: \mathbf{P}(\overline{\mathcal{S}}_2) \rightarrow \mathbf{P}(\overline{\mathcal{S}}_1)$$

so that for all  $p \in \mathbf{P}(\overline{\mathcal{S}}_2)$ , the Reeb chord or orbit marking  $p$  and  $\psi(p)$  have matching labels.

satisfying the following condition for each  $q \in \mathbf{P}(\overline{\mathcal{S}}_2)$ :

$$(s \circ \overline{u}_2(q), t \circ \overline{u}_2(q)) = (s \circ \overline{u}_1(\psi(q)), t \circ \overline{u}_1(\psi(q))).$$

for all  $q \in \mathbf{P}(\overline{\mathcal{S}}_2)$ . The story is called stable if there are no unstable east or west infinity curves on either side, and either  $u^1$  or  $u^2$  is stable.

**Definition 9.11.** A matched comb of height  $N$  is a sequence of stable matched stories running from  $(\mathbf{x}_1^j, \mathbf{x}_2^j)$  to  $(\mathbf{x}_1^{j+1}, \mathbf{x}_2^{j+1})$  for sequences of lower states  $\{\mathbf{x}_1^j\}_{j=1}^{N+1}$  (for  $\mathcal{H}^\vee$ ) and upper states  $\{\mathbf{x}_2^j\}_{j=1}^{N+1}$  (for  $\mathcal{H}^\wedge$ ).

In principle, the Gromov compactification could contain more complicated objects: closed components contained in some story, or  $\alpha$ -boundary degenerations. We exclude these possibilities in the next two lemmas.

**Lemma 9.12.** *Fix  $B_1 \in \mathcal{D}(\mathbf{x}_1, \mathbf{y}_1)$  and  $B_2 \in \mathcal{D}(\mathbf{x}_2, \mathbf{y}_2)$  so that  $\mathbf{w}_i(B_1) = \mathbf{w}_i(B_2)$  for  $i = 1, \dots, 2n$ , and at least one of  $n_{\mathbf{w}}(B_1)$  or  $n_{\mathbf{z}}(B_1)$  vanishes, and so that  $\text{ind}(B_1 \natural B_2) \leq 2$ . Then, curves in the Gromov compactification of  $MM_{\natural}^B(\mathbf{x}_1, \mathbf{y}_1; \mathbf{x}_2, \mathbf{y}_2)$  contain no boundary degenerations.*

**Proof.** Fix a curve  $(\bar{u}_1, \bar{u}_2)$  denote the matched comb in the Gromov compactification of matched curve pairs, so that  $\bar{u}_1$  denotes the portion in  $\mathcal{H}^\vee$  and  $\bar{u}_2$  in  $\mathcal{H}^\wedge$ .

We first prove that neither  $\bar{u}_1$  nor  $\bar{u}_2$  can contain a  $\beta$ -boundary degeneration. This is equivalent to showing that  $\bar{u}_i$  does not contain a puncture  $p_i$  marked with a Reeb orbit, and with the property that  $s(\bar{u}_i(p_i)) = 0$ .

To see this, we prove first that if there is a puncture  $p$  marked by a Reeb orbit in  $\bar{u}_i$  with  $\pi_{\mathbb{D}}(p) = (0, \tau)$ , then in fact for each  $j = 1, \dots, 2n$ , there are corresponding punctures  $q_1$  and  $q_2$  in  $\bar{u}_1$  and  $\bar{u}_2$  with

$$\pi_{\mathbb{D}}(\bar{u}_1(q_1)) = \pi_{\mathbb{D}}(u_2(q_2)) = (0, \tau),$$

so that  $q_1$  is marked by some orbit that covers  $\check{Z}_j$  and  $q_2$  is marked by some orbit that covers  $\hat{Z}_j$ . This follows from the following observations:

- The curve  $\bar{u}_1$  contains a puncture  $q_1$  marked by Reeb orbit that covers  $\check{Z}_j$  with  $\pi_{\mathbb{D}}u(q) = (0, \tau)$  if and only  $\bar{u}_2$  contains a puncture  $q_2$  marked by a Reeb orbits that covers  $\hat{Z}_j$  with  $\pi_{\mathbb{D}}u(q) = (0, \tau)$ . This is immediate from the matching condition.
- If  $\bar{u}_1$  contains a puncture  $q$  marked by a Reeb orbit that covers  $\check{Z}_j$  with  $\pi_{\mathbb{D}}u(q) = (0, \tau)$ , and  $\{j, k\} \in M^\vee$ , then there is another puncture  $q'$  marked by a Reeb orbit that covers  $\check{Z}_k$ . This follows at once from the fact that  $q$  is contained in a  $\beta$ -boundary degeneration component.
- If  $\bar{u}_2$  contains a puncture  $q$  marked by a Reeb orbit that covers  $\hat{Z}_j$  with  $\pi_{\mathbb{D}}u(q) = (0, \tau)$ , then it also contains another puncture  $q'$  marked by a Reeb orbit that covers  $\hat{Z}_k$  with  $\pi_{\mathbb{D}}u(q') = (0, \tau)$ , where  $\{j, k\} \in M^\wedge$ . This follows as above.

Compatibility of  $M^\wedge$  and  $M^\vee$  now allows us to conclude that statement at the beginning of the paragraph. Moreover, from that statement it follows that if  $\bar{u}_1$  or  $\bar{u}_2$  contains any boundary degeneration, then in fact it contains some boundary degeneration that contains  $\mathbf{w}$  and another boundary degeneration that contains  $\mathbf{z}$ . But this violates the hypothesis that  $n_{\mathbf{w}}(B_1) = 0$  or  $n_{\mathbf{z}}(B_1) = 0$ .

We turn to the possibility of a  $\mathbb{T}_\alpha$  boundary degeneration. Since  $B_1$  does not cover both  $\mathbf{w}$  and  $\mathbf{z}$ , our homological hypotheses on the type  $A$  side ensures that the limiting curve contains no  $\alpha$ -boundary degenerations on the  $\mathcal{H}^\vee$  side.

It remains to consider the possibility that an  $\alpha$ -boundary degenerations that occurs on the  $\mathcal{H}^\vee$  side, with projecting to  $(1, \tau)$  for some  $\tau \in \mathbb{R}$ .

The chords and orbits in the boundary degeneration in  $\bar{u}_2$  can match with chords and orbits on various East infinity curves in  $\bar{u}_1$ . Nonetheless, the  $(s, t)$ -projections of all of these chords and orbits are  $(1, \tau)$ , for some fixed  $\tau \in \mathbb{R}$ , by the matching condition. Moreover, the weight at each boundary component  $Z_i$  of these chords



in  $\bar{u}_1$  must be at least 1 (since the same is true for each boundary degeneration in  $\mathcal{H}^\vee$ ). Consider now the main component  $u_1$  of  $\bar{u}_1$ , obtained after removing East infinity curves. Note that the total weights of the Reeb chords and orbits of an East infinity curve are the same at both their Eastern and their Western boundary; it follows that  $u_1$  has a chord packet  $\rho$  at  $(s, t) = (1, \tau)$  with the property that  $\omega_i(\rho) \geq 1$  for all  $i = 1, \dots, 2n$ . Observe also the main component cannot have any orbits whose  $s$ -projection is 1. It follows that  $\rho^-$  contains points on all of the boundary components of  $\Sigma_1$ ; i.e.  $\rho^-$  contains at least  $2n$  points. But this violates boundary monotonicity:  $\rho^-$  can contain at most  $n$  points.  $\square$

**Lemma 9.13.** *Suppose that  $n > 1$ . Fix  $B_1 \in \mathcal{D}(\mathbf{x}_1, \mathbf{y}_1)$  and  $B_2 \in \mathcal{D}(\mathbf{x}_2, \mathbf{y}_2)$  so that  $\omega_i(B_1) = \omega_i(B_2)$  for  $i = 1, \dots, 2n$ , and at least one of  $n_w(B_1)$  or  $n_z(B_1)$  vanishes, and so that  $\text{ind}(B_1 \natural B_2) \leq 2$ . Curves in the Gromov compactification of  $mm_{\natural}^B(\mathbf{x}_1, \mathbf{y}_1; \mathbf{x}_2, \mathbf{y}_2)$  contain no closed components.*

**Proof.** By our hypotheses on the homology class, homologically non-trivial closed components cannot occur on the  $\mathcal{H}^\vee$  side.

Suppose there is a curve in the Gromov compactification of  $mm_{\natural}^B(\mathbf{x}_1, \mathbf{y}_1; \mathbf{x}_2, \mathbf{y}_2)$  which has a single closed component in  $\mathcal{H}^\wedge$ , and it has multiplicity  $k > 0$ . Let  $(u'_1, u'_2)$  be the main components of this limit, so that  $u'_1 \in \mathcal{M}^{B_1}(\mathbf{x}_1, \mathbf{y}_1; \mathcal{S}'_1)$  and  $u'_2 \in \mathcal{M}^{B_2-k[\Sigma_2]}(\mathbf{x}_2, \mathbf{y}_2; \mathcal{S}'_2)$ . We will show now that  $(u'_1, u'_2)$  lies in a moduli space whose expected dimension  $\text{ind}(u'_1, u'_2)$  satisfies

$$(9.5) \quad \text{ind}(u'_1, u'_2) \leq \text{ind}(B_1 \natural B_2) + 2 - 2nk.$$

Let  $o'_i$  denote the number of orbits in  $\mathcal{S}'_i$ ,  $c'_i$  denote the number of chords in  $\mathcal{S}'_i$ ,  $\omega$  denote  $\omega_\partial([B_1]) = \omega_\partial([B_2])$ ,  $\omega'_i$  denote  $\omega_\partial([B'_i])$ . Since there are no boundary degenerations, we conclude that  $B_1 = B'_1$ , and in particular  $\omega'_1 = \omega$ . Also, the matching conditions ensure that  $c'_1 = c'_2$ . If  $\delta$  is the number of interior punctures in  $\mathcal{S}'_1$  that match with punctures in the (removed) closed component, then  $o'_1 = o'_2 + \delta$ .

The pair  $(u'_1, u'_2)$  lies in a moduli space whose expected dimension is given by

$$\begin{aligned} \text{ind}(u'_1, u'_2) &= \text{ind}(B_1, \mathcal{S}'_1) + \text{ind}(B_2, \mathcal{S}'_2) - 2(\delta - 1) - 2o'_2 - c'_2 \\ &= \text{ind}(B_1, \mathcal{S}'_1) + \text{ind}(B_2, \mathcal{S}'_2) - 2o'_1 - c'_1 + 2 \end{aligned}$$

To see why, note that the  $\delta$  orbits in  $\mathcal{S}'_1$  are all required to have the same  $(s, t)$  projection (hence the term  $2(\delta - 1)$ ); the additional  $2o'_2 + c'_2$  constraints come from the orbits and chords in  $\mathcal{S}'_2$ , which project to the same  $(s, t)$  values as corresponding orbits and chords in  $\mathcal{S}'_1$ .

It is elementary to see that

$$e([\Sigma_2]) + n_{\mathbf{x}_2}([\Sigma_2]) + n_{\mathbf{y}_2}([\Sigma_2]) = 2 - 2g_2 + 2(g_2 + n - 1) = 2n.$$

Since  $[B'_1] = [B_1]$ , the index formula gives

$$\begin{aligned} \text{ind}(u'_1, u'_2) - \text{ind}(B_1 \natural B_2) &= e(B'_1) + n_{\mathbf{x}_1}(B_1) + n_{\mathbf{y}_1}(B_1) - e(B_2) - n_{\mathbf{x}_2}(B_2) - n_{\mathbf{y}_1}(B_2) \\ &\quad - 2\omega'_1 - 2\omega'_2 + 2\omega + 2o'_2 + c'_2 + 2 \\ &= -2nk - 2\omega'_2 + 2o'_2 + c'_2 + 2 \\ &\leq -2nk + 2, \end{aligned}$$

using the obvious inequality  $-2\omega'_2 + 2o'_2 + c'_2 \leq 0$ ; i.e. Inequality 9.5 holds.

Our hypothesis that  $\text{ind}(B_1 \natural B_2) = 2$  ensures that  $(u_1, u'_2)$  lives in a moduli space  $\mathcal{M}$  with a free  $\mathbb{R}$  action (since  $u'_1$  contains orbits, so it cannot be constant) and  $\dim(\mathcal{M}) = 4 - 2nk$ . Since  $n > 1$  and  $k \geq 1$ , we conclude that this moduli space is empty.

We have ruled out homologically non-trivial closed components. Homologically trivial “ghost” components are also ruled out by the dimension formula, as in [10, Lemma 5.57].  $\square$

**Remark 9.14.** When  $n = 1$ , spheres can occur in zero-dimensional moduli spaces, so that case must be handled separately; see Section 9.8.

**Definition 9.15.** Given a shadow  $B \in \mathcal{D}(\mathbf{x}_1 \# \mathbf{y}_1, \mathbf{x}_2 \# \mathbf{y}_2)$ , the embedded matched moduli space  $mm_{\natural}^B(\mathbf{x}_1, \mathbf{y}_1; \mathbf{x}_2, \mathbf{y}_2)$  is the union of all  $mm_{\natural}^B(\mathbf{x}_1, \mathbf{y}_1; \mathbf{x}_2, \mathbf{y}_2; \mathcal{S}_1, \mathcal{S}_2; \psi)$  taken over all compatible pairs  $\mathcal{S}_1$  and  $\mathcal{S}_2$  with  $\chi(\mathcal{S}_1 \natural \mathcal{S}_2) = \chi_{\text{emb}}(B)$ . Moreover,

$$\widehat{mm}^B(\mathbf{x}_1, \mathbf{y}_1; \mathbf{x}_2, \mathbf{y}_2) = mm_{\natural}^B(\mathbf{x}_1, \mathbf{y}_1; \mathbf{x}_2, \mathbf{y}_2) / \mathbb{R}.$$

**Proposition 9.16.** We can find a generic almost-complex structures on  $\mathcal{H}^{\wedge}$ ,  $\mathcal{H}^{\vee}$ , and  $\mathcal{H} = \mathcal{H}^{\vee} \#_Z \mathcal{H}^{\wedge}$  with the following property. For each  $\mathbf{x} = \mathbf{x}_1 \# \mathbf{x}_2$  and  $\mathbf{y} = \mathbf{y}_1 \# \mathbf{y}_2 \in \mathfrak{S}(\mathcal{H})$ ,  $B \in \mathcal{D}(\mathbf{x}, \mathbf{y})$  and  $\text{ind}(B) = 1$ , with at least one of  $n_w(B)$  or  $n_z(B)$  vanishing, there is an identification of moduli spaces of curves in  $\mathcal{H}$  with matched curves:

$$\widehat{m}^B(\mathbf{x}_1 \# \mathbf{x}_2, \mathbf{y}_1 \# \mathbf{y}_2) \cong \widehat{mm}^B(\mathbf{x}_1, \mathbf{y}_1; \mathbf{x}_2, \mathbf{y}_2).$$

**Proof.** With Lemmas 9.12 and 9.13 in place, this is a standard gluing argument; see [10, Proposition 9.6].  $\square$

**Definition 9.17.** Let  $\mathcal{H} = \mathcal{H}^{\wedge} \#_Z \mathcal{H}^{\vee}$  be a decomposition of a doubly-pointed Heegaard diagram for a knot in  $S^3$ , and assume that  $n > 1$ . The chain complex of matched curves is the pair  $(C, \partial^{(0)})$ , where, as before,  $C$  denotes the free  $\mathbb{R}$ -module generated by Heegaard states for  $\mathcal{H}$  or, equivalently, matching pairs of states (as in Definition 9.2). The operator

$$\partial^{(0)} : C \rightarrow C$$

is the  $\mathbb{R}$ -module endomorphism specified by

$$(9.6) \quad \partial^{(0)}(\mathbf{x}_1 \# \mathbf{x}_2) = \sum_{(\mathbf{y}_1, \mathbf{y}_2) \in \{B \mid \text{ind}(B)=1\}} \# \left( \widehat{mm}^B(\mathbf{x}_1, \mathbf{y}_1; \mathbf{x}_2, \mathbf{y}_2) \right) \cdot U^{n_w(B)} V^{n_z(B)} \cdot \mathbf{y}_1 \# \mathbf{y}_2.$$

**9.2. The chain complex of matched curves.** Although it is not technically necessary (it can be thought of as a consequence of Proposition 9.16, we include here a proof that  $\partial^{(0)}$  induces a differential. The methods appearing in the proof will appear again in the proof of Theorem 9.1.

The following is a slight adaptation of [10, Proposition 9.16]:

**Lemma 9.18.** Suppose that  $\text{ind}(B_1, \mathcal{S}_1; B_2, \mathcal{S}_2) = 2$ , then for generic  $J$ , the moduli space  $mm_{\natural}^B(\mathbf{x}_1, \mathbf{y}_1; \mathbf{x}_2, \mathbf{y}_2; \mathcal{S}_1, \mathcal{S}_2)$  can be compactified by adding the following objects:

(ME-1) two-story matched holomorphic curves (i.e. neither story contains curves at East or West infinity)

- (ME-2) matched stories  $(u^1, v^1)$  and  $(u^2, v^2)$  where the only non-trivial components of  $v_1$  and  $v_2$  are join curves, and where  $\mathbf{W}(v^1)$  and  $\mathbf{W}(v^2)$  are the two distinct length one Reeb chords that cover the same boundary component,
- (ME-3) matched stories  $(u^1, v^1)$  and  $(u^2, v^2)$  where the only non-trivial components of  $v^1$  and  $v^2$  are orbit curves, and  $\mathbf{W}(v^1)$  and  $\mathbf{W}(v^2)$  are the two distinct length one Reeb chords that cover the same boundary component.

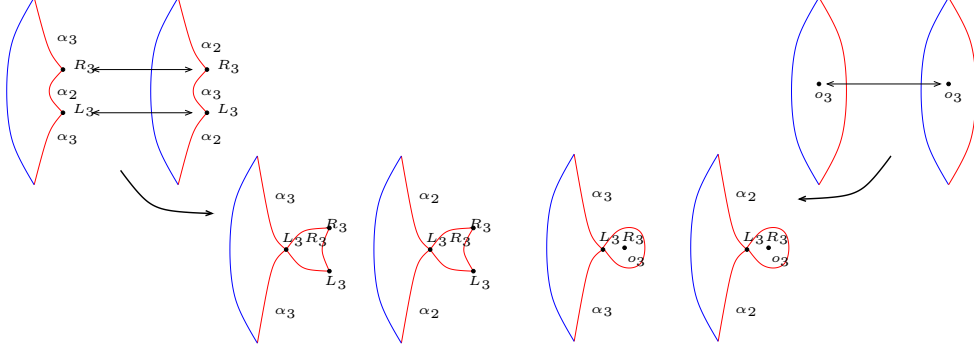


FIGURE 30. Cancellation of join ends with orbit ends.

**Proof.** The main components are strongly boundary monotone by the argument from Lemma 9.6. This rules out boundary double points, as in [10, Lemma 5.56]. Boundary degenerations are ruled out as in Lemma 9.12. Dimension considerations rule out closed components as in Lemma 9.13.

We follow proof of [10, Proposition 9.16]. Suppose there is some matched story that appears in the boundary of the moduli space. We could write that matched story as a pair of stories with a matching condition on the eastmost punctures; instead we combine the curves at East infinity into a single sequence, writing, more symmetrically,  $(u_1, v_1, \dots, v_\ell, u_2)$ . Let  $(\mathcal{S}'_1, \mathcal{T}_1, \dots, \mathcal{T}_\ell, \mathcal{S}'_2)$  denote the corresponding sequence of source curves. Let  $\mathcal{T} = \mathcal{T}_1 \natural \dots \natural \mathcal{T}_\ell$  (where we glue along all boundary punctures and all interior punctures, as well). There is an induced partition  $P_1$  on the east punctures of  $\mathcal{S}'_1$ : two punctures are in the same partition if they are assigned to same components of  $\mathcal{T}$ . There is a similar partition  $P_2$  on the east punctures of  $\mathcal{S}'_2$ . Combining Equations (9.2) and (9.3), we see that

$$\text{ind}(B_1, \mathcal{S}'_1; B_2, \mathcal{S}'_2) = g - \chi(\mathcal{S}'_1) - \chi(\mathcal{S}'_2) + 2e(B) + c + 2o,$$

where  $c = |\mathbf{E}(\mathcal{S}'_1)| = |\mathbf{E}(\mathcal{S}'_2)|$  and  $o = |\mathbf{\Omega}(\mathcal{S}'_1)| = |\mathbf{\Omega}(\mathcal{S}'_2)|$ . The limit curves  $(u_1, u_2)$  live in a fibered product  $\mathcal{M}$  whose dimension (after dividing out by the free  $\mathbb{R}$  action) is given by

$$\begin{aligned} \dim(\mathcal{M}) &= \text{ind}(B_1, \mathcal{S}'_1, P_1) + \text{ind}(B_2, \mathcal{S}'_2, P_2) - k - 1 - 2o', \\ &= g - \chi(\mathcal{S}'_1) - \chi(\mathcal{S}'_2) + 2e(B) + k - 1 + 2o'; \end{aligned}$$

where  $k$  is the number of components of  $\mathcal{T}$ , which agrees with  $|P_1| = |P_2|$ ; and  $o' = |\mathbf{\Omega}(\mathcal{S}'_1)| = |\mathbf{\Omega}(\mathcal{S}'_2)|$  is the number of interior punctures in  $\mathcal{S}'_1$ . By elementary topology,

$$\chi(\mathcal{S}'_1) + \chi(\mathcal{S}'_2) - c - 2o = \chi(\mathcal{S}'_1) + \chi(\mathcal{S}'_2) + \chi(\mathcal{T}) - c_1 - c_2 - 2o',$$

where  $c_i = |\mathbf{E}(\mathcal{S}'_i)|$  for  $i = 1, 2$ . It follows that

$$\dim(M) = \text{ind}(B_1, \mathcal{S}_1; B_2, \mathcal{S}_2) + (\chi(\mathcal{T}) - k) + (k - c_1) + (k - c_2) - 1.$$

Since  $\chi(\mathcal{T}) \leq k$  and  $k \leq c_i$  for  $i = 1, 2$ , we conclude that if  $\dim(M) \geq 0$  and  $\text{ind}(B_1, \mathcal{S}_1; B_2, \mathcal{S}_2) = 2$ , then exactly one of the following three possibilities can occur:

- (d-1) all the components of  $\mathcal{T}$  are disks, and  $\{c_1, c_2\} = \{k, k+1\}$
- (d-2)  $k = c_1 = c_2$ , exactly one component in  $\mathcal{T}$  is an annulus, and all other components are trivial strips.

Case (d-1) is excluded, as follows. Suppose that  $c_1 = k+1$  and  $c_2 = k$ , so that there are two punctures on  $\mathcal{S}'_1$  labelled by two chords  $\rho_1$  and  $\rho_2$  (for  $\mathcal{H}^\vee$ ) that are matched by  $\mathcal{T}$ ; and  $\rho_1 \oplus \rho_2$  is the corresponding chord in  $\mathcal{S}'_2$ . Both chords  $\rho_i$  have weight  $1/2$ , so clearly  $\{\rho_1^-, \rho_2^-\}$  are the two  $\alpha$ -curves on some fixed boundary component, while  $\rho_1 \oplus \rho_2^-$  is also an  $\alpha$ -curve on the corresponding boundary component in  $\mathcal{H}^\wedge$ . But this violates Lemma 9.6, according to which the sets of  $\alpha$ -occupied curves are complementary. The case where  $c_1 = k$  and  $c_2 = k+1$  is excluded the same way.

Consider next Case (d-2). Drop all the trivial strip components, letting  $\mathcal{T}_0$  be the annulus. Dropping all unstable components from east infinity, we have  $\mathcal{T}_0 = \mathcal{T}_1 \natural \dots \natural \mathcal{T}_\ell$ . Obviously, we cannot have  $\ell = 1$ : for an orbit at East infinity cannot match with an interior puncture. Consider next  $\ell = 2$ . This can occur in two ways. Suppose  $\mathcal{T} = \mathcal{T}_1 \natural \mathcal{T}_2$ . We have that

$$0 = \chi(\mathcal{T}) = \chi(\mathcal{T}_1) + \chi(\mathcal{T}_2) - 2o - c;$$

where  $o$  resp.  $c$  denotes the number of interior resp. boundary punctures in  $\mathcal{T}_1$  (which are matched with corresponding punctures in  $\mathcal{T}_2$ ). Clearly, this forces  $\mathcal{T}_1$  and  $\mathcal{T}_2$  to be disks, with either  $o = 0$  and  $c = 2$  or  $o = 1$  and  $c = 0$ . The first case is Case (ME-2), and the second is Case (ME-3). The same Euler characteristic considerations show that decompositions with  $\ell > 2$  have unstable components.

It remains to consider the case where there is more than one story. In that case, by the additivity of the index, it follows that there are two stories, both have index 1, and neither has curves at East infinity.  $\square$

**Remark 9.19.** In [10, Proposition 9.16], Case (d-2) is ruled by the existence of a basepoint on the boundary, while Case (d-1) does occur, unlike in the above proof, where it is ruled out by combinatorics of the Reeb chords.

**Lemma 9.20.** Let  $(u^1, v^1)$  and  $(u^2, v^2)$  be a matched story with sources  $(\mathcal{S}_1, \mathcal{T}_1)$  and  $(\mathcal{S}_2, \mathcal{T}_2)$  with the property that for  $i = 1, 2$ , the only non-trivial component of  $v^i$  is a join curve forming a length one Reeb chord, then there are arbitrary small open neighborhoods  $U$  of  $(u^1, v^1) \times (u^2, v^2)$  in  $M^{B_1}(\mathbf{x}_1, \mathbf{y}_1, \mathcal{S}_1 \natural \mathcal{T}_1) \times M^{B_2}(\mathbf{x}_2, \mathbf{y}_2, \mathcal{S}_2 \natural \mathcal{T}_2)$  so that  $\partial \overline{U}$  meets  $M^B(\mathbf{x}_1, \mathbf{y}_1, \mathcal{S}_1 \natural \mathcal{T}_1; \mathbf{x}_2, \mathbf{y}_2, \mathcal{S}_2; \mathcal{S}_2 \natural \mathcal{T}_2)$  in an odd number of points. The same conclusion holds if for each  $i = 1, 2$ , the only non-trivial component of  $v^i$  is an orbit curve.

**Proof.** If  $(u_1, v_1)$  and  $(v_2, v_2)$  is a matched story where the only non-trivial components of  $v^1$  and  $v^2$  are join curves, the result follows from Proposition 7.39.

When  $v^1$  and  $v^2$  are orbit curves, the result follows from Proposition 7.40. See Figure 31.  $\square$

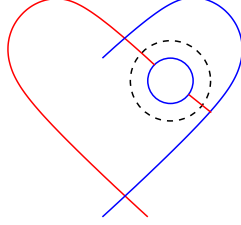


FIGURE 31. Cancellation of join ends with orbit ends; an example.

**Proposition 9.21.** *The endomorphism  $\partial^{(0)}$  is a differential.*

**Proof.** Fix  $\mathbf{x}_1 \# \mathbf{x}_2, \mathbf{y}_1 \# \mathbf{y}_2 \in \mathfrak{S}(\mathcal{H}^\vee \# \mathcal{H}^\wedge)$  and  $B \in \pi_2(\mathbf{x}_1 \# \mathbf{x}_2, \mathbf{y}_1 \# \mathbf{y}_2)$  with  $\text{ind}(B) = 2$ . Consider the ends of  $\mathcal{M}^B(\mathbf{x}_1, \mathbf{x}_2; \mathbf{y}_1, \mathbf{y}_2)$ , consisting of embedded, matched holomorphic curves representing  $B$ . By Lemma 9.18, ends of these moduli spaces are either two-story matched curves; or they correspond to matched combs, with height two, of two types (with join curves or orbit curves at East infinity). These two types of ends cancel in pairs according to Lemma 9.20; so the total number of two-story ends is even, and those count the  $\mathbf{y}_1 \# \mathbf{y}_2$  coefficient of  $\partial^{(0)} \circ \partial^{(0)}(\mathbf{x}_1 \# \mathbf{x}_2)$ .  $\square$

We identify  $(C, \partial^{(0)})$  with the Heegaard-Floer chain complex  $C_{\mathcal{R}}(\mathcal{H})$  associated to the doubly-pointed Heegaard diagram  $\mathcal{H}$ , via the following adaptation of [10, Theorem 9.10]:

**Theorem 9.22.** *Let  $\mathcal{H}$  be a Heegaard diagram representing  $K$ , equipped with a decomposition  $\mathcal{H} = \mathcal{H}^\vee \cup_Z \mathcal{H}^\wedge$  as a union of an upper and a lower diagram along  $2n$  circles, with  $n > 1$ . For suitable choices of almost-complex structures  $J$  used to define  $C_{\mathcal{R}}(K)$ , there is an isomorphism (of chain complexes)  $C_{\mathcal{R}}(K) \cong (C, \partial^{(0)})$ .*

**Proof.** This follows from Lipshitz’s reformulation of Heegaard Floer homology ([6, Theorem 2]) and Proposition 9.16.  $\square$

### 9.3. Self-matched curves.

**Definition 9.23.** *Let  $\mathcal{S}_1$  be a decorated source. Partition let  $\Omega_+(\mathcal{S}_1)$  resp.  $\Omega_-(\mathcal{S}_1)$  denote the set of interior punctures of  $\mathcal{S}_1$  that are labelled by even resp. odd orbits. A self-marked source is a decorated source, together with an injection  $\phi: \Omega_+(\mathcal{S}_1) \rightarrow \mathbf{E}(\mathcal{S}_1)$  with the property that if  $p \in \Omega_+(\mathcal{S}_1)$  is marked by some orbit  $o_j$ , then  $\phi(p)$  is marked by a length one chord that covers the boundary component  $Z_k$  with  $\{j, k\} \in M^\wedge$ . A self-matched curve  $u$  is an element  $u \in \mathcal{M}^{B_1}(\mathbf{x}, \mathbf{y}; \mathcal{S}_1, \phi)$ , subject to the following additional constraints: for each puncture  $p \in \Omega_+(\mathcal{S}_1)$ ,*

$$(9.7) \quad t \circ u(p) = t \circ u(\phi(p)).$$

Note although “self-matched curves” are supported in  $\mathcal{H}^\vee$ , the matching condition depends on  $\mathcal{H}^\wedge$ , through its induced matching  $M^\wedge$ .

**Definition 9.24.** A self-matched curve pair consists of the following data:

- a self-matched source  $(\mathcal{S}_1, \phi: \Omega_+(\mathcal{S}_1) \rightarrow \mathbf{E}(\mathcal{S}_1))$
- a marked source  $\mathcal{S}_2$
- an injection  $\psi: \mathbf{P}(\mathcal{S}_2) \rightarrow \mathbf{E}(\mathcal{S}_1)$ , where  $\mathbf{P}(\mathcal{S}_2) = \Omega(\mathcal{S}_2) \cup \mathbf{E}(\mathcal{S}_2)$
- a pseudo-holomorphic self-matched curve  $u_1$  with source  $\mathcal{S}_1$  in  $\mathcal{H}^\vee$  and
- a pseudo-holomorphic curve  $u_2$  with source  $\mathcal{S}_2$  in  $\mathcal{H}^\wedge$ ,

satisfying the following properties

- (smpc-1) The map  $\psi$  is a one-to-one correspondence between  $\mathbf{E}(\mathcal{S}_2)$  and  $\mathbf{E}(\mathcal{S}_1) \setminus \phi(\Omega_+(\mathcal{S}_2))$ .
- (smpc-2) If  $p \in \Omega(\mathcal{S}_2)$ , is labelled by an orbit  $o_j$ , then  $\phi(p)$  is labelled by a length one Reeb chord that covers the boundary component of  $\check{Z}_j$ .
- (smpc-3) If  $p \in \mathbf{E}(\mathcal{S}_2)$ , then the name of the Reeb chord in  $\mathcal{H}^\wedge$  marking  $p$  is the same as the name of the Reeb chord in  $\mathcal{H}^\vee$  marking  $\psi(p)$ .
- (smpc-4) For each puncture  $q \in \mathbf{P}(\mathcal{S}_2)$ :

$$(9.8) \quad t \circ u_1(\psi(q)) = t \circ u_2(q).$$

Let  $mm_{\sharp}^{B_1, B_2}(\mathbf{x}, \mathbf{y}; \mathcal{S}_1, \mathcal{S}_2, \phi, \psi)$  denote the moduli space of self-matched curve pairs.

Note that the even orbits in  $\mathcal{S}_1$  are constrained by the self-matching condition; and the odd orbits in  $\mathcal{S}_1$  are not constrained by any additional condition.

Let  $(u_1, u_2)$  be a self-matched curve pair with sources  $\mathcal{S}_1$  and  $\mathcal{S}_2$ . Let  $o_1^+$  resp.  $o_1^-$  denote the number of even resp. odd orbits in  $\mathcal{S}_1$ ; let  $c_i$  denote the number of boundary punctures in  $\mathcal{S}_i$ . For example, note that  $c_1 = c_2 + o_2 + o_1^+$ .

Given homology classes  $B_1 \in \pi_2(\mathbf{x}_1, \mathbf{y}_1)$  and  $B_2 \in \pi_2(\mathbf{x}_2, \mathbf{y}_2)$ , we construct a corresponding class  $B = B_1 \# B_2 \in \pi_2(\mathbf{x}_1 \# \mathbf{y}_1, \mathbf{x}_2 \# \mathbf{y}_2)$ , as follows. First, we obtain a homology class  $B'_2$  from  $B_2$  by summing, for each puncture in  $\mathcal{S}_1$  labelled by some orbit  $o_j$  with  $f(j) = 2k - 1$ , all the components of  $\Sigma_2 \setminus \beta$  that contain boundary components  $\hat{Z}_\ell$  with  $f(\ell) \leq 2k$ . Similarly, we obtain a homology class  $B'_1$  from  $B_1$  by adding, for each puncture in  $\mathcal{S}_1$  labelled by  $o_j$  with  $f(j) = 2k - 1$ , all the components of  $\Sigma_1 \setminus \beta$  that contain boundary components  $\check{Z}_\ell$  with  $f(\ell) \leq 2k$ . Let  $B_1 \# B_2 = B'_1 \natural B'_2$ .

We formalize now the expected dimension of the moduli space of pairs of curves, with the time constraints coming from Equations (9.7) and (9.8).

**Definition 9.25.** For a self-matched curve pair with  $\chi(\mathcal{S}_i) = \chi_{\text{emb}}(B_i)$ , define the index of the self-matched curve pair by

$$\text{ind}^\sharp(B_1, \mathcal{S}_1; B_2, \mathcal{S}_2) = \text{ind}(B_1, \mathcal{S}_1) + \text{ind}(B_2, \mathcal{S}_2) - c_1$$

**Proposition 9.26.** For a self-matched curve pair  $(u_1, u_2)$ , as above the domain  $B_1 \# B_2$  has the following properties:

$$\begin{aligned} B_1 \# B_2 &\in \mathcal{D}(\mathbf{x}_1 \# \mathbf{x}_2, \mathbf{y}_1 \# \mathbf{y}_2) \\ n_w(B_1 \# B_2) &= n_w(B_1) + o_1^- \\ n_z(B_1 \# B_2) &= n_z(B_1) \end{aligned}$$

Moreover, if  $\chi(\mathcal{S}_i) = \chi_{\text{emb}}(B_i)$  for  $i = 1, 2$ , then

$$\text{ind}(B_1 \# B_2) = \text{ind}^\sharp(B_1, \mathcal{S}_1; B_2, \mathcal{S}_2).$$

**Proof.** This is a straightforward consequence of the fact that if  $\mathcal{D}$  is any of the components in  $\Sigma_i \setminus \mathcal{B}$  then  $\text{ind}(B_i + \mathcal{D}) = \text{ind}(B_i) + 2$ .  $\square$

Let  $\mathbf{x} = \mathbf{x}_1 \# \mathbf{x}_2$  and  $\mathbf{y} = \mathbf{y}_1 \# \mathbf{y}_2$ . Define

$$\begin{aligned} mm_\sharp^B(\mathbf{x}, \mathbf{y}) &= \bigcup_{\left\{ \begin{array}{l} B_1 \in \pi_2(\mathbf{x}_1, \mathbf{y}_1) \\ B_2 \in \pi_2(\mathbf{x}_2, \mathbf{y}_2) \end{array} \middle| B = B_1 \# B_2 \right\}} \bigcup_{\{(\mathcal{S}_1, \mathcal{S}_2, \phi, \psi) \mid \text{ind}^\sharp(B_1, \mathcal{S}_1; B_2, \mathcal{S}_2) = \text{ind}(B)\}} mm_\sharp^{B_1, B_2}(\mathbf{x}, \mathbf{y}, \phi, \psi). \end{aligned}$$

We use these moduli spaces to construct an endomorphism of  $C$ , specified by its values  $\mathbf{x} = \mathbf{x}_1 \# \mathbf{x}_2$  by

$$(9.9) \quad \partial^\sharp(\mathbf{x}) = \sum_{\mathbf{y}} \sum_{\{B \in \pi_2(\mathbf{x}, \mathbf{y}) \mid \text{ind}(B) = 1\}} \# \left( \frac{mm_\sharp^B(\mathbf{x}, \mathbf{y})}{\mathbb{R}} \right) \cdot U^{n_w(B)} V^{n_z(B)} \cdot \mathbf{y}.$$

**Proposition 9.27.** *The endomorphism  $\partial^\sharp$  satisfies the identity  $\partial^\sharp \circ \partial^\sharp = 0$ .*

As usual, the proof involves understanding the ends of one-dimensional moduli spaces of self-matched curve pairs. These ends contain terms counted in  $\partial^\sharp \circ \partial^\sharp$ ; and all other terms cancel. We give the proof after some preliminary results; see Figures 32, 33, and 34 for pictures.

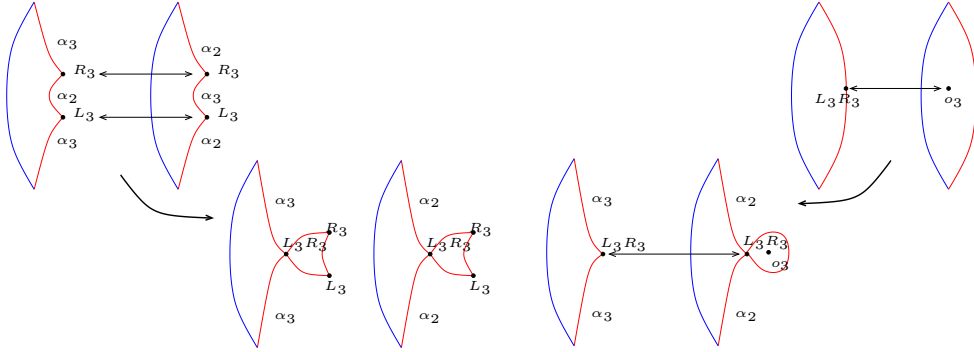


FIGURE 32. Ends of Type (sME-3) cancel ends of type (sME-5). This is a combination of Lemmas 9.31 and 9.32.

**Definition 9.28.** If  $\overline{\mathcal{S}}$  is the source of a holomorphic story  $(w_\ell, \dots, w_1, u, v_1, \dots, v_m)$ , let  $\Omega_-(\overline{\mathcal{S}})$  resp  $\Omega_+(\overline{\mathcal{S}}) \subset \Omega(\overline{\mathcal{S}})$  denote the subset of punctures in  $\overline{\mathcal{S}}$  marked by Reeb orbits which are odd resp. even. A self-matched story consists of the following data:

- a holomorphic story  $\overline{u} = (w_\ell, \dots, w_1, u, v_1, \dots, v_m)$
- an injective map  $\phi: \Omega_+(\overline{\mathcal{S}}) \rightarrow \mathbf{E}(\overline{\mathcal{S}})$  with the property that if  $p \in \overline{\mathcal{S}}$  is a puncture marked by some orbit  $o_j$ , then  $\phi(p)$  is marked by some chord  $v_k$  that covers  $Z_k$  with multiplicity one, so that  $\{j, k\} \in M^\wedge$ .

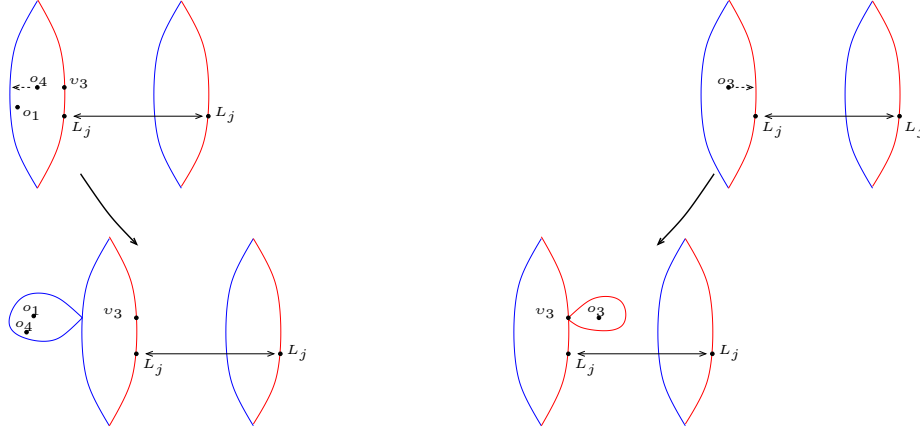


FIGURE 33. **Ends of Type (sME-4) with an odd orbit cancel against ends of Type (sME-6).** This cancellation is a combination of Lemmas 9.34 and 9.35.

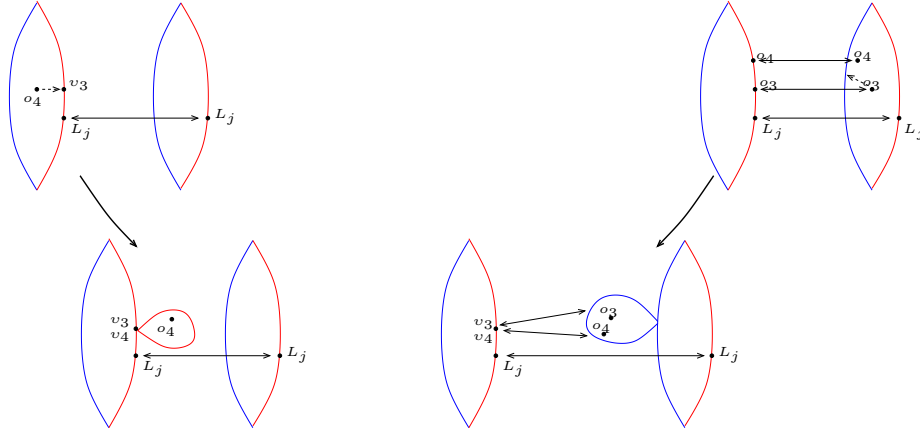


FIGURE 34. **Ends of Type (sME-4) with an even orbit cancel against ends of Type (sME-7).** This cancellation is a combination of Lemmas 9.36 and 9.37.

**Definition 9.29.** A self-matched story pair *consists of the following data:*

- a self-matched holomorphic story  $\overline{u}_1$  in  $\mathcal{H}^\vee$ , with source  $\overline{\mathcal{S}}_1$
- a holomorphic story  $\overline{u}_2$  in  $\mathcal{H}^\wedge$ , with source  $\overline{\mathcal{S}}_2$
- a one-to-one correspondence

$$\psi: \mathbf{P}(\overline{\mathcal{S}}_2) \rightarrow \mathbf{E}(\overline{\mathcal{S}}_1) \setminus \phi(\Omega(\overline{\mathcal{S}}_1)),$$

*satisfying the following properties:*

- if  $q \in \Omega(\overline{\mathcal{S}}_2)$  is marked by an orbit  $o_j$  (in  $\mathcal{H}^\wedge$ ), then  $\psi(q)$  is marked by one of the two length 1 chords that covers  $\check{Z}_j$



- if  $q \in \mathbf{E}(\overline{\mathcal{S}}_2)$ , the Reeb chord in  $\mathcal{H}^\wedge$  label on  $q$  has the same name as the Reeb chord in  $\mathcal{H}^\vee$  that marks  $\psi(q)$
- for each  $q \in \mathbf{P}(\mathcal{S}_2)$ ,

$$t \circ \overline{u}_1(\psi(q)) = t \circ \overline{u}_2(q).$$

**Proposition 9.30.** *Suppose that  $\text{ind}(B_1, \mathcal{S}_1; B_2, \mathcal{S}_2) = 2$ . Every comb pair appearing in the boundary of the moduli space  $MM_\#^B(\mathbf{x}, \mathbf{y}; \mathcal{S}_1, \mathcal{S}_2)$  is of one of the following types:*

- (sME-1) a two-story self-matched curve pair
- (sME-2) a self-matched story pair of the form  $(u_1, v_1), u_2$ , where  $v_1$  is a join curve
- (sME-3) a self-matched story pair of the form  $u_1, (u_2, v_2)$  where  $v_2$  is an orbit curve
- (sME-4) a self-matched story pair  $(u_1, v_1), u_2$  where  $v_1$  is an orbit curve
- (sME-5) a self-matched story pair of the form  $(u_1, v_1), (u_2, v_2)$  where  $v_1$  and  $v_2$  are join curves, and the corresponding punctures in  $u_1$  and  $u_2$  are the two distinct length one Reeb chords that cover the same boundary component.
- (sME-6) a self-matched story pair of the form  $(w_1, u_1), u_2$ , where  $w_1$  is a simple boundary degeneration
- (sME-7) a self-matched story pair of the form  $u_1, (w_2, u_2)$ , where  $w_2$  is a simple boundary degeneration.

**Proof.** Suppose that we have a sequence of self-matched curve pairs with fixed sources  $\mathcal{S}_1$  and  $\mathcal{S}_2$ , representing fixed homology classes  $B_1$  and  $B_2$ . The index of these is computed nby

$$\begin{aligned} \text{ind}^\#(\mathcal{S}_1, \mathcal{S}_2) &= \text{ind}(B_1; \mathcal{S}_1) + \text{ind}(B_2; \mathcal{S}_2) - o_+ - c_2 - o_2 \\ &= d_1 + n_{\mathbf{x}_1}(B_1) + n_{\mathbf{y}_1}(B_1) + e(B_1) - 2\mathbf{w}_\partial^1 \\ &\quad + d_2 + n_{\mathbf{x}_2}(B_2) + n_{\mathbf{y}_2}(B_2) + e(B_2) - 2\mathbf{w}_\partial^2 + 2o_- + o_+ + o_2 + c_1, \end{aligned}$$

where  $o_+$  resp.  $o_-$  denotes the number of punctures in  $\mathcal{S}_1$  marked by even resp. odd orbits;  $c_2$  denotes the number of East punctures in  $\mathcal{S}_2$  and  $o_2$  the number of interior punctures.

Take a Gromov limit, and assume that it does not contain any curves at West infinity, and that it consists of a singly story. Consider the main component  $(u'_1, u'_2)$ , with sources  $\mathcal{S}'_1$  and  $\mathcal{S}'_2$ . This limit inherits certain matching conditions, whose expected dimension we will now express. Let  $\lambda_+$  denote the number of East punctures that arise as limits of East marked orbits in  $\mathcal{S}_1$ . Let  $\lambda_-$  denote the number of East punctures that are not matched with any other punctures in either  $\mathcal{S}'_i$ . (These punctures arise as limits of interior punctures in  $\mathcal{S}_1$  marked by odd orbits.) Let  $c'_2$  denote the number of East punctures in  $\mathcal{S}'_2$  and  $o'_2$  denote the number of its interior punctures.

Each interior puncture of  $\mathcal{S}'_1$  marked by an even orbit is constrained to lie at the same  $t$ -level as some corresponding East puncture  $\mathcal{S}'_1$ ; and each puncture of  $\mathcal{S}'_2$  is constrained to lie at the same  $t$ -level as a corresponding East puncture in  $\mathcal{S}'_1$ . Thus, the expected dimension of the moduli space in which  $(u'_1, u'_2)$  lives is

computed by

$$\begin{aligned} \text{ind}(u'_1, u'_2) &\leq \text{ind}(B_1; \mathcal{S}'_1) + \text{ind}(B_2; \mathcal{S}'_2) - o'_+ - \lambda_+ - c'_2 - o'_2 \\ &= d_1 + n_{\mathbf{x}_1}(B_1) + n_{\mathbf{x}_2}(B_1) + e(B_1) - 2\mathfrak{w}_\partial^1 \\ &\quad + d_2 + n_{\mathbf{x}_1}(B_1) + n_{\mathbf{x}_2}(B_1) + e(B_2) - 2\mathfrak{w}_\partial^2 + c'_1 + o'_+ + 2o'_- + o'_2, \end{aligned}$$

Thus,

$$\text{ind}(u'_1, u'_2) - \text{ind}^\sharp(\mathcal{S}_1, \mathcal{S}_2) \leq (c'_1 - \lambda_- - \lambda_+ - c_1) + (o'_+ - o_+) + (2o'_- + \lambda_- - 2o_-) + (o'_2 - o_2).$$

Each quantity in parentheses is clearly non-positive. Since we assumed that  $\text{ind}^\sharp(\mathcal{S}_1, \mathcal{S}_2) = 2$ , at most one of the quantities can be  $-1$  (and the others zero) for  $(u'_1, u'_2)$  to exist.

If  $2o'_+ + \lambda_- - 2o_- = -1$ , then  $\lambda_- = 1$ . In this case, an (odd) orbit curve forms in  $\mathcal{S}_1$  (Case (sME-4)). On the other hand, if  $2o'_+ + \lambda_- - 2o_- = 0$ , then  $\lambda_- = 0$ .

Also,  $o'_+ + \lambda_+ \leq o_+$ , so if  $o'_+ - o_+ = -1$ , then  $\lambda_+ = 0$  or  $1$ . Assume first that  $\lambda_+ = 0$ . In this case,  $\mathcal{S}'_1$  must contain a multiple even orbit. In that case, it is also the case that  $c'_1 < c_1$ , which is a contradiction. Assume next that  $\lambda_+ = 1$ . In that case,  $c'_1 = c_1 + 1$ . This is the case of an (even) orbit curve appearing in  $\mathcal{S}_1$  (Case (sME-4), again).

If  $c'_1 - c_1 = -1$ , there are two possibilities. A join curve can form on  $\mathcal{S}_1$  without one on  $\mathcal{S}_2$  (Case (sME-2)), or it can form on both sides (Case (sME-5)).

If  $o'_2 - o_2 = -1$ , we have an orbit curve forming on  $\mathcal{S}_2$  (Case (sME-3)).

This finishes the cases where curves at West infinity do not form.

Suppose that the limiting curve  $(u', v')$  contains weight  $2k$  boundary degeneration with  $2m$  distinct orbits in it. Then,  $(u', v')$  lies in a moduli space whose index is computed by

$$\text{ind}(B_1, \mathcal{S}_1) + \text{ind}(B'_1, \mathcal{S}'_1) - (c_1 - 2k) - (2m - 1) :$$

there are  $c_1 - 2k$  height constraints coming from chords in  $\mathcal{S}'_1 = \mathcal{S}_1$  that are not matched with orbits in the boundary degeneration, and the remaining group of  $2m$  chords are required to occur at the same  $t$ -value.

$$\begin{aligned} \text{ind}(B_1, \mathcal{S}'_1) &\leq \text{ind}(B_1, \mathcal{S}_1) - c_1 + c'_1 = \text{ind}(B_1, \mathcal{S}_1) - 2(k - m) \\ \text{ind}(B'_2, \mathcal{S}'_2) &\leq \text{ind}(B_2, \mathcal{S}_2) - 2k. \end{aligned}$$

Thus,

$$\text{ind}(u'_1, u'_2) \leq \text{ind}^\sharp - 2k + 1.$$

Thus, for the limiting object to be non-empty, we require  $k = 1$ , i.e. the boundary degeneration is simple; this is Case (sME-7). More generally, each boundary degeneration level carries codimension at least 1, so it follows that no more than one boundary degeneration can occur, and if it does, then there are no other curves at East infinity.

Suppose next that there is a weight  $2k$  boundary degeneration West infinity on the  $\mathcal{S}_1$ -side; let  $a$  denote the total weight of the orbits, and let  $m$  denote the number

of chords in  $\mathcal{S}'_1$  that are matched with the boundary degeneration. Suppose that  $m > 0$ . Then,  $(u'_1, u'_2)$  lives in a moduli space with expected dimension

$$\text{ind}(u'_1, u'_2) = \text{ind}(B'_1, \mathcal{S}'_1) + \text{ind}(B_2, \mathcal{S}'_2) - c'_1 + 1,$$

since there are  $c'_1 - m$  matching conditions coming from the chords that do not go into the boundary degeneration, and the remaining  $m$  chords are required to lie at the same height, imposing  $m - 1$  further constraints. It is straightforward to see that

$$\begin{aligned} n_{\mathbf{x}_1}(B'_1) + n_{\mathbf{y}_1}(B'_1) + e(B'_1) &= n_{\mathbf{x}_1}(B_1) + n_{\mathbf{y}_1}(B_1) + e(B_1) - 4k \\ \omega_\partial^1(B'_1) &= \omega_\partial^1(B_1) - 2k \\ c'_1 &\leq c_1 - a + m \\ o'_1 &\leq o_1 - a \\ \omega_\partial^1(B'_1) &= \omega_\partial^1(B) - a \end{aligned}$$

so  $\text{ind}(u'_1, u'_2) \leq \text{ind}^\sharp + 1 - 2k$ . Thus,  $k > 1$  forces  $(u'_1, u'_2)$  to be in an empty moduli space; the case  $k = 1$  is allowed, and it is Case (sME-6).

We turn our attention to  $m = 0$ . In this case,

$$\text{ind}(u'_1, u'_2) = \text{ind}(B'_1, \mathcal{S}'_1) + \text{ind}(B_2, \mathcal{S}'_2) - c'_1,$$

and the boundary degeneration is forced to contain exactly one odd orbit: it is a special boundary degeneration with weight  $2k = 2a$ . In this case, computing as above, we find that  $\text{ind}(u'_1, u'_2) \leq \text{ind}^\sharp - 2k$ . The moduli space is once again empty if  $k > 1$ . When  $k = 1$ , there is a special case where it is non-empty: when  $(u'_1, u'_2)$  is constant. This case also falls under Case (sME-6). □

Let  $(u_1, v_1), (u_2, v_2)$  be a self-matched story pair where  $v_1$  and  $v_2$  are join curves, as in Case (sME-5). Then,  $(u_1, u_2)$  are self-matched pairs. Similarly, if  $u_1, (u_2, v_2)$  is a self-matched story pair where  $v_2$  is an orbit curve as in Case (sME-4), then  $(u_1, u_2)$  are also self-matched pairs. In these cases, we call  $(u_1, u_2)$  the *trimming* of the corresponding limit curve.

**Lemma 9.31.** *The number of ends of Type (sME-5) coincides with the number of self-matched pairs  $(u_1, \mathcal{S}_1, u_2, \mathcal{S}_2, \phi, \psi)$  for which  $\mathbf{E}(\mathcal{S}_2)$  consists of one length 1 chord and all other chords have length  $1/2$ .*

**Proof.** Let  $\mathcal{M}_b(\mathbf{x}, \mathbf{y}, \mathcal{S}_1; \mathcal{S}_2)$  be the moduli space of self-matched curve pairs, where exactly one of the boundary punctures  $q$  of  $\mathcal{S}_2$  is labelled by a length 1 chord, which we denote  $v$  (and all others boundary punctures are marked by length  $1/2$  chords). This moduli space embeds in a larger moduli space  $\widetilde{\mathcal{M}}_b$ , where we drop the condition from Equation (9.8) for the puncture  $q \in \mathcal{S}_2$  marked by the length 1 chord. This moduli space in turn admits an evaluation map

$$\text{ev}_q - \text{ev}_{\psi(q)} : \widetilde{\mathcal{M}}_b \rightarrow \mathbb{R}$$

with 0 as a regular value, whose preimage is  $\mathcal{M}_b(\mathbf{x}, \mathbf{y}, \mathcal{S}_1; \mathcal{S}_2)$ .

Given  $u = (u_1, u_2) \in mm_b(\mathbf{x}, \mathbf{y}; \mathcal{S}_1, \mathcal{S}_2)$ , let  $\tilde{U} \subset \widetilde{mm}_b$  be a neighborhood so that  $\text{ev}_q - \text{ev}_{\psi(q)}: \tilde{U} \rightarrow (-\epsilon, \epsilon)$  is a diffeomorphism (i.e. so that  $u$  is the preimage of 0).

Let  $\mathcal{S}'_1 = \mathcal{S}_1 \natural_{\psi(q)} \mathcal{I}_1$  and  $\mathcal{S}'_2 = \mathcal{S}_2 \natural_q \mathcal{I}_2$ . Thus,  $\mathcal{S}_2$  comes with an extra pair of punctures  $\{q_1, q_2\}$  (labelled by chords which can be joined to form  $v$ ). Let  $\widetilde{mm}$  be the moduli space like  $mm_{\sharp}(\mathbf{x}, \mathbf{y}, \mathcal{S}'_1, \mathcal{S}'_2)$ , except now that at the two distinguished punctures  $\{q_1, q_2\}$  in  $\mathcal{S}'_2$  coming from the east infinity curve, we do not require the time constraint from Equation (9.8). There is a map  $F = (F_1, F_2, F_3): \widetilde{mm} \rightarrow \mathbb{R}^3$ , with components

$$F_1 = t \circ \text{ev}_{\psi(q_1)} - t \circ \text{ev}_{q_1}, \quad F_2 = t \circ \text{ev}_{q_1} - t \circ \text{ev}_{q_2} \quad F_3 = t \circ \text{ev}_{\psi(q_1)} - t \circ \text{ev}_{\psi(q_2)},$$

with the property that if  $\Delta \subset \mathbb{R}^2$  denotes the diagonal, the Type (sME-5) end of  $mm_{\sharp}(\mathbf{x}, \mathbf{y}, \mathcal{S}'_1, \mathcal{S}'_2)$  at  $(u_1, \mathcal{S}_1, u_2, \mathcal{S}_2, \phi, \psi)$ .

Gluing the east infinity curves to  $u_1$  and  $u_2$ , we get a gluing map

$$\gamma: \tilde{U} \times (0, \epsilon) \times (0, \epsilon) \rightarrow \widetilde{mm}.$$

The gluing map continuously extends to a map from  $\tilde{U} \times [0, \epsilon) \times [0, \epsilon)$  to the Gromov compactification of  $\widetilde{mm}$  so that for all  $r_1, r_2 > 0$ ,

$$\begin{aligned} \gamma(u_1 \times u_2 \times \{0\} \times \{0\}) &= ((u_1, v_1), (u_2, v_2)) \\ F_1 \circ \gamma|_{\tilde{U} \times \{0\} \times \{0\}} &= \text{ev}_{\psi(q)} - \text{ev}_q|_{\tilde{U}} \\ F_2 \circ \gamma(\tilde{U} \times \{r_1\} \times \{0\}) &= 0 \\ F_2 \circ \gamma(\tilde{U} \times \{r_1\} \times \{r_2\}) &> 0 \\ F_3 \circ \gamma(\tilde{U} \times \{0\} \times \{r_2\}) &= 0 \\ F_3 \circ \gamma(\tilde{U} \times \{r_1\} \times \{r_2\}) &> 0. \end{aligned}$$

It follows that  $(F \circ \gamma)^{-1}(\{0\} \times \Delta)$  has a single endpoint over the origin, and that is the point  $((u_1, v_1), (u_2, v_2))$ , giving the stated correspondence between ends and self-matched curves stated in the lemma.  $\square$

**Lemma 9.32.** *The number of ends of Type (sME-3) coincides with the number of self-matched pairs for which  $\mathbf{E}(\mathcal{S}_2)$  consists of one length 1 chord and all other chords have length  $1/2$ .*

**Proof.** Let  $mm_b(\mathbf{x}, \mathbf{y}, \mathcal{S}_1, \mathcal{S}_2)$ ,  $\widetilde{mm}_b$ , and  $U$  be as in the proof of Lemma 9.31. Gluing the orbit curve to  $\mathcal{S}_2$  now gives a gluing map

$$\gamma: U \times (0, \epsilon) \rightarrow mm_{\sharp}(\mathbf{x}, \mathbf{y}, \mathcal{S}_1, \mathcal{S}'_2),$$

where now  $\mathcal{S}'_2 = \mathcal{S}_2 \natural \mathcal{I}$  is obtained by gluing on an orbit curve, which we denote here by  $v_2$ . (Note that  $\mathcal{S}'_2$  and  $v_2$  mean different objects than they did in the proof of Lemma 9.31.) Gluing extends continuously to the Gromov compactification, giving

$$\gamma: U \times [0, \epsilon) \rightarrow \widetilde{mm}_{\sharp}(\mathbf{x}, \mathbf{y}, \mathcal{S}_1, \mathcal{S}'_2),$$

so that for all  $r > 0$ ,

$$\begin{aligned}\gamma(u_1, \times u_2 \times \{0\}) &= (u_1, (u_2, v_2)) \\ \text{ev}_{v_i} - \text{ev}_{o'_i}|_{\gamma(U \times \{0\})} &= \text{ev}_{v_i} - \text{ev}_{v'_i} \\ s \circ \text{ev}_{o'_i}(\gamma(u, 0)) &= 1 \\ s \circ \text{ev}_{o'_i}(\gamma(u, r)) &< 1.\end{aligned}$$

There is a neighborhood  $U'$  of  $(u_1, (u_2, v_2))$  in  $\overline{mm}_\#(\mathbf{x}, \mathbf{y}, \mathcal{S}_1, \mathcal{S}_2')$  so that

$$U' \cap mm_\#(\mathbf{x}, \mathbf{y}; \mathcal{S}_1, \mathcal{S}_2') = (\text{ev}_{o_i} - \text{ev}_{o'_i})^{-1}(0),$$

so that  $s \circ \text{ev}_{o'_i}: U' \rightarrow (1 - \epsilon, 1]$  is a proper map near 1. It follows that the ends  $U' \cap mm_\#(\mathbf{x}, \mathbf{y}; \mathcal{S}_1, \mathcal{S}_2') = (\text{ev}_{o_i} - \text{ev}_{o'_i})^{-1}(0)$  is modelled on the preimage at  $s = 1$ .  $\square$

**Definition 9.33.** Let  $X$  be a set consisting of one or two Reeb chords. A  $X$ -partially self-matched curve pair (or  $X$ -partial-smcp) is the data  $(\mathcal{S}_1, \phi, \mathcal{S}_2, \psi)$  as in Definition 9.24, except Condition (smcp-1) is replaced by the following:

- $\mathbf{E}(\mathcal{S}_1)$  is partitioned into three disjoint sets:

$$\phi(\Omega_+(\mathcal{S}_1)) \quad \psi(\mathbf{E}(\mathcal{S}_2)) \quad X',$$

where  $X'$  is a set with  $|X'| = |X|$ , and the labels on the punctures of  $X'$  are specified in  $X$ .

Moreover, if  $|X| = 2$ , let  $X' = \{p_1, p_2\}$ . In this case, we also require

$$(9.10) \quad t \circ u_1(p_1) = t \circ u_1(p_2).$$

Let  $mm_{b,X}^B(\mathbf{x}, \mathbf{y})$  denote the moduli space of  $X$ -partial smcps, with homology class  $B$ .

Let  $(u_1, v_1), u_2$  be a self-matched story pair where  $v_1$  is an orbit curve; and let  $v$  be the chord labelling the boundary puncture of  $v_1$ . If the orbit in  $v_1$  is odd, then  $(u_1, u_2)$  is a  $\{v\}$ -partial smcp. If the orbit is even, then  $(u_1, u_2)$  is a  $X$ -partial smcp, where  $X$  consists of two length one chords that cover  $M^\wedge$ -matched boundary components. Similarly, if  $(w_1, v_1), u_2$  is a self-matched story pair where  $w_1$  is a boundary degeneration, the curves  $u_1$  and  $u_2$  is a partial smcp with one remaining chord, and if  $u_1, (w_2, u_2)$  is a self-matched story pair where  $w_2$  is a boundary degeneration, then  $(u_1, u_2)$  is a  $\{v\}$ -partial smcp, where  $v$  is a length one chord that covers some boundary component. In all the above cases, we call  $(u_1, u_2)$  the *trimming* of the self-matched story pair. The next few lemmas show that the number of ends are determined by the trimmings of the limiting configurations.

**Lemma 9.34.** Suppose that  $o_j$  is an odd orbit, and let  $v_j$  be the chord of length one that covers the corresponding boundary component  $\check{Z}_j$ . The number of curves in  $mm_{b;\{v_j\}}^B(\mathbf{x}, \mathbf{y}; \mathcal{S}_1, \mathcal{S}_2)$  has the same parity as the number of ends of  $mm_\#^B(\mathbf{x}, \mathbf{y}; \mathcal{S}_1', \mathcal{S}_2')$  of Type (sME-4), where  $v_1$  is an orbit curve that has a boundary puncture marked by  $o_j$ .

**Proof.** This follows from the gluing

$$\gamma: mm_{b;v_j}^B(\mathbf{x}, \mathbf{y}; \mathcal{S}_1', \mathcal{S}_2) \times (0, \epsilon) \rightarrow mm_\#^B(\mathbf{x}, \mathbf{y}, \mathcal{S}_1, \mathcal{S}_2),$$

gluing the orbit curve to  $\mathcal{S}'_1$  at  $v_j$ , which parameterizes the end with  $s(u(q)) \mapsto 0$ , where here  $q$  denotes the  $o_j$ -marked puncture; cf. Proposition 7.40.  $\square$

The following is a variant of Proposition 7.41:

**Lemma 9.35.** *Suppose that  $\{j, k\} \in M^\wedge$ , where  $f(j)$  is odd. Let  $v_j$  be a chord of length one that covers an boundary component  $\tilde{Z}_j$ . The number of curves in  $mm_{b; \{v_j\}}^B(\mathbf{x}, \mathbf{y}; \mathcal{S}_1, \mathcal{S}_2)$  has the same parity as the number of ends of  $mm_\#^B(\mathbf{x}, \mathbf{y}; \mathcal{S}'_1, \mathcal{S}'_2)$  of Type (sME-6), where  $w_1$  is a (smooth) simple boundary degeneration that contains  $o_j$ .*

**Proof.** Let  $\mathcal{S}'_1 = \mathcal{R}_1^* \mathcal{S}_1$ . This curve contains three distinguished punctures,  $q_1$  and  $q_2$  marked by orbits (coming from  $\mathcal{R}$ ), labelled so that  $q_2$  is the even orbit; and a third puncture  $q_3$  that marked by a length 1 chord, with  $q_3 = \phi(q_2)$ . (In the notation of the lemma statement,  $q_3$  is labelled by  $v_j$ .) Consider a moduli space  $\widetilde{mm}$  containing  $mm_\#(\mathbf{x}, \mathbf{y}, \mathcal{S}'_1, \mathcal{S}_2)$ , where we drop the height constraint from Equation (9.7) for the orbit  $q_2$  and its corresponding chord  $q_3 = \phi(q_2)$ . Thus, there is an evaluation map

$$t \circ \text{ev}_{q_1} - t \circ \text{ev}_{q_2}: \widetilde{mm} \rightarrow \mathbb{R}$$

so that 0 is a regular value, and whose preimage is identified with  $mm_\#(\mathbf{x}, \mathbf{y}, \mathcal{S}'_1, \mathcal{S}_2)$ .

We will consider a map  $F = (F_1, F_2): \widetilde{mm} \rightarrow \mathbb{R}^2$  whose components are given by

$$F_1 = t \circ \text{ev}_{q_1} - t \circ \text{ev}_{q_2} \quad F_2 = t \circ \text{ev}_{q_1} - t \circ \text{ev}_{q_3}.$$

This map extends continuously to the Gromov compactification of  $\widetilde{mm}$ .

Fix  $((u_1, w_1), u_2)$  in the Gromov compactification. Gluing gives a map

$$\gamma: \mathcal{M} \times_{\mathbb{T}_\beta} \mathcal{N}(\mathcal{R}) \times (-\epsilon, \epsilon) \times (0, \epsilon) \rightarrow \widetilde{mm}.$$

Here, the  $(-\epsilon, \epsilon)$  specifies the  $t$ -coordinate where the gluing is performed, and  $[0, \epsilon)$  represents the gluing scale. We restrict this to  $(u_1, u_2) \times w_1 \in \mathcal{M} \times_{\mathbb{T}_\beta} \mathcal{N}$ , and denote the resulting map

$$\gamma: (-\epsilon, \epsilon) \times (0, \epsilon) \rightarrow \widetilde{mm}.$$

Consider the two punctures  $q_1$  and  $q_2$  in  $\mathcal{R}$ . Since  $w_1$  is generic,  $t \circ w_1(q_1) \neq t \circ w_1(q_2)$ . Assume  $t \circ w_1(q_1) > t \circ w_1(q_2)$ . The map

$$(t \circ \text{ev}_{q_1} - t \circ \text{ev}_{q_3}) \circ \gamma(\cdot, 0): (-\epsilon, \epsilon) \rightarrow (-\epsilon, \epsilon)$$

has odd degree. By our assumption, for all  $r > 0$ ,

$$F_1 \circ \gamma(r, t) > 0.$$

Clearly, also

$$F_1(0, t) = 0.$$

Thus,

$$F \circ \gamma: (-\epsilon, \epsilon) \times [0, \epsilon) \rightarrow \mathbb{R}^{\geq 0} \times \mathbb{R}$$

is proper map of degree 1 to points in  $\mathbb{R}^{\geq 0} \times \mathbb{R}$  near the origin. The moduli space consists of points in the preimage of  $\mathbb{R}^{>0} \times \{0\}$ , a smooth one-manifold whose end consists of the preimage of the origin.

The same argument applies when  $t \circ w_1(q_1) < t \circ w_1(q_2)$ , with minor modifications.  $\square$

**Lemma 9.36.** *Suppose that  $o_j$  is an even orbit, and let  $v_j$  be a chord of length one that covers a the corresponding boundary component  $\check{Z}_j$ , and  $v_k$  be a chord of length one that covers  $\check{Z}_k$ , with  $\{j, k\} \in M^\wedge$ . The number of curves in  $mm_{b;\{v_j, v_k\}}^B(\mathbf{x}, \mathbf{y}; \mathcal{S}_1, \mathcal{S}_2)$  has the same parity as the number of ends of  $mm_\#^B(\mathbf{x}, \mathbf{y}; \mathcal{S}'_1, \mathcal{S}'_2)$  of Type (sME-4), where  $v_1$  is an orbit curve with boundary puncture marked by  $v_j$ .*

**Proof.** Let  $\widetilde{mm}_b$  denote the moduli space containing  $mm_{b;\{v_j, v_k\}}^B(\mathbf{x}, \mathbf{y}, \mathcal{S}_1, \mathcal{S}_2)$ , of data  $(u_1, u_2, \mathcal{S}_1, \phi, \mathcal{S}_2, \psi)$  satisfying the conditions from Definition 9.33, except that for the two distinguished punctures  $q_1$  and  $q_2$  on  $\mathcal{S}_1$  labelled by  $v_j$  and  $v_k$  (not contained in  $\phi(\Omega_+(\mathcal{S}_1))$  or  $\psi(\mathbf{E}(\mathcal{S}_2))$ ), we no longer require that  $t \circ u_1(q_1) = t \circ u_1(q_2)$ ; i.e. we drop the constraint from Equation (9.10).

We have a map

$$t \circ \text{ev}_{q_1} - t \circ \text{ev}_{q_2} : \widetilde{mm}_b \rightarrow \mathbb{R}$$

so that 0 is a regular value, and

$$(t \circ \text{ev}_{q_1} - t \circ \text{ev}_{q_2})^{-1}(0) = mm_{b;\{v_j, v_k\}}^B(\mathbf{x}, \mathbf{y}, \mathcal{S}_1, \mathcal{S}_2).$$

Each  $(u_1, u_2) \in mm_{b;\{v_j, v_k\}}^B(\mathbf{x}, \mathbf{y}, \mathcal{S}_1, \mathcal{S}_2)$  neighborhood  $\tilde{U} \in \tilde{M}$ , so that  $F_1 : \tilde{U} \rightarrow (-\epsilon, \epsilon)$  is a homeomorphism.

Let  $\widetilde{\widetilde{mm}}$  be the moduli space like  $\widetilde{mm}_b$ , except now  $q_1$  is marked by the orbit  $o_j$  rather than  $v_j$ . In particular, we have the map

$$F_1 = t \circ \text{ev}_{q_1} - t \circ \text{ev}_{q_2} : \widetilde{\widetilde{mm}} \rightarrow \mathbb{R}$$

with regular value 0, so that

$$F_1^{-1}(0) = mm_\#^B(\mathbf{x}, \mathbf{y}, \mathcal{S}'_1, \mathcal{S}'_2).$$

Let  $F_2 = s \circ \text{ev}_{q_1}$ , we have a map

$$F = (F_1, F_2) : \widetilde{\widetilde{mm}} \rightarrow \mathbb{R} \times \mathbb{R}^{<1}.$$

Gluing on the orbit curve at  $q_1$  gives a map  $\gamma : \tilde{U} \times [0, r) \rightarrow mm_\#^B(\mathbf{x}, \mathbf{y}, \mathcal{S}'_1, \mathcal{S}'_2)$ . We have that

$$F_1 \circ \gamma : \tilde{U} \times (0) \rightarrow (-\epsilon, \epsilon)$$

has degree 1 near 0; and for all  $\tilde{u} \in \tilde{U}$ ,  $r \in (0, \epsilon)$ .

$$F_2 \circ \gamma(\tilde{u}, 0) = 1$$

$$F_2 \circ \gamma(\tilde{u}, r) < 1$$

Thus,

$$F \circ \gamma(\tilde{U} \times [0, \epsilon)) \rightarrow \mathbb{R} \times \mathbb{R}^{\leq 1}$$

is proper of degree 1 for points near  $(0, 1)$  in  $\mathbb{R} \times \mathbb{R}^{\leq 1}$ . It follows at once that the smooth manifold

$$mm_\#^B(\mathbf{x}, \mathbf{y}, \mathcal{S}'_1, \mathcal{S}'_2) = F_1^{-1}(\{0\})$$

has one end over the point  $(0, 1) \in \mathbb{R} \times \mathbb{R}^{\leq 1}$ .  $\square$

**Lemma 9.37.** *Suppose that  $\{j, k\} \in M^\wedge$ , and let  $v_j$  and  $v_k$  be chords of length one that cover the boundary components  $\check{Z}_j$  and  $\check{Z}_k$  respectively. The number of curves in  $mm_{b; \{v_j, v_k\}}^B(\mathbf{x}, \mathbf{y}; \mathcal{S}_1, \mathcal{S}_2)$  has the same parity as the number of ends of  $mm_{\sharp}^B(\mathbf{x}, \mathbf{y}; \mathcal{S}_1, \mathcal{S}_2')$  of Type (sME- $\gamma$ ), where  $w_2$  is a simple boundary degeneration that contains  $o_j$  and  $o_k$ .*

**Proof.** Let  $\widetilde{mm}_b$  be as in Lemma 9.36.

Let  $\widetilde{mm}$  be the moduli space containing the moduli space of self-matched curve pairs  $mm_{\sharp}^B(\mathbf{x}, \mathbf{y}, \mathcal{S}_1, \mathcal{S}_2')$  as in Definition 9.24, except that now there are two distinguished (interior) punctures  $q_1, q_2$  in  $\mathcal{S}_2$  marked by orbits  $o_j$  and  $o_k$  respectively, where we do not impose the corresponding height constraints (from Equation (9.8)). Note that  $u_1$  represents the homology class  $B_1$  and  $u_2$  represents the homology class  $B_2 + \mathcal{D}$ , where  $\mathcal{D}$  is the elementary domain  $\Sigma_2$  containing  $\hat{Z}_j$  and  $\hat{Z}_k$ . Consider the map  $F = (F_1, F_2, F_3): \widetilde{mm} \rightarrow \mathbb{R}^3$  whose three components are the evaluation maps

$$\begin{aligned} F_1 &= t \circ \text{ev}_{\psi(q_1)} - t \circ \text{ev}_{q_1} \\ F_2 &= t \circ \text{ev}_{\psi(q_1)} - t \circ \text{ev}_{\psi(q_2)} \\ F_3 &= t \circ \text{ev}_{q_1} - t \circ \text{ev}_{q_2}. \end{aligned}$$

Clearly,

$$mm_{\sharp}^{B_1, B_2 + \mathcal{D}}(\mathbf{x}, \mathbf{y}, \mathcal{S}_1, \mathcal{S}_2') = F^{-1}(\Delta \times \{0\}),$$

where  $\Delta \subset \mathbb{R}^2$  is the diagonal.

For sufficiently small open subsets  $\tilde{U} \subset \widetilde{mm}_{\sharp}$ , gluing gives a map

$$\gamma: (-\epsilon, \epsilon) \times \widetilde{mm}_{\sharp} \times_{\mathbb{T}_{\beta}} n(\mathcal{D}) \times [0, \epsilon) \rightarrow \widetilde{mm},$$

where the  $(-\epsilon, \epsilon)$  factor specifies the  $t$ -coordinate where the gluing is performed, and the  $[0, \epsilon)$  represents the gluing scale. The fibered product over  $\mathbb{T}_{\beta}$  is taken with respect to an evaluation map  $\text{ev}_t: \mathcal{M} \rightarrow \mathbb{T}_{\beta}$ , defined by

$$\text{ev}_t(u_1) = u_1^{-1}(0, t) \in \mathbb{T}_{\beta};$$

and the (degree one) evaluation map  $\text{ev}^{\beta}: \mathcal{N} \rightarrow \mathbb{T}_{\beta}$ . Assume that  $\text{ev}^{\beta}(w_1)$  is a regular value, so that there is an open neighborhood  $W$  of  $w_2$  so that  $\text{ev}: W \rightarrow \mathbb{T}_{\beta}$  is a local diffeomorphism. Restricting to some sufficiently small neighborhood  $\tilde{U} \subset \widetilde{m}$ , we can guarantee that for  $t \in (-\epsilon, \epsilon)$ ,  $\text{ev}_t(\tilde{U}) \subset \text{ev}(W)$ , so  $\tilde{U} \times_{\mathbb{T}_{\beta}} W \cong \tilde{U}$ . Further shrinking  $\tilde{U}$  if needed, we can assume that

$$t \circ \text{ev}_{q_1} - t \circ \text{ev}_{q_2}: \tilde{U} \rightarrow (-\epsilon, \epsilon)$$

is a homeomorphism, so that the preimage of 0 is the nearly self-matched curve pair  $(u_1, u_2)$ . We abbreviate the gluing map (suppressing the choice of  $W$ ), writing instead

$$\gamma: \tilde{U} \times (-\epsilon, \epsilon) \times (0, \epsilon) \rightarrow \widetilde{mm}.$$

This map has a natural extension to  $\tilde{U} \times (-\epsilon, \epsilon) \times [0, \epsilon)$  to the Gromov compactification of  $\widetilde{mm}$ .



For any fixed  $\tilde{u} \in \tilde{U}$ ,  $r \in (0, 1)$ ,

$$F_1: \gamma(\cdot, \tilde{u}, r): (-\epsilon, \epsilon) \rightarrow (-\epsilon, \epsilon)$$

has degree one, since the same statement holds when  $r = 0$ . Also, for any fixed  $t \in (-\epsilon, \epsilon)$ ,

$$F_2 \circ \gamma(t, \cdot, r): \tilde{U} \rightarrow (-\epsilon, \epsilon)$$

has degree one, since the same statement holds setting  $r = 0$ . Finally,

$$F_3(t, \tilde{u}, 0) = 0 \quad \text{and} \quad F_3(t, \tilde{u}, r) > 0.$$

It follows that

$$F \circ \gamma: (-\epsilon, \epsilon) \times \widetilde{mm}_\natural \times [0, \epsilon) \rightarrow \mathbb{R} \times \mathbb{R} \times \mathbb{R}^{\geq 0}$$

has degree 1 near the origin; and the smooth manifold  $F^{-1}(\Delta \times \{0\})$  has one end over the origin.  $\square$

**Proof of Proposition 9.27.** As usual, we consider index two moduli spaces. Consider their ends, as in Proposition 9.30. Combining Lemma 9.31 and 9.32, it follows that the count of ends of Type (sME-5) cancels with the ends of Type (sME-3). Combining Lemma 9.35 and 9.34, it follows that ends of Type (sME-6) cancel with ends of Type (sME-4), where the orbit curve is odd, as illustrated in Figure 33. Combining Lemma 9.36 and 9.37, it follows that ends of Type (sME-7) cancel with ends of Type (sME-4) where the orbit curve is even, as illustrated in Figure 34.

The ends that are not accounted for are of Type (sME-1); and these ends count the  $\mathbf{y}$  coefficient of  $\partial^\sharp \circ \partial^\sharp$ .  $\square$

**9.4. Intermediate complexes.** Note that the self-matched compatible pairs from Definition 9.24 use the orbits curves quite differently from Definition 9.4; and so the chain complex defined using the two objects  $(C, \partial^{(0)})$  and  $(C, \partial_\natural)$  seem quite different. To construct a homopy equivalence between these complexes, we will use a sequence of intermediate complexes, defined here.

Fix an integer  $\ell$  and a marked source  $\mathcal{S}$ . Let  $\Omega^{\leq \ell}(\mathcal{S}) \subset \Omega(\mathcal{S})$  denote the subset of those punctures  $q \in \mathcal{S}$  that are marked by orbits  $o_j$  with  $f(j) \leq \ell$ . Define  $\Omega^\ell(\mathcal{S})$  and  $\Omega^{>\ell}(\mathcal{S})$  analogously

**Definition 9.38.** Let  $\ell$  be an integer between  $0, \dots, 2n$ . An  $\ell$ -self-matched curve pair is the following data.

- a holomorphic curve  $u_1$  in  $\mathcal{H}^\vee$ , with source  $\mathcal{S}_1$
- a holomorphic curve  $u_2$  in  $\mathcal{H}^\wedge$ , with source  $\mathcal{S}_2$
- an injection  $\phi: \Omega_+^{\leq \ell}(\mathcal{S}_1) \rightarrow \mathbf{E}(\mathcal{S}_1)$
- an injection  $\psi: \mathbf{E}(\mathcal{S}_2) \rightarrow \mathbf{E}(\mathcal{S}_1)$

with the following properties:

- $\mathbf{E}(\mathcal{S}_1)$  is a union of three disjoint sets,  $\phi(\Omega_+^{\leq \ell}(\mathcal{S}_1))$ ,  $\psi(\mathbf{E}(\mathcal{S}_2))$ , and  $\Omega^{\leq \ell}(\mathcal{S}_1)$

- If  $p \in \Omega_+^{\leq \ell}(\mathcal{S}_1)$  is labelled by some orbit  $o_j$ , then  $\phi(p)$  is marked by a length one Reeb chord that covers the boundary component of  $\check{Z}_k$ , where  $\{j, k\} \in M^\wedge$ , and

$$t \circ u_1(\phi(p)) = t \circ u_2(p).$$

- If  $q \in \mathbf{E}^{\leq \ell}(\mathcal{S}_2)$ , then  $\psi(q)$  is labelled by a length one Reeb chord that covers the boundary component of  $\check{Z}_j$ , and

$$t \circ u_1(\psi(q)) = t \circ u_2(q).$$

- If  $q \in \mathbf{E}^{> \ell}(\mathcal{S}_2) \cup \mathbf{E}(\mathcal{S}_2)$ , then the marking on the Reeb chord or orbit of  $q$  is the same as the marking on the Reeb chord or orbit of  $\psi(q)$ , and

$$(s \circ u_1(\psi(q)), t \circ u_1(\psi(q))) = (s \circ u_2(q), t \circ u_2(q)).$$

Let  $mm_{\natural; \ell}^{B_1, B_2}(\mathbf{x}, \mathbf{y}, \mathcal{S}_1, \mathcal{S}_2, \phi, \psi)$  denote the moduli space of  $\ell$ -morphism matched curves.

$$\begin{aligned} mm_{\star; \ell}^B(\mathbf{x}, \mathbf{y}) &= \bigcup \left\{ \begin{array}{l} B_1 \in \pi_2(\mathbf{x}_1, \mathbf{y}_1) \\ B_2 \in \pi_2(\mathbf{x}_2, \mathbf{y}_2) \end{array} \middle| B = B_1 \natural B_2 \right\} \bigcup mm_{\star; \ell}^{B_1, B_2}(\mathbf{x}, \mathbf{y}, \phi, \psi). \\ &\quad \left\{ (\mathcal{S}_1, \mathcal{S}_2, \phi, \psi) \middle| \text{ind}^\natural(B_1, \mathcal{S}_1; B_2, \mathcal{S}_2) = \text{ind}(B) \right\} \end{aligned}$$

**Definition 9.39.** Fix  $\ell \in \{0, \dots, 2n\}$ . Consider  $C$  equipped with the endomorphism determined by

$$\partial^{(\ell)}(\mathbf{x}) = \sum_{\mathbf{y}} \sum_{\{B \in \mathcal{D}(\mathbf{x}, \mathbf{y}) \mid \text{ind}(B)=1\}} \# \left( \frac{mm_{\natural; \ell}^B(\mathbf{x}, \mathbf{y})}{\mathbb{R}} \right) \cdot \mathbf{y}$$

**Remark 9.40.** Note that  $\partial^{(0)}$  is the operator from Equation (9.6); and  $\partial^{(2n)}$  is the operator  $\partial^\sharp$  is the operator from Equation (9.9)

Unlike the earlier cases, a sequence of  $\ell$ -self-matched curve pairs can have a Gromov limit to a pair of curves  $((w_1, u_1), (w_2, u_2))$  where both  $w_1$  and  $w_2$  are simple boundary degenerations, so that each puncture in  $w_2$  has a corresponding puncture in  $w_1$ , which is marked by the same orbit. This can happen in the special case where the odd orbit  $o_j$  in  $w_2$  has  $f(j) = \ell$ .

We will formulate the end counts in terms of the following types of curves (which naturally arise in Gromov limits of  $\ell$ -self-matched curve pairs):

**Definition 9.41.** Let  $\rho$  be a Reeb chord in  $\Sigma_1$ , and let  $\ell$  be an integer between  $0, \dots, 2n$ . An  $\ell$ -self-matched curve pair with remaining  $\{\rho\}$  is the following data.

- a holomorphic curve  $u_1$  in  $\mathcal{H}^\vee$ , with source  $\mathcal{S}_1$
- a holomorphic curve  $u_2$  in  $\mathcal{H}^\wedge$ , with source  $\mathcal{S}_2$
- an injection  $\phi: \Omega_+^{\leq \ell}(\mathcal{S}_1) \rightarrow \mathbf{E}(\mathcal{S}_1)$
- an injection  $\psi: \mathbf{E}(\mathcal{S}_2) \rightarrow \mathbf{E}(\mathcal{S}_1)$

with the following properties:

- $\mathbf{E}(\mathcal{S}_1)$  is a union of four disjoint sets,

$$\phi(\mathbf{E}_+^{\leq \ell}(\mathcal{S}_1)), \quad \psi(\mathbf{E}(\mathcal{S}_2) \cup \mathbf{E}(\mathcal{S}_2)), \quad \mathbf{E}_-^{\leq \ell}(\mathcal{S}_1), \quad \{q_0\},$$

where  $q_0$  is a puncture labelled by the Reeb chord  $\rho$ .

- If  $p \in \Omega_+^{\leq \ell}(\mathcal{S}_1)$  is labelled by some orbit  $o_j$ , then  $\phi(p)$  is marked by a length one Reeb chord that covers the boundary component of  $\check{Z}_k$ , where  $\{j, k\} \in M^\wedge$ , and

$$t \circ u_1(\phi(p)) = t \circ u_2(p).$$

- If  $q \in \mathbf{E}^{\leq \ell}(\mathcal{S}_2) \cup \mathbf{E}(\mathcal{S}_2)$ , then  $\psi(q)$  is labelled by a length one Reeb chord that covers the boundary component of  $\check{Z}_j$ , and

$$t \circ u_1(\psi(q)) = t \circ u_2(q).$$

- If  $q \in \mathbf{E}^{> \ell}(\mathcal{S}_2)$ , then the marking on the Reeb chord or orbit of  $q$  is the same as the marking on the Reeb chord or orbit of  $\psi(q)$ , and

$$(s \circ u_1(\psi(q)), t \circ u_1(\psi(q))) = (s \circ u_2(q), t \circ u_2(q)).$$

We denote the moduli space of these data by  $mm_{b; \ell, \{\rho\}}^B(\mathbf{x}, \mathbf{y}, \mathcal{S}_1, \mathcal{S}_2)$ .

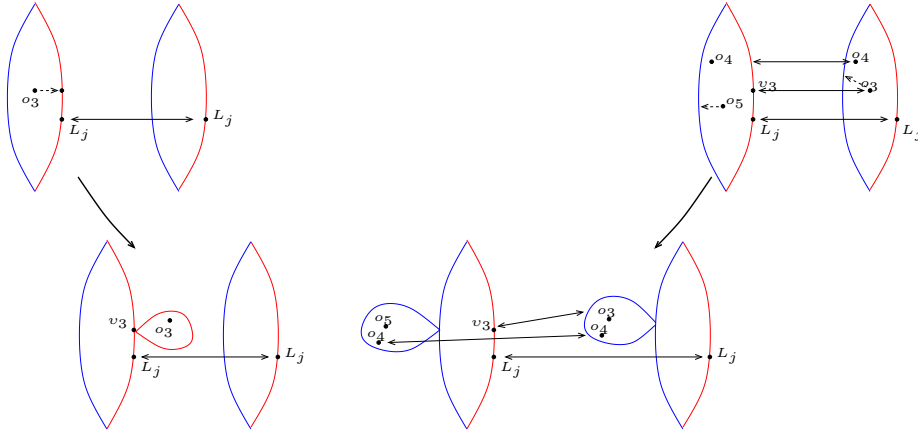


FIGURE 35. Ends of Type (sME-4) where the orbit is labelled by  $o_j$  with  $f(j) = \ell$  is odd, cancel against curves with boundary degenerations on both sides.

**Lemma 9.42.** *Let  $j$  be so that  $f(j) = \ell$  is odd. The number of curves in  $mm_{b; \ell, \{v_j\}}^B(\mathbf{x}, \mathbf{y}; \mathcal{S}_1, \mathcal{S}_2)$  has the same parity as the number of ends of  $mm_{b; \ell}^{B'}(\mathbf{x}, \mathbf{y}; \mathcal{S}'_1, \mathcal{S}'_2)$  of the form  $((u_1, w_1), (u_2, w_2))$ , where  $\mathcal{S}'_1 = \mathcal{R}_1 \natural \mathcal{S}_1$ ,  $\mathcal{S}'_2 = \mathcal{R}_2 \natural \mathcal{S}_2$ ,  $w_1$  and  $w_2$  are simple boundary degenerations with sources  $\mathcal{R}_1$  and  $\mathcal{R}_2$  both of which contain a puncture marked with  $o_j$ , and  $B'_i = B_i + \mathcal{D}_i$ , where  $\mathcal{D}_i$  is the shadow of  $w_i$  for  $i = 1, 2$ .*

**Proof.** Let  $q_1$  and  $q_2$  be the two punctures on  $\mathcal{S}'_2$  coming from  $w_2$ , labelled so that  $q_1$  is labelled by the odd Reeb orbit and  $q_2$  by the even one. In particular,  $\psi(q_1)$  is a puncture on  $\mathcal{S}'_1$  labelled by  $v_j$ . There is a moduli space  $\widetilde{mm}$  which is like  $mm_{b; \ell, \{v_j\}}^B(\mathbf{x}, \mathbf{y}, \mathcal{S}'_1, \mathcal{S}'_2)$ , except we now drop the conditions that

$$t \circ u_1(\psi(q_1)) = t \circ u_2(q_1) \quad \text{and} \quad t \circ u_1(\psi(q_2)) = t \circ u_2(q_2).$$

Thus, we have a map

$$F = (F_1, F_2, F_3, F_4): \widetilde{mm} \rightarrow \mathbb{R} \times \mathbb{R} \times (0, 1) \times (0, 1)$$

with components

$$\begin{aligned} F_1 &= t \circ u_1(\psi(q_1)) - t \circ u_2(q_1), \\ F_2 &= t \circ u_1(\psi(q_2)) - t \circ u_2(q_2), \\ F_3 &= s \circ u_1(\psi(q_2)), \\ F_4 &= s \circ u_2(q_2) \end{aligned}$$

so that  $F^{-1}(0 \times \Delta) = mm_{b;\ell;\{v_j\}}^B(\mathbf{x}, \mathbf{y}, \mathcal{S}'_1, \mathcal{S}'_2)$ .

Fix  $(u_1, u_2) \in mm_{b;\ell;\{v_j\}}^B(\mathbf{x}, \mathbf{y}; \mathcal{S}_1, \mathcal{S}_2)$ . Gluing  $w_1$  and  $w_2$  to  $u_1$  and  $u_2$  gives a map

$$\gamma: \times(-\epsilon, \epsilon) \times (0, \epsilon) \times (-\epsilon, \epsilon) \times (0, \epsilon) \rightarrow \widetilde{mm}.$$

(Note we are now gluing to both sides, giving two time parameters and two scale parameters.)

The gluing map extends to a map from  $(-\epsilon, \epsilon) \times [0, \epsilon) \times (-\epsilon, \epsilon) \times [0, \epsilon)$  to the Gromov compactification of  $\widetilde{mm}$ . This extension satisfies the following properties, for all  $t_1, t_2 \in (-\epsilon, \epsilon)$  and  $r_1, r_2 \in (0, \epsilon)$ :

- $F_1 \circ \gamma(\cdot, r_1, t_1 r_2): (-\epsilon, \epsilon) \rightarrow (-\epsilon, \epsilon)$  has degree one, since the same holds for  $r_1 = 0$ .
- $F_2 \circ \gamma(t_1, r_1, \cdot, r_2): (-\epsilon, \epsilon) \rightarrow (-\epsilon, \epsilon)$  has degree one, since the same holds for  $r_2 = 0$ .
- $F_3(t_1, \cdot, t_2, r_2): [0, \epsilon) \rightarrow (0, 1]$  has degree one near 1.
- $F_4(t_1, r_1, t_2, \cdot): [0, \epsilon) \rightarrow (0, 1]$  has degree one near 1.

It follows at once that  $(F \circ \gamma)^{-1}(\{0\} \times \{0\} \times \Delta)$  is a one-manifold with a single end over the origin.  $\square$

**Proposition 9.43.** *The endomorphism  $\partial^{(\ell)}$  satisfies  $\partial^{(\ell)} \circ \partial^{(\ell)} = 0$ .*

**Proof.** This is a straightforward synthesis of Propositions 9.21 and 9.27. Again, we look at two-dimensional moduli spaces. We find that their ends are of the following types:

- Two-story  $\ell$ -self-matched curve pairs.
- Type (ME-2).
- Type (ME-3), if the orbit curves are marked by  $o_j$  with  $j \notin \Omega_k$
- Type (sME-3), if the odd orbit  $o_j$  has  $f(j) \leq \ell$ .
- Type (sME-4), where the orbit curve on the left is marked by an odd orbit  $o_j$ , with  $f(j) \leq \ell$ .
- Type (sME-6).
- Type (sME-7).
- $\Omega$ -matched story pair ends, of the form  $(w_1, u_1), (w_2, u_2)$ , which occurs when  $\ell$  is odd and both  $w_1$  and  $w_2$  contain the puncture with  $f$ -value equal to  $\ell + 1$ .

Ends of Type (ME-3) and (sME-3) cancel with ends of Type (ME-2) by Lemma 9.20 when the orbit is has  $f$ -value greater than  $\ell$ ; and a combination of Lemmas 9.31 combined with Lemma 9.32 otherwise. Similarly, ends of type (sME-4) where the orbit is an odd orbit in  $\Omega_k$  cancel with those of Type (sME-6), as in Lemmas 9.34 and 9.35. Ends of Type (sME-4) where the orbit is even and has  $f$ -value less than or equal to  $\ell$  cancel with those of Type (sME-7) where the orbit has  $f$ -value less than or equal to  $\ell$ . By Lemma 9.42 and 9.34, the remaining ends of the form  $(w_1, u_1), (w_2, u_2)$  cancel with ends of Type (sME-4) where the orbit is odd, has and has  $f$ -value equal to  $\ell$ ; see Figure 35.  $\square$

Consider  $C$  equipped with the endomorphism

$$\partial^{(k)}(\mathbf{x}) = \sum_{\mathbf{y}} \sum_{\{B \in \pi_2(\mathbf{x}, \mathbf{y}) \mid \text{ind}(B)=1\}} \# \left( \frac{mm_{\mathfrak{z}; \ell}^B(\mathbf{x}, \mathbf{y})}{\mathbb{R}} \right) \cdot U^{n_w(B)} V^{n_z(B)} \cdot \mathbf{y}.$$

**9.5. Interpolating between the intermediate complexes.** In this section we prove the following:

**Proposition 9.44.** *When  $n > 1$ , there is an isomorphism of chain complexes over  $\mathcal{R}$*

$$\Phi_\ell: (C, \partial^{(\ell)}) \rightarrow (C, \partial^{(\ell+1)})$$

The map  $\Phi_\ell$  will be constructed by counting curves which generalize the  $\Omega$ -matched curves, as follows.

**Definition 9.45.** *Let  $\ell$  be an integer between  $1, \dots, 2n$ . An  $\ell$ -morphism matched curve, is the following data.*

- a holomorphic curve  $u_1$  in  $\mathcal{H}^\vee$ , with source  $\mathcal{S}_1$
- a holomorphic curve  $u_2$  in  $\mathcal{H}^\wedge$ , with source  $\mathcal{S}_2$
- a subset  $X \subset \mathbf{E}_+^\ell(\mathcal{S}_1)$ , (i.e. which is empty if  $\ell$  is odd)
- a subset  $Y \subset \mathbf{E}_-^\ell(\mathcal{S}_1)$
- an injection  $\phi: \Omega_+^{\leq \ell}(\mathcal{S}_1) \cup X \rightarrow \mathbf{E}(\mathcal{S}_1)$
- an injection  $\psi: \mathbf{E}(\mathcal{S}_2) \rightarrow \mathbf{E}(\mathcal{S}_1)$
- a real number  $t_0 \in \mathbb{R}$

with the following properties:

- $\mathbf{E}(\mathcal{S}_1)$  is a union of four disjoint sets,  $\phi(\mathbf{E}_+^{\leq \ell}(\mathcal{S}_1) \cup X)$ ,  $\psi(\mathbf{E}(\mathcal{S}_2))$ ,  $\mathbf{E}_-^{\leq \ell}(\mathcal{S}_1)$ , and  $Y$ .
- $X$  contains all punctures  $q \in \mathbf{E}_+^\ell(\mathcal{S}_1)$  with  $t \circ u_1(q) > t_0$
- $Y$  contains all punctures  $q \in \mathbf{E}_-^\ell(\mathcal{S}_1)$  with  $t \circ u_1(q) < t_0$
- If  $p \in \Omega_+^{\leq \ell}(\mathcal{S}_1) \cup X$  is labelled by some orbit  $o_j$ , then  $\phi(p)$  is marked by a length one Reeb chord that covers the boundary component of  $\tilde{Z}_k$ , where  $\{j, k\} \in M^\wedge$ , and

$$t \circ u_1(\phi(p)) = t \circ u_2(p).$$

- If  $q \in \mathbf{E}^{\leq \ell}(\mathcal{S}_2)$  or  $q \in \mathbf{E}^\ell(\mathcal{S}_2)$  and  $t \circ u_2(q) < t_0$ , then  $\psi(q)$  is labelled by a length one Reeb chord that covers the boundary component of  $\tilde{Z}_j$ , and

$$t \circ u_1(\psi(q)) = t \circ u_2(q)$$

- If  $q \in \mathbf{E}^{>\ell}(\mathcal{S}_2)$  or  $q \in \mathbf{E}^\ell(\mathcal{S}_2)$  and  $t \circ u_2(q) > t_0$ , then the marking on the Reeb chord or orbit of  $q$  is the same as the marking on the Reeb chord or orbit of  $\psi(q)$ , and

$$(s \circ u_1(\psi(q)), t \circ u_1(\psi(q))) = (s \circ u_2(q), t \circ u_2(q)).$$

- If  $q \in \mathbf{E}^\ell(\mathcal{S}_2)$  and  $t \circ u_2(q) = t_0$ , then  $\psi(q)$  is also labelled by the same Reeb orbit, and

$$t \circ u_1(\psi(q)) = t \circ u_2(q) = t_0.$$

Moreover, the following inequalities hold on the  $s$  projection. Order the punctures  $q \in \mathbf{E}^\ell(\mathcal{S}_2)$  with  $t \circ u_1(q) = t_0$   $\{q_i\}_{i=1}^m$  so that the sequence  $\{s \circ u_2(q_i)\}_{i=1}^m$  is increasing; then

$$s \circ u_2(q_i) < s \circ u_1(\psi(q_i))$$

and, if  $i < m$ ,

$$s \circ u_1(\psi(q_i)) < s \circ u_2(q_{i+1}).$$

Each  $\ell$ -morphism matched curve has three associated integers,  $m_-$ ,  $m$ , and  $m_+$ , where  $m_-$  resp.  $m_+$  denotes the number of punctures  $q$  in  $\mathbf{E}^\ell(\mathcal{S}_2)$  with  $t(q) < t_0$  resp.  $t(q) > t_0$ ; and  $m$  (as above) is the number of punctures in  $\mathbf{E}^\ell(\mathcal{S}_2)$  with  $t(q) = t_0$ . The triple  $(m_-, m, m_+)$  is called the profile of the  $\ell$ -morphism matched curve.

Let  $mm_{\star;\ell}(\mathbf{x}, \mathcal{S}_1, \mathcal{S}_2, \phi, \psi)$  denote the moduli space of  $\ell$ -morphism matched curves.

$$\begin{aligned} mm_{\star;\ell}^B(\mathbf{x}, \mathbf{y}) &= \bigcup \bigcup mm_{\star;\ell}^{B_1, B_2}(\mathbf{x}, \mathbf{y}, \phi, \psi). \\ &\left\{ \begin{array}{l} B_1 \in \pi_2(\mathbf{x}_1, \mathbf{y}_1) \\ B_2 \in \pi_2(\mathbf{x}_2, \mathbf{y}_2) \end{array} \middle| B = B_1 \natural B_2 \right\} \{(\mathcal{S}_1, \mathcal{S}_2, \phi, \psi) \mid \text{ind}^{\natural}(B_1, \mathcal{S}_1; B_2, \mathcal{S}_2) = \text{ind}(B)\} \end{aligned}$$

**Definition 9.46.** Define a map  $h_\ell: (C, \partial^{(\ell)}) \rightarrow (C, \partial^{(\ell+1)})$  by the formula

$$h_\ell(\mathbf{x}) = \sum_{\mathbf{y}} \sum_{\{B \in \pi_2(\mathbf{x}, \mathbf{y}) \mid \text{ind}(B)=1\}} \#mm_{\star;\ell}(\mathbf{x}, \mathbf{y}) \cdot U^{n_w(B)} V^{n_z(B)} \cdot \mathbf{y}.$$

**Lemma 9.47.**

$$\partial^{(\ell+1)} \circ h_\ell + h_\ell \circ \partial^{(\ell)} = \partial^{(\ell+1)} + \partial^{(\ell)}.$$

**Proof.** Consider ends of one-dimensional moduli spaces  $mm_{\star;\ell}(\mathbf{x}, \mathbf{y})$ . There are two cases, according to the parity of  $\ell$ . Suppose that  $\ell$  is odd.

There are ends as involving punctures other than the ones whose  $t$ -projection is  $t_0$ . These ends are as in the intermediate complexes in Proposition 9.44. Many of these ends cancel in pairs in the proof of that proposition, leaving the two-story buildings, and the ends that involve the special  $t_0$ -level.

Those ends in turn can be classified, as follows. Let  $\{q_1, \dots, q_m\} \in \mathbf{E}^\ell(\mathcal{S}_2)$  be the punctures with  $t \circ u_1(q_i) = t_0$ , labelled as in Definition 9.45.

- (b-1) The end corresponds to  $s(u_1(q_m)) \mapsto 1$ ; in this case, there is a Gromov limit to  $((u_1, v_1), u_2)$ , where  $v_1$  is an orbit curve (for an orbit whose  $f$ -value is  $\ell$ ), attached at the level  $t_0$ . These ends are labelled by integers  $(m_-, m-1, m_+)$ , where  $m_-$  and  $m_+$  are defined as in Definition 9.45.

- (b-2) The end corresponds to  $s(u_2(\psi(q_1))) \mapsto 0$ ; in this case, there is a Gromov limit to  $((w_1, u_1), (w_2, v_2))$ , where  $w_1$  and  $w_2$  are simple boundary degenerations, both of which contain an orbit  $o_j$  with  $f(j) = \ell$ . These ends are labelled by integers  $(m_-, m-1, m_+)$ .
- (b-3) Pairs  $(u_1, u_2)$  with  $s(u_1(q_i)) = s(u_2(\psi(q_i)))$  or  $s(u_2(\psi(q_i))) = s(u_1(q_{i+1}))$ . These ends are labelled  $(m_-, m, m_+, j)$  where with the convention  $j = 2i-1$ , if  $s(u_1(q_i)) = s(u_2(\psi(q_i)))$ ; and  $j = 2i$  if  $s(u_2(\psi(q_i))) = s(u_1(q_{i+1}))$ .
- (b-4) there is some  $q \in \mathbf{E}^\ell(\mathcal{S}_2)$  with  $t(u_2(q)) = t_0$ , but  $q$  arises as a limit point of punctures with  $t(u_2(q)) < t_0$ . Let  $s_0 = s(u_1(\psi(q))) = s(u_2(q))$ . These ends are labelled  $(m_-, m, m_+, j)$  where

$$(9.11) \quad j = \begin{cases} 1 & \text{if } s_0 < s \circ u_1(q_1) \\ 2i-1 & \text{if } s \circ u_2(\psi(q_{i-1})) < s_0 < s \circ u_2(q_i) \\ 2i & \text{if } s \circ u_2(q_i) < s_0 < s \circ u_1(\psi(q_{i+1})) \\ 2m & \text{if } s \circ u_1(q_m) < s_0 \end{cases}$$

Let  $m_+$  here be one greater than the number of  $q \in \mathbf{E}^\ell(\mathcal{S}_2)$  with  $t(u_2(q)) > t_0$ ; this is  $m_+$  for the curves before taking the Gromov limit.

- (b-5) there is some  $q \in \mathbf{E}^\ell(\mathcal{S}_2)$  with  $t(u_2(q)) = t_0$ , but  $q$  arises as a limit point of punctures with  $t(u_2(q)) > t_0$ . These ends are labelled  $(m_-, m, m_+, j)$ , where  $j$  is defined as in Equation (9.11); where now  $m_-$  is computed before taking the Gromov limit.
- (b-6) there is some  $q \in \mathbf{E}^\ell(\mathcal{S}_1)$  with  $t(u_1(q)) = t_0$ , arising as a limit point of punctures with  $t(u_1(q)) > t_0$ . These ends are labelled  $(m_-, m, m_+, j)$ , where  $j$  is defined as in Equation (9.11); and  $m_-$  is computed before taking the Gromov limit.

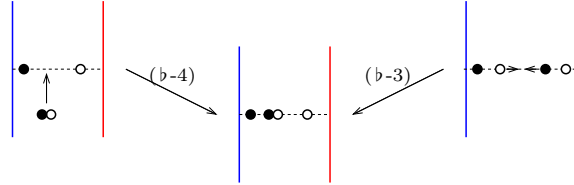


FIGURE 36. **Ends of Types (b-4) and (b-3) cancel** We have drawn here the strip: the light dots represent the images under the projection to  $[0, 1] \times \mathbb{R}$  of the punctures on  $\mathcal{S}_1$ ; the dark ones represent the punctures on  $\mathcal{S}_2$ .

End of Type (b-3)  $(m_-, m, m_+, j)$  cancel with end of Type (b-4)  $(m_-, m-1, m_+ + 1, j)$  except when  $m = 1$ ; see Figure 36.

Ends of Type (b-5)  $(m_-, m, m_+, j)$  cancel in pairs except in the special case where  $j = m$ .

Ends of Type (b-1)  $(m_-, m, m_+)$  cancel with ends of Type (b-5)  $(m_- + 1, m-1, m_+, m-1)$  except when  $m = 1$ .

Ends of Type (b-2)  $(m_-, m, m_+)$  cancel with ends of Type (b-6)  $(m_- + 1, m-1, m_+)$  except when  $m = 1$ .

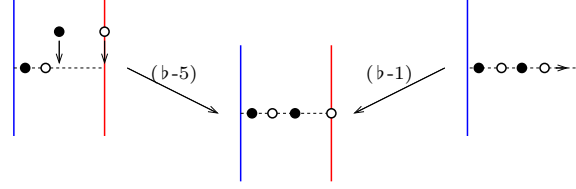


FIGURE 37. **Ends of Type (b-1) cancel certain ends of Type (b-5)**, when the ennd of Type (b-5) has the form  $(m_-, m, m_+, m)$ .

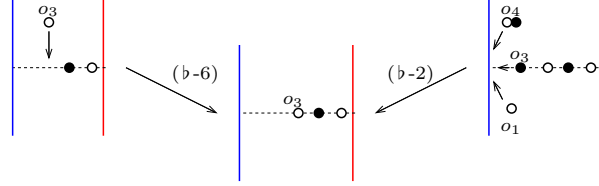


FIGURE 38. **Ends of Types (b-6) and (b-2) cancel**

The remaining ends are: Type (b-3)  $(m_-, 1, m_+, 1)$ , Type (b-1)  $(m_-, 1, m_+)$ , and Type (b-2)  $(m_-, 1, m_+)$ . Now, provided that  $m_- > 0$ , ends of Type (b-3)  $(m_-, 1, m_+, 1)$  correspond to ends of Type (b-1) and (b-2)  $(m_- - 1, 1, m_+ + 1)$ .

After these further cancellations, the remaining ends are of Type (b-3)  $(0, 1, m_+, 1)$  – which correspond to the terms in  $\partial^{(\ell)}$  – and ends of type Type (b-1) and (b-2)  $(m_-, 1, 0)$  – which correspond to the terms in  $\partial^{(\ell+1)}$ .

The remaining two-story buildings count terms in  $\partial^{(\ell+1)} \circ h_\ell + h_\ell \circ \partial^{(\ell)}$ , verifying that  $\partial^{(\ell+1)} \circ h_\ell + h_\ell \circ \partial^{(\ell)} = 0$  when  $\ell$  is odd.

This discussion requires slight modifications in case  $\ell$  is even. Let  $\{q_1, \dots, q_m\} \in \mathbf{E}^\ell(\mathcal{S}_2)$  be the punctures with  $t \circ u_1(q_i) = t_0$ , labelled as in Definition 9.45.

- (b'-1) The end corresponds to  $s(u_1(q_m)) \mapsto 1$ ; in this case, there is a Gromov limit to  $((u_1, v_1), u_2)$ , where  $v_1$  is an orbit curve (for an orbit whose  $f$ -value is  $\ell$ ), attached at the level  $t_0$ .
- (b'-2) The end corresponds to  $s(u_2(\psi(q_1))) \mapsto 0$ ; in this case, there is a Gromov limit to  $((w_1, u_1), u_2)$ , where  $w_1$  is a simple boundary degeneration containing an orbit  $o_j$  with  $f(j) = \ell$ , and  $u_2$  contains an extra unmatched chord  $v_k$ , which covers the boundary component  $\check{Z}_k$  so that  $f(k) = \ell - 2$ .
- (b'-3) Pairs  $(u_1, u_2)$  with  $s(u_1(q_i)) = s(u_2(\psi(q_i)))$  or  $s(u_2(\psi(q_i))) = s(u_1(q_{i+1}))$ .
- (b'-4) There is some  $q \in \mathbf{E}^\ell(\mathcal{S}_2)$  with  $t(u_2(q)) = t_0$ , but  $q$  arises as a limit point of punctures with  $t(u_2(q)) < t_0$ .
- (b'-5) There is some  $q \in \mathbf{E}^\ell(\mathcal{S}_1)$  with  $t(u_1(q)) = t_0$ , arising as a limit point of punctures with  $t(u_1(q)) > t_0$ . Note that in this case there is an extra puncture  $q'$  (the limit of  $\phi(q)$ ) with  $t(q') = t_0$  on  $u_1$  labelled by  $v_k$ , where  $f(k) = \ell - 1$ .

With the above remarks in place, verification of the stated relation when  $\ell$  is even proceeds much as before. The most significant difference is that the cancellation



of ends of Type  $(b'-5)$  with those of Type  $(b'-2)$  is slightly simpler than the corresponding cancellation in the odd case; see Figure 39.

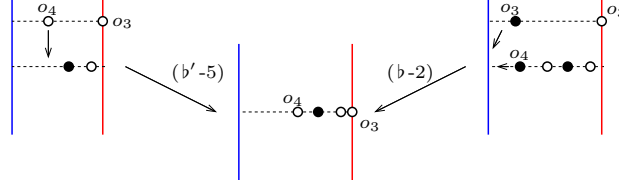


FIGURE 39. Ends of Types  $(b'-5)$  and  $(b'-2)$  cancel

□

**9.6. Time dilation.** Consider  $(C, \partial^\sharp)$ . The differential  $\partial^\sharp$  counts self-matched curve pairs. As in [10], we deform the matching appearing. In our case, we deform the constraints appearing in the definition of a self-matched curve pair (Equation (9.8)) by conditions indexed by a real parameter  $T$ , as follows:

$$T \cdot t \circ u_1(\psi(q)) = t \circ u_2(q).$$

The corresponding moduli spaces are denoted  $MM_\sharp(T; \mathbf{x}, \mathbf{y})$ , which we call the *moduli space of  $T$ -modified paritally self-matched curve pairs*.

Taking the limit as  $T \mapsto \infty$ , the curves converge to combs, whose algebraic information is contained in their main components. These limiting objects are natural analogues of the “trimmed simple ideal matched curves” from [10, Definition 9.31]:

**Definition 9.48.** A trimmed simple ideal partially self-matched curve is a pair of holomorphic combs  $(u_1, u_2)$  connecting two Heegaard states generators  $\mathbf{x} = \mathbf{x}_1 \# \mathbf{x}_2$  and  $\mathbf{y} = \mathbf{y}_1 \# \mathbf{y}_2$ , where  $u_1$  is a self-matched curve (in the sense of Definition 9.23), equipped with a one-to-one correspondence  $\varphi: \mathbf{E}(\mathcal{S}_1) \setminus \phi(\Omega_+(\mathcal{S}_1)) \rightarrow \mathbf{E}(\mathcal{S}_2)$  such that either one of  $u_1$  or  $u_2$  is trivial, and the other has index 1, and  $\mathbf{E}(\mathcal{S}_1) \setminus \phi(\Omega_+(\mathcal{S}_1))$  and  $\mathbf{E}(\mathcal{S}_2)$  are empty; or all of the following conditions hold:

- (TSIC-1) The comb  $u_1$  is a holomorphic curve for  $\mathcal{H}^\vee$  asymptotic to a sequence of non-empty sets of Reeb chords  $\vec{\rho} = (\rho_1, \dots, \rho_m)$
- (TSIC-2)  $u_1$  has index 1 with respect to  $\vec{\rho}$ .
- (TSIC-3)  $u_2$  is a height  $m$  holomorphic building for  $\mathcal{H}^\wedge$  with no components at east infinity
- (TSIC-4) each story of  $u_2$  has index one.
- (TSIC-5)  $u_1$  and  $u_2$  are strongly boundary monotone
- (TSIC-6) for each  $i = 1, \dots, m$ , the east punctures of the  $i^{\text{th}}$  story of  $u_2$  are labelled, in order, by a non-empty sequence of Reeb chords  $(-\rho_1^i, \dots, -\rho_{\ell_i}^i)$  with the property that the sequence of singleton sets of chords  $\vec{\rho}^i = (\{\rho_1^i\}, \dots, \{\rho_{\ell_i}^i\})$  are composable.
- (TSIC-7) The composition of the sequence of singleton sets of Reeb chords  $\rho^i$  on the  $i^{\text{th}}$  story of  $u_2$  coincides with the  $i^{\text{th}}$  set of reeb chords  $\rho_i$  in the partition for  $w$ .

Let  $MM_{b; \star}^{B_1 \natural B_2}(\mathbf{x}, \mathbf{y})$  denote the moduli space of trimmed simple ideal partially self-matched curves.

**Proposition 9.49.** *Fix  $\mathbf{x} = \mathbf{x}_1 \# \mathbf{x}_2, \mathbf{y} = \mathbf{y}_1 \# \mathbf{y}_2 \in \mathfrak{S}(\mathcal{H} = \mathcal{H}^\wedge \# \mathcal{H}^\vee)$ ,  $B_1 \in \mathcal{D}(\mathbf{x}_1, \mathbf{y}_1)$ , and  $B_2 \in \mathcal{D}(\mathbf{x}_2, \mathbf{y}_2)$ . For each generic  $T$  sufficiently large,*

$$\#mm_{\flat, \star}^{B_1 \natural B_2}(\mathbf{x}, \mathbf{y}) = \#mm_{\sharp}^{B_1 \natural B_2}(T; \mathbf{x}, \mathbf{y}).$$

**Proof.** The proof is as in [10, Proposition 9.40]; the key difference being that in [10], there is no self-matching (in particular  $u_1$  a holomorphic curve rather than a self-matched curve), but this does not affect the argument.

In a little more detail, Gromov compactness shows that as  $T \mapsto \infty$ , the  $T$ -selfmatched curves converge to a pair of combs  $U_1$  and  $U_2$  (in  $\mathcal{H}^\vee$  and  $\mathcal{H}^\wedge$  respectively) satisfying a matching condition. Throwing out the East infinity curves, we arrive at a pair of combs  $(u_1, u_2)$ . The matching conditions (Condition (TSIC-7)) is clear; the fact that  $u_1$  is a (one-story) holomorphic curve (Condition (TSIC-1)) of index one (Property (TSIC-2)) follows from the index formula.

Boundary monotonicity of  $u_1$  follows from Lemma 7.2. It follows then from Lemma 8.7 that the algebra elements from each packet are non-zero. It now follows that  $u_2$  has no  $\alpha$ -boundary degenerations; for such a boundary degeneration would give rise to a vanishing algebra element. Having eliminated  $\alpha$ -boundary degenerations from  $u_2$ , Condition (TSIC-3) and (TSIC-4) follows from the index formula. Boundary monotonicity of  $u_2$  follows now from Lemma 8.7 combined with Proposition 5.9. The matching conditions (TSIC-7) is straightforward.

Conversely, the existence of  $T$ -self-matched curves for sufficiently large  $T$  follows from a gluing argument as in the proof of [10, Proposition 9.40].  $\square$

**9.7. Putting together the pieces.** We can now assemble the steps to provide the main theorem:

**Proof of Theorem 9.1.** Start from the complex  $C_{\mathcal{R}}(\mathcal{H}) = (C, \partial)$  for the doubly-pointed Heegaard diagram, with differential as in Equation (9.1). When  $n > 1$ , Theorem 9.22 (neck stretching) identifies  $C_{\mathcal{R}}(\mathcal{H}) \simeq (C, \partial^{(0)})$ , where the latter differential counts matched holomorphic curves. Proposition 9.44 gives the sequence of isomorphisms

$$(C, \partial^{(0)}) \cong \cdots \cong (C, \partial^{(2n)}).$$

Note that  $(C, \partial^{(2n)}) = (C, \partial^\sharp)$ . When  $n = 1$ ,

Next, we replace the differential  $\partial^\sharp$  by a new differential  $\partial^{T; \sharp}$  which counts  $T$ -modified partially self-matched pairs; i.e. points in  $mm_{\sharp}(T; \mathbf{x}, \mathbf{y})$ . When  $T = 1$ , clearly  $\partial^\sharp = \partial^{T; \sharp}$ . The chain homotopy type of  $(C, \partial^{T; \sharp})$  is independent of the choice of  $T$ : i.e. varying  $T$  gives chain homotopy equivalences between the various choices of complex. (This is the analogue of [10, Proposition 9.22], with the understanding that now, in one-dimensional families, we have orbit curve end cancellation ends in addition to the cancellation of join curve ends as in [10]; cf. Lemma 9.20 above.) Taking  $T$  sufficiently large as in Proposition 9.49, and composing homotopy equivalences, we find that  $C_{\mathcal{R}}(\mathcal{H})$  is chain homotopic to  $(C, \partial')$ , where now  $\partial'$  counts trimmed simple ideal partially self-matched curves (Definition 9.48). Since  $u_1$  is strongly boundary monotone (which can be phrased in terms of chord packets, thanks to Lemma 7.3), Lemma 8.7 guarantees that the objects counted in  $\partial'$  correspond to the algebraic counts appearing in the differential on  $Q(\mathcal{H}^\wedge) \boxtimes R(\mathcal{H}^\vee)$ .  $\square$

**9.8. The case where  $n = 1$ .** The case where  $n = 1$  works technically a little differently from the case where  $n > 1$ . The key distinguishing feature is that in the case where  $n = 1$ , closed components do exist in the Gromov compactification. (It is also, of course a bit simpler, since we have to deal with deforming only one pair of matched orbits.)

As we shall see in our proof of Theorem 1.1 (Section 15), we will need the case  $n = 1$  only in a very specific special case: gluing on the standard lower diagram, which has the property that any homotopy class that covers both  $Z_1$  and  $Z_2$  also covers the two basepoints  $w$  and  $z$ . This property would allow us to simplify the arguments considerably; but in the interest of giving a clean statement of Theorem 9.1, we give a proof when  $n = 1$  without these restrictions hypotheses.

**9.8.1. Matched curves.** Consider the notion of matched curves (as in Definition 9.4), except where the objects  $\bar{u}_1$  and  $\bar{u}_2$  are stories, rather than simply curves. When  $n > 1$ , Lemma 9.13 shows that in sufficiently small index (and in homology classes not covering both  $w$  and  $z$ ), the combs contain no closed components; Lemma 9.12 shows that they can contain no boundary degenerations. Thus, with these hypotheses, the matched stories are automatically matched curves.

This is no longer the case where  $n = 1$ . Specifically, Lemma 9.13 fails in this case: moduli spaces of self-matched stories are expected to contain closed components (on the  $\mathcal{H}^\wedge$  side); and indeed, after removing those components, we obtain a (suitably) generalized matched curve in a moduli space of the same expected dimension.

We formalize these curves as follows:

**Definition 9.50.** A special matched pair *consists of*

- a holomorphic curve  $u_1$  in  $\mathcal{H}^\vee$  with source  $\mathcal{S}_1$  representing homology class  $B_1 \in \mathcal{D}(\mathbf{x}_1, \mathbf{y}_1)$
- a holomorphic curve  $u_2$  in  $\mathcal{H}^\wedge$  with source  $\mathcal{S}_2$  representing homology class  $B_2 \in \mathcal{D}(\mathbf{x}_2, \mathbf{y}_2)$
- a subset  $X \subset \mathbf{E}(\mathcal{S}_1)$  of punctures marked by the orbit  $\alpha_1$ ,
- a subset  $Y \subset \mathbf{E}(\mathcal{S}_1)$  of punctures marked by the orbit  $\alpha_2$ ,
- a one-to-one correspondence  $\phi: X \rightarrow Y$
- an injection  $\psi: \mathbf{E}(\mathcal{S}_2) \rightarrow \mathbf{E}(\mathcal{S}_1)$

with the following properties:

- $\mathbf{E}(\mathcal{S}_1)$  is a disjoint union of  $\psi(\mathbf{E}(\mathcal{S}_2))$ ,  $X$ , and  $Y$ .
- For each  $q \in \mathbf{E}(\mathcal{S}_2)$  is marked with a Reeb orbit or chord in  $\mathcal{H}^\wedge$ , the corresponding puncture  $\psi(q) \in \mathbf{E}(\mathcal{S}_1)$  is marked with the Reeb orbit or chord in  $\mathcal{H}^\vee$  with the same name.
- For each  $q \in \mathbf{E}(\mathcal{S}_2)$ ,

$$(s \circ u_1(\psi(q)), t \circ u_1(\psi(q))) = (s \circ u_2(q), t \circ u_2(q)).$$

- For each  $p \in X$

$$(s \circ u_1(\phi(p)), t \circ u_1(\phi(p))) = (s \circ u_2(p), t \circ u_2(p)).$$

If  $B_1$  and  $B_2$  induce  $B \in \mathcal{D}(\mathbf{x}, \mathbf{y})$ , let  $\mathcal{SM}_{\mathfrak{h}}^B(\mathbf{x}_1, \mathbf{y}_1; \mathbf{x}_2, \mathbf{y}_2; \mathcal{S}_1, \mathcal{S}_2; \psi, \phi)$  denote the moduli space of matched pairs.

We have the following analogue of Lemmas 9.13 for special matched curves.

**Lemma 9.51.** *Suppose  $n = 1$ . Fix  $B_1 \in \mathcal{D}(\mathbf{x}_1, \mathbf{y}_1)$  and  $B_2 \in \mathcal{D}(\mathbf{x}_2, \mathbf{y}_2)$  so that  $\omega_i(B_1) = \omega_i(B_2)$  for  $i = 1, \dots, 2n$ , and at least one of  $n_w(B_1)$  or  $n_z(B_1)$  vanishes, and so that  $\text{ind}(B_1 \natural B_2) \leq 2$ . Then, curves in the Gromov compactification of  $\mathcal{SM}_\natural^B(\mathbf{x}_1, \mathbf{y}_1; \mathbf{x}_2, \mathbf{y}_2)$  contain no closed components or boundary degenerations.*

**Proof.** For a closed component to form, at least two pairs of matched orbits must come together (i.e. it could either be that two punctures in  $X$  along with their two corresponding punctures in  $Y$ ; or punctures  $q_1$  and  $q_2$  in  $\mathcal{S}_2$  along with their matching punctures  $p_1$  and  $p_2$  in  $\mathcal{S}_1$ ). In any case, this occurs in codimension 2, and is therefore excluded from the index computation.

Let  $(\bar{u}_1, \bar{u}_2)$  denote a Gromov limit. Suppose that  $\bar{u}_2$  contains a boundary degeneration. It follows that there are two punctures in  $\mathcal{S}_2$  marked by Reeb orbits that cover both boundary components, and which project to  $(1, \tau)$ . There must be two matching punctures in  $\mathcal{S}_1$ , which project to the same point  $(1, \tau)$ . It follows that  $\mathcal{S}_1$  contains either a closed component projecting to  $(1, \tau)$ , or two boundary degenerations (covering  $\check{Z}_1$  and  $\check{Z}_2$ ). In either case, it follows that  $n_w(B_1) > 0$  and  $n_z(B_1) > 0$ , violating our hypothesis.

Similarly, if  $\bar{u}_1$  contains a boundary degeneration, then it follows that  $\bar{u}_2$  must also contain a closed component or a boundary degeneration, contradicting the above.  $\square$

We can form an endomorphism of  $C$ , obtained by counting index one special matched curves. We denote this by  $(C, \partial^{(0)})$ . In view of the above compactness result,  $\partial^{(0)}$  is a differential. (Compare Proposition 9.21.)

**Theorem 9.52.** *When  $n = 1$ , suitable choices of almost-complex structures  $J$  used to define  $C_{\mathcal{R}}(K)$ , there is an isomorphism (of chain complexes)  $C_{\mathcal{R}}(K) \cong (C, \partial^{(0)})$ .*

**Proof.** Using the neck stretching from Theorem 9.22, we find limiting objects which are now matched stories. Those stories contain closed components on the  $\mathcal{H}^\wedge$ -side. Removing each such closed component, we arrive at a corresponding special matched curve. Conversely, given a special matched curve, at each puncture  $p \in X$ , and matching puncture  $\phi(p) \in Y$ , we attach a sphere that covers  $\mathcal{H}^\wedge$ . Gluing that sphere gives the stated identification.

To justify this, we need to observe that the count of curves after gluing spheres at each  $\{p, \phi(p)\}$  puncture (with  $p \in X$ ) agrees with the original count of special marked curves. It suffices to verify this in a special case; see Figure 40.

We have exhibited a region in a Heegaard diagram. It is known that for any almost-complex structure, the displayed shadow from  $\{x_1, x_2\}$  to  $\{y_1, y_2\}$  has an odd number of representatives. View the annular region as an upper diagram. The moduli space from the lower diagram now consists of a bigon from  $x_1$  to  $y_1$  superimposed on a bigon from  $x_2$  to itself. The first moduli space is one-dimensional, with a free  $\mathbb{R}$  action, and an orbit  $o_1$  in the interior. The second moduli space is two-dimensional, parameterized by a cut and an  $\mathbb{R}$  action, with an orbit  $o_2$  in its interior. We can scale the  $\mathbb{R}$  action and the cut parameter so that

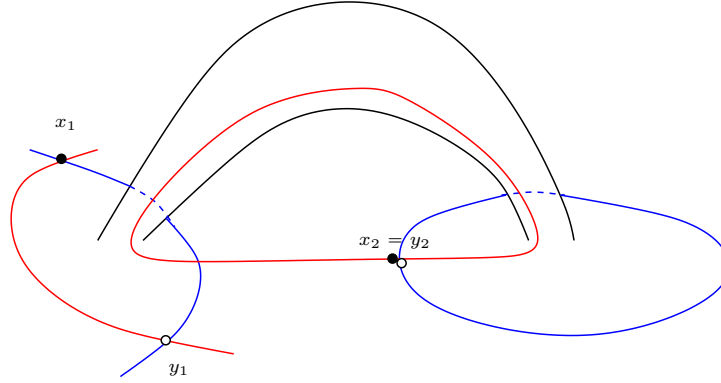


FIGURE 40. Local contributions of spheres.

$o_1$  and  $o_2$  occur at the same  $(s, t)$  coordinate; gluing in the sphere gives rise to the needed differential.  $\square$

**Remark 9.53.** *The gluing of closed components is very similar to the stabilization invariance proof in Heegaard Floer homology [20, Section 10]. The key difference is that here we are gluing spheres with two punctures, rather than the one puncture considered there.*

9.8.2. *Comparison with self-matched curves.* The intermediate complexes considered when  $n = 1$  have a slightly different form. For  $(C, \partial^{(1)})$ , we count points in moduli spaces satisfying the matching conditions for special matched curves, except now punctures on the  $\mathcal{H}^\wedge$ -side marked by  $o_1$  are matched with punctures on the  $\mathcal{H}^\vee$ -side, marked by the corresponding length one Reeb chord. Similarly, in  $(C, \partial^{(2)})$ , all orbits on the  $\mathcal{H}^\wedge$ -side are matched with the corresponding length one Reeb chord; while orbits on the  $\mathcal{H}^\vee$  side are matched with long chords on the  $\mathcal{H}^\wedge$  side.

We have the following analogue of Proposition 9.44:

**Proposition 9.54.** *There is an isomorphism of chain complexes over  $\mathcal{R}$*

$$\Phi: (C, \partial^{(0)}) \rightarrow (C, \partial^{(2)})$$

**Proof.** We construct first an isomorphism  $\Phi_0: (C, \partial^{(0)}) \rightarrow (C, \partial^{(1)})$  as in the proof of Proposition 9.44. Specifically, we modify the definition of 0-morphism matched curves as in Definition 9.45, which comes equipped with a special time  $t_0$  with the following properties:

- Each puncture in  $\mathcal{S}_2$  marked by  $o_2$  is matched with a length one chord in  $\mathcal{S}_1$  that covers the corresponding boundary component, with the same  $t$ -projection.
- Each puncture in  $\mathcal{S}_2$  marked with the orbit  $o_1$  and which projects to  $t > t_0$  is matched with an orbit on  $\mathcal{S}_1$  with the same  $(s, t)$  projection.
- Each puncture in  $\mathcal{S}_2$  marked with the orbit  $o_1$  and which projects to  $t < t_0$  is matched with a chord on  $\mathcal{S}_1$  marked with the corresponding length one chord, with the same  $t$ -projection.

- The punctures  $\{q_i\}_{i=1}^m$  in  $\mathcal{S}_2$  that project to  $t = t_0$  are all marked by  $o_1$  have corresponding punctures  $\{\psi(q_i)\}_{i=1}^m$  in  $\mathcal{S}_1$  that project to  $t = t_0$ . For all  $i = 1, \dots, m$   $s \circ u_2(q_i) < s \circ u_1(\psi(q_i))$ ; and moreover for  $i = 1, \dots, m-1$ , and  $s \circ u_1(\psi(q_i)) < s \circ u_2(q_{i+1})$ .
- The remaining punctures on  $\mathcal{S}_1$  marked with  $o_1$  are paired off with punctures on  $\mathcal{S}_1$  marked with  $o_2$ , with the same  $(s, t)$  projection.

Define a map  $h_0: C \rightarrow C$  counting rigid such objects, as in the proof of Lemma 9.47.

We adapt the proof of Lemma 9.47, to show that

$$\partial^{(1)} \circ h_0 + h_0 \circ \partial^{(0)} = \partial^{(0)} + \partial^{(1)}.$$

In this adaptation, we consider once again ends of one-dimensional moduli spaces. Some of the ends considered in that proof cannot occur: ends of Type (b-1) can occur. Ends of Type (b-2) are excluded: the argument of Lemma 9.51 would show that if a boundary degeneration occurs in  $\mathcal{H}^\wedge$ , then in fact the homology class on  $\mathcal{H}^\vee$  has  $n_w > 0$  and  $n_z > 0$ . Ends of Types (b-3), (b-4), and (b-5) can occur; but ends of Type (b-6) are replaced by ends where there are two matching punctures on  $\mathcal{S}_1$ ,  $q$  and  $\phi(q)$ , labelled by  $o_1$  and  $o_2$ , which project to the same  $(s, t)$  coordinate. These latter ends cancel in pairs (where the double puncture comes from  $t > t_0$  or  $t < t_0$ . The remaining ends cancel in pairs as in the proof of Lemma 9.47. (Note also that there are no join curve ends to the moduli spaces, since the boundary Reeb chords appearing in join curves do not exist for  $n = 1$  diagrams.)

The isomorphism  $\Phi_0$  is now given by  $\text{Id} + h_0$ .

A similar isomorphism is constructed  $\Phi_1: (C, \partial^{(1)}) \rightarrow (C, \partial^{(2)})$  is constructed analogously.  $\square$

We wish to compare  $(C, \partial^{(2)})$  with the chain complex  $(C, \partial^\#)$  defined by counting self-matched curves (Definition 9.23). (Note that for  $\partial^{(2)}$ , we allow punctures in  $\mathcal{S}_1$  marked by  $o_2$  to project to the same  $(s, t)$ -coordinate as some puncture marked by  $o_1$ ; while punctures in  $\mathcal{S}_2$  marked by  $o_i$  project to the same  $t$ -coordinate as some boundary puncture on  $\mathcal{S}_1$  marked by a corresponding length 1 Reeb chord.) An isomorphism between the two complexes is constructed as follows:

**Proposition 9.55.** *When  $n = 1$ , there is an isomorphism of complexes over  $\mathcal{R}$*

$$(C, \partial^{(0)}) \cong (C, \partial^{(2)}).$$

**Proof.** As in the proof of Proposition 9.44, we construct an isomorphism

$$\Phi: (C, \partial^{(2)}) \rightarrow (C, \partial^\#),$$

by counting certain curves.

The curves we count in this morphism are equipped with a distinguished  $t$ -value  $t_0$ , with the following properties:

- All punctures on  $\mathcal{S}_2$  labelled with some orbit are paired off with punctures in  $\mathcal{S}_1$  labelled with the matching length one Reeb chord.
- The punctures  $\{q_i\}_{i=0}^{2m-1}$  on  $\mathcal{S}_1$  with  $t(q_i) = t_0$  have the following properties:
  - $q_i$  is marked by the orbit  $o_j$  for  $j = 1, 2$  where  $i \equiv j \pmod{2}$

- $s(u_1(q_i))$  is a monotone increasing function of  $i = 0, \dots, 2m - 1$ .
- The remaining punctures  $q$  on  $\mathcal{S}_1$  labelled with the orbit  $o_2$  are paired off with punctures  $\phi(q)$  in  $\mathcal{S}_1$ :
- if  $t(q) > t_0$ , then  $\phi(q)$  is labelled with  $o_1$ , and  $q$  and  $\phi(q)$  have the same  $(s, t)$  projection.
- if  $t(q) < t_0$ , then  $\phi(q)$  is labelled with the length one chord covering  $\check{Z}_1$ ; and  $t(u(\phi(q))) = t(u(q))$ .

Counting such curves induces a map  $h: (C, \partial^{(2)}) \rightarrow (C, \partial^\#)$ . We claim that

$$\partial^\# \circ h + h \circ \partial^{(2)} = \partial^{(2)} + \partial^\#.$$

This is obtained by looking at ends of one-dimensional moduli spaces of the above kind. The following kinds of ends can occur

- (b'-1)  $s(u_1(q_{2m-1})) \mapsto 1$ , so that in the Gromov limit, we get  $((u_1, v_1), u_2)$ , where  $v_1$  is an orbit curve (with orbit  $o_1$ ) attached at the level  $t_0$ .
- (b'-2) Ends where  $s(u_2(\psi(q_0))) \mapsto 0$ ; in this case, there is a Gromov limit to  $((w_1, u_1), u_2)$ , where  $w_1$  is a simple boundary degeneration containing  $o_2$  and  $w$ .
- (b'-3) Pairs  $(u_1, u_2)$  with  $s(u_1(q_i)) = s(u_2(\psi(q_i)))$  or  $s(u_2(\psi(q_i))) = s(u_1(q_{i+1}))$ .
- (b'-4) there is some  $q \in \mathbf{E}(\mathcal{S}_2)$  labelled by an orbit with  $t(u_2(q)) = t_0$ , but  $q$  arises as a limit point of punctures with  $t(u_2(q)) < t_0$ .
- (b'-5) there is some  $q \in \mathbf{E}(\mathcal{S}_2)$  labelled by an orbit with  $t(u_2(q)) = t_0$ , but  $q$  arises as a limit point of punctures with  $t(u_2(q)) > t_0$ .
- (b'-6) Ends where  $s(u_2(\psi(q))) \mapsto 0$  and  $t(u_1(q)) > t_0$ ; in this case, there is a Gromov limit to  $((u_1, v_1), u_2)$ , where  $v_1$  is an orbit curve.
- (b'-7) Ends where  $s(u_2(\psi(q))) \mapsto 1$  and  $t(u_1(q)) > t_0$ ; in this case, there is a Gromov limit to  $((w_1, u_1), v_2)$ , where  $w_1$  is a simple boundary degeneration.

Consider ends of Type (b'-6). When  $w_1$  contains  $o_1$ , it also contains  $z$ . These cases do not count algebraically, since we have specialized to  $UV = 0$ . Thus, ends of Type (b'-6) count when  $w_1$  contains  $o_2$  and  $w$ ; and these cancel against ends of Type (b'-7).

Ends of type (b'-1) drop out in pairs, or cancel with ends of Type (b'-5), when the latter orbit is labelled  $o_2$ . Ends of Type (b'-2) drop out with orbits of Type (b'-5), when the latter orbit is labelled  $o_1$ . Ends of Type (b'-3) cancel with ends of Type (b'-4) (noting that the latter punctures come in pairs). See Figure 41 for an illustration.  $\square$

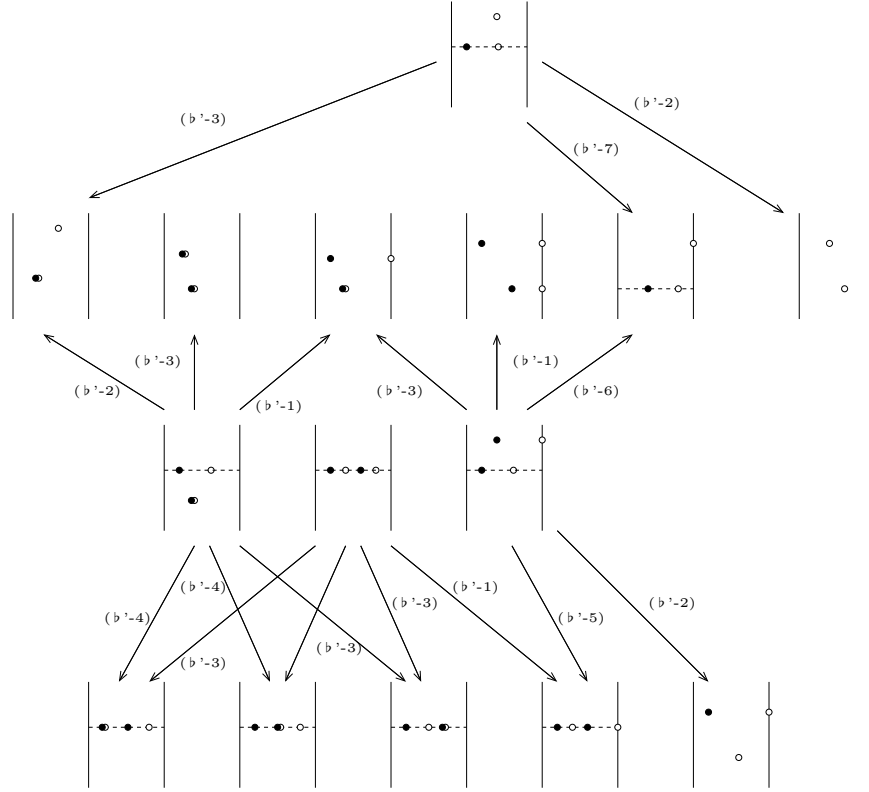


FIGURE 41. **Cancellation of ends in the moduli spaces in the construction of  $h: (C, \partial^{(2)}) \rightarrow (C, \partial^\#)$ .** The drawings are shorthand: we have illustrated the projections of punctures in  $\mathcal{S}_1$  to the strip, coloring the ones labelled by  $o_1$  white and those labelled by  $o_2$  black. There are four moduli spaces, with arrows coming out of them; and their ends are at the ends of the arrows. Ends with two incoming arrows cancel, and ends with only one incoming arrow are the terms in  $\partial_\#$  and  $\partial^{(2)}$ .



## 10. BIMODULES

In this section, we describe how to associate a type DA bimodule to a middle Heegaard diagram (cf. Definition 2.8), together with a matching on the incoming boundary components. Loosely speaking, the incoming boundary is treated as type  $A$ , and the outgoing as type  $D$ . (See [9] for the corresponding construction in bordered Floer homology.)

In more detail, fix a middle diagram

$$\mathcal{H}^{\parallel} = (\Sigma_0, (\check{Z}_1, \dots, \check{Z}_{2m}), (\hat{Z}_1, \dots, \hat{Z}_{2n}), \{\check{\alpha}_1, \dots, \check{\alpha}_{2m-1}\}, \{\hat{\alpha}_1, \dots, \hat{\alpha}_{2n-1}\}, \{\alpha_1^c, \dots, \alpha_g^c\}, \{\beta_1, \dots, \beta_{g+m+n-1}\}),$$

and let  $\check{M}$  be a matching on  $\{1, \dots, 2m\}$ , thought of as indexing the components of  $\check{Z}$ . The Heegaard diagram induces a matching  $M^{\parallel}$  on all the boundary components of  $\Sigma_0$ .<sup><</sup>

Together,  $\check{M}$  and  $M^{\parallel}$  given an equivalence relation on the components of  $\partial\Sigma$ .

**Definition 10.1.** *We say that  $\check{M}$  is compatible with  $\mathcal{H}^{\parallel}$  if every equivalence class has some component of  $\check{Z}$  in it.*

Form  $W^{\parallel} = W(\mathcal{H}^{\parallel})$  as in Definition 2.4, and  $\check{W} = W(\check{M})$ . The compatibility condition is equivalent to the condition that the one-manifold  $W = W^{\parallel} \cup \check{W}$  has no closed components.

**Definition 10.2.** *Let  $\mathcal{H}^{\parallel}$  be a middle diagram, equipped with a matching  $\check{M}$  on the incoming boundary components. The full incoming algebra  ${}^*\check{\mathcal{C}}(\mathcal{H}^{\parallel})$  and full outgoing algebra  ${}^*\hat{\mathcal{C}}(\mathcal{H}^{\parallel})$  are defined by*

$$\check{\mathcal{C}}(\mathcal{H}^{\parallel}) = \bigoplus_{k=0}^{2m-1} \mathcal{C}(2m, k); \quad \hat{\mathcal{C}}(\mathcal{H}^{\parallel}) = \bigoplus_{k=0}^{2n-1} \mathcal{C}(2n, k).$$

*We will be primarily interested in the  $k = n$ , summands, which we call the incoming algebra and the outgoing algebra respectively:*

$$\check{\mathcal{C}}(\mathcal{H}^{\parallel}) = \mathcal{C}(2m, m); \quad \hat{\mathcal{C}}(\mathcal{H}^{\parallel}) = \mathcal{C}(2n, n).$$

Each middle Heegaard state  $\mathbf{x}$  determines two subsets

$$\check{\alpha}(\mathbf{x}) \subset \{1, \dots, 2m\} \quad \text{resp.} \quad \hat{\alpha}(\mathbf{x}) \subset \{1, \dots, 2n\}$$

consisting of those  $i \in \{1, \dots, 2m\}$  resp.  $\{1, \dots, 2n\}$  with  $\mathbf{x} \cap \check{\alpha}_i \neq \emptyset$  resp  $\mathbf{x} \cap \hat{\alpha}_i \neq \emptyset$ . Each middle Heegaard state  $\mathbf{x}$  has an *idempotent type*  $k = |\check{\alpha}(\mathbf{x})|$ .

Let  ${}^*RQ(\mathcal{H}^{\parallel})$  be the  $\mathbb{F}$ -vector space spanned by the middle Heegaard states of  $\mathcal{H}^{\parallel}$ . Let

$$\check{I}(\mathbf{x}) = \mathbf{I}_{\check{\alpha}(\mathbf{x})} \quad \text{and} \quad \hat{I}(\mathbf{x}) = \mathbf{I}_{\{1, \dots, 2n-1\} \setminus \hat{\alpha}(\mathbf{x})}.$$

An  $I(2n, k - m + n) - I(2m, k)$ -bimodule structure is specified by

$$\hat{I}(\mathbf{x}) \cdot \mathbf{x} \cdot \check{I}(\mathbf{x}) = \mathbf{x}.$$

There is a splitting

$${}^*RQ(\mathcal{H}^{\parallel}) = \bigoplus_{k \in \mathbb{Z}} I(2n, k - m + n) RQ(\mathcal{H}^{\parallel})_{I(2m, k)},$$

where  $k$  is the idempotent type of  $\mathbf{x}$ . We will be primarily interested in the summand where  $k = m$ ,

$$I(2n,n)RQ(\mathcal{H}^\parallel)_{I(2m,m)}.$$

Our goal here is to endow  $RQ(\mathcal{H}^\parallel)$  with the structure of a type  $DA$  bimodule structure  $RQ(\mathcal{H}^\parallel, \widetilde{M}) = {}^{\hat{C}}RQ(\mathcal{H}^\parallel)_{\check{C}}$ , where  $\check{C} = \check{C}(\mathcal{H}^\parallel)$  and  $\hat{C} = \hat{C}(\mathcal{H}^\parallel)$ .

To equip  $RQ(\mathcal{H}^\parallel)$  with the structure of a  $DA$  bimodule, we choose further an orientation  $\vec{W}$  on  $W = W^\parallel \cup \widetilde{W}$ . Each boundary component  $\check{Z}_i$  or  $\hat{Z}_j$  of  $\mathcal{H}^\parallel$  corresponds to some point on  $W$ .

This data specifies an orbit marking, in the following sense:

**Definition 10.3.** *A special orbit in  $\mathcal{H}^\parallel$  covers an orbit in  $\check{Z}_i$  that is matched with  $\hat{Z}_j$ . An orbit marking in a middle diagram  $\mathcal{H}^\parallel$  is a partition of the simple orbits of  $\check{Z}$  so that:*

- $\widetilde{M}$  matches even with odd orbits,
- if components of  $\check{Z}$  are matched by  $M^\parallel$ , then one one is even and the other is odd.

Let  $\check{\Omega}^+ \subset \{1, \dots, 2m\}$  denote the even boundary components of  $\check{Z}$ ; and  $\check{\Omega}^- \subset \{1, \dots, 2m\}$  denote the odd ones.

An orientation on  $W$  is equivalent to an orbit marking: each segment of  $W$  in  $W^\parallel$  is oriented from even to odd, and each segment in  $\widetilde{W}$  is oriented from odd to even.

The orientation on  $W$  also induces a pair of functions

$$\sigma: \{1, \dots, 2m\} \rightarrow \{1, \dots, 2n\}, \quad \tau: \{1, \dots, 2m\} \rightarrow \{1, \dots, 2n\},$$

the *starting* and *terminal* points respectively. Namely,  $\sigma(p) = i$  and  $\tau(p) = j$  if  $\check{Z}_p$  is contained on the oriented interval in  $W$  starting at  $\hat{Z}_i$ , and  $\tau(p) = j$  if  $\check{Z}_p$  is contained on the oriented interval terminating in  $\hat{Z}_j$ .

See Figure 42 for an example.

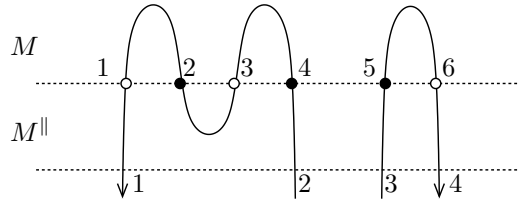


FIGURE 42. **Orbit markings in a middle diagram.** The even orbits (1,3,6) are colored white and the odd ones (2,4,5) are colored black. Moreover,  $\sigma(1) = \sigma(2) = \sigma(3) = \sigma(4) = 2$ ;  $\tau(1) = \tau(2) = \tau(3) = \tau(4) = 1$ ;  $\sigma(5) = \sigma(6) = 3$ ;  $\tau(5) = \tau(6) = 4$ .

The  $DA$  bimodule  $RQ(\mathcal{H}^\parallel)$  depends on the incoming matching, but we typically suppress data from the notation; in fact, even the curvature element in the incoming algebra  $\check{C}$  depends on this choice. The bimodule also depends on an orientation of  $W$ , which we also suppress.

**10.1. Type  $DA$  bimodules.** We adapt the definitions from Section 8.1 in the following straightforward manner. Suppose that  $\boldsymbol{\rho}$  is a set of Reeb chords for  $\mathcal{H}^\parallel$  that is algebraic in the sense of Definition 8.2, and that is supported entirely on  $\check{Z}$ . For each  $\rho \in \boldsymbol{\rho}$ ,  $\alpha(\rho^+)$  resp.  $\alpha(\rho^-)$  be the curve  $\check{\alpha}_i$  with  $\rho^+ \in \check{\alpha}_i$  resp.  $\rho^- \in \check{\alpha}_i$ . Let

$$I^-(\boldsymbol{\rho}) = \sum_{\{\mathbf{s} \mid \{\check{\alpha}(\rho_1^-), \dots, \check{\alpha}(\rho_j^-)\} \subset \{\check{\alpha}_i\}_{i \in \mathbf{s}}\}} I_{\mathbf{s}} \quad \text{and} \quad I^+(\boldsymbol{\rho}) = \sum_{\{\mathbf{s} \mid \{\check{\alpha}(\rho_1^+), \dots, \check{\alpha}(\rho_j^+)\} \subset \{\check{\alpha}_i\}_{i \in \mathbf{s}}\}} I_{\mathbf{s}}$$

Then,  $\check{b}_0(\boldsymbol{\rho})$  be the algebra element  $a_0 \in \mathcal{B}_0(2m, m)$  with  $a = I^- \cdot a \cdot I^+$  and whose weight  $w_i(a)$  is the average local multiplicity at  $\check{Z}_i$  for  $i = 1, \dots, 2m$ . Let  $\check{b}(\boldsymbol{\rho})$  be the image of  $\check{b}_0(\boldsymbol{\rho})$  in  $\check{C}$ .

The definition of constraint packets has the following immediate generalization to middle diagrams:

**Definition 10.4.** Fix a Heegaard state  $\mathbf{x}$  and a sequence  $\vec{a} = (a_1, \dots, a_\ell)$  of pure algebra elements of  $\check{C}(\mathcal{H}^\parallel)$ . A sequence of constraint packets  $\boldsymbol{\rho}_1, \dots, \boldsymbol{\rho}_k$  is called  $(\mathbf{x}, \vec{a})$ -compatible if there is a sequence  $1 \leq k_1 < \dots < k_\ell \leq k$  so that the following conditions hold:

- the constraint packets  $\boldsymbol{\rho}_{k_i}$  consist of chords in  $\check{Z}$ , and they are algebraic, in the sense of Definition 8.2,
- $\check{I}(\mathbf{x}) \cdot \check{b}(\boldsymbol{\rho}_{k_1}) \otimes \dots \otimes \check{b}(\boldsymbol{\rho}_{k_\ell}) = \mathbf{I}(\mathbf{x}) \cdot a_1 \otimes \dots \otimes a_\ell$ , as elements of  $RQ(\mathcal{H}^\vee) \otimes \check{C}^{\otimes \ell}$
- for each  $t \notin \{k_1, \dots, k_\ell\}$ , the constraint packet  $\boldsymbol{\rho}_t$  is one of the following types:
  - ( $DA\rho$ -1) it consists of the orbit  $\{o_i\}$ , where  $o_i$  is odd for the  $\vec{W}$ -induced orbit marking.
  - ( $DA\rho$ -2) it is of the form  $\{o_i, v_j\}$ , where  $o_i$  is even  $\{i, j\} \in M$ , and  $v_j$  is one of the two Reeb chords that covers  $\check{Z}_j$  with multiplicity one.
  - ( $DA\rho$ -3) it is of the form  $\{o_k\}$ , where  $o_k$  is the simple Reeb orbit around some component in  $\hat{Z}$
  - ( $DA\rho$ -4) it is of the form  $\{\rho_j\}$ , where  $\rho_j$  is a Reeb chord of length  $1/2$  supported in some  $\hat{Z}$ .

Let  $\llbracket \mathbf{x}, a_1, \dots, a_\ell \rrbracket$  be the set of all sequences of constraint packets  $\boldsymbol{\rho}_1, \dots, \boldsymbol{\rho}_k$  that are  $(\mathbf{x}, \vec{a})$ -compatible.

Given  $(\boldsymbol{\rho}_1, \dots, \boldsymbol{\rho}_k) \in \llbracket \mathbf{x}, a_1, \dots, a_\ell \rrbracket$ , we can consider  $\pi_2(\mathbf{x}, \boldsymbol{\rho}_1, \dots, \boldsymbol{\rho}_k, \mathbf{y})$ , the space of homology classes of maps with asymptotics at  $\check{Z}$  specified by the given Reeb chords.

We define the index  $\text{ind}(B, \mathbf{x}, \mathbf{y}; \vec{\rho})$  exactly as in the case of type A modules (Definition 7.9):

$$\begin{aligned} \text{ind}(B, \mathbf{x}, \mathbf{y}; \vec{\rho}) &= e(B) + n_{\mathbf{x}}(B) + n_{\mathbf{y}}(B) + \ell \\ &\quad - \mathbf{w}(\vec{\rho}) + \iota(\text{cho}(\vec{\rho})) + \sum_{o \in o(\vec{\rho})} (1 - \mathbf{w}(o)), \end{aligned}$$

**Lemma 10.5.** Given  $B \in \mathcal{D}(\mathbf{x}, \mathbf{y})$ , the quantity

$$\mathbf{m}(B) = e(B) + n_{\mathbf{x}}(B) + n_{\mathbf{y}}(B) - \mathbf{w}_{\partial}(B)$$

is independent of  $B$  (depending only on  $\mathbf{x}$  and  $\mathbf{y}$ ). Also, if  $\{j, k\} \in M^\parallel$ , oriented in  $W^\parallel$  from  $k$  to  $j$ , then the integer

$$\mathbf{A}_{\{j,k\}} = \mathbf{w}_j(B) - \mathbf{w}_k(B),$$

is independent of the choice of  $B$  (depending only on  $\mathbf{x}$  and  $\mathbf{y}$ ).

**Proof.** Clearly,  $\{j, k\} \in M^\parallel$  if and only if  $i$  and  $j$  are contained in the same component  $\mathcal{B}_{\{j,k\}}$  of

$$\Sigma_0 \setminus (\beta_1 \cup \cdots \cup \beta_{g+m+n-1}).$$

Now,

$$\pi_2(\mathbf{x}, \mathbf{y}) \cong \bigoplus_{\{j,k\}} \mathbb{Z} \cdot \mathcal{B}_{\{j,k\}}.$$

The lemma follows from the following:

$$\begin{aligned} e(\mathcal{B}_{\{j,k\}}) + n_{\mathbf{x}}(\mathcal{B}_{\{j,k\}}) + n_{\mathbf{y}}(\mathcal{B}_{\{j,k\}}) &= 2 \\ \mathbf{w}_j(\mathcal{B}_{\{j,k\}}) &= \mathbf{w}_k(\mathcal{B}_{\{j,k\}}) = 1. \end{aligned}$$

□

We can think of  $\mathbf{A}(B)$  as defining an element  $\mathbb{A}(B) \in H^1(W^\parallel, \partial W^\parallel) \cong \mathbb{Z}^{m+n}$ , the *Alexander grading*. Now, the Alexander grading, with values in  $H^1(W^\parallel, \partial W^\parallel)$ ; and the  $\delta$ -grading  $\mathbf{gr}$ , with values in  $\mathbb{Q}$ , are determined up to overall constants by

$$\begin{aligned} \mathbf{A}(\mathbf{x}) - \mathbf{A}(\mathbf{y}) &= \mathbf{A}(B) \\ \mathbf{gr}(\mathbf{x}) - \mathbf{gr}(\mathbf{y}) &= e(B) + n_{\mathbf{x}}(B) + n_{\mathbf{y}}(B) - \mathbf{w}_\partial(B) \end{aligned}$$

Given  $B \in \pi_2(\mathbf{x}, \boldsymbol{\rho}_1, \dots, \boldsymbol{\rho}_h, \mathbf{y})$ , let  $\hat{b}_0(B) = a \in \mathcal{B}_0(2n, n)$  be the algebra element with  $\hat{\mathbf{I}}(\mathbf{x}) \cdot a = a$  and whose weight at  $i \in \{1, \dots, 2n\}$  agrees with the local multiplicity of  $B$  at  $\hat{Z}_i$ . Let  $\hat{b}(B)$  denote the image of  $\hat{b}_0(B)$  in  $\hat{C}$ . Given, an  $(\mathbf{x}, \vec{a})$ -compatible sequence of constraint packets  $\boldsymbol{\rho}_1, \dots, \boldsymbol{\rho}_h$ , we define a corresponding monomial in the variables  $U_1, \dots, U_{2n}$ , denoted  $\gamma(\boldsymbol{\rho}_1, \dots, \boldsymbol{\rho}_h)$ , to be product over all packets of Type  $(DA\boldsymbol{\rho}-1)$  of the element  $U_{\tau(i)}$ . Let

$$(10.1) \quad \hat{b}(B, \boldsymbol{\rho}_1, \dots, \boldsymbol{\rho}_h) = \gamma(\boldsymbol{\rho}_1, \dots, \boldsymbol{\rho}_h) \cdot \hat{b}(B).$$

Let  $\mathcal{M}(\mathbf{x}, \mathbf{y}, \boldsymbol{\rho}_1, \dots, \boldsymbol{\rho}_h)$  denote the moduli space of flowlines as in Definition 5.4, with the understanding that now the asymptotics at  $\pm\infty$  go to middle Heegaard states  $\mathbf{x}$  and  $\mathbf{y}$ . Note also that for middle diagrams, the number of  $\beta$ -curves is given by  $d = g + m + n - 1$ .

Define

$$(10.2) \quad \begin{aligned} &\delta_{\ell+1}^1(\mathbf{x}, a_1, \dots, a_\ell) \\ &= \sum_{\substack{\mathbf{y} \in \mathfrak{S} \\ (\boldsymbol{\rho}_1, \dots, \boldsymbol{\rho}_k) \in \llbracket \mathbf{x}, a_1, \dots, a_\ell \rrbracket \\ B \in \pi_2(\mathbf{x}, \boldsymbol{\rho}_1, \dots, \boldsymbol{\rho}_h, \mathbf{y})}} \# \hat{\mathcal{M}}(\mathbf{x}, \mathbf{y}, \boldsymbol{\rho}_1, \dots, \boldsymbol{\rho}_h) \cdot \hat{b}(B, \boldsymbol{\rho}_1, \dots, \boldsymbol{\rho}_h) \otimes \mathbf{y}. \end{aligned}$$

Lemma 8.10 has the following straightforward adaptation:

**Lemma 10.6.** *Fix  $\mathbf{x}, \mathbf{y} \in \mathfrak{S}$ , a sequence of pure algebra elements  $\vec{a} = (a_1, \dots, a_\ell)$ , an  $(\mathbf{x}, \vec{a})$ -compatible sequence of constraint packets  $\rho_1, \dots, \rho_h$ , and  $B \in \mathcal{D}(\mathbf{x}, \mathbf{y})$ . If there is a pre-flowline  $u$  whose shadow is  $B$  and whose packet sequence is  $(\rho_1, \dots, \rho_\ell)$ , then*

$$\mathbf{gr}(\mathbf{x}) + \ell - \sum_{i=1}^{\ell} \mathbf{w}(a_i) = \mathbf{gr}(\mathbf{y}) - \mathbf{w}_{\widehat{Z}}(\widehat{b}(B)) + \text{ind}(B, \mathbf{x}, \mathbf{y}, \rho_1, \dots, \rho_h).$$

**Proof.** We have that

$$\mathbf{gr}(\mathbf{x}) - \mathbf{gr}(\mathbf{y}) = e(B) + n_{\mathbf{x}}(B) + n_{\mathbf{y}}(B) - \mathbf{w}_{\partial}(B),$$

and

$$\text{ind}(B) = e(B) + n_{\mathbf{x}}(B) + n_{\mathbf{y}}(B) + h - \mathbf{w}_{\partial}(B) + \sum \iota(\text{cho}(\rho_i)).$$

Taking the difference, we find that

$$\mathbf{gr}(\mathbf{x}) - \mathbf{gr}(\mathbf{y}) - \text{ind}(B, \mathbf{x}, \mathbf{y}, \vec{\rho}) = -h - \sum \iota(\text{cho}(\rho_i)).$$

Now, if  $\rho_i$  is an algebraic packet, then  $\iota(\text{cho}(\rho_i)) = -\mathbf{w}(\rho_i)$ ; if it is of Type  $(DA\rho-1)$ ,  $\iota(\text{cho}(\rho_i)) = 0$ ; if it is of Type  $(DA\rho-2)$ ,  $\iota(\text{cho}(\rho_i)) = -1$ ; if it is of Type  $(DA\rho-3)$ , the contribution is 0; if it is of Type  $(DA\rho-4)$ , we get  $-1/2$ . It follows that

$$\begin{aligned} \mathbf{gr}(\mathbf{x}) - \mathbf{gr}(\mathbf{y}) - \text{ind}(B, \mathbf{x}, \mathbf{y}, \vec{\rho}) &= -\ell + \left( \sum_{i=1}^{\ell} \mathbf{w}_{\widehat{Z}}(a_i) \right) \\ &\quad - \#(\text{odd orbits coming in}) - \mathbf{w}_{\widehat{Z}}(B) \\ &= -\ell + \left( \sum_{i=1}^{\ell} \mathbf{w}_{\widehat{Z}}(a_i) \right) - \mathbf{w}(\widehat{b}(B, \vec{\rho}_i)). \end{aligned}$$

□

**Lemma 10.7.** *Given  $\mathbf{x}$  and a sequence of algebra elements  $(a_1, \dots, a_\ell)$ , there are only a finite number of non-negative homology classes  $B \in \pi_2(\mathbf{x}, \mathbf{y}, \vec{\rho})$  where  $\rho_1, \dots, \rho_h$  are  $(\mathbf{x}, \vec{a})$ -compatible and with  $\text{ind}(B, \mathbf{x}, \mathbf{y}, \vec{\rho}) = 1$ .*

**Proof.** According to Lemma 10.5,  $(\mathbf{x}, \vec{a})$ ,  $\mathbf{y}$ , and  $\text{ind}(B, \mathbf{x}, \mathbf{y}, \vec{\rho}) = 1$  determines the total weight of  $b$ . The lemma also shows that  $\{i, j\} \in M^{\parallel}$ , then  $\mathbf{w}_i(B) - \mathbf{w}_j(B)$  is independent of  $B$  (depending only on  $\mathbf{x}$  and  $\mathbf{y}$ ).

Suppose next that  $\{i, j\} \in \widetilde{M}$ , and  $i$  is an odd orbit, then if  $c_{i,j} = \mathbf{w}_i(a_1 \otimes \dots \otimes a_\ell) - \mathbf{w}_j(a_1 \otimes \dots \otimes a_\ell)$ , then clearly

$$c_{i,j} \leq \mathbf{w}_i(B) - \mathbf{w}_j(B) \leq c_{i,j} + \mathbf{w}_{\tau(i)}(b).$$

Finally, if  $i \in \widehat{Z}$  is  $W$ -initial, then  $\mathbf{w}_i(B) = \mathbf{w}_i(b)$ .

Since every in-coming boundary component is equivalent (using the equivalence relation generated by  $M^{\parallel}$  and  $\widetilde{M}$ ) to an  $W$ -initial out boundary component, we have universal upper bounds on the weights of  $B$  at all of its boundary points (which we also assumed to be non-negative). Since the map  $B \mapsto \bigoplus_i \mathbf{w}_i(B)$  gives an injection of  $\pi_2(\mathbf{x}, \mathbf{y})$  into  $\mathbb{Z}^{m+n}$ , the lemma follows. □

Theorem 7.18 has the following straightforward adaptation to middle diagrams.

**Remark 10.8.** We will need the following theorem in the case where the incoming sequence of packets are compatible with some sequence of algebra elements  $(a_1, \dots, a_\ell)$ . To underscore the similarity with Theorem 7.18, we have stated it under slightly weaker hypotheses. (Compare Definition 7.15.)

**Theorem 10.9.** Choose a middle diagram  $\mathcal{H}^\parallel$ , and fix a compatible matching  $M^\wedge$ . Choose also an orbit marking (Definition 10.3). Fix a lower Heegaard state  $\mathbf{x}$  and a sequence of constraint packets  $\vec{\rho}$  with the following properties:

- $(\mathbf{x}, \vec{\rho})$  is strongly boundary monotone.
- The chords appearing in each packet  $\rho_i$  are disjoint from one another
- Each packet contains at most one orbit, and that orbit is simple.
- If a packet contains an even (in-coming) orbit, then it contains exactly one other Reeb chord, as well; and that chord is disjoint from the orbit.
- If the packet contains an orbit which is not even, then it contains no other chord.

Let  $\mathbf{y}$  be a lower Heegaard state, and  $B \in \pi_2(\mathbf{x}, \mathbf{y})$ , whose local multiplicity vanishes somewhere. Choose  $\mathcal{S}$  and  $\vec{P}$  so that  $[\vec{P}] = (\rho_1, \dots, \rho_\ell)$  and so that the  $\chi(\mathcal{S}) = \chi_{\text{emb}}(B)$ ; and suppose that  $\text{ind}(B, \mathbf{x}, \mathbf{y}; \vec{\rho}) = 2$ , and abbreviate  $\widehat{M} = \widehat{M}^B(\mathbf{x}, \mathbf{y}; \mathcal{S}; \vec{P})$ . The total number of ends of  $\widehat{M}$  of the following types are even in number:

(DAE-1) Two-story ends, which are of the form

$$\widehat{M}(\mathbf{x}, \mathbf{w}; \mathcal{S}_1; \rho_1, \dots, \rho_i) \times \widehat{M}(\mathbf{w}, \mathbf{y}; \mathcal{S}_2; \rho_{i+1}, \dots, \rho_\ell),$$

taken over all lower Heegaard states  $\mathbf{w}$  and choices of  $\mathcal{S}_1$  and  $\mathcal{S}_2$  so that  $\mathcal{S}_1 \natural \mathcal{S}_2 = \mathcal{S}$ , and  $B_1 \natural B_2 = B$ .

(DAE-2) Orbit curve ends, of the form  $\widehat{M}^B(\mathbf{x}, \mathbf{y}, \mathcal{S}'; \rho_1, \dots, \rho_{i-1}, \sigma, \rho_{i+1}, \dots, \rho_\ell)$ , where  $\text{orb}(\sigma) = \text{orb}(\rho_i) \setminus \{o_r\}$ ,  $\text{cho}(\sigma) = \text{cho}(\rho_i) \cup \{v_r\}$  where  $v_r$  is a Reeb chord that covers the boundary component  $Z_r$  with multiplicity 1.

(DAE-3) Contained collision ends for two consecutive packets  $\rho_i$  and  $\rho_{i+1}$ , which correspond to points in  $\widehat{M}^{B'}(\mathbf{x}, \mathbf{y}, \mathcal{S}; \rho_1, \dots, \rho_{i-1}, \sigma, \rho_{i+2}, \dots, \rho_\ell)$  with the following properties:

- The collision is visible.
- The packets  $\rho_i$  and  $\rho_{i+1}$  are strongly composable.
- The packet  $\sigma$  is a contained collision of  $\rho_i$  and  $\rho_{i+1}$
- The chords in  $\sigma$  are disjoint from one another.

(DAE-4) Join ends, of the form  $\widehat{M}^B(\mathbf{x}, \mathbf{y}, \mathcal{S}'; \rho_1, \dots, \rho_{i-1}, \sigma, \rho_{i+1}, \dots, \rho_\ell)$ ,  $\text{orb}(\sigma) = \text{orb}(\rho_i)$ , and the following conditions hold:

- $(\mathbf{x}, \rho_1, \dots, \rho_{i-1}, \sigma, \rho_{i+1}, \dots, \rho_\ell)$  is strongly boundary monotone.
- There is some  $\rho \in \text{cho}(\rho_i)$  with the property that  $\rho = \rho_1 \uplus \rho_2$ , and  $\text{cho}(\sigma) = (\text{cho}(\rho_i) \setminus \{\rho\}) \cup \{\rho_1, \rho_2\}$ .
- In the above decomposition, at least one of  $\rho_1$  and  $\rho_2$  covers only half of a boundary component.

(DAE-5) Boundary degeneration collisions  $\sigma$  between two consecutive packets  $\rho_i$  and  $\rho_{i+1}$ ; when  $o_j \in \text{orb}(\rho_i)$ ,  $o_k \in \text{orb}(\rho_{i+1})$  and  $\{j, k\} \in M^\parallel$ . When  $\sigma = \rho_i \setminus \{o_j, o_k\}$  is non-empty, these correspond to points in

$$\widehat{M}^{B'}(\mathbf{x}, \mathbf{y}, \mathcal{S}'; \rho_1, \dots, \rho_{i-1}, \sigma, \rho_{i+1}, \dots, \rho_\ell)$$

in the chamber  $\mathcal{C}^{o_j < o_k}$ , where the homology class  $B'$  is obtained from  $B$  by removing a copy of  $\mathcal{B}_{\{j,k\}}$ . When  $\sigma = \emptyset$ , then  $\ell = 1$ ,  $\mathbf{x} = \mathbf{y}$ ,  $B' = 0$ , and the end is unique.

**Proof.** The proof is exactly as in the proof of Theorem 7.18. The key difference is that in a middle diagram, we do not treat special boundary degenerations separately. (Theorem 7.18 would have had a similar statement if we had treated the marked points  $w$  and  $z$  as orbits around the punctures.)  $\square$

**Proposition 10.10.** *Let  $\mathcal{H}^\parallel$  be a middle diagram that is compatible with a given matching  $M$  on its incoming boundary. Choose an orientation on  $W = W(\mathcal{H}^\parallel) \cup W(M)$ . The  $I(2n) - I(2m)$ -bimodule  $RQ(\mathcal{H}^\parallel)$ , equipped the operations*

$$\delta_{\ell+1}^1 : RQ(\mathcal{H}^\parallel) \otimes \check{\mathcal{C}}^{\otimes \ell} \rightarrow \hat{\mathcal{C}} \otimes RQ(\mathcal{H}^\parallel)$$

*defined above endows  $RQ(\mathcal{H}^\parallel)$  with the structure of a curved  $\mathcal{C}(n, \widehat{M}) - \mathcal{C}(m, M)$  DA bimodule (cf. Equations (3.4) and (3.5)), where  $\widehat{M}$  is the matching on  $\{1, \dots, 2n\}$  induced by  $M^\parallel$  and  $M$ .*

**Proof.** This is a combination of Propositions 6.3 and Proposition 8.12.

In more detail, look at ends of one-dimensional moduli spaces. Note that the moduli spaces that contribute to the outgoing algebra element cannot cover all of the outgoing boundary with positive weight, so we can restrict attention to homology classes  $B$  that do not cover all of  $\Sigma$ ; i.e. Theorem 10.9 applies.

Consider first the  $\mathcal{A}_\infty$  relation with no incoming algebra elements.

When  $\mathbf{x} \in \mathcal{C}^{o > o'}$ , there is a corresponding end of  $\mathcal{M}(\mathbf{x}, \mathbf{x}, \{o\}, \{o'\})$ . In turn, that moduli space contributes to  $\mu_2 \circ (\text{Id} \otimes \delta^1) \circ \delta^1$  only in two cases:

- when both  $o$  and  $o'$  are Reeb orbits on the out-going boundary, or
- one of the two is a Reeb orbit on the out-going boundary and the other is an odd orbit on the in-coming boundary.

Each equivalence class of orbits contains exactly one pair of orbits which can be paired in a simple boundary degeneration as above: the boundary degeneration is the unique simple boundary degeneration that contains the orbit corresponding to the endpoint of the given  $W$ -equivalence class. Explicitly, when the  $W$ -equivalence class contains no in-coming boundary components, then  $o$  and  $o'$  are the two (out-going) orbits in the equivalence class; otherwise, if  $o$  is outgoing and it is paired with an in-coming  $o'$ , then that  $o'$  must be the last odd orbit in the  $W$ -equivalence class (under the ordering induced by its orientation).

By switching the order of  $o$  and  $o'$  if needed (since  $\mathbf{x} \in \mathcal{C}^{o > o'}$  or  $\mathcal{C}^{o' > o}$ ), we can conclude each equivalence class of orbits contributes  $U_j U_k$ , where  $\widehat{Z}_j$  and  $\widehat{Z}_k$  are the two out-going boundary components in the equivalence class. Thus, these boundary degenerations to  $\mu_2 \circ (\text{Id} \otimes \delta^1) \circ \delta^1(\mathbf{x})$  gives a term of the form  $\mu_0^{\hat{\mathcal{C}}} \otimes \mathbf{x}$ .

As in the proof of Proposition 8.12, there are orbit curve ends which can be identified with  $\delta^1(\mathbf{x}, \mu_0^{\check{\mathcal{C}}})$ .

All other contributions cancel in pairs as in the proof of Proposition 8.12, verifying the weighted type  $DA$  structure equation with no algebra inputs, Equation (3.4). Note that we do have collision ends when packets on  $\check{Z}$  collide with packets on  $\hat{Z}$ ; but once again, these cancel with ends where the two packets are permuted.  $\square$

**10.2. Another pairing theorem.** Let  $\mathcal{H}^\wedge$  be an upper diagram and  $\mathcal{H}^\parallel$  be a middle diagram, so that  $\partial\mathcal{H}^\wedge$  is identified with  $\partial^\vee\mathcal{H}^\parallel$ . Then, we can form a new upper diagram  $\mathcal{H}^\parallel\#\mathcal{H}^\wedge$ . Evidently, there is a one-to-one correspondence between pairs of states  $\mathbf{x}$  and  $\mathbf{y}$ , where  $\mathbf{x}$  is an partial Heegaard state for  $\mathcal{H}^\parallel$  and  $\mathbf{y}$  is an upper Heegaard state for  $\mathcal{H}^\wedge$ , and  $\alpha(\mathbf{x}) = \{1, \dots, 2n\} \setminus \hat{\alpha}(\mathbf{y})$ .

We have the following analogue of the pairing theorem Theorem 9.1; compare also [9, Theorem 11]:

**Theorem 10.11.** *Let  $\mathcal{H}^\parallel$  and  $\mathcal{H}^\wedge$  be as above. Let  $C_1 = C(\mathcal{H}^\wedge) = \check{C}(\mathcal{H}^\parallel)$ ;  $C_2 = \hat{C}(\mathcal{H}^\parallel)$ . Under the above hypotheses, there is a quasi-isomorphism of curved type  $D$  structures*

$${}^{C_2}R(\mathcal{H}^\parallel\#\mathcal{H}^\wedge) \simeq {}^{C_2}RQ(\mathcal{H}^\parallel)_{C_1} \boxtimes^{C_1} R(\mathcal{H}^\wedge).$$

**10.3. Proof of the DA bimodule pairing theorem.** The proof of Theorem 10.11 is very similar to the proof of Theorem 9.1. The key algebraic difference is that in the present context, there is a curvature in the result; and analytically, the curvature is produced by boundary degenerations. We give the details presently.

Let  $\mathcal{H}_2^\wedge$  be an upper diagram with  $2m$  outgoing boundary components and  $\mathcal{H}^\parallel$  be a middle diagram with  $2m$  incoming boundary components and  $2n$  outgoing ones. Fix an identification between  $\hat{Z}(\mathcal{H}_1^\wedge)$  and  $\check{Z}(\mathcal{H}^\parallel)$ , and use this to form the upper  $\mathcal{H}^\wedge = \mathcal{H}^\parallel\#\mathcal{H}_2^\wedge$ .

Definition 9.2 has the following straightforward generalization:

**Definition 10.12.** *Let  $\mathcal{H}^\wedge = \mathcal{H}^\parallel\#\mathcal{H}_2^\wedge$ . States  $\mathbf{x}_1 \in \mathfrak{S}(\mathcal{H}^\parallel)$ ,  $\mathbf{x}_2 \in \mathfrak{S}(\mathcal{H}^\wedge)$  are called matching states if  $\check{\alpha}(\mathbf{x}_1)$  is the complement of  $\alpha(\mathbf{x}_2)$  (i.e.  $\check{\mathbf{I}}(\mathbf{x}_1) = \hat{\mathbf{I}}(\mathbf{x}_2)$ ).*

There is a one-to-one correspondence between pairs of matching states  $\mathbf{x}_1$  and  $\mathbf{x}_2$ , and upper states for  $\mathcal{H}^\wedge$ ; and hence there is a one-to-one correspondence between generators of  $RQ(\mathcal{H}^\parallel) \boxtimes R(\mathcal{H}_2^\wedge)$  and  $R(\mathcal{H}^\wedge)$ .

**Definition 10.13.** *Suppose that  $(\mathbf{x}_1, \mathbf{y}_1)$  and  $(\mathbf{x}_2, \mathbf{y}_2)$  are matching states, and  $B_1 \in \mathcal{D}(\mathbf{x}_1, \mathbf{y}_1)$  and  $B_2 \in \mathcal{D}(\mathbf{x}_2, \mathbf{y}_2)$ . We say that  $B_1$  and  $B_2$  are matching domains if the local multiplicities of  $B_2$  around each component of  $\hat{Z}_i(\mathcal{H}_2^\wedge)$  coincide with the local multiplicities around each component of  $\check{Z}_i(\mathcal{H}^\parallel)$ .*

For  $\mathbf{x} = \mathbf{x}_1\#\mathbf{x}_2$  and  $\mathbf{y} = \mathbf{y}_1\#\mathbf{y}_2$ , there is a one-to-one correspondence between  $B \in \mathcal{D}(\mathbf{x}, \mathbf{y})$  and matching domains  $B_1 \in \mathcal{D}(\mathbf{x}_1, \mathbf{y}_1)$  and  $B_2 \in \mathcal{D}(\mathbf{x}_2, \mathbf{y}_2)$ . In that case, we write  $B = B_1\#B_2$ .

Definition 9.4 has the following generalization:

**Definition 10.14.** *Suppose  $n > 1$ . Fix two pairs  $(\mathbf{x}_1, \mathbf{x}_2)$  and  $(\mathbf{y}_1, \mathbf{y}_2)$  of matching states, i.e. where  $\mathbf{x}_1, \mathbf{y}_1 \in \mathfrak{S}(\mathcal{H}^\parallel)$ ,  $\mathbf{x}_2, \mathbf{y}_2 \in \mathfrak{S}(\mathcal{H}_2^\wedge)$ , so that  $\mathbf{x} = \mathbf{x}_1\#\mathbf{x}_2$  and  $\mathbf{y} = \mathbf{y}_1\#\mathbf{y}_2$  are Heegaard states for  $\mathcal{H}$ . A matched pair consists of the following data*



- a holomorphic curve  $u_1$  in  $\mathcal{H}^\parallel$  with source  $\mathcal{S}_1$  representing homology class  $B_1 \in \mathcal{D}(\mathbf{x}_1, \mathbf{y}_1)$
- a holomorphic curve  $u_2$  in  $\mathcal{H}_2^\wedge$  with source  $\mathcal{S}_2$  representing homology class  $B_2 \in \mathcal{D}(\mathbf{x}_2, \mathbf{y}_2)$
- a bijection  $\psi: \mathbf{P}(\mathcal{S}_2) \rightarrow \check{\mathbf{P}}(\mathcal{S}_1)$ , where  $\check{\mathbf{P}}(\mathcal{S}_1) \subset \mathbf{P}(\mathcal{S}_1)$  denotes the set of punctures on  $\mathcal{S}_1$  that are labelled by chords and orbits supported on  $\check{Z}$ ,

with the following properties:

- For each  $q \in \mathbf{P}(\mathcal{S}_2)$  is marked with a Reeb orbit or chord, the corresponding puncture  $\psi(q) \in \mathbf{P}(\mathcal{S}_1)$  is marked with the matching Reeb orbit or chord (in the sense of Definition 9.3).
- For each  $q \in \mathbf{P}(\mathcal{S}_2)$ ,

$$(s \circ u_1(\psi(q)), t \circ u_1(\psi(q))) = (s \circ u_2(q), t \circ u_2(q)).$$

If  $(u_1, u_2)$  is a matched pair with homology class  $B_1$  and  $B_2$ , then  $B_1$  and  $B_2$  are matching domains. Let  $MM_{\natural}^B(\mathbf{x}_1, \mathbf{y}_1; \mathbf{x}_2, \mathbf{y}_2; \mathcal{S}_1, \mathcal{S}_2; \psi)$  denote the moduli space of matched pairs with shadow  $B = B_1 \# B_2$ .

We have the following analogue of Lemma 9.6:

**Lemma 10.15.** *Let  $(\mathbf{x}_1, \mathbf{x}_2)$  and  $(\mathbf{y}_1, \mathbf{y}_2)$  be two pairs of matching states, and fix a matched pair  $(u_1, u_2)$  connecting  $\mathbf{x}_1 \# \mathbf{x}_2$  to  $\mathbf{y}_1 \# \mathbf{y}_2$ , with  $u_1 \in \mathcal{M}(\mathbf{x}_1, \mathbf{y}_1, \boldsymbol{\rho}_1, \dots, \boldsymbol{\rho}_m)$  and  $u_2 \in \mathcal{M}(\mathbf{x}_2, \mathbf{y}_2, \boldsymbol{\rho}'_1, \dots, \boldsymbol{\rho}'_m)$  (where the chords in  $\boldsymbol{\rho}_i$  all match, in the sense of Definition 9.3 with chords in  $\boldsymbol{\rho}'_i$ ). Then, both  $u_1$  and  $u_2$  are strongly boundary monotone; moreover,  $\alpha(\mathbf{x}_1, \boldsymbol{\rho}_1, \dots, \boldsymbol{\rho}_\ell)$  is complementary to  $\alpha(\mathbf{x}_2, \boldsymbol{\rho}'_1, \dots, \boldsymbol{\rho}'_\ell)$  for all  $\ell = 0, \dots, m$ .*

Given a holomorphic curve  $u_1$  for a middle diagram, let  $\check{c}_1$  denote the number of chords in  $u_1$  on  $\check{Z}(\mathcal{H}^\parallel)$ ,  $\check{o}_1$  denote the number of orbits in  $u_1$  on  $\check{Z}(\mathcal{H}^\parallel)$ , and  $\check{w}_1$  denote the total weight of  $u_1$  at  $\check{Z}(\mathcal{H}^\parallel)$ .

If  $(u_1, u_2)$  is a matched pair of curves, if  $c_2$ ,  $o_2$ , and  $w_2$  denote the number of chords, orbits, and total weight at  $\hat{Z}(\mathcal{H}_2^\wedge)$  respectively, then  $\check{c}_1 = c_2$ ,  $\check{o}_1 = o_2$ ,  $\check{w}_1 = w_2$ . The space of matched pairs lies in a moduli space whose expected dimension is given by

$$(10.3) \quad \text{ind}(B_1, \mathcal{S}_1; B_2, \mathcal{S}_2) = \text{ind}(B_1, \mathcal{S}_1) + \text{ind}(B_2, \mathcal{S}_2) - c_2 - 2o_2.$$

**Definition 10.16.** *The embedded index of a matched pair is defined by the formula*

$$(10.4) \quad \begin{aligned} \text{ind}(B_1; B_2) &= e(B_1) + n_{\mathbf{x}_1}(B_1) + n_{\mathbf{y}_1}(B_1) + e(B_2) + n_{\mathbf{x}_2}(B_2) + n_{\mathbf{y}_2}(B_2) - 2\omega_{\check{Z}}(B_1) \\ &= e(B_1 \natural B_2) + n_{\mathbf{x}}(B_1 \natural B_2) + n_{\mathbf{y}}(B_1 \natural B_2). \end{aligned}$$

Lemma 10.17 has the following analogue:

**Lemma 10.17.** *Fix  $B_1 \in \mathcal{D}(\mathbf{x}_1, \mathbf{y}_1)$  and  $B_2 \in \mathcal{D}(\mathbf{x}_2, \mathbf{y}_2)$  so that  $\mathbf{w}_i(B_1) = \mathbf{w}_i(B_2)$  for  $i = 1, \dots, 2m$ , and the local multiplicity of  $B_1$  vanishes somewhere. For generic admissible almost complex structures on  $\Sigma_i \times [0, 1] \times \mathbb{R}$ , and  $\text{ind}(B_1, \mathcal{S}_1; B_2, \mathcal{S}_2) \leq 2$ , the moduli space of matched pairs*

$$MM_{\natural}^B(\mathbf{x}_1, \mathbf{y}_1; \mathbf{x}_2, \mathbf{y}_2; \mathcal{S}_1, \mathcal{S}_2; \psi)$$

is transversely cut out by the  $\bar{\partial}$ -equation and the evaluation map; in particular, this moduli space is a manifold whose dimension is given by Equation (10.3).

Proposition 9.9 has the following analogue:

**Proposition 10.18.** *Fix  $\mathbf{x} = \mathbf{x}_1 \# \mathbf{x}_2$  and  $\mathbf{y} = \mathbf{y}_1 \# \mathbf{y}_2$ , and decompose  $B \in \mathcal{D}(\mathbf{x}, \mathbf{y})$  as  $B = B_1 \natural B_2$ , with  $B_i \in \mathcal{D}(\mathbf{x}_i, \mathbf{y}_i)$ . Fix source curves  $\mathcal{S}_1$  and  $\mathcal{S}_2$  together with a one-to-one correspondence  $\psi: \mathbf{P}(\mathcal{S}_2) \rightarrow \mathbf{P}(\mathcal{S}_1)$  which is consistent with the chord and orbit labels, so we can form  $\mathcal{S} = \mathcal{S}_1 \natural_\psi \mathcal{S}_2$ . Suppose that  $M^B(\mathbf{x}, \mathbf{y}; \mathcal{S})$  (i.e. the moduli space for curves in  $\mathcal{H}$ ) and  $M^{B_i}(\mathbf{x}_i, \mathbf{y}_i; \mathcal{S}_i)$  (which are moduli spaces for curves in  $\mathcal{H}_i$ ) are non-empty for  $i = 1, 2$ . Then,  $\text{ind}(B_1, \mathcal{S}_1; B_2, \mathcal{S}_2) \leq \text{ind}(B)$  if and only if  $\chi(\mathcal{S}_i) = \chi_{\text{emb}}(B_i)$  for  $i = 1, 2$ ; and all the chords in  $\mathcal{S}_1$  have weight  $1/2$  and all the orbits in  $\mathcal{S}_1$  have weight  $1$ .*

In the present case, the Gromov compactification can contain  $\beta$ -boundary degenerations. Nonetheless, excluding the  $\alpha$ -boundary degenerations and closed curve components work as before, as in the following. Compare Lemmas 9.12 and 9.13 respectively:

**Lemma 10.19.** *Fix  $B_1 \in \mathcal{D}(\mathbf{x}_1, \mathbf{y}_1)$  and  $B_2 \in \mathcal{D}(\mathbf{x}_2, \mathbf{y}_2)$  with so that*

- *the local multiplicities of  $B_1$  along  $\check{Z}(\mathcal{H}_1)$  agree with the local multiplicities of  $\hat{Z}(\mathcal{H}_2)$*
- *$B_1$  has vanishing local multiplicity somewhere.*

*Then, curves in the Gromov compactification of  $MM_{\natural}^B(\mathbf{x}_1, \mathbf{y}_1; \mathbf{x}_2, \mathbf{y}_2; \mathcal{S}_1, \mathcal{S}_2)$  contain no  $\alpha$ -boundary degenerations.*

**Lemma 10.20.** *Suppose that  $m > 1$ . Fix matching domains  $B_1 \in \mathcal{D}(\mathbf{x}_1, \mathbf{y}_1)$  and  $B_2 \in \mathcal{D}(\mathbf{x}_2, \mathbf{y}_2)$ , so that  $B_1$  has a vanishing local multiplicity somewhere, and so that  $\text{ind}(B_1 \natural B_2) \leq 2$ . Curves in the Gromov compactification of  $MM_{\natural}^B(\mathbf{x}_1, \mathbf{y}_1; \mathbf{x}_2, \mathbf{y}_2; \mathcal{S}_1, \mathcal{S}_2)$  contain no closed components.*

**Lemma 10.21.** *Fix matching domains  $B_1 \in \mathcal{D}(\mathbf{x}_1, \mathbf{y}_1)$  and  $B_2 \in \mathcal{D}(\mathbf{x}_2, \mathbf{y}_2)$  so that  $w_i(B_1) = w_i(B_2)$  so that  $\text{ind}(B_1 \natural B_2) \leq 2$ . Then, curves in the Gromov compactification of  $MM_{\natural}^B(\mathbf{x}_1, \mathbf{y}_1; \mathbf{x}_2, \mathbf{y}_2; \mathcal{S}_1, \mathcal{S}_2)$  contain no  $\beta$ -boundary degenerations, except in the special case where  $B = B_{\{j,k\}}$  for some matched pair  $j$  and  $k$ .*

**Proof.** The proof of Lemma 9.12 actually shows that if there is  $\beta$ -boundary degeneration (on either side), then in fact, it forms along with a sequence of boundary degenerations that contain all the orbits in a single component of  $W$ . A straightforward computation shows that the remaining components have index 0, and therefore, if it has a pseudo-holomorphic representative, the remainder must correspond to a constant map. It follows that  $B = B_{\{j,k\}}$ .  $\square$

### 10.3.1. Type $D$ structures of matched curves.

**Definition 10.22.** *Let  $\mathcal{H}^\wedge = \mathcal{H}^\parallel \cup \mathcal{H}_2^\wedge$  be a decomposition of an upper diagram. Let  $X$  denote the vector space generated by upper states for  $\mathcal{H}^\wedge$ , equipped with an operator*

$$\delta_{\natural}^1: X \rightarrow \mathcal{C} \otimes X$$

characterized by

$$\delta_{\natural}^1(\mathbf{x}) = \sum_{\{B=B_1 \# B_2 \mid \text{ind}(B)=1\}} \#mm_{\natural}^B(\mathbf{x}, \mathbf{y}) \cdot \hat{b}(B) \otimes \mathbf{y}.$$

The analogue of Theorem 9.22 is the following:

**Theorem 10.23.** *Provided  $m > 1$ .  $(X, \delta_{\natural}^1)$  is a curved type  $D$  structure, which is homotopy equivalent to  $R(\mathcal{H}^{\wedge})$ .*

**Proof.** The stretching argument from Theorem 10.23 proves that  $\delta_{\natural}^1$  agrees with  $\delta^1$  for a suitable complex structure on  $\mathcal{H}^{\wedge}$ . It follows that  $\delta_{\natural}^1$  is a curved type  $D$  structure.  $\square$

**Remark 10.24.** *The above argument shows that boundary degenerations which are allowed in Lemma 10.21 indeed do occur; and their algebraic count is 1.*

10.3.2. *Self-matched curves.* We adapt Definition 9.23 to middle diagrams as follows:

**Definition 10.25.** *Let  $\mathcal{S}_1$  be a decorated source for  $\mathcal{H}^{\parallel}$ . according to whether the punctures are marked by chords or orbits on  $\hat{Z}$  or  $\check{Z}$  respectively. Further partition the punctures of  $\mathcal{S}_1$  labelled by chords and orbits in  $\check{Z}$ , as*

$$\check{\mathbf{E}}(\mathcal{S}_1) \cup \check{\Omega}^+(\mathcal{S}_1) \cup \check{\Omega}^-(\mathcal{S}_1),$$

where  $\check{\mathbf{E}}(\mathcal{S}_1)$  consists of boundary punctures,  $\check{\Omega}^+(\mathcal{S}_1)$  consists of interior punctures marked by even Reeb orbits, and  $\check{\Omega}^-(\mathcal{S}_1)$  consists of interior punctures marked by odd Reeb orbits. A self-marked source is a decorated source, together with an injection  $\phi: \check{\Omega}^+(\mathcal{S}_1) \rightarrow \check{\mathbf{E}}(\mathcal{S}_1)$  with the property that if  $p \in \check{\Omega}^+(\mathcal{S}_1)$  is marked by some orbit  $o_j$ , then  $\phi(p)$  is marked by a length one chord that covers the boundary component  $Z_k$  so that  $\{j, k\} \in M^{\wedge}$ . A self-matched curve  $u$  is an element  $u \in m^{B_1}(\mathbf{x}, \mathbf{y}; \mathcal{S}_1, \phi)$ , subject to the following additional constraints: for each puncture  $p \in \check{\Omega}^+(\mathcal{S}_1)$ ,

$$(10.5) \quad t \circ u(p) = t \circ u(\phi(p)).$$

Let  $mm_{\natural}^{B_1, B_2}(\mathbf{x}, \mathbf{y}; \mathcal{S}_1, \mathcal{S}_2, \phi, \psi)$  denote the moduli space self-matched curve pairs.

Let  $X$  be the  $\mathbb{F}$ -vector space generated by matching states  $\mathbf{x}_1$  and  $\mathbf{x}_2$ . We use the self-matched moduli spaces to construct a map

$$\delta_{\natural}^1: X \rightarrow \mathcal{B} \otimes X$$

defined as in Definition 10.22, only using  $mm_{\natural}^B(\mathbf{x}, \mathbf{y})$  instead of  $mm_{\natural}^B(\mathbf{x}, \mathbf{y})$ .

**Proof of Theorem 10.11.** The proof is very similar to the proof of Theorem 9.1. Theorem 10.23 provides the  $D$ -module isomorphism  $R(\mathcal{H}^{\wedge}) \cong (X, \delta_{\natural}^1)$ . Suppose  $m > 1$ .

We wish to define a sequence of intermediate complexes. Specifically, in the definitions of the intermediate complexes, we chose a particular ordering on  $\{1, \dots, m\}$  in which to deform the matching condition; specifically, choose a one-to-one correspondence  $f: \{1, \dots, 2m\} \rightarrow \{1, \dots, 2m\}$  so that if  $n_1, \dots, n_{2k}$  are the orbits in

$\check{Z}$  on a given component of  $W$ , arranged in the opposite to the order they appear in  $W$  (with its orientation), then  $\{f(n_2), f(n_1), f(n_3), \dots, f(n_{2k}), f(n_{2k-1})\}$  is a sequence of consecutive integers. See Figure 43 for an example.

We can now define the sequence of intermediate type  $D$  structures  $(X, \delta_\ell^1: X \rightarrow \mathcal{C} \otimes X)$  using operators  $\delta_\ell^1$  that count  $\ell$ -self-matched curve pairs, adapting Definition 9.38.

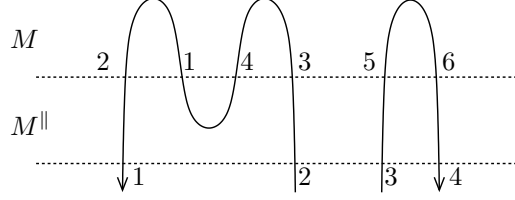


FIGURE 43. **Labeling the orbits for a middle diagram.** For this picture, we have listed a valid numbering  $f$ .

Isomorphisms are constructed as in Proposition 9.44. Finally, the identification of  $(X, \delta_\#^1)$  with the tensor product is achieved by time dilation.

The case where  $m = 1$  is handled separately, using special matched pairs, as in Subsection 9.8.  $\square$

11. EXTENDING THE  $DA$  BIMODULES

As defined so far, our type  $DA$  bimodules are curved bimodules over  $\mathcal{C}$ . Our aim here is to extend these modules to modules over  $\mathcal{B}$ . Specifically, if  $\mathcal{H}^\parallel$  is a middle diagram, let  $\check{\mathcal{B}} = \check{\mathcal{B}}(\mathcal{H}^\parallel) = \bigoplus_{k=0}^{2m-1} \mathcal{B}(2m, k)$ ,  $\hat{\mathcal{B}} = \hat{\mathcal{B}}(\mathcal{H}^\parallel) = \bigoplus_{k=0}^{2n-1} \mathcal{B}(2n, k)$ , so that

$$\check{\mathcal{C}} = \left( \sum_{\{\mathbf{x} | \mathbf{x} \cap \{0, 2m\} = \emptyset\}} \mathbf{I}_{\mathbf{x}} \right) \cdot \check{\mathcal{B}} \cdot \left( \sum_{\{\mathbf{x} | \mathbf{x} \cap \{0, 2m\} = \emptyset\}} \mathbf{I}_{\mathbf{x}} \right)$$

$$\hat{\mathcal{C}} = \left( \sum_{\{\mathbf{x} | \mathbf{x} \cap \{0, 2m\} = \emptyset\}} \mathbf{I}_{\mathbf{x}} \right) \cdot \hat{\mathcal{B}} \cdot \left( \sum_{\{\mathbf{x} | \mathbf{x} \cap \{0, 2m\} = \emptyset\}} \mathbf{I}_{\mathbf{x}} \right).$$

In particular, there are inclusion maps  $\iota: \check{\mathcal{C}} \rightarrow \check{\mathcal{B}}$  and  $\iota: \hat{\mathcal{C}} \rightarrow \hat{\mathcal{B}}$ . In the next statement we will use the corresponding bimodules  $\check{\mathcal{B}}[\iota]_{\check{\mathcal{C}}}$  and  $\hat{\mathcal{B}}[\iota]_{\hat{\mathcal{C}}}$ .

**Proposition 11.1.** *Let  $\mathcal{H}^\parallel$  be a middle diagram, and  ${}^{\hat{\mathcal{C}}}RQ(\mathcal{H}^\parallel)_{\check{\mathcal{C}}}$  be the corresponding type  $DA$  bimodule. Then, there is a type  $DA$  bimodule  ${}^{\hat{\mathcal{B}}}RQ_{\check{\mathcal{B}}}$ , with the property that*

$$\hat{\mathcal{B}}[\iota]_{\hat{\mathcal{C}}} \boxtimes {}^{\hat{\mathcal{C}}}RQ(\mathcal{H}^\parallel)_{\check{\mathcal{C}}} = {}^{\hat{\mathcal{B}}}RQ_{\check{\mathcal{B}}} \boxtimes \check{\mathcal{B}}[\iota]_{\check{\mathcal{C}}}.$$

The bimodule over  $\mathcal{B}$  in the statement of Proposition 11.1 is constructed by extending the notion of middle diagrams, and defining their associated type  $DA$  bimodules, as we do presently. The proof of the above theorem is given in Section 11.3.

**11.1. Extended middle diagrams.** We define now relevant generalization of middle diagrams used in the construction of the module from Proposition 11.1.

**Definition 11.2.** *An extended middle diagram is a Heegaard diagram obtained from an upper diagram with  $2m+2n+2$  boundary components  $\{Z_0, \dots, Z_{2m+2n+1}\}$ , and adding a new arc  $\alpha_{2m+2n+1}$  connecting  $Z_0$  and  $Z_{2m+2n+1}$ , and adding two new beta circles, so that the  $\beta$  circles now are labelled  $\{\beta_i\}_{i=1}^{g+m+n+1}$ .*

We think of  $2m$  of these components as “incoming” boundary, writing  $\check{Z}_i = Z_i$  for  $i = 1, \dots, 2m$ ;  $2n$  “outgoing” boundary components, writing  $\hat{Z}_i = Z_{2m+2n+2-i}$  for  $i = 1, \dots, 2n$ ; and two “middle” boundary components  $Z_0^\parallel = Z_0$  and  $Z_1^\parallel = Z_{2m+1}$ . We also let  $\check{\alpha}_i = \alpha_i$  for  $i = 0, \dots, 2m$ ;  $\hat{\alpha}_i = \alpha_{2m+2n+1-i}$  for  $i = 0, \dots, 2n$ . We write this data

$$\mathcal{H}^{\parallel, x} = (\Sigma_0, \{\check{Z}_i\}_{i=1}^{2m}, \{\hat{Z}_i\}_{i=1}^{2n}, \{Z_0^\parallel, Z_1^\parallel\}, \{\check{\alpha}_i\}_{i=0}^{2m}, \{\hat{\alpha}_i\}_{i=0}^{2n}, \{\alpha_i^c\}_{i=1}^g, \{\beta_i\}_{i=1}^{g+m+n+1}).$$

Note that  $\check{\alpha}_0$  connects  $\check{Z}_1$  to  $Z_0^\parallel$ ,  $\hat{\alpha}_0$  connects  $Z_0^\parallel$  to  $\hat{Z}_1$ ,  $\check{\alpha}_{2m}$  connects  $\check{Z}_{2m}$  to  $Z_1^\parallel$ , and  $\hat{\alpha}_{2n}$  connects  $Z_1^\parallel$  to  $\hat{Z}_{2n}$ .

**Example 11.3.** *Let*

$$\mathcal{H}^\parallel = (\Sigma_0, \{\check{Z}_i\}_{i=1}^{2m}, \{\hat{Z}_i\}_{i=1}^{2n}, \{\check{\alpha}_i\}_{i=1}^{2m-1}, \{\hat{\alpha}_i\}_{i=1}^{2n-1}, \{\alpha_i^c\}_{i=1}^g, \{\beta_i\}_{i=1}^{g+m+n-1})$$

be a middle diagram. We can form an extended middle diagram as follows. Connect  $\check{Z}_1$  and  $\hat{Z}_1$  by a path that crosses only  $\beta$ -circles. Remove a disk centered at a point on the path from  $\Sigma_0$  to obtain a new boundary component  $Z_0^\parallel$ , and introduce new arcs  $\check{\alpha}_0$  connecting  $\check{Z}_1$  to  $Z_0^\parallel$  and  $\hat{\alpha}_0$  connecting  $Z_0^\parallel$  to  $\hat{\alpha}_1$ . Add also a new small  $\beta$ -circle  $\beta_0$  in a collar neighborhood of  $Z_0^\parallel$ . Connect  $\check{Z}_{2m}$  and  $\hat{Z}_{2n}$  by another path, remove another disk to obtain the boundary component  $Z_1^\parallel$ , and introduce arcs  $\check{\alpha}_{2m}$  connecting this to  $\check{Z}_{2m}$  and  $\hat{\alpha}_{2n}$  connecting it to  $\hat{Z}_{2n}$ , and introduce a circle  $\beta_{g+m+n}$  which encircles  $Z_1^\parallel$ , intersecting  $\check{\alpha}_{2m}$  and  $\hat{\alpha}_{2n}$  in one point apiece. In this manner, we obtain a new extended middle diagram,  $\mathcal{H}^{\parallel,x}$ , called a stabilization of  $\mathcal{H}^\parallel$ .

See Figure 44 for an example.

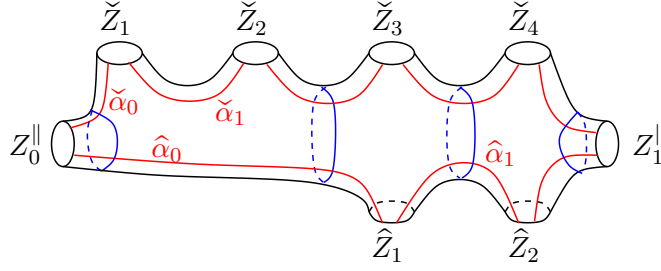


FIGURE 44. Extended middle diagram of local minimum.

**Definition 11.4.** An extended partial Heegaard state is a  $g + m + n + 1$ -tuple of points, where one lies on each  $\beta$ -circle, one lies on each  $\alpha$ -circle, and no more than one lies on each  $\alpha$ -arc. Let  $\check{\alpha}(\mathbf{x}) \subset \{0, \dots, 2m\}$  be the set of  $i \in \{0, \dots, 2m\}$  so that  $\mathbf{x} \cap \check{\alpha}_i \neq \emptyset$ ; and  $\hat{\alpha}(\mathbf{x}) \subset \{0, \dots, 2n\}$  be the set of  $i \in \{0, \dots, 2n\}$  so that  $\mathbf{x} \cap \hat{\alpha}_i \neq \emptyset$ . An extended middle Heegaard state has an idempotent type  $k = |\check{\alpha}(\mathbf{x})|$ .

**11.2. DA bimodules for extended diagrams.** An extended middle diagram induces a matching on the components of  $\partial\Sigma$ ; in fact, if  $\mathcal{H}^{\parallel,x}$  is an extension of  $\mathcal{H}^\parallel$ , then the matchings are the same.

**Definition 11.5.** Let  $\mathcal{H}^{\parallel,x}$  be an extended middle diagram compatible with a matching  $M$  on the incoming boundary components. The incoming algebra  $\check{\mathcal{B}}(\mathcal{H}^{\parallel,x})$  and the outgoing algebra  $\hat{\mathcal{B}}(\mathcal{H}^{\parallel,x})$  are defined by

$$\check{\mathcal{B}}(\mathcal{H}^\parallel) = \bigoplus_{k=0}^{2m-1} \mathcal{B}(2m, k); \quad \hat{\mathcal{B}}(\mathcal{H}^\parallel) = \bigoplus_{k=0}^{2n-1} \mathcal{B}(2n, k).$$

We will define a type DA bimodule  $RQ^x(\mathcal{H}^{\parallel,x}) = \hat{\mathcal{B}} RQ^x(\mathcal{H}^{\parallel,x})_{\check{\mathcal{B}}}$ . As a vector space, it is spanned by the extended middle Heegaard states of  $\mathcal{H}^{\parallel,x}$ .

$$\mathbf{I}_{\{0, \dots, 2n\} \setminus \hat{\alpha}(\mathbf{x})} \cdot \mathbf{x} \cdot \mathbf{I}_{\check{\alpha}(\mathbf{x})} = \mathbf{x}.$$

Again, there is a splitting

$$RQ^x(\mathcal{H}^{\parallel,x}) = \bigoplus_{k \in \mathbb{Z}} I(2n, k-m+n) RQ^x(\mathcal{H}^\parallel)_{I(2m, k)},$$

where  $k$  is the idempotent type of  $\mathbf{x}$ . We will be primarily interested in the summand where  $k = m$ ,

$$I(2n,n)RQ^x(\mathcal{H}^\parallel)_{I(2m,m)}.$$

The material from Section 10.1 has a straightforward adaptation to extended diagrams, with the understanding that the pseudo-holomorphic curves in consideration now have zero multiplicity at the middle boundary  $Z_0^\parallel$  and  $Z_1^\parallel$ .

In particular, the definition of  $(\mathbf{x}, \vec{a})$ -compatible sequences given in Definition 10.4 can be readily defined when  $\mathbf{x}$  is an extended partial Heegaard state, and the sequence  $\vec{a} = (a_1, \dots, a_\ell)$  lies in  $\check{\mathcal{B}}(\mathcal{H}^{\parallel,x})$  (rather than  $\check{\mathcal{C}}(\mathcal{H}^\parallel)$ , as it was there).

Observe given  $(B, \rho_1, \dots, \rho_h)$ , the associated element  $\hat{b}(B, \rho_1, \dots, \rho_h)$  defined as in Equation (10.1) naturally lies in  $\hat{\mathcal{B}}(\mathcal{H}^{\parallel,x})$  for extended diagrams, rather than merely in  $\hat{\mathcal{C}}$ .

With these observations in place, Equation (8.5) induces now a map

$$\delta_{\ell+1}^1: RQ^x(\mathcal{H}^{\parallel,x}) \otimes \check{\mathcal{B}}^{\otimes \ell} \rightarrow \hat{\mathcal{B}} \otimes RQ^x(\mathcal{H}^{\parallel,x}).$$

Proposition 10.10 has the following analogue for extended middle diagrams:

**Proposition 11.6.** *Let  $\mathcal{H}^{\parallel,x}$  be an extended middle diagram that is compatible with a given matching  $M$  on its incoming boundary. Choose an orientation on  $W = W(\mathcal{H}^\parallel) \cup W(M)$ . The  $I(2n) - I(2m)$ -bimodule  $RQ^x(\mathcal{H}^{\parallel,x})$ , equipped the operations  $\delta_{\ell+1}^1: RQ^x(\mathcal{H}^{\parallel,x}) \otimes \check{\mathcal{B}}^{\otimes m} \rightarrow \hat{\mathcal{B}} \otimes RQ^x(\mathcal{H}^{\parallel,x})$  defined above endows  $RQ^x(\mathcal{H}^{\parallel,x})$  with the structure of a curved  $\check{\mathcal{B}} - \hat{\mathcal{B}}$  type DA bimodule.*

**Proof.** Theorem 10.9 has a straightforward adaptation to extended middle diagrams. The proposition then is an immediate consequence.  $\square$

**11.3. Destabilizing extended diagrams.** Our aim now is to prove the following version of Proposition 11.1:

**Proposition 11.7.** *Let  $\mathcal{H}^{\parallel,x}$  be an extension of a middle diagram  $\mathcal{H}^\parallel$ , as in Example 11.3. The type DA bimodules associated to  $\mathcal{H}^\parallel$  and  $\mathcal{H}^{\parallel,x}$  are related by the formula*

$$\hat{\mathcal{B}}[\iota]_{\hat{\mathcal{C}}} \boxtimes^{\hat{\mathcal{C}}} RQ(\mathcal{H}^\parallel)_{\check{\mathcal{C}}} = \hat{\mathcal{B}} RQ^x_{\check{\mathcal{B}}}(\mathcal{H}^{\parallel,x}) \boxtimes^{\check{\mathcal{B}}} \check{\mathcal{B}}[\iota]_{\check{\mathcal{C}}}.$$

This is proved in two steps.

**Step 1: Remove  $\check{\alpha}_0$  and  $\check{\alpha}_m$ .** From  $\mathcal{H}^\parallel$  we constructed  $\mathcal{H}^{\parallel,x}$ . There is another diagram,  $\mathcal{H}^{\parallel,\frac{x}{2}}$  which is obtained from  $\mathcal{H}^{\parallel,x}$  by removing  $\check{\alpha}_0$  and  $\check{\alpha}_{2m+1}$ . (See Figure 45 for an illustration of removing  $\check{\alpha}_0$ .) We call such diagrams *half-extended middle diagrams*. We can define the associated DA bimodule as before, except that now the input algebra for a half extended middle diagram is obviously  $\check{\mathcal{C}}$ , whereas the output algebra is *a priori*  $\hat{\mathcal{B}}$ .

**Lemma 11.8.** *The DA bimodules for an extended middle diagram and a half-extended middle diagram are related by*

$$\hat{\mathcal{B}} RQ^{\frac{x}{2}}(\mathcal{H}^{\parallel,\frac{x}{2}})_{\check{\mathcal{C}}} = \hat{\mathcal{B}} RQ^x(\mathcal{H}^{\parallel,x})_{\check{\mathcal{B}}} \boxtimes^{\check{\mathcal{B}}} \check{\mathcal{B}}[\iota]_{\check{\mathcal{C}}}.$$

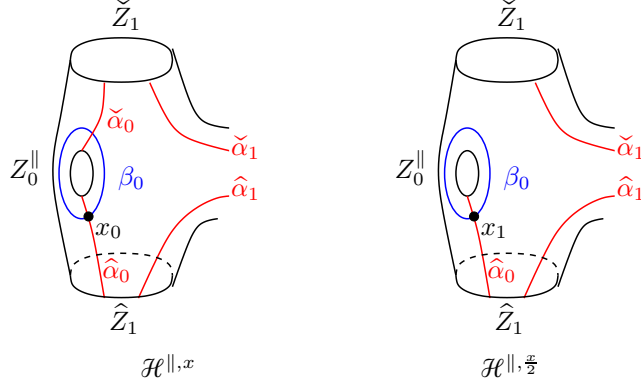


FIGURE 45. **Removing  $\check{\alpha}_0$ .** At the left, we have a portion of an extended middle diagram; at the right, we have the corresponding half-extended middle diagram.

**Proof.** Recall that  $\beta_0$  and  $\beta_{g+m+n}$  denote the two  $\beta$ -circles that encircle  $Z_0^||$  and  $Z_1^||$  respectively. Let  $x_0 = \beta_0 \cap \hat{\alpha}_0$  and  $x_{2m+1} = \beta_{g+m+n} \cap \hat{\alpha}_{2n}$ ; and  $y_0 = \beta_0 \cap \check{\alpha}_0$  and  $y_{2n+1} = \beta_{g+m+n} \cap \hat{\alpha}_{2n+1}$ ; The generators of  ${}^{\hat{\beta}}RQ^x(\mathcal{H}^{||,x})_{\check{\beta}} \boxtimes {}^{\check{\beta}}[\iota]_{\check{\mathcal{C}}}$  are those middle states with  $\{x_0, x_{2m+1}\} \subset \mathbf{x}$ , which in turn are the states generating  $RQ^{\frac{x}{2}}(\mathcal{H}^{||, \frac{x}{2}})$ . Similarly, the holomorphic curves counted in the module actions for  ${}^{\hat{\beta}}RQ^x(\mathcal{H}^{||,x})_{\check{\beta}} \boxtimes {}^{\check{\beta}}[\iota]_{\check{\mathcal{C}}}$  cannot have an  $\alpha$ -interval which maps to  $\check{\alpha}_0$  or  $\check{\alpha}_{2m+1}$ : for the endpoints would have to either be at Reeb chords, but the incoming algebra does not allow Reeb chords with boundary on  $\check{\alpha}_0$  or  $\check{\alpha}_{2m+1}$ ; or they would have to be  $\pm\infty$  punctures, but the generators we are considering contain  $x_0$  and  $x_{2m+1}$ , not the corresponding  $y_0$  or  $y_{2n+1}$ . Thus, the holomorphic curves used to define the  $\mathcal{A}_\infty$  operations on  ${}^{\hat{\beta}}RQ^x(\mathcal{H}^{||,x})_{\check{\beta}} \boxtimes {}^{\check{\beta}}[\iota]_{\check{\mathcal{C}}}$  coincide with the ones used to define  ${}^{\hat{\beta}}RQ^x(\mathcal{H}^{||, \frac{x}{2}})_{\check{\mathcal{C}}}$ .  $\square$

**Step 2: Remove  $\hat{\alpha}_0$  and  $\hat{\alpha}_{2n}$ .** This is a neck stretching argument, in the spirit of Step 1 in the pairing theorem.

We start by analyzing moduli spaces that are relevant after the neck stretching. To this end, let  $\mathcal{H}_0^||$  consist of a punctured disk, whose puncture we think of as the (filled) middle boundary  $Z^||$ , and whose boundary we label  $\mathcal{Z}$ , equipped with a single embedded  $\beta$ -circle that separates the puncture from the boundary, and a single  $\alpha$ -arc, denoted  $\alpha$ , that runs from the boundary to the puncture, meeting  $\beta$  in a single point, which we denote  $x$ . See Figure 46.

A homology class of flows from  $x$  to itself is determined by its local multiplicity  $k$  at the puncture; denote the space  $\mathcal{M}^{[k]}(x, x)$ .

**Lemma 11.9.** *The space  $\mathcal{M}^{[k]}(x, x)$  is  $2k$ -dimensional. There is a dense, open subset of  $\mathcal{M}^k(x, x)$  consisting of those curves whose Reeb orbits are simple.*

**Proof.** The dimension is a straightforward application of the dimension formula: the Euler measure of the region is  $k$ , and the point measure is  $k$ . Smoothness is a consequence of the fact that the domain curve is also planar.  $\square$



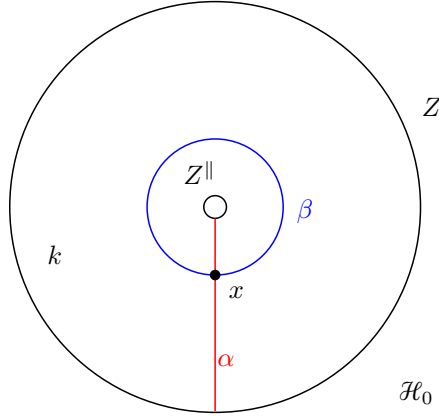


FIGURE 46. **The diagram  $\mathcal{H}_0$ .** We will consider homology classes with local multiplicity  $k$  near the boundary  $Z$ , as indicated.

Consider the evaluation map  $\text{ev}: \mathcal{M}^k(x, x) \rightarrow \text{Sym}^k([0, 1] \times \mathbb{R})$ , which projects the punctures of the source curves in  $\mathcal{M}^k(x, x)$  to  $[0, 1] \times \mathbb{R}$ .

**Lemma 11.10.** *The map  $\text{ev}: \mathcal{M}^{[k]}(x, x) \rightarrow \text{Sym}^k([0, 1] \times \mathbb{R})$  is a proper map of odd degree.*

**Proof.** Properness can be thought of as a consequence of Gromov's compactness theorem, since any non-constant holomorphic curves from  $x$  to  $x$  projects to some symmetric product  $\text{Sym}^k([0, 1] \times \mathbb{R})$ . It remains to compute the degree, which we do with a model computation.

Invert the Heegaard surface, so that it is a disk  $D$  in the complex plane,  $Z$  corresponds to the origin,  $\beta$  corresponds to the unit circle. We can think of the domain of the holomorphic curve  $D^+$  as the upper half disk (i.e.  $z \in D$  whose imaginary part is non-negative). The holomorphic disks we are considering are holomorphic maps from  $D^+$  to  $D$  which carry the real interval  $[-1, 1]$  in  $\partial D^+$  to the real interval in  $D$ , the upper half circle in  $\partial D^+$  to the boundary of  $D$ , and the points  $\{\pm 1\}$  to 1. By the Schwartz reflection principle, these correspond to holomorphic maps  $f: D \rightarrow D$  so that

$$(B-1) \quad f(\partial D) \subset \partial D$$

$$(B-2) \quad f(D \cap \mathbb{R}) \subset \mathbb{R}; \text{ i.e. } \overline{f(z)} = f(\bar{z}).$$

Consider those  $f$  for which  $f(D \cap \mathbb{R}) \neq 0$ . (These correspond to those holomorphic curves that have no Reeb chord on their boundary.) By classical complex analysis holomorphic maps  $f$  as above can be uniquely written in the form

$$f(z) = \prod_{i=1}^k \frac{(z - \alpha_i)(z - \bar{\alpha}_i)}{(1 - \bar{\alpha}_i z) \cdot (1 - \alpha_i z)},$$

where  $\{\alpha_1, \dots, \alpha_k\} \in \text{Sym}^k(D^+)$ . This shows that  $\text{ev}$  induces a homeomorphism, for suitable choices of complex structure  $\beta$ . It follows that the degree is odd in general.  $\square$

**Proposition 11.11.** *There is an identification*

$$\hat{\mathcal{B}} RQ^{\frac{x}{2}}(\mathcal{H}^{\parallel, \frac{x}{2}})_{\check{c}} \simeq^{\hat{\mathcal{B}}} [\iota]_{\hat{c}} \boxtimes {}^{\hat{c}} RQ(\mathcal{H}^{\parallel})_{\check{c}}$$

**Proof.** Start from  $R(\mathcal{H}^{\parallel})$ . We will add first  $Z_0^{\parallel}$ ,  $\beta_0$ ,  $\hat{\alpha}_0$  to obtain a diagram  $\mathcal{H}'$ ; and then add  $Z_1^{\parallel}$ ,  $\beta_{g+m+n}$ , and  $\hat{\alpha}_{2n}$  to obtain  $\mathcal{H}^{\parallel, \frac{x}{2}}$ .

Fix a curve  $\gamma_0$  in  $\mathcal{H}'$  which is parallel to  $\beta_0$ , dividing  $\mathcal{H}^{\parallel, \frac{x}{2}}$  into two components, one of which is homeomorphic to  $\mathcal{H}_0^{\parallel}$ , and another looks like  $\mathcal{H}^{\parallel, \frac{x}{2}}$  with  $\beta_0$  removed. Stretch the neck normal to  $\gamma_0$ , so that  $\mathcal{H}^{\parallel, \frac{x}{2}} = \mathcal{H}' \cup \mathcal{H}_0^{\parallel}$ . The diagram  $\mathcal{H}'$  can also be used to define a  $DA$  bimodule of the form  $\hat{\mathcal{B}} RQ'_{\check{c}}$ .

Let  $m^B(\mathbf{x}, \mathbf{y}; \rho_1, \dots, \rho_k)$  be some moduli space of holomorphic curves which appears in the definition of the module actions for  $\mathcal{H}^{\parallel}$ , equipped with a puncture point  $z_0$  (thought of as a filling of  $Z_0^{\parallel}$ ). We have an analogous moduli spaces  $m_{\mathcal{H}'}^B(\mathbf{x}, \mathbf{y}; \rho_1, \dots, \rho_k)$  which define the actions on  $\hat{\mathcal{B}} RQ'_{\check{c}}$ .

Stretching the neck gives a fibered product description:

$$m_{\mathcal{H}'}^B(\mathbf{x}, \mathbf{y}; \rho_1, \dots, \rho_k) = m^B(\mathbf{x}, \mathbf{y}; \rho_1, \dots, \rho_k) \times_{\text{Sym}^d([0,1] \times \mathbb{R})} m^{[d]}(\mathcal{H}_0^{\parallel}),$$

where the fibered product is taken over the evaluation at the puncture  $z_0$

$$m^B(\mathbf{x}, \mathbf{y}; \rho_1, \dots, \rho_k) \rightarrow \text{Sym}^d([0,1] \times \mathbb{R})$$

(where here  $d$  depends on the homotopy class of  $B$ ), and the evaluation map from Lemma 11.10. Indeed, by Lemma 11.10, it follows that  $RQ(\mathcal{H}^{\parallel}) \cong RQ'(\mathcal{H}')$ .

Adding  $\beta_{g+m+n}$ ,  $Z_1^{\parallel}$ , and  $\hat{\alpha}_{2n}$  to  $\mathcal{H}'$  in the same manner, we obtain an isomorphism  $RQ'(\mathcal{H}') \cong RQ^x(\mathcal{H}^{\parallel, x})$ .  $\square$

We now have all the ingredients to prove the following:

**Proof of Proposition 11.7.** Combine Lemma 11.8 and Proposition 11.11.  $\square$

## 12. SOME ALGEBRAICALLY DEFINED BIMODULES

Having defined the holomorphic objects of study, we now turn to their computation. In [22], we associated bimodules to crossings, maxima, and minima. Their description did not involve pseudo-holomorphic curves: rather, they were defined via explicit, algebraic descriptions. These bimodules were defined over the algebra  $\mathcal{A}$ , and some versions were defined over a related algebra  $\mathcal{A}'$ . In this section, we adapt these constructions to the curved framework. These modified bimodules will play a central role in an explicit computation of the holomorphic objects (e.g. Theorem 1.1 and Theorem 14.1 below).

**12.1. Algebraically defined, curved bimodules.** Consider the  $DA$  bimodules from [22] associated to a positive crossings, a negative crossing, a maximum, and a minimum,  $\mathcal{A}_2 \mathcal{P}_{\mathcal{A}_1}^i$ ,  $\mathcal{A}_2 \mathcal{N}_{\mathcal{A}_1}^i$ ,  $\mathcal{A}_2 \Omega_{\mathcal{A}_1}^c$ , and  $\mathcal{A}_2 \mathcal{U}_{\mathcal{A}_1}^c$ . (We suppress here the parameters (matching and strand numbers) of the algebras appearing in these bimodules.) By slightly modifying the construction, we obtain corresponding curved bimodules over  $\mathcal{B}^*$ , which are related to the original bimodule as follows:

**Proposition 12.1.** *There are curved bimodules associated to crossings, maxima, and minima over  $\mathcal{B}$ ,  $\mathcal{B}_2^* \mathcal{P}_{\mathcal{B}_1^*}^i$ ,  $\mathcal{B}_2^* \mathcal{N}_{\mathcal{B}_1^*}^i$ ,  $\mathcal{B}_2^* \Omega_{\mathcal{B}_1^*}^c$ , and  $\mathcal{B}_2^* \mathcal{U}_{\mathcal{B}_1^*}^c$ , which are related to the corresponding bimodules over  $\mathcal{A}$  defined in [22] by the following relations:*

$$\begin{aligned} \mathcal{A}_2 T_{\mathcal{B}_2^*} \boxtimes^{\mathcal{B}_2^*} \mathcal{P}_{\mathcal{B}_1^*}^i &\simeq \mathcal{A}_2 \mathcal{P}_{\mathcal{A}_1}^i \boxtimes^{\mathcal{A}_1} T_{\mathcal{B}_1^*} \\ \mathcal{A}_2 T_{\mathcal{B}_2^*} \boxtimes^{\mathcal{B}_2^*} \mathcal{N}_{\mathcal{B}_1^*}^i &\simeq \mathcal{A}_2 \mathcal{N}_{\mathcal{A}_1}^i \boxtimes^{\mathcal{A}_1} T_{\mathcal{B}_1^*} \\ \mathcal{A}_2 T_{\mathcal{B}_2^*} \boxtimes^{\mathcal{B}_2^*} \Omega_{\mathcal{B}_1^*}^c &\simeq \mathcal{A}_2 \Omega_{\mathcal{A}_1}^c \boxtimes^{\mathcal{A}_1} T_{\mathcal{B}_1^*} \\ \mathcal{A}_2 T_{\mathcal{B}_2^*} \boxtimes^{\mathcal{B}_2^*} \mathcal{U}_{\mathcal{B}_1^*}^c &\simeq \mathcal{A}_2 \mathcal{U}_{\mathcal{A}_1}^c \boxtimes^{\mathcal{A}_1} T_{\mathcal{B}_1^*}, \end{aligned}$$

where  $\mathcal{A}_i T_{\mathcal{B}_i^*}$  is the  $\mathcal{B}$ -to- $\mathcal{A}$  transformer from Definition 3.3.

**Proof.** This follows from the fact that the bimodules defined over  $\mathcal{A}$  are “standard” in the sense of [22, Section 2], which we recall presently. First, recall that the algebras  $\mathcal{A}_i$  are equipped with preferred elements  $C_i$ , and each is equipped with a subalgebra  $\mathcal{B}_i \subset \mathcal{A}_i$ , with the property that  $dC_i \in \mathcal{B}_i$ ; indeed,  $dC_i$  is the curvature  $\mu_0^{\mathcal{B}_i}$  associated to the matching. A *standard sequence* is a sequence  $a_1, \dots, a_{\ell-1}$  of elements of  $\mathcal{A}_1$  with the property that each  $a_i$  is either equal to  $C_1$  or it is an element of  $\mathcal{B}_1 \subset \mathcal{A}_1$ .

**Definition 12.2.** *A type  $DA$  bimodule  $\mathcal{A}_2 X_{\mathcal{A}_1}$  is called standard if the following conditions hold:*

(DA-1) *The bimodule  $X$  is finite-dimensional (over  $\mathbb{F}$ ), and it has a  $\mathbb{Q}$ -grading  $\Delta$  and a further grading  $\mathbf{A}$ , as follows. Think of  $\mathcal{A}_i$  as associated to a union of points  $Y_i$ , and fix a cobordism  $W_1$  from  $Y_1$  to  $Y_2$ . The weights of a homogenous algebra element can be viewed as an element of  $H^0(Y_i)$ ; taking the coboundary then induces an element  $\mathbf{A}(a)$  in  $H^1(W, \partial W)$ . These various gradings are related by the formulas:*

$$\begin{aligned} \Delta(\delta_\ell^1(\mathbf{x}, a_1, \dots, a_{\ell-1})) &= \Delta(\mathbf{x}) + \Delta(a_1) + \dots + \Delta(a_{\ell-1}) - \ell + 2 \\ \mathbf{A}(\delta_\ell^1(\mathbf{x}, a_1, \dots, a_{\ell-1})) &= \mathbf{A}(\mathbf{x}) + \mathbf{A}(a_1) + \dots + \mathbf{A}(a_{\ell-1}); \end{aligned}$$

- (This is the condition that  $X$  is adapted to  $W_1$  in the sense of [22, Definition 2.5].)
- (DA-2) The one-manifold  $W$  is compatible with the matching  $M_1$  used in the algebra  $\mathcal{A}_1$ , in the sense that  $W \cup W(M_1)$  has no closed components.
- (DA-3) For any standard sequence of elements  $a_1, \dots, a_{\ell-1}$  with at least some  $a_i \in \mathcal{B}_1$ ,  $\delta_\ell^1(\mathbf{x}, a_1, \dots, a_{\ell-1}) \in \mathcal{B}_2 \otimes X$ .
- (DA-4) For any  $\mathbf{x} \in X$ ,

$$C^2 \otimes \mathbf{x} + \sum_{\ell=0}^{\infty} \delta_{1+\ell}^1(\mathbf{x}, \overbrace{C^1, \dots, C^1}^{\ell}) \in \mathcal{B}_2 \otimes X.$$

If  $\mathcal{A}_2 X_{\mathcal{A}_1}$  is standard in the above sense, then the actions on  $\mathcal{A}_2 X_{\mathcal{A}_1} \boxtimes^{\mathcal{A}_1} T_{\mathcal{B}_1}^*$  are sums of actions on  $X$  where the input is a standard sequence in the above sense. It follows from Property (DA-3) that the output lies in  $\mathcal{B}_2$ , except in the special case of the  $\delta_1^1$  action on the tensor product, in which case Proposition (DA-4) expresses the output in  $\mathcal{B}_2 \otimes X$  plus  $C^2 \otimes X$ . Dropping the term in  $C^2 \otimes X$ , we obtain actions defining  $\mathcal{B}_2^* X_{\mathcal{B}_1}^*$ . As the notation suggests, the operations so defined give a curved DA bimodule. Indeed, the curved bimodule relations can be seen as direct consequence of the ordinary bimodule relations for  $\mathcal{A}_2 X_{\mathcal{A}_1}$ : in our construction of  $\mathcal{B}_2 X_{\mathcal{B}_1}$ , we have dropped the term  $C^2 \otimes \mathbf{x}$ , but its contribution to the  $\mathcal{A}_\infty$  relation in  $\mathcal{B}_2 \otimes X$  is precisely  $(\partial C^2) \otimes \mathbf{x} = \mu_0^{\mathcal{B}_2} \otimes \mathbf{x}$ ; moreover, the terms involving for  $\mu_0^{\mathcal{B}_1}$  account for the terms in the  $\mathcal{A}_\infty$  relation containing  $\partial C^1$ .

By construction,

$$\mathcal{A}_2 T_{\mathcal{B}_2}^* \boxtimes^{\mathcal{B}_2^*} X_{\mathcal{B}_1}^* = \mathcal{A}_2 X_{\mathcal{A}_1} \boxtimes^{\mathcal{A}_1} T_{\mathcal{B}_1}^* :$$

The proposition now follows since all the bimodules listed above are standard. (See [22, Proposition 3.3 and Theorems 5.3 and 7.10].)  $\square$

(Note that the actions on  $\mathcal{B}_2^* X_{\mathcal{B}_1}^*$  are precisely the actions  $\gamma_k$  defined in [22, Section 13].)

**12.2. Bimodules over  $\mathcal{A}'$ .** Recall that in [22], we considered an algebra  $\mathcal{A}'$  that was dual to  $\mathcal{A}$ . Sometimes, it is convenient to work with bimodules over this algebra (and its quotient, described in Subsection 12.3).

It is natural to consider idempotents in  $\mathcal{A}'$  that are complementary to those in  $\mathcal{A}$ . In the present paper, when we write  $\mathcal{B}^*$ , we understand  $\mathcal{B}(2n, n)$ , with curvature specified by some matching  $M$ . Correspondingly, when we write  $\mathcal{A}'$  without decoration, we understand  $\mathcal{A}'(2n, n+1, M)$  from [22].

In [22, Section 6], we constructed bimodules associated to crossings over the algebras  $\mathcal{A}'$ , denoted  $\mathcal{A}'_1 \mathcal{P}_{\mathcal{A}'_2}^i$  and  $\mathcal{A}'_1 \mathcal{N}_{\mathcal{A}'_2}^i$ , which become homotopy equivalent to the type DA bimodule over  $\mathcal{A}$ , after tensoring with the canonical DD bimodule. (See Proposition 12.6 below). Before giving the precise statement, we describe a similar bimodule for a local minimum, as well. (This latter bimodule was not needed in [22]; rather, it was sufficient to have only its corresponding type DD module.)

12.2.1. *The local minimum*  $\mathcal{A}'_1 \mathcal{U}_{\mathcal{A}'_2}^c$ . Let  $\mathcal{B}_2 \mathcal{U}_{\mathcal{B}_1}^c$  denote the DA bimodule for a minimum from [22]. We define now the corresponding DA bimodule  $\mathcal{A}'_1 \mathcal{U}_{\mathcal{A}'_2}^c$  (i.e. where the input algebra  $\mathcal{A}'_2$  has 2 fewer strands than the output algebra  $\mathcal{A}'_1$ ). This discussion is very similar to the construction of the corresponding bimodule for a local maximum (over  $\mathcal{A}$ ) from [22, Section 5]; see also [21, Section 7].

Let  $\phi_c: \{1, \dots, 2n\} \rightarrow \{1, \dots, 2n+2\}$  be the map

$$(12.1) \quad \phi_c(j) = \begin{cases} j & \text{if } j < c \\ j+2 & \text{if } j \geq c. \end{cases}$$

Let

$$(12.2) \quad \mathcal{A}'_1 = \mathcal{A}'(n+1, M_1) \quad \text{and} \quad \mathcal{A}'_2 = \mathcal{A}(n, M_2),$$

where  $M_2$  is obtained from  $M_1$  by the property that:

$$(12.3) \quad \begin{aligned} &\{\phi_c(i), \phi_c(j)\} \in M_1 \Rightarrow \{i, j\} \in M_2; \\ &\{c, \phi_c(s)\}, \{c+1, \phi_c(t)\} \in M_1 \Rightarrow \{s, t\} \in M_2. \end{aligned}$$

We call an idempotent state  $\mathbf{y}$  for  $\mathcal{A}'_1$  an *allowed idempotent state* for  $\mathcal{A}'_1$  if

$$(12.4) \quad |\mathbf{y} \cap \{c-1, c, c+1\}| \leq 2 \quad \text{and} \quad c \in \mathbf{y}.$$

There is a map  $\psi'$  from allowed idempotent states  $\mathbf{y}$  for  $\mathcal{A}'_1$  to idempotent states for  $\mathcal{B}_2(n)$ , where  $\mathbf{x} = \psi'(\mathbf{y}) \subset \{0, \dots, 2n\}$  is characterized by

$$(12.5) \quad |\mathbf{y} \cap \{c-1, c, c+1\}| + |\mathbf{x} \cap \{c-1\}| = 2 \quad \text{and} \quad \phi_c(\mathbf{x}) \cap \mathbf{y} = \emptyset.$$

Similarly, we can define  $\psi$  from idempotent states for  $\mathcal{A}'_1$  to idempotent states for  $\mathcal{A}'_2$  by

$$(12.6) \quad \psi(\mathbf{y}) = \{0, \dots, 2n\} \setminus \psi'(\mathbf{y}).$$

We have the following:

**Lemma 12.3.** *If  $\mathbf{x}$  is an allowed idempotent state (for  $\mathcal{A}'_1$ ) and  $\mathbf{y}$  is an idempotent state for  $\mathcal{A}'_2$  so that  $\psi(\mathbf{x})$  and  $\mathbf{y}$  are close enough (i.e.  $\mathbf{I}_{\psi(\mathbf{x})} \cdot \mathcal{B}_1 \cdot \mathbf{y} \neq 0$ ), then there is an allowed idempotent state  $\mathbf{z}$  (for  $\mathcal{A}'_1$ ) with  $\psi(\mathbf{z}) = \mathbf{y}$  so that there is a map*

$$\Phi_{\mathbf{x}}: \mathbf{I}_{\psi(\mathbf{x})} \cdot \mathcal{A}'_2 \cdot \mathbf{I}_{\mathbf{y}} \rightarrow \mathbf{I}_{\mathbf{x}} \cdot \mathcal{A}'_1 \cdot \mathbf{I}_{\mathbf{z}}$$

with the following properties:

- $\Phi_{\mathbf{x}}$  maps the portion of  $\mathbf{I}_{\psi(\mathbf{x})} \cdot \mathcal{B}_2 \cdot \mathbf{I}_{\mathbf{y}}$  with weights  $(v_1, \dots, v_{2n})$  surjectively onto the portion of  $\mathbf{I}_{\mathbf{x}} \cdot \mathcal{B}_1 \cdot \mathbf{I}_{\mathbf{z}}$  with  $w_{\phi_c(i)} = v_i$  and  $w_c = w_{c+1} = 0$ ,
- $\Phi_{\mathbf{x}}$  further satisfies the relations

$$\Phi_{\mathbf{x}}(U_i \cdot a) = U_{\phi_c(i)} \cdot \Phi_{\mathbf{x}}(a)$$

$$\Phi_{\mathbf{x}}(E_i \cdot a) = \begin{cases} E_{\phi_c(i)} \cdot \Phi_{\mathbf{x}}(a) & \text{if } i \neq t \\ (E_{\phi_c(t)} + E_c \llbracket E_{\phi_c(t)}, E_{c+1} \rrbracket) \cdot \Phi_{\mathbf{x}}(a) & \text{if } i = t \end{cases}$$

for any  $i \in 1, \dots, 2n$  and  $a \in \mathbf{I}_{\psi(\mathbf{x})} \cdot \mathcal{A}'_2 \cdot \mathbf{I}_{\mathbf{y}}$ .

Moreover, the state  $\mathbf{z}$  is uniquely characterized by the existence of such a map  $\Phi_{\mathbf{x}}$ .

**Proof.** This is a straightforward adaptation of [22, Lemma 5.2]; the only novelty is that here we are using the algebra elements  $E_i$  extending  $\mathcal{B}$  to  $\mathcal{A}'$  rather than the algebra elements  $C_p$  extending  $\mathcal{B}$  to  $\mathcal{A}$  as in that lemma.  $\square$

**Definition 12.4.** Let  $\mathcal{A}'_1 \mathcal{U}_{\mathcal{A}'_2}^c$  be the vector space generated by elements  $\mathbf{Q}_y$  generated by allowed idempotent states  $y$  for  $\mathcal{A}'_1$ . Endow this with the structure of a  $I(\mathcal{A}'_1) - I(\mathcal{A}'_2)$  bimodule by

$$\mathbf{I}_{\psi(y)} \cdot \mathbf{Q}_y \cdot \mathbf{I}_y = \mathbf{Q}_y.$$

Let

$$\delta_1^1: \mathcal{A}'_1 \Omega_{\mathcal{A}'_2}^c \rightarrow \mathcal{A}'_1 \otimes_{\mathcal{A}'_1} \Omega_{\mathcal{A}'_2}^c$$

be the map specified by

$$\delta_1^1(\mathbf{Q}_y) = \mathbf{I}_y \cdot (R_{c+1}R_c + L_cL_{c+1} + U_cE_{c+1}) \otimes \sum_{\mathbf{z}} \mathbf{Q}_{\mathbf{z}}.$$

where the sum is taken over all allowed idempotents  $\mathbf{z}$  for  $\mathcal{A}'_2$ . Let

$$\delta_2^1: \mathcal{A}'_1 \Omega_{\mathcal{A}'_2}^c \otimes \mathcal{A}'_2 \rightarrow \mathcal{A}'_1 \otimes_{\mathcal{A}'_1} \Omega_{\mathcal{A}'_2}^c$$

be the map characterized by the property that if  $a = \mathbf{I}_{\psi(\mathbf{x})} \cdot a \cdot \mathbf{I}_y \in \mathcal{A}'_1$  is a non-zero algebra element, then  $\delta_2^1(\mathbf{Q}_{\mathbf{x}} \cdot a) = \Phi_{\mathbf{x}} \cdot \mathbf{Q}_{\mathbf{z}}$ , where  $\mathbf{z}$  is as in Lemma 12.3.

**Proposition 12.5.** The above specified actions  $\delta_1^1$  and  $\delta_2^1$  (and  $\delta_\ell^1 = 0$  for all  $\ell > 2$ ) give  $\mathcal{A}'_2 \mathcal{U}_{\mathcal{A}'_1}^c$  the structure of a DA bimodule, equipped with a  $\Delta$ -grading and a grading by  $H^1(W, \partial)$ , where  $W$  is the one-manifold specified in the diagram.

**Proof.** The proof is straightforward. (Compare [22, Theorem 5.3].) The differential of the term  $E_c \llbracket E_{c+1}, E_t \rrbracket$  in  $\Phi_{\mathbf{x}}(E_s)$ , which is  $U_c \cdot \llbracket E_{c+1}, E_t \rrbracket$ , cancels against the anti-commutator of the other term in  $\Phi_{\mathbf{x}}(E_t)$ ,  $E_{\phi_c(t)}$ , with the term  $\delta_1^1(\mathbf{x}) = U_c \cdot E_{c+1}$ .  $\square$

**12.2.2. DA bimodules over  $\mathcal{A}'$ .** The bimodule over  $\mathcal{A}'$  associated to a local minimum defined above and the bimodules over  $\mathcal{A}'$  associated to crossings in [22, Section 3.4] are related to the corresponding bimodules over  $\mathcal{A}$ .

In a little more detail, given an integer  $n$ , a matching  $M$  on  $\{1, \dots, 2n\}$ , and an integer  $i \in 1, \dots, 2n - 1$ , there are associated algebras which we abbreviate  $\mathcal{A}_1$ ,  $\mathcal{A}'_1$ ,  $\mathcal{A}_2$ , and  $\mathcal{A}'_2$ , and imodules  $\mathcal{A}_2 \mathcal{P}_{\mathcal{A}_1}^i$  and  $\mathcal{A}_2 \mathcal{N}_{\mathcal{A}_1}^i$ . In [22, Section 3.4], we also associated bimodules  $\mathcal{A}'_1 \mathcal{P}_{\mathcal{A}'_2}$  and  $\mathcal{A}'_1 \mathcal{N}_{\mathcal{A}'_2}$ .

**Proposition 12.6.** For algebras  $\mathcal{A}_j$  and  $\mathcal{A}'_j$  as above, we have relations

$$\begin{aligned} \mathcal{A}_2 \mathcal{P}_{\mathcal{A}_1}^i \boxtimes^{\mathcal{A}_1, \mathcal{A}'_1} \mathcal{K} &\simeq^{\mathcal{A}'_1} \mathcal{P}_{\mathcal{A}'_2}^i \boxtimes^{\mathcal{A}'_2, \mathcal{A}_1} \mathcal{K} \\ \mathcal{A}_2 \mathcal{N}_{\mathcal{A}_1}^i \boxtimes^{\mathcal{A}_1, \mathcal{A}'_2} \mathcal{K} &\simeq^{\mathcal{A}'_1} \mathcal{N}_{\mathcal{A}'_2}^i \boxtimes^{\mathcal{A}'_2, \mathcal{A}_2} \mathcal{K} \end{aligned}$$

Similarly, now using algebras  $\mathcal{A}'_j$  as in Equation 12.2 (and corresponding algebras  $\mathcal{A}_j$ ), we have that

$$\mathcal{A}_2 \mathcal{U}_{\mathcal{A}_1} \boxtimes^{\mathcal{A}_1, \mathcal{A}'_1} \mathcal{K} \simeq^{\mathcal{A}'_1} \mathcal{U}_{\mathcal{A}'_2} \boxtimes^{\mathcal{A}'_2, \mathcal{A}_2} \mathcal{K}$$

**Proof.** Note that the  $DA$  bimodules over  $\mathcal{A}'$  are all bounded, so the above tensor products all make sense. The relation involving the positive crossing is [22, Proposition 3.3]. The relationship with the negative crossing follow formally, since both negative crossing bimodules are constructed as “opposite modules” to the positive crossing bimodules; see [22, Definition 3.5 and Subsection 6.2].

For the relation involving the minimum, note that in [22, Section 7.1], we defined the type  $DD$  bimodule associated to a minimum, denoted  $\mathcal{A}, \mathcal{A}' \mathcal{U}$ . In Theorem 7.10, it is verified that

$$\mathcal{A}_2 \mathcal{U}_{\mathcal{A}_1}^c \boxtimes^{\mathcal{A}_1, \mathcal{A}'_1} \mathcal{K} \simeq^{\mathcal{A}_2, \mathcal{A}'_1} \mathcal{U}.$$

The similar verification that

$$\mathcal{A}_2, \mathcal{A}'_1 \mathcal{U} \simeq^{\mathcal{A}'_1} \mathcal{U}_{\mathcal{A}'_2} \boxtimes^{\mathcal{A}'_2, \mathcal{A}_2} \mathcal{K}$$

is a straightforward exercise in the definitions.  $\square$

**Remark 12.7.** Observe that for all  $X \in \mathcal{U}^c$ ,  
(12.7)

$$\delta_2^1(X, \llbracket E_i, E_j \rrbracket) = \begin{cases} \llbracket E_{\phi_c(i), \phi_c(j)} \rrbracket \otimes X & \text{if } \{i, j\} \in M_2, \{i, j\} \neq \{s, t\} \\ \llbracket E_{\phi_c(s)}, E_c \rrbracket \cdot \llbracket E_{\phi_c(t)}, E_{c+1} \rrbracket \otimes X & \text{if } \{i, j\} = \{s, t\}. \end{cases}$$

**12.3. A new algebra  $\mathcal{A}''$ .** We will find it convenient to work in a quotient of  $\mathcal{A}'$ . Specifically, let  $\mathcal{A}''$  be the quotient of  $\mathcal{A}'$  by the relations  $\llbracket E_i, E_j \rrbracket = 1$  for all  $\{i, j\} \in M$ . There is a quotient map  $q: \mathcal{A}' \rightarrow \mathcal{A}''$ .

Recall that  $\mathcal{A}'$  is equipped with a  $\Delta$ -grading defined by

$$\Delta(a) = \#(E_j \text{ that divide } a) - \sum_i \mathbf{w}_i(a).$$

Since  $\llbracket E_i, E_j \rrbracket$  is homogeneous with  $\Delta(\llbracket E_i, E_j \rrbracket) = 0$ , it follows that the  $\Delta$  grading descends to  $\mathcal{A}''$ .

The weight vector, which was a grading on  $\mathcal{A}'$ , no longer descends to  $\mathcal{A}''$ . However, there is an Alexander grading on  $\mathcal{A}'$ , induced by the matching and the orientation on its associated one-manifold, defined by

$$\mathbf{A}(a) = \bigoplus_{\{i, j\} \in M} \mathbf{w}_i(a) - \mathbf{w}_j(a),$$

where  $W$  represents an arc oriented from  $i$  to  $j$ . This grading descends to  $\mathcal{A}''$ .

Evidently, the set of algebra elements in  $\mathcal{A}''$  with a fixed  $\Delta$ -grading is finite-dimensional (unlike for  $\mathcal{A}'$ ). It follows that bimodules over  $\mathcal{A}''$  automatically satisfy the boundedness properties required to form their tensor products, as in [22, Proposition 2.7]. Specifically, a bimodule is called *adapted*  $W$  if it has a grading by  $\mathbb{Q}$  and  $H^1(W)$ , as in Property (DA-1) from Definition 12.2 (using the algebras  $\mathcal{A}''$  in place of  $\mathcal{A}$ , equipped with the above Alexander grading).

**Proposition 12.8.** Choose  $W_1: Y_1 \rightarrow Y_2$ ,  $W_2: Y_2 \rightarrow Y_3$ ,  $\mathcal{A}_1'', \mathcal{A}_2'',$  and  $\mathcal{A}_3''$  as above. Suppose moreover that  $W_1 \cup W_2$  has no closed components, i.e. it is a disjoint union of finitely many intervals joining  $Y_1$  to  $Y_3$ . Given any two bimodules  $\mathcal{A}_2'' X_{\mathcal{A}_1''}^1$  and  $\mathcal{A}_3'' X_{\mathcal{A}_2''}^2$  adapted to  $W_1$  and  $W_2$  respectively, we can form their tensor product  $\mathcal{A}_3'' X_{\mathcal{A}_2''}^2 \boxtimes \mathcal{A}_2'' X_{\mathcal{A}_1''}^1$  (i.e. only finitely many terms in the infinite

sums in its definition are non-zero); and moreover, it is a bimodule that is adapted to  $W = W_1 \cup W_2$ .

**Proof.** This follows exactly as in [22, Proposition 2.7], in view of the fact that the set of algebra elements in  $\mathcal{A}''$  with a fixed  $\Delta$ -grading is finite-dimensional. (The same property holds for the algebras  $\mathcal{A}$  considered in that proposition.)  $\square$

We construct bimodules over  $\mathcal{A}''$  that are related to bimodules over  $\mathcal{A}'$  in the following:

**Lemma 12.9.** *There are DA bimodules  $\mathcal{A}_1'' \mathcal{P}_{\mathcal{A}_2''}^i$ ,  $\mathcal{A}_1'' n_{\mathcal{A}_2''}^i$ ,  $\mathcal{A}_1'' \mathcal{U}_{\mathcal{A}_2''}^c$  related to the above bimodules by the relations*

$$(12.8) \quad \mathcal{A}_1'' q_{\mathcal{A}_1'} \boxtimes \mathcal{A}_1' \mathcal{U}_{\mathcal{A}_2'}^c \simeq \mathcal{A}_1'' \mathcal{U}_{\mathcal{A}_2''}^c \boxtimes \mathcal{A}_2'' q_{\mathcal{A}_2'}$$

$$(12.9) \quad \mathcal{A}_1'' q_{\mathcal{A}_1'} \boxtimes \mathcal{A}_1' \mathcal{P}_{\mathcal{A}_2'}^i \simeq \mathcal{A}_1'' \mathcal{P}_{\mathcal{A}_2''}^i \boxtimes \mathcal{A}_2'' q_{\mathcal{A}_2'}$$

$$(12.10) \quad \mathcal{A}_1'' q_{\mathcal{A}_1'} \boxtimes \mathcal{A}_1' n_{\mathcal{A}_2'}^i \simeq \mathcal{A}_1'' n_{\mathcal{A}_2''}^i \boxtimes \mathcal{A}_2'' q_{\mathcal{A}_2'}$$

**Proof.** Equation (12.7) ensures that all the operations where some element of the input algebra lies in the ideal in  $\mathcal{A}'$  whose quotient is  $\mathcal{A}''$  have the property that the output is contained in the corresponding ideal in the output algebra. It follows at once that there is an induced module  $\mathcal{A}_1'' \mathcal{U}_{\mathcal{A}_2''}^c$  satisfying Equation (12.8).

The bimodule associated to a positive crossing is constructed in Section [22, Section 6]. It is constructed so that all operations commute with multiplication by  $\llbracket E_i, E_j \rrbracket$ . Specifically, there are relations

$$\delta_2^1(X, \llbracket E_i, E_j \rrbracket \cdot a) = \llbracket E_{\tau(i)}, E_{\tau(j)} \rrbracket \cdot \delta_2^1(X, a)$$

$$\delta_3^1(X, \llbracket E_i, E_j \rrbracket \cdot a_1, a_2) = \delta_3^1(X, a_1, \llbracket E_i, E_j \rrbracket \cdot a_2) = \llbracket E_{\tau(i)}, E_{\tau(j)} \rrbracket \cdot \delta_3^1(X, a_1, a_2),$$

where  $\tau: \{1, \dots, 2n\} \rightarrow \{1, \dots, 2n\}$  is the transposition that switches the two adjacent elements, corresponding to the strands that enter the crossing. (Note that  $\delta_k^1 = 0$  for  $k > 3$ .) It follows at once that there is a bimodule  $\mathcal{A}_1'' \mathcal{P}_{\mathcal{A}_2''}$  satisfying Equation (12.9).

The corresponding construction for the negative crossing follow similarly. (Compare [22, Section 6.2].)  $\square$

We wish to state an analogue of Proposition 12.6, using the algebras  $\mathcal{A}''$ . To this end, we will define the canonical type  $DD$  bimodule  $\mathcal{B}^*, \mathcal{A}'' \mathcal{K}$ . Generators of  $\mathcal{B}^*, \mathcal{A}'' \mathcal{K}$ , as a vector space, correspond to  $n$ -element subsets  $\mathbf{x} \subset \{0, \dots, 2n\}$ , i.e.  $I$ -states for  $\mathcal{B}(2n, n)$ . Let  $K_{\mathbf{x}}$  be the generator corresponding to  $\mathbf{x}$ . The left  $I(2n, n) \otimes I(2n, n+1)$ -module structure is specified by

$$(\mathbf{I}_{\mathbf{x}} \otimes \mathbf{I}_{\{0, \dots, 2n\} \setminus \mathbf{x}}) \cdot K_{\mathbf{x}} = K_{\mathbf{x}}.$$

The differential is specified by the element

$$A = \sum_{i=1}^{2n} (L_i \otimes R_i + R_i \otimes L_i) + \sum_{i=1}^{2n} U_i \otimes E_i \in \mathcal{B} \otimes \mathcal{A}'',$$

$$\delta^1: \mathcal{K} \rightarrow \mathcal{A} \otimes \mathcal{A}'' \otimes \mathcal{K}.$$



by  $\delta^1(v) = A \otimes v$ . That is,  $\mathcal{B}^{\star, \mathcal{A}''} \mathcal{K}$  is obtained from the description of  $\mathcal{A}, \mathcal{A}' \mathcal{K}$  by dropping the terms involving  $C_{\{i,j\}}$ , and then taking the quotient to go from  $\mathcal{A}'$  to  $\mathcal{A}''$ , or, more formally,

$$\mathcal{A} T_{\mathcal{B}^{\star}} \boxtimes^{\mathcal{B}^{\star}, \mathcal{A}''} \mathcal{K} =_{\mathcal{A}_1''} q_{\mathcal{A}'} \boxtimes^{\mathcal{A}', \mathcal{A}} \mathcal{K}.$$

For future reference, we describe analogous type  $DD$  bimodules for a local minimum and for a crossing.

**12.3.1. Algebraically defined curved  $DD$ -bimodule of a local minimum.** Fix some positive integers  $n$  and  $c$ , with  $1 \leq c \leq 2n+1$ , and a matching  $M_1$  on  $\{1, \dots, 2n+2\}$ . Let

$$\mathcal{A}_1'' = \mathcal{A}''(n+1, M_1) \quad \text{and} \quad \mathcal{B}_2^{\star} = \mathcal{B}^{\star}(n, M_2),$$

where  $M_2$  is induced from  $M_1$  as in Equation 12.3. Define  $\mathcal{B}_2^{\star, \mathcal{A}_1''} \mathcal{U}_c = \mathcal{U}$ , as follows.

We call an idempotent state  $\mathbf{y}$  for  $\mathcal{B}_1$  an *allowed idempotent state* for  $\mathcal{B}_1$  if

$$|\mathbf{y} \cap \{c-1, c+1\}| \neq \emptyset \quad \text{and} \quad c \notin \mathbf{y}.$$

Note that the allowed idempotent states  $\mathbf{y}$  for  $\mathcal{B}_1$  are those that are of the form  $\{0, \dots, 2n+2\} \setminus \mathbf{y}'$ , where  $\mathbf{y}'$  is an allowed idempotent state for  $\mathcal{A}_1'$ , in the sense of Equation (12.4).

As a vector space,  $\mathcal{U}$  is spanned by vectors that are in one-to-one correspondence with allowed idempotent states for  $\mathcal{A}_1''$ ; if  $\mathbf{y}$  is an allowed idempotent state for  $\mathcal{A}_1''$ , let  $\mathbf{P}_{\mathbf{y}}$  be its corresponding generator. The bimodule structure, over the rings of idempotents  $I(\mathcal{B}_2) \otimes I(\mathcal{A}_1'')$  is specified by the relation

$$(\mathbf{I}_{\psi(\mathbf{y})} \otimes \mathbf{I}_{\{0, \dots, 2n+2\} \setminus \mathbf{y}}) \cdot \mathbf{P}_{\mathbf{y}} = \mathbf{P}_{\mathbf{y}},$$

where  $\psi$  is as in Equation (12.5).

The differential is specified by the the following element in  $\mathcal{B}_2 \otimes \mathcal{A}_1''$ :

(12.11)

$$\begin{aligned} A'' &= (1 \otimes L_c L_{c+1}) + (1 \otimes R_{c+1} R_c) + \sum_{j=1}^{2n} R_j \otimes L_{\phi(j)} + L_j \otimes R_{\phi_c(j)} + U_j \otimes E_{\phi_c(j)} \\ &\quad + 1 \otimes E_c U_{c+1} + U_s \otimes E_{c+1}. \end{aligned}$$

(Note that in [22, Section 7.1], we described a  $DD$  bimodule  $\mathcal{A}_1'', \mathcal{A}_2 \mathcal{U}_c$  associated to a local minimum. The above description is obtained by eliminating all the terms involving  $C_{i,j}$ , and specializing from  $\mathcal{A}'$  to  $\mathcal{A}''$ .)

The bimodule can be described in a little more detail, in terms of the classification of idempotents for  $\mathcal{A}_1''$  into three types, labelled  $\mathbf{X}$ ,  $\mathbf{Y}$ , and  $\mathbf{Z}$ :

- $\mathbf{y}$  is of type  $\mathbf{X}$  if  $\mathbf{y} \cap \{c-1, c, c+1\} = \{c, c+1\}$ ,
- $\mathbf{y}$  is of type  $\mathbf{Y}$  if  $\mathbf{y} \cap \{c-1, c, c+1\} = \{c-1, c\}$ ,
- $\mathbf{y}$  is of type  $\mathbf{Z}$  if  $\mathbf{y} \cap \{c-1, c, c+1\} = \{c-1, c+1\}$ .

There is a corresponding classification of the generators  $\mathbf{P}_{\mathbf{y}}$  into  $\mathbf{X}$ ,  $\mathbf{Y}$ , and  $\mathbf{Z}$ .

With respect to this decomposition, terms in the differential are of the following four types:

- (P-1)  $R_j \otimes L_{\phi_c(j)}$  and  $L_c \otimes R_{\phi_c(j)}$  for all  $j \in \{1, \dots, 2n\} \setminus \{c-1, c\}$ ; these connect generators of the same type.
- (P-2)  $U_j \otimes E_{\phi_c(j)}$
- (P-3)  $1 \otimes E_c U_{c+1}$
- (P-4)  $U_s \otimes E_{c+1}$
- (P-5) Terms in the diagram below that connect generators of different types.

$$(12.12) \quad \begin{array}{ccc} & & \\ & \xrightarrow{1 \otimes L_c L_{c+1}} & \\ \mathbf{X} & & \mathbf{Y} \\ & \xleftarrow{1 \otimes R_{c+1} R_c} & \\ & & \\ & \swarrow \begin{array}{l} L_{c-1} \oplus R_{c-1} \\ R_{c-1} \oplus L_{c-1} \end{array} \searrow & \swarrow \begin{array}{l} L_c \oplus R_{c+2} \\ R_c \oplus L_{c+2} \end{array} \searrow \\ & & \mathbf{Z} \end{array}$$

With the understanding that if  $c = 1$ , then the terms containing  $L_{c-1}$  or  $R_{c-1}$  are missing; similarly, if  $c = 2n$ , the terms containing  $R_{c+2}$  and  $L_{c+2}$  are missing.

**12.3.2. Algebraically defined curved bimodule of a positive crossing.** We construct the bimodule  $\mathcal{B}_2^*, \mathcal{A}_1'' \mathcal{P}_i$ . Fix  $i$  with  $1 \leq i \leq 2n-1$ , fix a matching  $M$  on  $\{1, \dots, 2n\}$ . Let  $\tau = \tau_i: \{1, \dots, 2n\} \rightarrow \{1, \dots, 2n\}$  be the transposition that switches  $i$  and  $i+1$ , and let  $\tau(M)$  be the induced matching; i.e.  $\{j, k\} \in M$  iff  $\{\tau(j), \tau(k)\} \in \tau(M)$ . Let

$$(12.13) \quad \mathcal{A}_1'' = \mathcal{A}''(n, \tau_i(M)) \quad \text{and} \quad \mathcal{B}_2^* = \mathcal{B}^*(n, M).$$

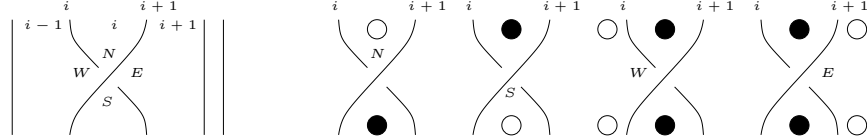


FIGURE 47. **Positive crossing DD bimodule generators.**

The four generator types are pictured to the right.

As an  $I(\mathcal{B}_1) - I(\mathcal{A}_2'')$ -bimodule,  $\mathcal{P}_i$  is the submodule of  $I(\mathcal{B}_1) \otimes_{\mathbb{F}} I(\mathcal{A}_2')$  generated by elements  $\mathbf{I}_{\mathbf{x}} \otimes \mathbf{I}_{\mathbf{y}}$  where  $\mathbf{x} \cap \mathbf{y} = \emptyset$  or

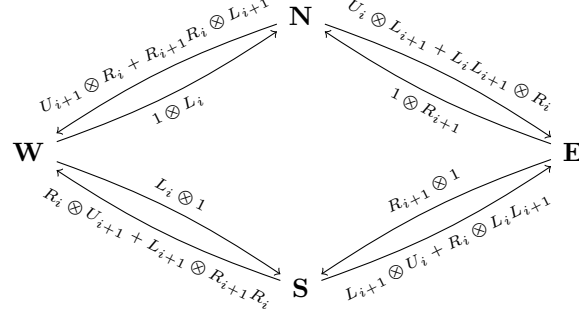
$$(12.14) \quad \mathbf{x} \cap \mathbf{y} = \{i\} \quad \text{and} \quad \{0, \dots, 2n\} \setminus (\mathbf{x} \cup \mathbf{y}) = \{i-1\} \text{ or } \{i+1\}.$$

Generators can be classified into four types, **N**, **S**, **W**, and **E**: for generators of type **N** the subsets  $\mathbf{x}$  and  $\mathbf{y}$  are complementary subsets of  $\{0, \dots, 2n\}$  and  $i \in \mathbf{x}$ ; for generators of type **S**,  $\mathbf{x}$  and  $\mathbf{y}$  are complementary subsets of  $\{0, \dots, 2n\}$  with  $i \in \mathbf{y}$ ; for generators of type **W**,  $i-1 \notin \mathbf{x}$  and  $i-1 \notin \mathbf{y}$ , and  $\mathbf{x} \cap \mathbf{y} = \{i\}$ ; for generators of type **E**,  $i+1 \notin \mathbf{x}$  and  $i+1 \notin \mathbf{y}$ , and  $\mathbf{x} \cap \mathbf{y} = \{i\}$ .

The differential has the following types of terms:

- (P-1)  $R_j \otimes L_j$  and  $L_j \otimes R_j$  for all  $j \in \{1, \dots, 2n\} \setminus \{i, i+1\}$ ; these connect generators of the same type.
- (P-2)  $U_j \otimes E_{\tau(j)}$  for all  $j = 1, \dots, 2n$

(P-3) Terms in the diagram below that connect generators of different types:



(12.15)

Note that for a generator of type **E**, the terms of Type (P-1) with  $j = i + 2$  vanish; while for one of type **W**, the terms of Type (P-1) with  $j = i - 1$  vanish.

There is a  $\mathbb{Q}$ -grading on  $\mathcal{P}_i$  defined by

$$(12.16) \quad \Delta(\mathbf{N}) = \Delta(\mathbf{S}) = \Delta(\mathbf{W}) - \frac{1}{2} = \Delta(\mathbf{E}) - \frac{1}{2},$$

which is homological in the sense that if  $(a \otimes b) \otimes Y$  appears with non-zero coefficient in  $\delta^1(X)$ , then

$$\Delta(X) - 1 = \Delta(Y) + \Delta(a) + \Delta(b) = \Delta(Y) - \omega(a) - \omega(b) + \#(E \text{ in } b).$$

There is an additional  $S = \mathbb{Q}^{2n}$ -valued grading on  $\mathcal{P}_i$ . The grading set can be thought of as the vector space spanned by the strands in the picture.)

Fix a standard basis  $e_1, \dots, e_{2n}$  for  $\mathbb{Q}^{2n}$  (where we can think of  $e_k$  as labelling the strand whose output is the  $k^{\text{th}}$  spot from the left, in the algebra corresponding to  $\mathcal{B}$ ), and set

$$(12.17) \quad \mathbf{gr}(\mathbf{N}) = \frac{e_i + e_{i+1}}{4} \quad \mathbf{gr}(\mathbf{W}) = \frac{e_i - e_{i+1}}{4} \quad \mathbf{gr}(\mathbf{E}) = \frac{-e_i + e_{i+1}}{4} \quad \mathbf{gr}(\mathbf{S}) = \frac{-e_i - e_{i+1}}{4}.$$

This induces an Alexander grading on the bimodule, in the following sense. Let  $\mathbf{A}^M$  denote the Alexander grading on the algebra from Subsection 3.3. Now, if  $(a \otimes b) \otimes Y$  appears with non-zero multiplicity in  $\delta^1(X)$ , then

$$\Pi(\mathbf{gr}(X)) = \mathbf{A}^M(a) - \mathbf{A}^{\tau_i(M)}(b) + \Pi(\mathbf{gr}(Y)),$$

where  $\Pi: \mathbb{Q}^{2n} \rightarrow \mathbb{Q}^n$  is the quotient by the matching.

(More abstractly, if  $W_1$  is the 1-manifold with  $n$  components associated to the matching, and  $W_2$  denotes 1-manifold with  $2n$  components appearing in the picture of the crossing, the map  $\Pi$  is induced by the inclusion map  $H^1(W_2, \partial W_2) \rightarrow H^1(W_2 \cup W_1, \partial W_2 \cup W_1) \cong H^1(W_1, \partial W_1)$ .)

The definition is almost the same as the  $DD$  bimodule  $\mathcal{A}_2, \mathcal{A}'_1 \mathcal{P}_i$  associated to a crossing from [22, Section 3.1], except that the terms involving  $C_{\{i,j\}}$  are dropped; i.e. by its construction, it is clear that

$$\mathcal{A}_1'' q_{\mathcal{A}'_1} \boxtimes^{\mathcal{A}_2, \mathcal{A}'_1} \mathcal{P}_i = \mathcal{A}_2 T_{\mathcal{B}_2^*} \boxtimes^{\mathcal{B}_2^*, \mathcal{A}_1''} \mathcal{P}_i.$$

12.3.3. *Algebraically defined curved bimodule of a negative crossing.* Taking opposite modules, we can form

$$\overline{\mathcal{A}_1, \mathcal{A}'_2 \mathcal{P}_i} = \overline{\mathcal{P}_i}^{\mathcal{A}_1, \mathcal{A}'_2} =_{\mathcal{A}_1^{\text{op}}, (\mathcal{A}'_2)^{\text{op}}} \overline{\mathcal{P}_i}.$$

Combining this with the identification  $o$  of  $\mathcal{A}_1$  and  $\mathcal{A}'_2$  with their opposites (an identification that switches the roles of  $R_i$  and  $L_i$ ), we arrive at a type  $DD$  bimodule, denoted  ${}^{\mathcal{A}_1, \mathcal{A}'_2} \mathcal{N}_i$ . Concretely, we reverse all the arrows in Figure 12.15 and replace algebra elements  $L_j$  and  $R_j$  with  $R_j$  and  $L_j$  respectively (leaving  $U_j$  unmodified).

Note that this is related to the  $DD$  bimodule associated to a crossing  ${}^{\mathcal{A}', \mathcal{A}} \mathcal{P}$  from [22, Section 3.1] by the relation

$${}^{\mathcal{A}} T_{\mathcal{B}^*} \boxtimes^{\mathcal{B}^*, \mathcal{A}''} \mathcal{P} = {}^{\mathcal{A}''} q_{\mathcal{A}'} \boxtimes^{\mathcal{A}', \mathcal{A}} \mathcal{P}.$$

12.4. **Curved  $DA$  bimodules over  $\mathcal{B}$  and those over  $\mathcal{A}''$ .** We have the following analogue of Proposition 12.6:

**Proposition 12.10.** *There is the following relationship between the curved bimodules associated to a minimum  ${}^{\mathcal{B}_2^*} \mathcal{U}_{\mathcal{B}_1^*}^c$ ,  ${}^{\mathcal{B}_2^*} \mathcal{P}_{\mathcal{B}_1^*}^i$ , and  ${}^{\mathcal{B}_2^*} \mathcal{N}_{\mathcal{B}_1^*}^i$  (from Proposition 12.1) and the corresponding  $DA$  bimodules over  $\mathcal{A}''$  (from Lemma 12.9):*

$$\begin{aligned} {}^{\mathcal{B}_2^*} \mathcal{U}_{\mathcal{B}_1^*}^c \boxtimes^{\mathcal{B}_1^*, \mathcal{A}''} \mathcal{K} &\simeq {}^{\mathcal{A}''} \mathcal{U}_{\mathcal{A}_2''}^c \boxtimes^{\mathcal{A}_2'', \mathcal{B}_2^*} \mathcal{K} \\ {}^{\mathcal{B}_2^*} \mathcal{P}_{\mathcal{B}_1^*}^i \boxtimes^{\mathcal{B}_1^*, \mathcal{A}''} \mathcal{K} &\simeq {}^{\mathcal{A}''} \mathcal{P}_{\mathcal{A}_2''}^i \boxtimes^{\mathcal{A}_2'', \mathcal{B}_2^*} \mathcal{K} \\ {}^{\mathcal{B}_2^*} \mathcal{N}_{\mathcal{B}_1^*}^i \boxtimes^{\mathcal{B}_1^*, \mathcal{A}''} \mathcal{K} &\simeq {}^{\mathcal{A}''} \mathcal{N}_{\mathcal{A}_2''}^i \boxtimes^{\mathcal{A}_2'', \mathcal{B}_2^*} \mathcal{K} \end{aligned}$$

**Proof.** It is straightforward to see that  ${}^{\mathcal{B}_1^*} \mathcal{U}_{\mathcal{B}_2^*}^c \boxtimes^{\mathcal{B}_2^*, \mathcal{A}''} \mathcal{K} = {}^{\mathcal{B}_1^*, \mathcal{A}''} \mathcal{U}_c$ , where the latter is the type  $DD$  bimodule from Subsection 12.2.1. The verification:  ${}^{\mathcal{A}''} \mathcal{U}_{\mathcal{A}_2''}^c \boxtimes^{\mathcal{A}_2'', \mathcal{B}_2^*} \mathcal{K} = {}^{\mathcal{B}_1^*, \mathcal{A}''} \mathcal{U}_c$  follows similarly.

The identification  ${}^{\mathcal{B}_2^*, \mathcal{A}''} \mathcal{P}_i = {}^{\mathcal{B}_2^*} \mathcal{P}_{\mathcal{B}_1^*}^i \boxtimes^{\mathcal{B}_1^*, \mathcal{A}''} \mathcal{K}$  is similarly straightforward. A homotopy equivalence  ${}^{\mathcal{A}''} \mathcal{P}_{\mathcal{A}_2''}^i \boxtimes^{\mathcal{A}_2'', \mathcal{B}_2^*} \mathcal{K} \simeq {}^{\mathcal{A}''} \mathcal{P}_i$  is given exactly as in the proof of [22, Lemma 6.2] (where it is shown that  ${}^{\mathcal{A}'_1} \mathcal{P}_{\mathcal{A}'_2}^i \boxtimes^{\mathcal{A}'_2, \mathcal{A}_2} \mathcal{K} \simeq {}^{\mathcal{A}', \mathcal{A}} \mathcal{P}_i$ ).

The relation with a negative crossing follows formally, since  ${}^{\mathcal{B}^*, \mathcal{A}''} \mathcal{K}$  is preserved by the symmetry induced by taking the algebra to its opposite.  $\square$

12.5. **Restricting idempotents.** Consider  $\mathcal{B}(n)$ , and let

$$(12.18) \quad \mathbf{j}(n) = \sum_{\{\mathbf{x} \mid \mathbf{x} \cap \{0, 2n\} = \emptyset\}} \mathbf{I}_{\mathbf{x}}.$$

Recall that  $\mathcal{C}(n)$  is the subalgebra of  $\mathcal{B}(n)$  determined by  $\mathcal{C}(n) = \mathbf{j}(n) \cdot \mathcal{B}(n) \cdot \mathbf{j}(n)$ . We can think of the inclusion map  $i: \mathcal{C}(n) \rightarrow \mathcal{B}(n)$  as a curved type  $DA$  bimodule  ${}^{\mathcal{B}^*(n)} i_{\mathcal{C}^*(n)}$ . As usual, we drop  $n$  (in the notation for  $\mathcal{C}^*$ ,  $\mathcal{B}^*$ , and  $\mathbf{j}$ ) when it clear from the context.

**Lemma 12.11.** *There are DA bimodules  ${}^{c_2^*}\mathcal{P}_{c_1^*}^i$ ,  ${}^{c_2^*}\mathcal{N}_{c_1^*}$ ,  ${}^{c_2^*}\mathcal{U}_{c_1^*}$  related to the above bimodules by the relations*

$$\begin{aligned} {}^{\mathcal{B}_2^*}i_{c_2^*} \boxtimes {}^{c_2^*}\mathcal{P}_{c_1^*} &\simeq {}^{\mathcal{B}_2^*}\mathcal{P}_{\mathcal{B}_1^*} \boxtimes {}^{\mathcal{B}_1^*}i_{c_1^*} \\ {}^{\mathcal{B}_2^*}i_{c_2^*} \boxtimes {}^{c_2^*}\mathcal{N}_{c_1^*} &\simeq {}^{\mathcal{B}_2^*}\mathcal{N}_{\mathcal{B}_1^*} \boxtimes {}^{\mathcal{B}_1^*}i_{c_1^*} \\ {}^{\mathcal{B}_2^*}i_{c_2^*} \boxtimes {}^{c_2^*}\mathcal{U}_{c_1^*} &\simeq {}^{\mathcal{B}_2^*}\mathcal{U}_{\mathcal{B}_1^*} \boxtimes {}^{\mathcal{B}_1^*}i_{c_1^*} \end{aligned}$$

**Proof.** It suffices to notice that all three bimodules  ${}^{\mathcal{B}_2^*}X_{\mathcal{B}_1^*} = {}^{\mathcal{B}_2^*}\mathcal{U}_{\mathcal{B}_1^*}$ ,  ${}^{\mathcal{B}_2^*}\mathcal{P}_{\mathcal{B}_1^*}^i$ , and  ${}^{\mathcal{B}_2^*}\mathcal{N}_{\mathcal{B}_1^*}^i$ , and have the property that if  $X \cdot j = j \cdot X$ , with  $j$  as in Equation (7.2). (Note that  $j$  depends on the underlying algebra; in particular for  $\mathcal{U}$ , the left and right “ $j$ ” differ.) This in turn it follows from properties of these three objects as (ordinary) bimodules over the idempotent algebras; c.f. [22, Proposition 8.2].  $\square$

13. COMPUTING THE  $DD$  BIMODULES OF STANDARD MIDDLE DIAGRAMS

Given an extended middle diagram  $\mathcal{H}^{\parallel, x}$ , we can think of the bimodule

$$\hat{\mathcal{B}} RQ^x(\mathcal{H}^{\parallel, x})_{\hat{\mathcal{B}}} \boxtimes \check{\mathcal{B}}, \check{\mathcal{A}}'' \mathcal{K}$$

as the type  $DD$  bimodule associated to  $\mathcal{H}^{\parallel, x}$ . Our aim here is to compute these bimodules for some standard middle diagrams, expressed in terms of the algebraically defined  $DD$  bimodules from Section 12.

**Theorem 13.1.** *For each number  $n$  of strands equipped with some matching  $\widetilde{M}$ , there are extended middle Heegaard diagrams for local minima (provided that  $\{c, c+1\} \notin \widetilde{M}$ ), positive, and negative crossings, denoted  $\mathcal{H}_c^\cup$ ,  $\mathcal{H}_i^+$ ,  $\mathcal{H}_i^-$ ; and whose associated  $DA$  bimodules  ${}^{\mathcal{B}_2^*}RQ^x(\mathcal{H}_c^\cup)_{\mathcal{B}_1^*}$ ,  ${}^{\mathcal{B}_2^*}RQ^x(\mathcal{H}_i^+)_{\mathcal{B}_1^*}$ ,  ${}^{\mathcal{B}_2^*}RQ^x(\mathcal{H}_i^-)_{\mathcal{B}_1^*}$  are related to the bimodules from Lemma 12.9 by:*

$$(13.1) \quad \mathcal{A}_1'' \mathcal{U}_{\mathcal{A}_2''}^c \boxtimes \mathcal{A}_2', \mathcal{B}_2^* \mathcal{K} \simeq {}^{\mathcal{B}_2^*}RQ^x(\mathcal{H}_c^\cup)_{\mathcal{B}_1^*} \boxtimes \mathcal{B}_1^*, \mathcal{A}_1'' \mathcal{K}$$

$$(13.2) \quad \mathcal{A}_1'' \mathcal{P}_{\mathcal{A}_2''}^i \boxtimes \mathcal{A}_2', \mathcal{B}_2^* \mathcal{K} \simeq {}^{\mathcal{B}_2^*}RQ^x(\mathcal{H}_i^+)_{\mathcal{B}_1^*} \boxtimes \mathcal{B}_1^*, \mathcal{A}_1'' \mathcal{K}$$

$$(13.3) \quad \mathcal{A}_2'' \mathcal{N}_{\mathcal{A}_1''} \boxtimes \mathcal{A}_1', \mathcal{B}_1^* \mathcal{K} \simeq {}^{\mathcal{B}_2^*}RQ^x(\mathcal{H}_i^-)_{\mathcal{B}_1^*} \boxtimes \mathcal{B}_1^*, \mathcal{A}_1'' \mathcal{K}.$$

We split the verification of Theorem 13.1 into parts (Subsections 13.2, 13.3, and 13.4), starting first with a warm-up (Subsection 13.1).

**13.1. The canonical  $DD$  bimodule.** Although this is not logically needed for the subsequent computations, we compute the bimodule associated to the middle diagram for the identity cobordism, as follows:

**Proposition 13.2.** *For the (extended middle) Heegaard diagram  $\mathcal{H}^{\natural}$  for the identity cobordism from Figure 7, stabilized as in Section 11, we have that*

$${}^{\mathcal{B}^*}RQ(\mathcal{H}^{\natural})_{\mathcal{B}^*} \boxtimes \check{\mathcal{B}}, \check{\mathcal{A}}'' \mathcal{K} \simeq {}^{\mathcal{B}^*}, \check{\mathcal{A}}'' \mathcal{K},$$

**Proof.** The stabilized identity diagram Figure 7 is redrawn in Figure 48.

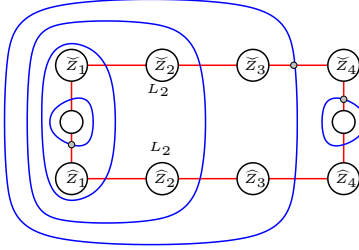


FIGURE 48. Extended middle diagram of the identity, again.

We claim that for the diagram,

$$\delta_2^1(\mathbf{1}, L_i) = L_i \otimes \mathbf{1} \quad \delta_2^1(\mathbf{1}, R_i) = R_i \otimes \mathbf{1}, \quad \delta_2^1(\mathbf{1}, U_i) = U_i \otimes \mathbf{1}.$$

The holomorphic disks counting the first two kinds of actions are polygons (in fact, in cases where  $1 < i < 2n$ , they are rectangles). For example, the rectangles counting the operations

$$\delta_2^1(\mathbf{I}_{\{2,3,4\}}, L_2) = L_2 \otimes \mathbf{I}_{\{1,3,4\}} \quad \delta_2^1(\mathbf{I}_{\{1,3,4\}}, R_2) = R_2 \otimes \mathbf{I}_{\{2,3,4\}}$$

are shown in the top line of Figure 49.

The holomorphic disk representing the action  $\delta_2^1(\mathbf{1}, U_i) = U_i \otimes \mathbf{1}$  is a (twice punctured) annulus, which is the region bounded by  $\beta_{i-1}$  and  $\beta_i$  (labelled so that  $\beta_0$  and  $\beta_{2n}$  encircle the two “middle” boundary components  $Z_0^\parallel$  and  $Z_1^\parallel$ ); but the precise combinatorics are dictated by the idempotent type of the input. When only one of  $i-1$  or  $i$  is present in the in-coming generator, there is a cut from the generator to  $\check{Z}_i$ , and another cut along  $\hat{\alpha}_{i-1} \cup \hat{\alpha}_i$ , which might or might not cut through  $\hat{Z}_i$ . In both cases, this annulus always has an odd number of pseudo-holomorphic representatives that can be realized as branched double-covers of the disk, and the output algebra element is always  $U_i$ .

When both  $i-1$  and  $i$  are present in the in-coming generator, there are two cuts going in towards  $\check{Z}_i$ ; one goes exactly until  $\check{Z}_i$  and the other not quite. The total number of such ends is odd. To see this, we consider the one-dimensional moduli space with the given homotopy class, and which contains the Reeb orbit. This has one end, which is a boundary degeneration. The other ends of this moduli space occur when a cut goes exactly out till  $\check{Z}_i$ ; thus there is an odd number of such ends.

It follows that the generators of  ${}^{\mathcal{B}^*}DA(\mathcal{H}^\natural)_{\mathcal{B}^*} \boxtimes^{\mathcal{B}^*, \mathcal{A}''} \mathcal{K}$  correspond to complementary idempotents, and the terms  $L_i \otimes R_i$ ,  $R_i \otimes L_i$ , and  $U_i \otimes E_i$  appear with non-zero coefficient in the differential.

The  $DD$  bimodule inherits a  $\Delta$ -grading, defined by

$$(13.4) \quad \Delta((a \otimes b) \otimes \mathbf{x}) = \#(E \text{ in } b) - \omega(a) - \omega(b).$$

By the Alexander grading, the coefficients  $(a \otimes b)\mathbf{x}$  in  $\delta^1(\mathbf{y})$  satisfy the relation that  $\omega(a) = \omega(b)$ . Thus,  $L_i \otimes R_i$ ,  $R_i \otimes L_i$ , and  $U_i \otimes E_i$  are all the elements with grading  $-1$ , and all other algebra elements have  $\leq -2$ , so they cannot appear in the differential. It follows that

$${}^{\mathcal{B}^*}DA(\mathcal{H}^\natural)_{\mathcal{B}^*} \boxtimes^{\mathcal{B}^*, \mathcal{A}''} \mathcal{K} = {}^{\mathcal{B}^*, \mathcal{A}''} \mathcal{K}.$$

□

**13.2. A local minimum.** Take the standard middle diagram for the local minimum occurring between strands  $c$  and  $c+1$ , and consider its stabilized middle diagram  $\mathcal{H}_c^\cup$ , as pictured in Figure 50. Equip the strands with a matching  $M$  with  $\{c, c+1\} \notin M$  (i.e., so that  $M$  is compatible with  $\mathcal{H}^\parallel$ .)

We now prove the following:

**Proposition 13.3.** *For each  $n$ , there is a Heegaard diagram for which Equation (13.1) holds.*

**Proof.** It is clear that the Heegaard states are in one-to-one correspondence with allowed idempotents for  $\mathbf{y}$ ; the correspondence is simply given by  $\mathbf{x} \mapsto \check{\alpha}(\mathbf{x})$ .

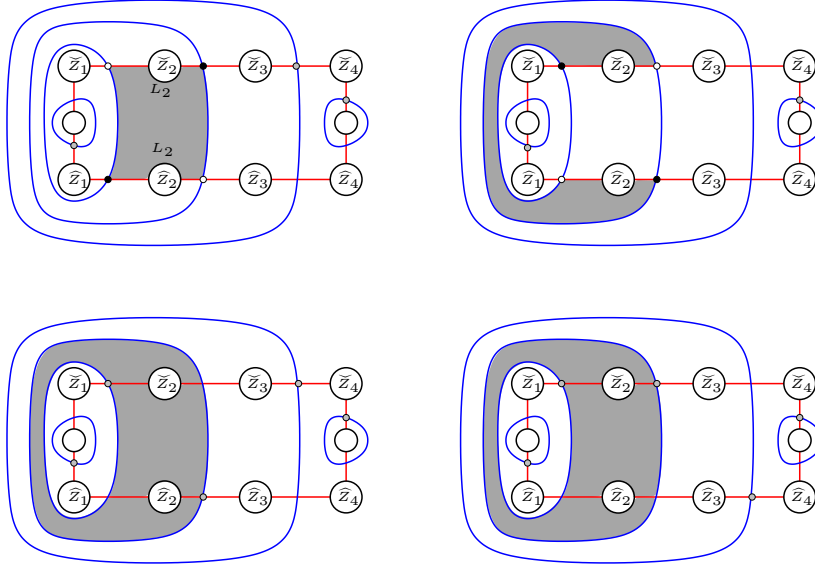


FIGURE 49. **Some holomorphic disks.** Redrawing the picture from Figure 7.

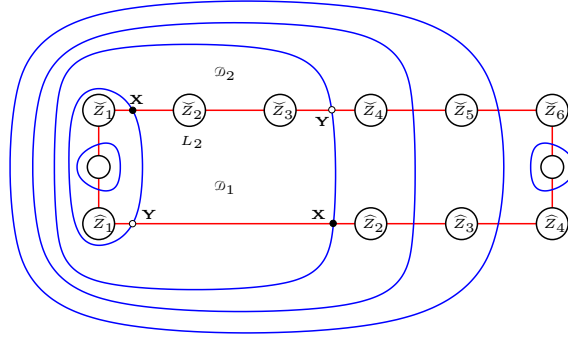


FIGURE 50. **Heegaard diagram for a minimum, stabilized.** Compare Figure 9. We have labelled two domains.

We verify actions that connect different terms of the following form:

$$\begin{array}{ccc}
 1 \otimes (R_c, U_{c+1}, L_c) + U_t \otimes U_c & & 1 \otimes (L_{c+1}, U_c, R_{c+1}) + q \cdot U_s \otimes U_{c+1} \\
 \downarrow & \begin{array}{c} \text{---} 1 \otimes (L_{c+1}, L_c) \text{---} \\ \text{---} 1 \otimes (R_c, R_{c+1}) \text{---} \end{array} & \downarrow \\
 \mathbf{X} & & \mathbf{Y} \\
 \swarrow L_c \oplus L_{c+2} & & \searrow L_{c-1} \oplus L_{c-1} \\
 & \mathbf{Z} & \\
 \nwarrow R_c \oplus R_{c+2} & & \nearrow R_{c-1} \oplus R_{c-1} \\
 & \downarrow & \\
 & 1 \otimes (R_c, U_{c+1}, L_c) + U_t \otimes U_c &
 \end{array}$$



(Note, though, that there are other actions as well.) Here,  $q = 0$  or  $1$  (though we shall see afterwards that it must be  $1$ ). We also prove that  $\delta_2^1(\mathbf{X}, U_{c+1}) = 0 = \delta_2^1(\mathbf{Y}, U_c) = \delta_2^1(\mathbf{Z}, U_{c+1})$ .

To set up the computation, we introduce some notation. Let  $\{\phi_c(s), c\} \in M_1$  and  $\{c+1, \phi_c(t)\} \in M_2$ , and orient the strand through the minimum as indicated in Figure 51; i.e.  $c$  corresponds to an even orbit,  $c+1$  to an odd orbit, and  $\tau(c) = \tau(c+1) = t$ . (See Figure 51.)

The six arrows that connect different generator types are represented by polygons. For example, the verification  $\mathbf{X}$  appears with non-zero multiplicity in  $\delta_3^1(\mathbf{Y}, L_{c+1}, L_c)$  can be seen by considering the quadrialteral (denoted  $\mathcal{D}_1$  in Figure 50), and noting that it represents a unique rigid holomorphic flow-line. Traversing the  $\alpha$ -curves,  $L_{c+1}$  occurs before  $L_c$ .

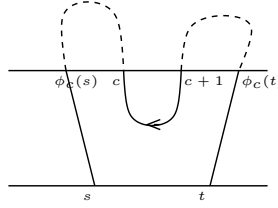


FIGURE 51. **Orienting a local minimum.**

Next we consider other terms from  $\mathbf{X}$  to  $\mathbf{X}$ . Consider holomorphic curves with shadow the annulus,  $\mathcal{D}_1 + \mathcal{D}_2$ . If we cut exactly to  $\check{Z}_c$ , there is a holomorphic disk containing  $e_{c+1}$  in its interior; if we cut further, exactly to  $\check{Z}_{c+1}$ , the holomorphic disk is interpreted as a  $\delta_4^1$ . Thus, this homotopy class gives two terms

$$\mathbf{X} \xrightarrow[\mathcal{D}_1 + \mathcal{D}_2]{U_t \otimes U_c} \mathbf{X} \quad \text{and} \quad \mathbf{X} \xrightarrow[\mathcal{D}_1 + \mathcal{D}_2]{1 \otimes (R_c, U_{c+1}, L_c)} \mathbf{X}.$$

Observe that there are no other holomorphic representatives for this homology class: the order of the algebra elements  $R_c$ ,  $U_{c+1}$ , and  $L_c$  is pre-determined by the order they appear on the  $\alpha$ -arc. Moreover,  $\delta_2^1(\mathbf{X}, U_{c+1}) = 0$ .

Consider next  $\mathbf{Y}$ . In this case, if we cut exactly to  $\check{Z}_{c+1}$ , there is a holomorphic disk containing  $e_c$  in its interior. But this homotopy class alone does not contribute to the differential, since  $e_c$  is an “even” Reeb orbit.

For this to count in an action for the DA bimodule, there must also be some  $v_s$  occurring at the same time. When  $s$  is distinct from  $c-1$  and  $c+2$ , it is easy to find a corresponding action

$$\mathbf{Y} \xrightarrow[\mathcal{D}_1 + \mathcal{D}_2 + \mathcal{D}_s]{U_s \otimes U_{c+1}} \mathbf{Y},$$

for a choice of  $\mathcal{D}_s$  which is an annular domain containing  $\check{Z}_{\phi_c(s)}$  and  $\hat{Z}_s$  in its interior.

Cutting further, we obtain the action

$$\mathbf{Y} \xrightarrow[\mathcal{D}_1 + \mathcal{D}_2]{1 \otimes (L_{c+1}, U_c, R_{c+1})} \mathbf{Y},$$

(which is obvious for any choice of  $s$ ). Moreover,  $\delta_2^1(\mathbf{Y}, U_c) = 0$ .

Tensor with the identity type  $DD$  bimodule, we obtain terms

$$\begin{aligned} \mathbf{X} & \xrightarrow{U_t \otimes E_c + 1 \otimes (U_c E_{c+1})} \mathbf{X} \\ \mathbf{Y} & \xrightarrow{q \cdot (U_s \otimes E_c) + 1 \otimes (E_c U_{c+1})} \mathbf{Y}. \end{aligned}$$

So far, we have verified that  $q = 1$  only under hypotheses on  $s$ ; but  $q = 1$  is forced from algebraic considerations, and the existing other terms, as follows. We refer to the structural equation for a  $DD$  bimodule simply as  $\delta \circ \delta = 0$ : this includes both terms that multiply terms in  $\delta^1$  with other such terms, and terms that differentiate terms in  $\delta^1$ . The term in  $\delta \circ \delta$  arising from anti-commuting the terms  $\mathbf{Y} \mapsto (U_s \otimes E_{\phi_c(s)}) \otimes \mathbf{Y}$  and the above  $\mathbf{Y} \mapsto ((1 \otimes (E_c U_{c+1})) \otimes \mathbf{Y}$  gives a term  $\mathbf{Y} \mapsto (U_s \otimes U_{c+1}) \otimes \mathbf{Y}$ . Note that  $(1 \otimes U_{c+1}) \otimes \mathbf{Y} \neq 0$ , so we need a term in  $\delta \circ \delta$  to cancel this term  $(U_s \otimes U_{c+1}) \otimes \mathbf{Y}$ . In fact, the only possible term that can cancel  $U_s \otimes U_{c+1}$  is the differential of  $U_s \otimes E_{c+1}$ .

Starting at  $\mathbf{Z}$ , the space of almost-complex structures has a chamber structure: pseudo-holomorphic flows correspond to annuli obtained by cutting the annulus  $A = \mathcal{D}_1 \cup \mathcal{D}_2$  in along  $\check{\alpha}_{c-1}$  (from the left) and  $\check{\alpha}_{c+1}$  (from the right). To determine which  $\mathcal{A}_\infty$  operations these induce involves understanding whether the cut from the left reaches the boundary punctures before the cuts on the right.

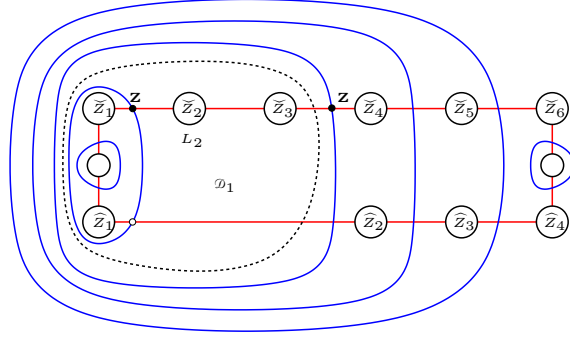


FIGURE 52. **Stretch along the dotted curve.**

Choose a complex structure where the length of the curve  $(\check{\alpha}_{c-1} \cup \check{\alpha}_c) \cap (\mathcal{D}_1 \cup \mathcal{D}_2)$  is much shorter than  $(\check{\alpha}_{c+1} \cup \check{\alpha}_c) \cap (\mathcal{D}_1 \cup \mathcal{D}_2)$ . (This choice is equivalent to stretching sufficiently much normal to the dotted curve in Figure 52.) Thus, for the pseudo-holomorphic flowlines, the cuts from the left reach all the punctures before the cuts from the right. In this case, the annulus supports exactly two non-trivial operations

$$\mathbf{Z} \xrightarrow[\mathcal{D}_1 + \mathcal{D}_2]{U_t \otimes U_c} \mathbf{Z} \quad \text{and} \quad \mathbf{Z} \xrightarrow[\mathcal{D}_1 + \mathcal{D}_2]{1 \otimes (R_c, U_{c+1}, L_c)} \mathbf{Z}$$

(which looks like the operations from  $\mathbf{X}$  to itself.) Thus, as in the case of generators of type  $\mathbf{X}$ , we obtain terms in the  $DD$  bimodule of the form.

$$\mathbf{Z} \xrightarrow{U_t \otimes E_c + 1 \otimes (U_c E_{c+1})} \mathbf{Z}$$

Having verified some of the terms in the type  $DD$  bimodule  ${}^{\mathcal{B}_2}RQ(\mathcal{H}_c^\cup)_{\mathcal{B}_1} \boxtimes^{\mathcal{B}_1, \mathcal{A}_1''} \mathcal{K}$ , algebra also forces some additional terms

$$\begin{aligned} \mathbf{X} &\xrightarrow{1 \otimes L_c L_{c+1} E_c E_{c+1}} \mathbf{Y} \\ \mathbf{Y} &\xrightarrow{1 \otimes R_{c+1} R_c E_c E_{c+1}} \mathbf{X}. \end{aligned}$$

(The first are needed cancel terms in  $\delta \circ \delta$  arising from composing the terms from  $\mathbf{X}$  to  $\mathbf{Y}$  labelled by  $1 \otimes L_c L_{c+1}$ , with terms from  $\mathbf{X}$  to  $\mathbf{X}$  labelled  $1 \otimes U_c E_{c+1}$  or (on the other side) terms from  $\mathbf{Y}$  to  $\mathbf{Y}$  labelled  $1 \otimes E_c U_{c+1}$ . The second terms follow similarly.)

Maslov index considerations allow the following additional types of terms in the differential:  $L_i \otimes R_i E_c E_{c+1}$ ,  $R_i \otimes L_i E_c E_{c+1}$ , and  $U_i \otimes E_i E_c E_{c+1}$ . But these would contribute terms to  $\delta \circ \delta$  that cannot be cancelled. Consider the case where the generator is of type  $\mathbf{X}$ . Then,  $d(U_i \otimes E_i E_c E_{c+1})$  contains the non-zero term  $U_i \otimes E_i E_c U_{c+1}$ , which can be factored as  $(U_i \otimes E_i) \cdot (1 \otimes E_c U_{c+1})$ , but  $1 \otimes E_c U_{c+1}$  does not connect two generators of type  $\mathbf{X}$ . The same argument for type  $\mathbf{Y}$  idempotents, using the other non-zero term  $U_i \otimes E_i U_c E_{c+1}$ , excludes the existence of terms of the form  $U_i \otimes E_i E_c U_{c+1}$ . Similar considerations apply to the other types of terms listed above.

A  $DD$  isomorphism from

$${}^{\mathcal{B}_2}RQ(\mathcal{H}_c^\cup)_{\mathcal{B}_1} \boxtimes^{\mathcal{B}_1, \mathcal{A}_1''} \mathcal{K} \rightarrow {}^{\mathcal{B}_2^*, \mathcal{A}_1''} \mathcal{U}$$

is now defined by

$$h^1(\mathbf{X}) = (1 + E_c E_{c+1}) \otimes \mathbf{X}, \quad h^1(\mathbf{Y}) = \mathbf{Y}, \quad h^1(\mathbf{Z}) = (1 + E_c E_{c+1}) \otimes \mathbf{Z}.$$

□

**13.3. A positive crossing.** Consider a positive crossing between the  $i^{th}$  and  $(i+1)^{st}$  strands.

A Heegaard diagram for this crossing (stabilized) is shown in Figure 53. Our aim here is to verify Theorem 13.1 for this diagram.

There are two cases, according to whether or not  $i$  and  $i+1$  are matched. We consider these two cases separately.

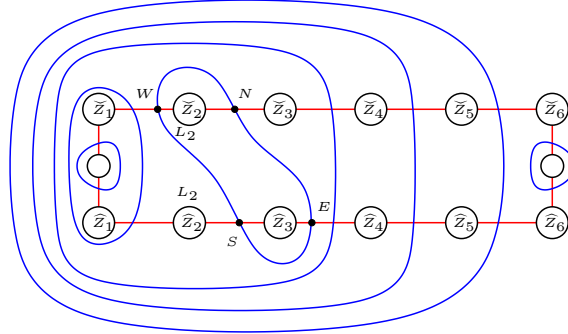
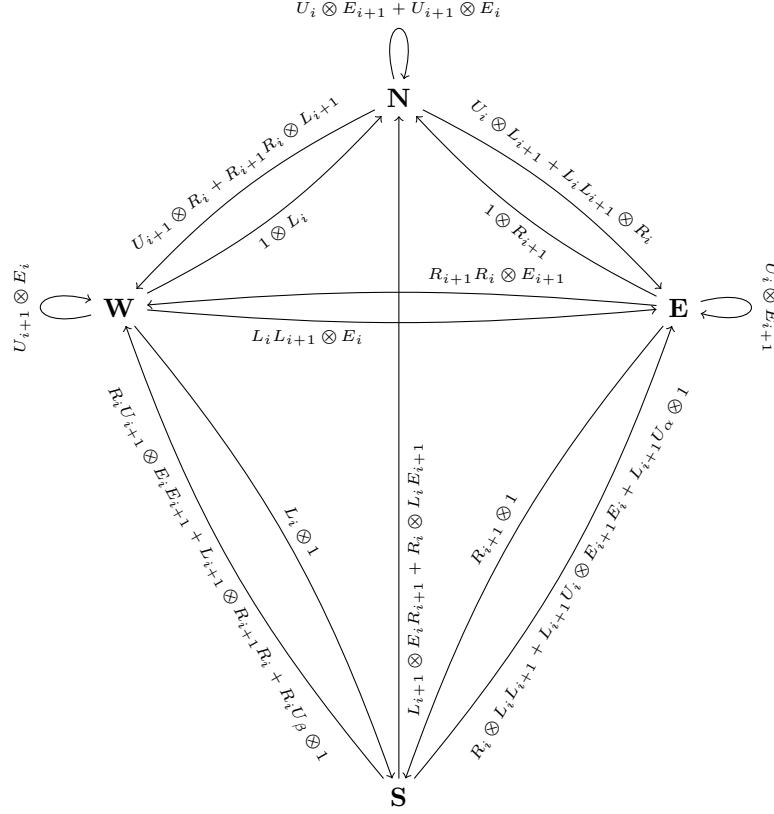


FIGURE 53. **Positive crossing diagram.** Stabilize Figure 10.

FIGURE 54. *DD bimodule of a positive crossing.*

**Lemma 13.4.** *Suppose that  $i$  and  $i + 1$  are not matched; indeed,  $\{\alpha, i\}, \{i + 1, \beta\} \in M_1$ . There is a unique type DD bimodule over  $\mathcal{B}_2, \mathcal{A}_1'' M$  with the following properties:*

- The generators of  $M$  over the idempotent ring are of the four types **N**, **S**, **E**, and **W** as in the bimodule  $\mathcal{B}_2, \mathcal{A}_1' \mathcal{P}_i$  described in Section 12.3.2
- The bimodule  $M$  has a  $\Delta$  grading is as specified in Equation (12.16)
- The bimodule  $M$  has an Alexander grading is as specified in Equation (12.17).
- The **N** coefficient of  $\delta_1^1(\mathbf{N})$  is  $U_i \otimes E_{i+1} + U_{i+1} \otimes E_i + \sum_{j \notin \{i, i+1\}} U_j \otimes E_j$ .
- The **W** coefficient of  $\delta_1^1(\mathbf{W})$  is  $U_{i+1} \otimes E_i + \sum_{j \notin \{i, i+1\}} U_j \otimes E_j$ .
- The **E** coefficient of  $\delta_1^1(\mathbf{E})$  is  $U_i \otimes E_{i+1} + \sum_{j \notin \{i, i+1\}} U_j \otimes E_j$ .
- The **S** coefficient of  $\delta_1^1(\mathbf{S})$  is  $\sum_{j \notin \{i, i+1\}} U_j \otimes E_j$ .
- The **E** coefficient of  $\delta^1(\mathbf{W})$  is  $R_{i+1} R_i \otimes E_{i+1}$ .
- The **W** coefficient of  $\delta^1(\mathbf{W})$  is  $L_i L_{i+1} \otimes E_i$ .

Moreover, there is an isomorphism  $\mathcal{B}_2, \mathcal{A}_1'' M \cong \mathcal{B}_2, \mathcal{A}_1' \mathcal{P}_i$ , where the right-hand-side bimodule is the one described in Section 12.3.2.

**Proof.** Consider the  $\mathbf{N}$  coefficient of  $\delta^1 \circ \delta^1(\mathbf{N})$ . There is a term of  $U_{i+1} \otimes U_i$  coming from differentiating the self-arrows. Gradings now ensure the term can arise only from a term of  $(1 \otimes L_i) \otimes \mathbf{N}$  in  $\delta^1(\mathbf{W})$  and  $(U_{i+1} \otimes R_i) \otimes \mathbf{W}$  in  $\delta^1(\mathbf{N})$ . The coefficient of  $R_i \otimes L_i E_{i+1}$  on the arrow from  $\mathbf{S}$  to  $\mathbf{N}$  is forced from the  $\mathbf{N}$  component of  $\delta^1 \circ \delta^1(\mathbf{W})$ .

The term of  $R_i U_{i+1} \otimes E_{i+1} E_i$  on the arrow from  $\mathbf{S}$  to  $\mathbf{W}$  is forced from the  $\mathbf{W}$  coefficient of  $\delta^1 \circ \delta^1(\mathbf{W})$ . (Note that degree considerations alone allow also for terms  $R_i U_{i+1} \otimes E_i E_{i+1}$  and  $R_i U_{i+1} \otimes 1$ ; but the  $DD$  structure relations and our hypotheses about the existing coefficients eliminates these possibilities.)

Symmetric arguments give  $L_{i+1} \otimes R_{i+1} E_i$  on the arrow from  $\mathbf{S}$  to north,  $L_{i+1} U_i \otimes E_i E_{i+1}$  on the arrow from  $\mathbf{S}$  to  $\mathbf{E}$ .

Now, considering the  $\mathbf{S}$  coefficient for  $\delta^1 \circ \delta^1(\mathbf{N})$  ensures the terms  $R_{i+1} R_i \otimes L_{i+1}$  on the arrow from  $\mathbf{N}$  to  $\mathbf{W}$  and  $L_i L_{i+1} \otimes R_i$  on the arrow from  $\mathbf{N}$  to  $\mathbf{E}$ .

The curvature term in  $\delta^1 \circ \delta^1(\mathbf{W})$  (of  $U_i U_\beta \otimes 1$ ) ensures the arrow from  $\mathbf{S}$  to  $\mathbf{E}$  labelled by  $R_i U_\beta$ .

This constructs all the actions in  $\mathcal{B}_2^*, \mathcal{A}'' M$ . The isomorphism is provided by the map

$$h^1: M \rightarrow \mathcal{P}_i$$

defined by

$$h^1(X) = \begin{cases} \mathbf{S} + (L_2 \otimes E_1) \cdot \mathbf{E} + (R_1 \otimes E_2) \cdot \mathbf{W} & \text{if } X = \mathbf{S} \\ X & \text{otherwise.} \end{cases}$$

□

**Proposition 13.5.** *If  $i$  and  $i + 1$  are unmatched, then Equation (13.2) holds.*

**Proof.** It is straightforward to see that Lemma 13.4 computes  $\mathcal{A}_1'' \mathcal{P}_{\mathcal{A}_2''}^i \boxtimes \mathcal{A}_2'', \mathcal{B}_2^* \mathcal{K}$ .

It remains to verify that there is a complex structure for which  $\mathcal{B}_2^* RQ^x(\mathcal{H}_i^+)_{\mathcal{B}_1^*} \boxtimes \mathcal{B}_1^*, \mathcal{A}_1'' \mathcal{K}$  is also computed by Lemma 13.4.

We consider the actions on  $\mathcal{B}_2^* RQ^x(\mathcal{H}_i^+)_{\mathcal{B}_1^*}$  which could pair to give the actions required by the lemma.

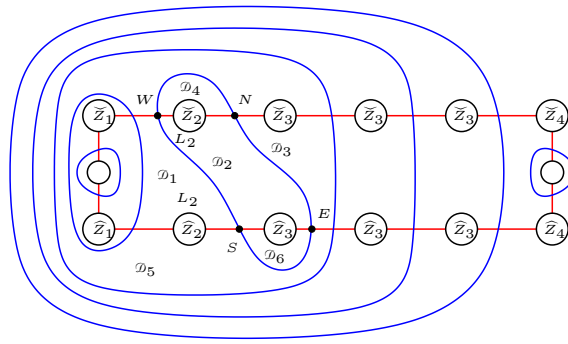


FIGURE 55. Labeling domains in the positive crossing diagram.

Consider labels shown in Figure 55. We have polygons that exhibit actions

For  $X \in \{\mathbf{N}, \mathbf{W}\}$

$$X \xrightarrow[\mathcal{D}_2 + \mathcal{D}_4 + \mathcal{D}_6]{U_{i+1} \otimes U_i} X.$$

For  $X' \in \{\mathbf{S}, \mathbf{E}\}$ , there is no action

$$Y \xrightarrow[\mathcal{D}_2 + \mathcal{D}_4 + \mathcal{D}_6]{U_{i+1} \otimes U_i} Y,$$

as can be seen from the geometry of that bigon.

The following action is given by a polygon, and hence it exists for all choices of almost-complex structure:

$$\mathbf{W} \xrightarrow[\mathcal{D}_1 + \mathcal{D}_2 + \mathcal{D}_4]{L_i L_{i+1} \otimes U_i} \mathbf{E}$$

Consider possible actions

$$(13.5) \quad Y' \xrightarrow[\mathcal{D}_1 + \mathcal{D}_3 + \mathcal{D}_5]{U_i \otimes U_{i+1}} Y'.$$

for  $Y' \in \{\mathbf{S}, \mathbf{W}\}$ . We can choose a complex structure so that neither exists, but

$$(13.6) \quad \mathbf{E} \xrightarrow[\mathcal{D}_1 + \mathcal{D}_3 + \mathcal{D}_5]{R_{i+1} R_i \otimes E_{i+1}} \mathbf{W}$$

exists. This can be seen as follows.

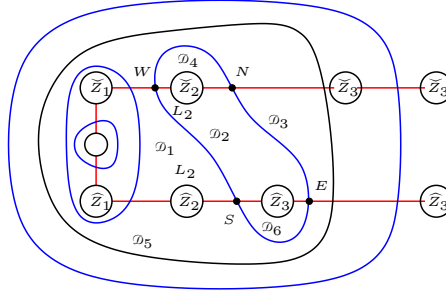


FIGURE 56. Stretch normal to the black curve.

First, we stretch normal to the black curve from Figure 56. In the limit, this curve degenerates to the point  $p$ ; this is indicated in Figure 57 (once we identify the two curves labelled  $p$  to points).

The domain  $\mathcal{D}_3 + \mathcal{D}_5$  can be thought of as the shadow of a pseudo-holomorphic flow from  $\mathbf{S}$  to  $\mathbf{W}$  with Maslov index 0. As the domain is degenerated, the domain decomposes into two regions as shown in Figure 57. One is  $\mathcal{D}'_3 + \mathcal{D}'_5$ , which is now an index one flow from  $\mathbf{S}$  to  $\mathbf{W}$  on the left; and the remaining region which we denote here  $\mathcal{D}''$ , thought of as connecting a generator to itself, and following the Reeb chord covering  $\check{Z}_{i+1}$  once. Both flows contain Reeb orbits at  $p$  in their interior. Let  $s_1 = s \circ \text{ev}_p(m^{\mathcal{D}'_3 + \mathcal{D}'_5}(\mathbf{S}, \mathbf{W}))$  and  $s_2 = s \circ \text{ev}_p(m^{\mathcal{D}''}(x, x; \rho))$ , where  $\rho$  is the length one Reeb orbit that covers  $\check{Z}_{i+1}$  once. We will choose our complex structure so that  $s_1 < s_2$ .

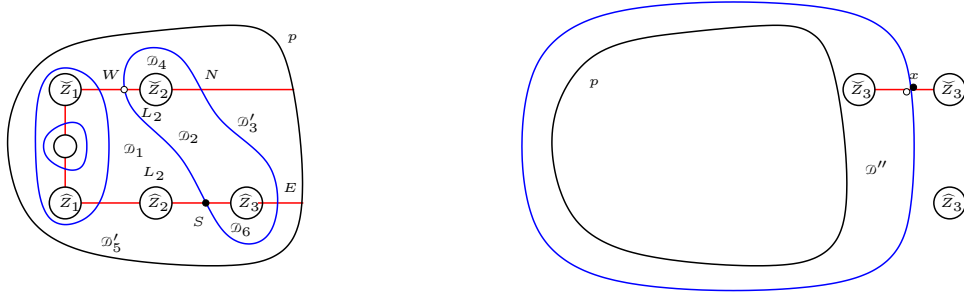


FIGURE 57. Degenerating the black curve from Figure 56.

Consider the maps

(13.7)

$$s \circ \text{ev}_p: \mathcal{M}^{\mathcal{D}_1 + \mathcal{D}_3' + \mathcal{D}_5'}(Y', Y') \rightarrow [0, 1] \quad \text{and} \quad s \circ \text{ev}_p: \mathcal{M}^{\mathcal{D}_3' + \mathcal{D}_5' + \mathcal{D}_6}(\mathbf{E}, \mathbf{W}) \rightarrow [0, 1]$$

We claim that these two moduli spaces map degree one to  $[0, s_1]$  and  $[s_1, 1]$  respectively. For example, consider the first of these maps  $Y' = \mathbf{S}$ . The moduli space  $\mathcal{M}^{\mathcal{D}_1 + \mathcal{D}_3' + \mathcal{D}_5'}(\mathbf{S}, \mathbf{S})$  has two ends: one is a  $\beta$ -boundary degeneration, where  $s \circ \text{ev}_p$  converges to 0; and the other is a broken flowline, juxtaposing the flow with shadow  $\mathcal{D}_1$  from  $\mathbf{S}$  to  $\mathbf{W}$ , followed by the flowline with shadow  $\mathcal{D}_3' + \mathcal{D}_5'$  from  $\mathbf{W}$  to  $\mathbf{S}$ . Here,  $s \circ \text{ev}_p$  converges to  $s_1$ . When  $Y' = \mathbf{W}$ , the order of the two parts of the broken flowline are reversed. It follows that the first map from Equation (13.7) has degree one onto  $[0, s_1]$ . The analysis of the second map from Equation (13.7) follows similarly (except in that case, rather than a boundary degeneration, the flow degenerates to an index one flowline containing a Reeb chord along its  $\alpha$ -boundary).

By the usual stretching arguments, the degree of the first map at  $s_2$  counts the number of representatives of Equation (13.5) (for either choice of  $Y'$ ), while the degree of the second map counts the number of representatives of Equation (13.6). Thus, for our choice of  $s_1 < s_2$ , the actions from Equation (13.5) are excluded and the one from Equation (13.6) is included.

We can now apply Lemma 13.4 to  $\mathcal{B}_2^* RQ^x(\mathcal{H}_i^+)_{\mathcal{B}_1^*} \boxtimes \mathcal{B}_1^* \mathcal{A}_1'' \mathcal{K}$  □

**Proposition 13.6.** *Equation (13.2) holds when  $i$  and  $i + 1$  are matched.*

**Proof.** First note that if  $i$  and  $i + 1$  are matched, then the  $DD$  bimodule of a positive crossing exhibited in Figure 54, with  $\alpha = i + 1$  and  $\beta = i$ , is uniquely characterized by the properties listed in the statement of Lemma 13.4. The proof follows exactly as in the proof of Lemma 13.4. In the present application, note that we expect a curvature term of  $U_i U_{i+1} \otimes 1$  in  $\delta \circ \delta$ .

With this said, the proof of Proposition 13.5 applies. □

#### 13.4. A negative crossing.

**Proposition 13.7.** *For the extended middle diagram for a negative crossing, Equation (13.3) holds.*

**Proof.** Observe that there is a symmetry (which is reflection through a vertical axis in Figure 53) taking the positive crossing diagram to the negative crossing diagram (shown in Figure 58) This switches **W** and **E**,  $i$  and  $2n - i$ , and reverses the orientation of the Heegaard diagram,

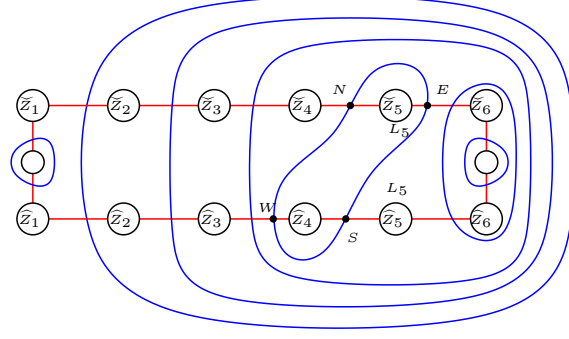


FIGURE 58. The (extended) negative crossing diagram.

Thus, the differential in the type  $DD$  bimodule associated to  $\mathcal{H}_i^-$  is computed by taking the differential the type  $DD$  bimodule  $\mathcal{H}_{2n-i}^+$ , reversing the arrows, switching **W** and **E**, and switching strand  $j$  with strand  $2n - j$ . This operation also transforms  $\mathcal{B}_2^* \mathcal{A}_1'' \mathcal{P}_i$  to the  $DD$  bimodule for  $n_{2n-i}$ .

With these remarks, the proposition follows immediately from Proposition 13.5 or 13.6.  $\square$

**Proof of Theorem 13.1.** The proof follows immediately from Propositions 13.3, 13.5, 13.6. and 13.7.  $\square$



14. COMPUTING THE TYPE  $D$  STRUCTURES OF AN UPPER DIAGRAM

Suppose that  $\hat{\mathbf{D}}$  is an upper knot diagram (thought of as a diagram in an upper half space). After Reidemeister moves and isotopies, we can arrange for all the local maxima of  $\hat{\mathbf{D}}$  to be global maxima, and for each of the local minima and crossings to occur at different heights. We can construct an upper Heegaard diagram for each upper slice of an *acceptable* diagram, as follows. We start from the standard upper diagram corresponding to all the local maxima, and then glue on the standard middle diagrams for the remaining crossings and local minima. In this manner we associate the *canonical upper diagram*  $\mathcal{H}^\wedge(\hat{\mathbf{D}})$  associated to the acceptable diagram  $\hat{\mathbf{D}}$ .

Given an acceptable upper knot diagram  $\hat{\mathbf{D}}$  with  $n$  strands at the bottom and matching  $M$ , there is an associated *algebraically defined type  $D$  structure*  $\mathcal{B}^* R^{alg}(\hat{\mathbf{D}})$ , where  $\mathcal{B}^* = \mathcal{B}^*(n, M)$ , obtained by starting with  ${}^{C^*(n, M)}k$  for the global maxima, and then tensoring with the bimodules  ${}^{C_2^*} \mathcal{P}_{C_1^*}^i$ ,  ${}^{C_2^*} \mathcal{N}_{C_1^*}^i$ ,  ${}^{C_2^*} \mathcal{U}_{C_1^*}^c$  as dictated by the local slices of  $\hat{\mathbf{D}}$ . (This is very closely related to the algebraic description appearing in [22]; see the proof of Theorem 1.1 below.)

**Theorem 14.1.** *Let  $\hat{\mathbf{D}}$  be any acceptable knot diagram  $\hat{\mathbf{D}}$ , and let  $\mathcal{H}^\wedge$  be its associated upper Heegaard diagram. Then there is an identification*

$$(14.1) \quad {}^{C^*(n, M)}R(\mathcal{H}^\wedge) \simeq {}^{C^*(n, M)}R^{alg}(\hat{\mathbf{D}}).$$

We will prove the above theorem at the end of this section. The hypothesis that  $\hat{\mathbf{D}}$  is acceptable is removed in Section 16 (see especially Theorem 16.3); though it is not logically necessary for the computation of knot Floer homology (Theorem 1.1, proved in Section 15).

**Definition 14.2.** *For  $\mathcal{C} = \mathcal{C}(n, M)$ , a type  $D$  structure  ${}^{\mathcal{C}^*}X$  is called relevant if there is an  $\mathcal{A}_\infty$  module  $Z_{\mathcal{A}''}$  over  $\mathcal{A}'' = \mathcal{A}''(n, M)$  with the property that*

$${}^{\mathcal{B}^*}i_{\mathcal{C}^*} \boxtimes {}^{\mathcal{C}^*}X = Z_{\mathcal{A}''} \boxtimes {}^{\mathcal{A}'', \mathcal{B}^*}\mathcal{K}.$$

Consider the type  $D$  structure  ${}^{\mathcal{C}^*}k$  from Section 6.1 (which is identified in Lemma 6.6 with the type  $D$  structure of the standard upper diagram). We shall see that  ${}^{\mathcal{C}^*}k$  is relevant, in the sense of Definition 14.2. Since  ${}^{\mathcal{C}^*}k$  is a one-dimensional vector space, so is  $Z_{\mathcal{A}''}$ . The  $\mathcal{A}_\infty$ -actions on this module are fairly complicated. Letting  $\mathbf{x}$  be the generator, we have that

$$\mathbf{x} \cdot E_{2i-1} \cdot E_{2i} + \mathbf{x} \cdot E_{2i} \cdot E_{2i-1} = \mathbf{x};$$

i.e. exactly one of the two following equations holds:

$$\mathbf{x} \cdot E_{2i-1} \cdot E_{2i} = \mathbf{x} \quad \text{or} \quad \mathbf{x} \cdot E_{2i} \cdot E_{2i-1} = \mathbf{x}.$$

Suppose that the first equation holds. Then, applying the  $\mathcal{A}_\infty$  relation with  $\mathbf{x}$ ,  $E_{2i-1}$  and  $E_{2i}$ , we can conclude that exactly one of

$$m_3(\mathbf{x}, E_{2i-1}, U_{2i}) = \mathbf{x} \quad \text{or} \quad m_3(\mathbf{x}, U_{2i-1}, E_{2i}) = \mathbf{x}$$

holds. The  $\mathcal{A}_\infty$  relations then imply many further actions. We organize this construction in the following:

**Lemma 14.3.** *The type  $D$  structure  ${}^{\mathcal{C}^*}k$  is relevant.*

**Proof.** Let  $\mathbf{x}_1$  denote the idempotent state for  $\mathcal{A}''$   $\mathbf{x}_1$  that consists of all odd numbers between 1 and  $2n-1$ , together with 0. Let  $P$  be the right  $\mathcal{B}(2n, n+1)$ -module consisting of  $2^n$  copies of  $\mathbf{I}_{\mathbf{x}_1} \cdot (L_1 L_2 \backslash \mathcal{B}(2n, n+1))$ , indexed by subsets  $S$  of  $\{1, \dots, n\}$ ; i.e.

$$P = \bigoplus_{S \subset \{1, \dots, n\}} P_S,$$

and there are preferred identifications of  $P_S \cong P_T$  for all  $S, T \subset \{1, \dots, n\}$ .

We endow  $P$  with a differential, as follows. Given  $i = 1, \dots, n$ , if  $i \notin S$ , let

$$\partial_i: P_S \rightarrow P_{S \cup \{i\}}$$

be multiplication by  $U_{2i-1}$  (composed with the preferred identification  $P_S \cong P_{S \cup \{i\}}$ ) and

$$\partial_i: P_{S \cup \{i\}} \rightarrow P_S;$$

be multiplication by  $U_{2i}$ . Note that  $\partial = \sum_{i=1}^n \partial_i: P \rightarrow P$  satisfies  $\partial \circ \partial = 0$ . (This follows from the fact that  $\partial^2$  is multiplication by  $z = \sum_{i=1}^n U_{2i-1} U_{2i}$ , and  $\mathbf{I}_{\mathbf{x}_1} \cdot z = \mathbf{I}_{\mathbf{x}_1} \cdot U_1 U_2 = \mathbf{I}_{\mathbf{x}_1} L_1 L_2 \cdot R_2 R_1$ .)

We can extend the action on  $P$  by  $\mathcal{B}(2n, n+1)$  to all of  $\mathcal{A}''$ , as follows. For fixed  $S$  with  $i \notin S$ , let

$$m_2(\cdot, E_{2i-1}): P_S \rightarrow P_{S \cup \{i\}} \quad \text{and} \quad m_2(\cdot, E_{2i}): P_{S \cup \{i\}} \rightarrow P_S$$

be the zero map, while

$$m_2(\cdot, E_{2i}): P_S \rightarrow P_{S \cup \{i\}} \quad \text{and} \quad m_2(\cdot, E_{2i-1}): P_{S \cup \{i\}} \rightarrow P_S$$

are the standard identifications. On each  $P_S$  multiplication by exactly one of  $E_{2i-1} \cdot E_{2i}$  or  $E_{2i} \cdot E_{2i-1}$  is non-zero, and the non-zero one is the preferred identification. It follows that the action by  $\mathcal{A}'$  descends to an action by  $\mathcal{A}''$ . Moreover, if  $\{j, k\}$  are unmatched, then  $E_j \cdot E_k$  acts the same as  $E_k E_j$ . It follows that there is an induced action of  $\mathcal{A}''$  on  $P$ .

We also claim that the homology of  $P$  is one-dimensional, generated by  $P_{\{\}} \cdot \left( \prod_{i=1}^{n-1} R_{2i} \right)$ .

We see this as follows. Let  $Q_j \subset P$  be the vector subspace generated by elements of the form  $b \cdot P_S$  with the property that

$$b = \prod_{i=1}^j R_{2i} \cdot c$$

with  $w_i(c) = 0$  for  $i = 1, \dots, 2j-1$  and  $\{1, \dots, j\} \cap S = \emptyset$ . In particular,  $Q_0 = P \supset Q_1 \supset \dots \supset Q_n$ , and  $Q_n$  is the one-dimensional vector space spanned by  $P_{\{\}} \cdot \left( \prod_{i=1}^{n-1} R_{2i} \right)$ . Observe that  $Q_j$  is a subcomplex. Define

$$H(a \cdot P_S) = \begin{cases} b \cdot (E_{2i-1} \cdot P_S) & \text{if } a = U_{2i-1} \cdot b \text{ and } w_j(b) < 1 \text{ for all } j < 2i-1 \\ b \cdot (E_{2i} \cdot P_S) & \text{if } a = U_{2i} \cdot b \text{ and } w_j(b) < 1 \text{ for all } j < 2i \end{cases}$$

We claim that  $\text{Id} + \partial \circ H + H \circ \partial$  maps  $Q_j$  to  $Q_{j+1}$ . Thus, iterating the chain map  $F = \text{Id} + \partial \circ H + H \circ \partial$   $n$  times, we obtain a chain homotopy contraction of  $P$  onto the one-dimensional subcomplex spanned by  $P_{\{\}} \cdot \left( \prod_{i=1}^{n-1} R_{2i} \right)$ , as claimed.

The homological perturbation lemma now endows the one-dimensional vector space  $Z_{\mathcal{A}''} = H(P, \partial)$ , with an  $\mathcal{A}_{\infty}$  action by  $\mathcal{A}''$ . We claim that  $Z_{\mathcal{A}''} \boxtimes^{\mathcal{A}'', \mathcal{B}^*} \mathcal{K}$  has trivial differential. This follows from the  $\Delta$ -gradings: the algebra output in  $\mathcal{A}''$  of

each element is either 0 (if it is some  $E_i$ )  $-1/2$  (if it is some  $L_i$  or  $R_i$ ). But such sequences of algebra elements act trivially on  $Z_{\mathcal{A}''}$ , for if

$$\Delta(x) = m_{\ell+1}(x, a_1, \dots, a_\ell) = \Delta(x) + \ell - 1 + \Delta(a_1) + \dots + \Delta(a_\ell) \geq \Delta(x) + \frac{\ell}{2} - 1$$

so  $\ell = 1$ . The case where  $\ell = 1$  is excluded since  $m_2(\mathbf{x}, E_i) = 0$ . The case where  $\ell = 2$  is also excluded by direct consideration. Moreover,

$$\mathbf{I}_{\{0,2,\dots,2i,\dots,2n\}} \cdot \left( Z_{\mathcal{A}''} \boxtimes^{\mathcal{A}'', \mathcal{B}^*} \mathcal{K} \right) = Z_{\mathcal{A}''} \boxtimes^{\mathcal{A}'', \mathcal{B}^*} \mathcal{K}.$$

The lemma follows.  $\square$

**Proposition 14.4.** *Let  $C_1^* = C^*(n, M_1)$ . Suppose  ${}^{C_1}X$  is relevant, then*

$$(14.2) \quad {}^{C_2^*} \mathcal{U}_{C_1^*}^c \boxtimes {}^{C_1^*} X \simeq {}^{C_2^*} RQ^x(\mathcal{H}_c^\cup)_{C_1^*} \boxtimes {}^{C_1^*} X$$

$$(14.3) \quad {}^{C_2^*} \mathcal{P}_{C_1^*}^i \boxtimes {}^{C_1^*} X \simeq {}^{C_2^*} RQ^x(\mathcal{H}_i^+)_{C_1^*} \boxtimes {}^{C_1^*} X$$

$$(14.4) \quad {}^{C_2^*} \mathcal{N}_{C_1^*} \boxtimes {}^{C_1^*} X \simeq {}^{C_2^*} RQ^x(\mathcal{H}_i^-)_{C_1^*} \boxtimes {}^{C_1^*} X;$$

and moreover all the type  $D$  structures appearing on the left are relevant.

**Proof.** Consider Equation (14.2). Combining Lemma 12.11, the relevance of  ${}^{\mathcal{B}_1}X$ , and the associativity of tensor product, we have that

$$\begin{aligned} {}^{\mathcal{B}_2^*} i_{C_2^*} \boxtimes ({}^{C_2^*} \mathcal{U}_{C_1^*}^c \boxtimes {}^{C_1^*} X) &\simeq {}^{\mathcal{B}_2^*} \mathcal{U}_{\mathcal{B}_1^*}^c \boxtimes {}^{\mathcal{B}_2^*} i_{C_2^*} \boxtimes {}^{C_1^*} X \\ &\simeq {}^{\mathcal{B}_2^*} \mathcal{U}_{\mathcal{B}_1^*}^c \boxtimes (Z_{\mathcal{A}_1''} \boxtimes^{\mathcal{A}_1'', \mathcal{B}_1^*} \mathcal{K}) \\ &\simeq Z_{\mathcal{A}_1''} \boxtimes ({}^{\mathcal{B}_2^*} \mathcal{U}_{\mathcal{B}_1^*}^c \boxtimes {}^{\mathcal{B}_1^*, \mathcal{A}_1''} \mathcal{K}). \end{aligned}$$

By Proposition 12.10,

$$Z_{\mathcal{A}_1''} \boxtimes ({}^{\mathcal{B}_2^*} \mathcal{U}_{\mathcal{B}_1^*}^c \boxtimes {}^{\mathcal{A}_1'', \mathcal{B}_1^*} \mathcal{K}) \simeq (Z_{\mathcal{A}_1''} \boxtimes^{\mathcal{A}_1''} \mathcal{U}_{\mathcal{A}_2''}^c) \boxtimes^{\mathcal{A}_2'', \mathcal{B}_2^*} \mathcal{K};$$

so  ${}^{C_2^*} \mathcal{U}_{C_1^*}^c \boxtimes {}^{C_1^*} X$  is relevant.

Applying Theorem 13.1 and Proposition 11.7,

$$\begin{aligned} Z_{\mathcal{A}_1''} \boxtimes ({}^{\mathcal{B}_2^*} \mathcal{U}_{\mathcal{B}_1^*}^c \boxtimes {}^{\mathcal{A}_1'', \mathcal{B}_1^*} \mathcal{K}) &\simeq Z_{\mathcal{A}_1''} \boxtimes ({}^{\mathcal{B}_2^*} RQ^x(\mathcal{H}_c^\cup)_{\mathcal{B}_1^*} \boxtimes {}^{\mathcal{B}_1^*, \mathcal{A}_1''} \mathcal{K}) \\ &\simeq {}^{\mathcal{B}_2^*} RQ^x(\mathcal{H}_c^\cup)_{\mathcal{B}_1^*} \boxtimes (Z_{\mathcal{A}_1''} \boxtimes^{\mathcal{A}_1'', \mathcal{B}_1^*} \mathcal{K}) \\ &\simeq {}^{\mathcal{B}_2^*} RQ(\mathcal{H}_c^\cup)_{\mathcal{B}_1^*} \boxtimes {}^{\mathcal{B}_1^*} i_{C_1^*} \boxtimes {}^{C_1^*} X \\ &\simeq {}^{\mathcal{B}_1^*} i_{C_1^*} \boxtimes {}^{C_2^*} RQ(\mathcal{H}_c^\cup)_{C_1^*} \boxtimes {}^{C_1^*} X. \end{aligned}$$

It follows that

$$(14.5) \quad {}^{\mathcal{B}_2^*} i_{C_2^*} \boxtimes {}^{C_2^*} \mathcal{U}_{C_1^*}^c \boxtimes {}^{C_1^*} X \simeq {}^{\mathcal{B}_2^*} i_{C_2^*} \boxtimes {}^{C_2^*} RQ^x(\mathcal{H}_c^\cup)_{C_1^*} \boxtimes {}^{C_1^*} X.$$

Equation (14.2) follows from Equation (14.5) and the following observation: if  ${}^{C_2^*}P$  and  ${}^{C^*}Q$  are any two type  $D$  structures, then

$$\text{Mor}^{C_2^*}(C_2^*P, C_2^*Q) = \text{Mor}^{\mathcal{B}_2^*}({}^{\mathcal{B}_2^*} i_{C_2^*} \boxtimes {}^{C_2^*} P, {}^{\mathcal{B}_2^*} i_{C_2^*} \boxtimes {}^{C^*} Q),$$

since

$${}^{C^*} i^{\mathcal{B}^*} \boxtimes {}^{\mathcal{B}^*} \mathcal{B}_{\mathcal{B}^*} \boxtimes {}^{\mathcal{B}^*} i_{C^*} = \iota \cdot \mathcal{B} \cdot \iota = C^*$$

(with  $\iota$  as in Equation (7.2)); so  ${}^{C_2^*}P \simeq {}^{C_2^*}Q$  iff  ${}^{\mathcal{B}_2^*} i_{C_2^*} \boxtimes {}^{C_2^*} P \simeq {}^{\mathcal{B}_2^*} i_{C_2^*} \boxtimes {}^{C_2^*} Q$ .

Equations (14.3) and (14.4) follows similarly.  $\square$

**Proof of Theorem 14.1.** We prove Theorem 14.1, together with the statement that  ${}^cR(\mathcal{H}^\wedge)$  is homotopy equivalent to a relevant type  $D$  structure, by induction on the sum of the number of crossings and local minima. When this sum is zero,  $\mathcal{H}^\wedge$  is the standard upper diagram, and the theorem follows from Lemma 6.6. Moreover, this module is relevant by Lemma 14.3.

The inductive step is now provided by Proposition 14.4 and Theorem 10.11.  $\square$

**Remark 14.5.** *With a little extra work, one can show that the type  $D$  structure  $R(\mathcal{H}^\wedge)$  is independent of the choice of upper Heegaard diagram  $\mathcal{H}^\wedge$ .*

## 15. COMPARING THE KNOT INVARIANTS

An *acceptable knot diagram*  $\mathbf{D}$  is a diagram for an oriented knot whose local maxima are at the same level, all of whose other events occur at different heights, and whose global minimum is the marked edge; thus, an acceptable knot diagram is obtained from an acceptable upper knot diagram in the sense of Section 14 by adding a single global minimum.

The methods of this paper now give the following explicit computation of knot Floer homology:

**Theorem 15.1.** *Let  $\mathbf{D}$  be an acceptable knot diagram, obtained by adding a global minimum to  $\hat{\mathbf{D}}$ , and let  $\mathcal{H}^\wedge$  be upper diagram associated to  $\hat{\mathbf{D}}$ . Then, there is a homotopy equivalence*

$${}^{\mathcal{R}}C_{\mathcal{R}}(\vec{K}) \simeq {}^{\mathbb{F}[U,V]}[\Psi]_{C^\star(1)} \boxtimes {}^{C^\star(1)}R^{alg}(\mathcal{H}^\wedge),$$

where  $\Psi: C(1) \rightarrow \mathbb{F}[U, V]$  is the isomorphism from Equation (8.8).

**Proof.** To compute  ${}^{\mathcal{R}}C_{\mathcal{R}}(\vec{K})$ , we use By the pairing theorem (Theorem 9.1)

$${}^{\mathcal{R}}C_{\mathcal{R}}(\vec{K}) = {}^{\mathcal{R}}Q(\mathcal{H}^\vee)_{C(1)} \boxtimes {}^{C(1)}R(\mathcal{H}^\wedge).$$

The result now follows from Lemma 8.14 with Theorem 14.1.  $\square$

**Remark 15.2.** *The application of Theorem 9.1 in the above proof in fact uses the special case where  $n = 1$ , where we glue to the standard lower diagram. This is a particularly simple special case of the pairing theorem; the more interesting applications of the pairing theorem are contained in the use of Theorem 14.1.*

The above description of knot Floer homology is not exactly the construction formulated in [22], but it is close enough that the proof of Theorem 1.1 follows quickly:

**Proof of Theorem 1.1.** In [22], we defined  $\mathcal{G}(\vec{K})$  as the homology of a complex  $\mathcal{C}(\mathbf{D})$  associated to a diagram. The complex  $\mathcal{C}(\mathbf{D})$  is constructed similarly to  $R^{alg}(\hat{\mathbf{D}})$  described above: the diagram  $\mathbf{D}$  is broken into pieces, and to each elementary piece we associate bimodules, and  $\mathcal{C}(\mathbf{D})$  is obtained by tensoring together these pieces. Specifically, to an upper diagram  $\hat{\mathbf{D}}$ , tensoring together local bimodules defines an algebraically defined type  $D$  structure  ${}^{\mathcal{A}(n,M)}\mathcal{Q}(\hat{\mathbf{D}})$ , where  $2n$  is the number of strands out of  $\hat{\mathbf{D}}$  and  $M$  is the matching induced by  $\hat{\mathbf{D}}$ ; and if  $\mathbf{D}$  is obtained by adding a global minimum to  $\hat{\mathbf{D}}$ , then  $\mathcal{C}(\mathbf{D}) = {}^{\mathbb{F}[U,V]}t\mathcal{U}_{\mathcal{A}(1)} \boxtimes {}^{\mathcal{A}(1)}\mathcal{Q}(\hat{\mathbf{D}})$ , where  ${}^{\mathbb{F}[U,V]}t\mathcal{U}_{\mathcal{A}(1)}$  is the a bimodule described in [22, Section 8.2].

We claim that

$$(15.1) \quad {}^{\mathcal{A}}T_{\mathcal{B}^\star} \boxtimes {}^{\mathcal{B}^\star}i_{C^\star} \boxtimes {}^{C^\star}R^{alg}(\hat{\mathbf{D}}) \simeq {}^{\mathcal{A}}\mathcal{Q}(\hat{\mathbf{D}}),$$

where  $\mathcal{A} = \mathcal{A}(n, M)$ ,  $\mathcal{B} = \mathcal{B}(n, M)$ ,  $C = C(n, M)$  for  $M$  as determined by  $\hat{\mathbf{D}}$ . This is seen by induction on the number of events in  $\hat{\mathbf{D}}$ . For the basic case, where  $\hat{\mathbf{D}}$  contains only maxima, recall from [22] that  ${}^{\mathcal{A}}\mathcal{Q}(\hat{\mathbf{D}})$  is generated by a single element  $\mathbf{x}$ , and  $\delta^1(\mathbf{x}) = C \otimes \mathbf{x}$ , where  $C = \sum_{i=1}^n C_{\{2i-1, 2i\}}$ ; i.e. there is an identification of  ${}^{\mathcal{A}}\mathcal{Q}(\hat{\mathbf{D}})$  with

$${}^{\mathcal{A}}T_{\mathcal{B}^\star} \boxtimes {}^{\mathcal{B}^\star}i_{C^\star} \boxtimes {}^{C^\star}k = {}^{\mathcal{A}}T_{\mathcal{B}^\star} \boxtimes {}^{\mathcal{B}^\star}i_{C^\star} \boxtimes {}^{C^\star}R^{alg}(\hat{\mathbf{D}}).$$

For the inductive step, when we add the bimodule associated to one more standard piece, we use Proposition 12.1 and Lemma 12.11.

Next, we consider  ${}^{\mathcal{R}}t\mathcal{U}_{\mathcal{A}(1)}$ , used in the definition of  $\mathcal{C}(\mathbf{D})$ . The bimodule  $t\mathcal{U}$  has three generators  $\mathbf{X}$ ,  $\mathbf{Y}$ , and  $\mathbf{Z}$ , with

$$\mathbf{X} \cdot \mathbf{I}_{\{0\}} = \mathbf{X}, \quad \mathbf{Y} \cdot \mathbf{I}_{\{1\}} = \mathbf{Y}, \quad \mathbf{Z} \cdot \mathbf{I}_{\{2\}} = \mathbf{Z}.$$

When 1 is oriented upwards,  $t\mathcal{U}$  is the  $DA$  bimodule with  $\delta_k^1 = 0$  for  $k \neq 2$ , and all  $\delta_2^1$  are determined by

$$\begin{aligned} \delta_2^1(\mathbf{Y}, L_1) &= u \otimes \mathbf{X}, & \delta_2^1(\mathbf{X}, R_1) &= u \otimes \mathbf{Y}, \\ \delta_2^1(\mathbf{Y}, R_2) &= v \otimes \mathbf{Z}, & \delta_2^1(\mathbf{Z}, L_2) &= v \otimes \mathbf{Y}, \\ \delta_2^1(\mathbf{X}, C_{\{1,2\}}) &= \delta_2^1(\mathbf{Y}, C_{\{1,2\}}) = \delta_2^1(\mathbf{Z}, C_{\{1,2\}}) = 0. \end{aligned}$$

(When 1 is oriented downwards, we define the actions as above, exchanging the roles of  $u$  and  $v$ .) It follows immediately from this description that

$$(15.2) \quad {}^{\mathcal{R}}t\mathcal{U}_{\mathcal{A}(1)} \boxtimes {}^{\mathcal{A}(1)}T_{\mathcal{B}^*(1)} \boxtimes {}^{\mathcal{B}^*(1)}i_{\mathcal{C}^*(1)} = {}^{\mathcal{R}}[\Psi]_{\mathcal{C}^*(1)},$$

where  $\Psi$  is as in Equation (8.8).

Thus, combining the definition of  $\mathcal{C}$  with Equations (15.1), (15.2), and Theorem 15.1, we find that

$$\begin{aligned} \mathcal{C}(\mathbf{D}) &= {}^{\mathcal{R}}t\mathcal{U}_{\mathcal{A}(1)} \boxtimes {}^{\mathcal{A}(1)}\mathcal{Q}(\mathcal{H}^\wedge) \\ &= {}^{\mathcal{R}}t\mathcal{U}_{\mathcal{A}(1)} \boxtimes {}^{\mathcal{A}(1)}T_{\mathcal{B}^*(1)} \boxtimes {}^{\mathcal{B}^*(1)}i_{\mathcal{C}^*(1)} \boxtimes {}^{\mathcal{C}^*(1)}R^{alg}(\widehat{\mathbf{D}}) \\ &= {}^{\mathcal{R}}[\Psi]_{\mathcal{C}^*(1)} \boxtimes {}^{\mathcal{C}^*(1)}R^{alg}(\mathcal{H}^\wedge) \\ &= {}^{\mathcal{R}}C_{\mathcal{R}}(\vec{K}), \end{aligned}$$

as required. □

## 16. FURTHER REMARKS ON INVARIANCE

This section is a further elaboration on Theorem 14.1, wherein we explore the invariance properties of the two sides of Equation (14.1).

Observe that the object appearing on the right hand side of Equation (14.1),  ${}^{c^*}R^{alg}(\hat{\mathbf{D}})$ , is associated to an acceptable upper diagram  $\hat{\mathbf{D}}$ . We explain first how to define  ${}^{c^*}R^{alg}(\hat{\mathbf{D}})$  for a more generic kind of knot diagram.

By analogy with [21, Section 11], we say that an upper diagram  $\hat{\mathbf{D}}$  is in *bridge position* if it is drawn on the  $y \geq 0$  plane so that:

- (1) all the critical points are local minima or maxima
- (2) minima, maxima, and crossings all have distinct  $y$  coordinates
- (3)  $\hat{\mathbf{D}}$  has no closed components

To an upper diagram in bridge position, we can associate an algebraically defined, curved type  $D$  structure  ${}^{c^*}R^{alg}(\hat{\mathbf{D}})$  in the obvious way: we tensor together the curved DA bimodules associated to the crossings local maxima, and local minima ( $\mathcal{B}_2^* \mathcal{P}_{\mathcal{B}_1^*}^i$ ,  $\mathcal{B}_2^* \mathcal{N}_{\mathcal{B}_1^*}^i$ ,  $\mathcal{B}_2^* \Omega_{\mathcal{B}_1^*}^c$ , and  $\mathcal{B}_2^* \mathcal{U}_{\mathcal{B}_1^*}^c$  from Proposition 12.1) as they appear in  $\hat{\mathbf{D}}$ .

Adapting methods from [21, Section 11] (see also [22, Section 8]), we can show that  ${}^{c^*}R^{alg}(\hat{\mathbf{D}})$  depends only on the planar isotopy class of the diagram  $\mathbf{D}$ .

**Proposition 16.1.** *If  $\hat{\mathbf{D}}$  and  $\hat{\mathbf{D}}'$  are two upper diagrams that differ by planar isotopies (fixing  $y = 0$ ), then the associated curved type  $D$  structures  ${}^{c^*}R^{alg}(\hat{\mathbf{D}})$  and  ${}^{c^*}R^{alg}(\hat{\mathbf{D}}')$  are homotopy equivalent (as curved type  $D$  structures).*

The above is proved in Section 16.2, after some algebraic background is set up in Section 16.1.

With a little more work, we can show that this curved type  $D$ -structure is in fact an invariant of the tangle represented by  $\hat{\mathbf{D}}$ .

**Proposition 16.2.** *If  $\hat{\mathbf{D}}$  and  $\hat{\mathbf{D}}'$  are two upper diagrams that represent the same tangle in  $S^3$ , then the associated curved type  $D$  structures  ${}^{c^*}R^{alg}(\hat{\mathbf{D}})$  and  ${}^{c^*}R^{alg}(\hat{\mathbf{D}}')$  are homotopy equivalent.*

To an upper diagram  $\hat{\mathbf{D}}$  in bridge position, there is an associated Heegaard diagram  $\mathcal{H}(\hat{\mathbf{D}})$ , obtained by stacking the middle diagrams associated to the crossings and critical points as they appear in  $\hat{\mathbf{D}}$ .

We have the following variant of Theorem 14.1:

**Theorem 16.3.** *Let  $\hat{\mathbf{D}}$  be an upper diagram in bridge position, and let  $\mathcal{H}^\wedge$  be its associated upper Heegaard diagram. Then there is an identification*

$$(16.1) \quad {}^{c^*(n,M)}R(\mathcal{H}^\wedge) \simeq {}^{c^*(n,M)}R^{alg}(\hat{\mathbf{D}}).$$

Combining Theorem 16.3 with Proposition 16.1, we can conclude that the homotopy class of the analytically defined  ${}^{c^*(n,M)}R(\mathcal{H}^\wedge)$ , which appears to depend on the choice of Heegaard diagram, in fact is an invariant for tangles. (One could alternatively prove invariance  ${}^{c^*(n,M)}R(\mathcal{H}^\wedge)$  using more analytical methods by showing invariance under isotopies, handleslides, and stablizations, in the spirit of [20].)

Theorem 16.3 is proved in Section 16.3

**16.1. Local maxima.** Consider the curved DA bimodule  $\mathcal{B}_1^\star \Omega_{\mathcal{B}_2^\star}^c$  from Proposition 12.1; i.e. where

$$\mathcal{B}_1^\star = \mathcal{B}(n, M_1) \quad \text{and} \quad \mathcal{B}_1^\star = \mathcal{B}(n, M_2),$$

where  $M_1$  is some matching on  $\{1, \dots, 2n\}$ , and  $M_2$  is the matching on  $\{1, \dots, 2n+2\}$  obtained by adding to  $\phi_c(M_1)$ , the additional pair  $\{c, c+1\}$ , with  $\phi_c$  as in Equation (12.1). By construction,  $\mathcal{B}_2^\star \Omega_{\mathcal{B}_1^\star}^c \cdot \iota = \iota \cdot \mathcal{B}_1^\star \Omega_{\mathcal{B}_2^\star}^c$  (compare Lemma 12.11); i.e. there is a corresponding bimodule

$$\mathcal{B}_2^\star i_{C_2^\star} \boxtimes \mathcal{C}_2^\star \Omega_{C_1^\star}^c \simeq \mathcal{B}_2^\star \Omega_{\mathcal{B}_1^\star}^c \boxtimes \mathcal{B}_1^\star i_{C_1^\star}$$

The key algebraic step required to adapt the invariance proof from [22] is the existence of a bimodule  $\mathcal{A}_1'' \Omega_{\mathcal{A}_2''}^c$  that is dual to  $\mathcal{B}_2^\star \Omega_{\mathcal{B}_1^\star}^c$ , as follows:

**Proposition 16.4.** *Given  $\mathcal{B}_1^\star$  and  $\mathcal{B}_2^\star$  as above, there is a bimodule  $\mathcal{A}_1'' \Omega_{\mathcal{A}_2''}^c$  with the property that*

$$\mathcal{B}_2^\star \Omega_{\mathcal{B}_1^\star}^c \boxtimes \mathcal{B}_1^\star, \mathcal{A}_1'' \mathcal{K} \simeq \mathcal{A}_1'' \Omega_{\mathcal{A}_2''}^c \boxtimes \mathcal{A}_2'', \mathcal{B}_2^\star \mathcal{K}.$$

The proof occupies the rest of this subsection.

The construction of  $\mathcal{A}_1'' \Omega_{\mathcal{A}_2''}^c$  is similar to the constructions of the bimodules associated to local minimum from [22] and [21]. As in [22, Section 7], we start with the construction of  $\Omega^c$  in the case where  $c = 1$ .

A *preferred idempotent state* for  $\mathcal{A}_2''$  is an idempotent state  $\mathbf{x}$  with

$$\mathbf{x} \cap \{0, 1, 2\} \in \{\{0\}, \{2\}, \{0, 2\}\}.$$

We have a map  $\psi$  from preferred idempotent states  $\mathbf{x} = \{x_1, \dots, x_{k+1}\}$  of  $\mathcal{A}_2''$  to idempotents of  $\mathcal{A}_1''$  defined by Let  $\mathcal{A}_1'' = \mathcal{A}'(n+1, k+1, M_1)$  and  $\mathcal{A}_2'' = \mathcal{A}'(n, k, M_2)$

$$\psi(\mathbf{x}) = \begin{cases} \{0, x_3 - 2, \dots, x_{k+1} - 2\} & \text{if } |\mathbf{x} \cap \{0, 1, 2\}| = 2 \\ \{x_2 - 2, \dots, x_{k+1} - 2\} & \text{if } |\mathbf{x} \cap \{0, 1, 2\}| = 1 \end{cases}$$

Generators of  $\Omega^1 = \mathcal{A}_1'' \Omega_{\mathcal{A}_2''}^1$  correspond to preferred idempotent states. Letting  $\mathbf{S}_\mathbf{x}$  denote the generator corresponding to the preferred idempotent state  $\mathbf{x}$ , the bimodule action is specified by

$$\mathbf{I}_\mathbf{x} \cdot \mathbf{S}_\mathbf{x} \cdot \mathbf{I}_{\psi(\mathbf{x})} = \mathbf{S}_\mathbf{x}.$$

The module is constructed via the homological perturbation lemma, following [22, Section 7.3].

Fix a matching  $M_2$  on  $\{1, \dots, 2n\}$ , and let  $M_1$  be the matching  $\{1, 2\} \cup \phi_1(M_1)$ . Let

$$\mathcal{B}_1^\circ = \mathcal{B}(2n+2, n+2) \quad \text{and} \quad \mathcal{B}_2^\circ = \mathcal{B}(2n, n+1).$$

Consider the idempotent in  $\mathcal{B}_1^\circ$  given by

$$\mathbf{I} = \sum_{\{\mathbf{x} \mid x_1=1\}} \mathbf{I}_\mathbf{x}.$$



Consider the right  $\mathcal{B}^\circ$ -module

$$M = (L_1 L_2 \mathcal{B}^\circ \setminus \mathbf{I} \cdot \mathcal{B}^\circ) \oplus (L_1 L_2 \mathcal{B}^\circ \setminus \mathbf{I} \cdot \mathcal{B}^\circ),$$

which can also be viewed as a left module over the subalgebra of  $\mathbf{I} \cdot \mathcal{B}^\circ \cdot \mathbf{I}$  consisting of elements with  $\mathbf{w}_1 = \mathbf{w}_2 = 0$ , which in turn is identified with  $\mathcal{B}^\circ 2$ . Denote this identification

$$\phi: \mathcal{B}_2^\circ \rightarrow \mathbf{I} \cdot \mathcal{B}^\circ \cdot \mathbf{I}.$$

Let  $\mathbf{X}$  and  $\mathbf{Y}$  be the generators of the two summands of  $M$ . Let

$$m_{1|1|0}(b_2, \mathbf{X} \cdot b_1) = \mathbf{X} \cdot \phi(b_2) \cdot b_1 \quad m_{1|1|0}(b_2, \mathbf{Y} \cdot b_1) = \mathbf{Y} \cdot \phi(b_2) \cdot b_1,$$

where  $b_2 \in \mathcal{B}_2^\circ$  and  $b_1 \in \mathbf{I} \cdot \mathcal{B}^\circ \setminus L_1 L_2 \cdot \mathcal{B}^\circ$ . Equip  $M$  with the differential

$$m_{0|1|0}(\mathbf{X}) = \mathbf{Y} \cdot U_2 \quad m_{0|1|0}(\mathbf{Y}) = \mathbf{X} \cdot U_1.$$

Think of the right  $\mathcal{B}^\circ$ -action as inducing further operations

$$m_{0|1|1}(\mathbf{X} \cdot b_1, b'_1) = \mathbf{X} \cdot (b_1 \cdot b'_1) \quad m_{0|1|1}(\mathbf{Y} \cdot b_1, b'_1) = \mathbf{Y} \cdot (b_1 \cdot b'_1).$$

All the operations described above give  $M$  the structure of a  $\mathcal{B}_2^\circ - \mathcal{B}^\circ$  bimodule, written  ${}_{\mathcal{B}_2^\circ} M_{\mathcal{B}^\circ}$ .

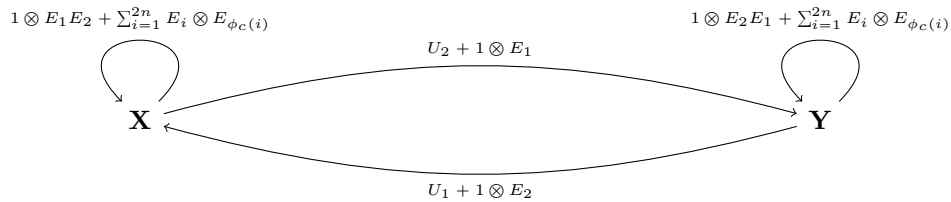
As explained in [22, Lemma 7.6],  $M$  can be viewed as arising from a type DA bimodule  ${}^{\mathcal{B}_2^\circ} \Theta_{\mathcal{B}_1^\circ}$  via  ${}_{\mathcal{B}_2^\circ} M_{\mathcal{B}_1^\circ} = {}_{\mathcal{B}_2^\circ} (\mathcal{B}_2^\circ)_{\mathcal{B}_2^\circ} \boxtimes {}^{\mathcal{B}_2^\circ} \Theta_{\mathcal{B}_1^\circ}$ . (The key notational difference here is we have restricted the incoming algebra from the algebra  $\mathcal{B}$  of [22, Lemma 7.6] to its subalgebra  $\mathcal{B}_1^\circ$  where the idempotent states have  $n+2$  elements; and correspondingly the output algebra has a similar constraint.)

In [22], this DA bimodule  $\Theta$  is promoted to a bimodule over versions of  $\mathcal{A}$ . Instead, we promote here the incoming algebra to  $\mathcal{A}_1''$  (and the outgoing one to  $\mathcal{A}_2''$ ). This is done by introducing the following actions:

$$\begin{aligned} \delta_2^1(\mathbf{X}, E_1) &= 1 \otimes \mathbf{Y} & \delta_2^1(\mathbf{Y}, E_2) &= 1 \otimes \mathbf{X} \\ \delta_2^1(\mathbf{X}, E_2) &= 0 & \delta_2^1(\mathbf{Y}, E_1) &= 0 \\ \delta_2^1(\mathbf{X}, E_{\phi_c(i)}) &= E_i \otimes \mathbf{X} & \delta_2^1(\mathbf{Y}, E_{\phi_c(i)}) &= E_i \otimes \mathbf{Y} \\ \delta_2^1(\mathbf{X}, E_1 E_2) &= 1 \otimes \mathbf{X} & \delta_2^1(\mathbf{Y}, E_2 E_1) &= 1 \otimes \mathbf{Y} \\ \delta_2^1(\mathbf{X}, E_2 E_1) &= 0 & \delta_2^1(\mathbf{Y}, E_1 E_2) &= 0 \end{aligned}$$

These actions are illustrated in the following picture:

(16.2)



(Here the arrow labels with  $U_2$  and  $U_1$  alone represent  $\delta_1^1$ , actions where the outgoing algebra element is 1.)

We denote the result by  ${}^{\mathcal{A}_2''} \Theta''_{{\mathcal{A}_1''}}$ .

**Lemma 16.5.** *The operations described above make  ${}^{\mathcal{A}_2''} \Theta''_{{\mathcal{A}_1''}}$  into a type DA bimodule.*

**Proof.** This is straightforward.  $\square$

Consider the map  $h^1: \Theta'' \rightarrow \Theta''$  determined on the generating set  $\mathbf{X} \cdot a$  and  $\mathbf{Y} \cdot a$  for  $a \in \Gamma$ ) by

$$\begin{aligned} h^1(\mathbf{X}a) &= \begin{cases} \mathbf{Y}a' & \text{if there is a } a' \in \Gamma \text{ with } a = U_1 a' \\ 0 & \text{otherwise} \end{cases} \\ h^1(\mathbf{Y}a) &= \begin{cases} \mathbf{X}a' & \text{if there is a pure } a' \in \Gamma \text{ with } a = U_2 a' \\ 0 & \text{otherwise} \end{cases} \end{aligned}$$

Let  $Q \subset \Theta''$  be the two-dimensional vector space  $\mathbf{X}L_1$  and  $\mathbf{Y}R_2$ . There are inclusions  $i^1: Q \rightarrow \Theta'' \subset \mathcal{A}_2'' \otimes \Theta''$  and a projection  $\pi^1: \Theta'' \rightarrow Q$

**Lemma 16.6.** *For the above operators, we have the identities:*

$$(\pi^1 \circ i^1) = \text{Id}_Q, \quad i^1 \circ \pi^1 = \text{Id}_{\Theta''} + dh^1, \quad h^1 \circ h^1 = 0, \quad h^1 \circ i^1 = 0, \quad \pi^1 \circ h^1 = 0.$$

The homological perturbation lemma, we can give  $\mathbf{X}L_1 \oplus \mathbf{Y}R_2$  the structure of a type  $DA$  bimodule.

**Definition 16.7.** *Let  $\mathcal{A}_1'' \Omega_{\mathcal{A}_2''}^c$  be the  $DA$  bimodule structure on  $\mathbf{X}L_1 \oplus \mathbf{Y}R_2$  induced by the homological perturbation lemma.*

We can now verify duality:

**Lemma 16.8.** *The bimodule  $\mathcal{A}_1'' \Omega_{\mathcal{A}_2''}^1$  as defined above satisfies the requirements of Proposition 16.4 when  $c = 1$ .*

**Proof.** This is a simple computation using the homological perturbation lemma, exactly as in [22, Lemma 7.5].  $\square$

**Proof of Proposition 16.4.** By analogy with [22, Section 7.5], we can define  $\mathcal{A}_1'' \Omega_{\mathcal{A}_2''}^c$  inductively in  $c$ , using the action of the bimodules of crossings; i.e.

$$\mathcal{A}_1'' \Omega_{\mathcal{A}_2''}^c = \mathcal{A}_1'' \Omega_{\mathcal{A}_4''}^{c-1} \boxtimes \mathcal{A}_4'' \mathcal{P}_{\mathcal{A}_3''}^c \boxtimes \mathcal{A}_3'' \mathcal{P}_{\mathcal{A}_2''}^{c-1},$$

for suitably chosen  $\mathcal{A}_3''$  and  $\mathcal{A}_4''$ . Property 16.4 is then proved by induction, with the basic case given by Lemma 16.8, and the inductive step using Proposition 12.10 (for the positive crossing). (The steps are as in the proof of [22, Theorem 7.10].)  $\square$

## 16.2. Algebraic invariance.

**Proof of Proposition 16.1.** Following terminology from [21, Section 11.3], Proving that the invariant  ${}^{c^*}R^{alg}(\widehat{\mathbf{D}})$  is an isotopy invariant amounts to proving invariance under bridge moves, which are:

- (1) Commutations of distant crossings
- (2) Trident moves
- (3) Critical points commute with distant crossings
- (4) Commuting distant critical points
- (5) Pair creation and annihilation.

In [21, 22], these are verified as obtained identities between corresponding  $DA$  bimodules. To expedite computations, we worked instead with  $DD$  bimodules.

In the notation of the present paper, the requisite identities for the  $DD$  module versions of commutation moves (for distant crossings and critical points) are of the form

$$X^i \boxtimes Y^j \boxtimes \mathcal{K} \simeq Y^{j'} \boxtimes X^{i'} \boxtimes \mathcal{K}$$

where  $X, Y$  can be either of  $\mathcal{P}, \mathcal{N}, \Omega$  or  $\mathcal{U}$ ,  $|i-j| > 1$  (and the superscripts  $i'$  and  $j'$  have to be chosen accordingly), curved modules over  $\mathcal{B}^*$  (as in Subsection 12.1), and  $\mathcal{K} =_{\mathcal{B}^*, \mathcal{A}''} \mathcal{K}$ . Trident moves come from identities

$$\mathcal{U}^c \boxtimes \mathcal{P}^{c+1} \boxtimes \mathcal{K} \simeq \mathcal{P}^{c+1} \boxtimes \mathcal{U}^c \boxtimes \mathcal{K}$$

$$\mathcal{P}^{c+1} \boxtimes \Omega^c \boxtimes \mathcal{K} \simeq \mathcal{U}^c \boxtimes \mathcal{P}^{c+1} \boxtimes \mathcal{K}$$

Pair creation and annihilation invariance from the identities

$$\Omega^{c+1} \boxtimes \mathcal{U}^c \simeq \text{Id} \simeq \Omega^c \boxtimes \mathcal{U}^{c+1}.$$

The verifications from [22] (dropping  $C_{i,j}$ , and viewing the algebras over  $\mathcal{B}$  as curved) now apply verbatim to give the stated identities.

In [22], the type  $DD$  identities implied corresponding identities of type  $DA$  modules, due to a Koszul duality, which we have not established here. Nonetheless, the above identities do establish corresponding identities where the  $DA$  modules act on any “relevant” type  $D$  structure, in the sense of Definition 14.2. Thus, the needed invariance follows once we know that  ${}^{c^*}R^{alg}(\mathbf{D})$  is relevant.

Relevance of  ${}^{c^*}R^{alg}(\mathbf{D})$  is proved by induction on the number of crossings and critical points in  $\mathbf{D}$  (as in the proof of Proposition 14.4), with the inductive step furnished by the fact that for  $X$  is  $\mathcal{P}, \mathcal{N}, \Omega$ , or  $\mathcal{U}$  (curved  $DA$  bimodules over  $\mathcal{B}$ ), there are corresponding  $DA$  bimodules  $X''$  so that

$${}^{\mathcal{B}_2}X_{\mathcal{B}_1} \boxtimes_{\mathcal{B}_1, \mathcal{A}_1''} \mathcal{K} \simeq_{\mathcal{A}_1''} X_{\mathcal{A}_2''} \boxtimes_{\mathcal{B}_1, \mathcal{A}_1''} \mathcal{K}.$$

For  $X \in \{\mathcal{P}, \mathcal{N}, \mathcal{U}\}$ , this was verified in Proposition 12.1, while for  $\Omega$ , it was Proposition 16.4.  $\square$

**Proof of Proposition 16.2.** In view of Proposition 16.1, it suffices to verify invariance of  ${}^{c^*}R^{alg}(\mathbf{D})$  under the Reidemeister moves. The corresponding  $DD$  module identities for  $\mathcal{A}$  and  $\mathcal{A}'$

Reidemeister 1 invariance follows from the identity  $\mathcal{P}^c \boxtimes \Omega^c \boxtimes \mathcal{K} \simeq \mathcal{P}^c \boxtimes \mathcal{K}$ , whereas the other Reidemeister moves follow from the braid relations from [22, Section 4]. The identities are verified exactly as they are done there, appealing to the fact that  ${}^{c^*}R(\mathbf{D})$  is relevant, as shown in the proof of Proposition 16.1 above.  $\square$

### 16.3. Computing the holomorphically defined invariant.

**Proof of Theorem 16.3.** The proof of Theorem 14.1 applies, once we have shown the analogue of Theorem 13.1 for a local maximum; i.e.

$${}^{c_2^*}\Omega_{c_1^*}^c \boxtimes {}^{c_1^*, \mathcal{A}_1''} \mathcal{K} \simeq_{{}^{c_2^*}} RQ^x(\mathcal{H}_c^\cap)_{c_1^*} \boxtimes {}^{c_1^*, \mathcal{A}_1''} \mathcal{K}.$$

This verification is very similar to the proof of Proposition 13.3, and is left to the reader.  $\square$

## REFERENCES

- [1] J. S. Birman. *Braids, links, and mapping class groups*. Princeton University Press, Princeton, N.J.; University of Tokyo Press, Tokyo, 1974. Annals of Mathematics Studies, No. 82.
- [2] F. Bourgeois. *A Morse-Bott Approach to Contact Homology*. PhD thesis, Stanford University, 2006.
- [3] Y. Eliashberg, A. Givental, and H. Hofer. Introduction to symplectic field theory. *Geom. Funct. Anal.*, (Special Volume, Part II):560–673, 2000. GAFA 2000 (Tel Aviv, 1999).
- [4] K. Fukaya, Y.-G. Oh, K. Ono, and H. Ohta. *Lagrangian intersection Floer theory—anomaly and obstruction*. Kyoto University, 2000.
- [5] M. Khovanov and L. Rozansky. Matrix factorizations and link homology. *Fund. Math.*, 199(1):1–91, 2008.
- [6] R. Lipshitz. A cylindrical reformulation of Heegaard Floer homology. *Geom. Topol.*, 10:955–1097 (electronic), 2006.
- [7] R. Lipshitz, P. S. Ozsváth, and D. P. Thurston. Bordered  $HF^-$  modules for the torus. In preparation.
- [8] R. Lipshitz, P. S. Ozsváth, and D. P. Thurston. Computing  $\widehat{HF}$  by factoring mapping classes. *Geom. Topol.*, 18(5):2547–2681, 2014.
- [9] R. Lipshitz, P. S. Ozsváth, and D. P. Thurston. Bimodules in bordered Heegaard Floer homology. *Geom. Topol.*, 19(2):525–724, 2015.
- [10] R. Lipshitz, P. S. Ozsváth, and D. P. Thurston. Bordered Heegaard Floer homology. *Mem. Amer. Math. Soc.*, 254(1216):viii+279, 2018.
- [11] A. Manion. Khovanov-Seidel quiver algebras and Ozsváth-Szabó’s bordered theory. *J. Algebra*, 488:110–144, 2017.
- [12] A. Manion. On the decategorification of Ozsváth and Szabó’s bordered theory for knot Floer homology. *Quantum Topol.*, 10(1):77–206, 2019.
- [13] C. Manolescu, P. Ozsváth, and S. Sarkar. A combinatorial description of knot Floer homology. *Ann. of Math. (2)*, 169(2):633–660, 2009.
- [14] C. Manolescu, P. Ozsváth, Z. Szabó, and D. Thurston. On combinatorial link Floer homology. *Geom. Topol.*, 11:2339–2412, 2007.
- [15] D. McDuff and D. Salamon. *J-holomorphic curves and symplectic topology*, volume 52 of *American Mathematical Society Colloquium Publications*. American Mathematical Society, Providence, RI, second edition, 2012.
- [16] Y.-G. Oh. Fredholm theory of holomorphic discs under the perturbation of boundary conditions. *Math. Z.*, 222(3):505–520, 1996.
- [17] P. Ozsváth and Z. Szabó. Heegaard Floer homology and alternating knots. *Geom. Topol.*, 7:225–254, 2003.
- [18] P. Ozsváth and Z. Szabó. Heegaard Floer homology and alternating knots. *Geom. Topol.*, 7:225–254 (electronic), 2003.
- [19] P. Ozsváth and Z. Szabó. Holomorphic disks and knot invariants. *Adv. Math.*, 186(1):58–116, 2004.
- [20] P. Ozsváth and Z. Szabó. Holomorphic disks and topological invariants for closed three-manifolds. *Ann. of Math. (2)*, 159(3):1027–1158, 2004.
- [21] P. Ozsváth and Zoltán Szabó. Kauffman states, bordered algebras, and a bigraded knot invariant. *Adv. Math.*, 328:1088–1198, 2018.
- [22] P. Ozsváth and Zoltán Szabó. Bordered knot algebras with matchings. *Quantum Topol.*, 10(3):481–592, 2019.
- [23] P. S. Ozsváth and Z. Szabó. Knot Floer homology calculator. <http://www.math.princeton.edu/~szabo/HFKcalc.html>.
- [24] J. A. Rasmussen. *Floer homology and knot complements*. PhD thesis, Harvard University, 2003.
- [25] S. Sarkar. Maslov index formulas for Whitney  $n$ -gons. *J. Symplectic Geom.*, 9(2):251–270, 2011.

DEPARTMENT OF MATHEMATICS, PRINCETON UNIVERSITY, PRINCETON, NEW JERSEY 08544

*E-mail address:* `petero@math.princeton.edu`

DEPARTMENT OF MATHEMATICS, PRINCETON UNIVERSITY, PRINCETON, NEW JERSEY 08544

*E-mail address:* `szabo@math.princeton.edu`